Engineering-Economic Methods for Power Transmission Planning under Uncertainty and Renewable Resource Policies

by

Francisco David Muñoz Espinoza

A dissertation submitted to The Johns Hopkins University in conformity with the requirements for the degree of Doctor of Philosophy.

Baltimore, Maryland

January, 2014

Abstract

Power transmission networks are some of the world's largest machines. Investments in these assets have historically been driven by projections of load growth, interconnection of baseload conventional power plants, reliability standards, and the economic exchange of electricity. However, today the transmission system is also seen as a key enabler to meet the new public policy goals that seek to incorporate large amounts of generation from renewable resources into the grid. In this dissertation I analyze three different engineering-economic challenges of power transmission planning that arise from the large scale integration of renewable energy technologies.

In the first essay I study the effects of transmission approximations on the design and performance of Renewable Portfolio Standards. In particular, I analyze how disregarding the indivisibility of transmission investments (i.e., lumpiness) or Kirchhoff's Voltage Law yield distorted estimates of the type and location of infrastructure, as well as inaccurate estimates of the cost of complying with renewable goals. I also utilize multi-stage investment models to study the potential benefits of coordinating the timing of transmission investments and the design of multi-year renewable energy policies.

In the second essay I propose a stochastic programming-based tool for adaptive transmission planning under market and regulatory uncertainties. The model considers investments in two stages, generators' response, and Kirchhoff's Voltage Law enforced through disjunctive constraints. I use a 240-bus representation of the Western Electricity Coordinating Council to illustrate its application, calculate the Expected Value of Perfect Information and the Expected Cost of Ignoring Uncertainty, and compare its performance to heuristic investment decision rules based on scenario planning.

The third essay describes a new, two-phase bounding and decomposition method to solve large-scale transmission and generation investment planning problems under various environmental constraints designed to incentivize high amounts of intermittent generation in electric power systems. The first phase exploits Jensen's inequality which I extend to stochastic problems with expected-value constraints. The second phase is an enhancement of Benders decomposition that I utilize to reduce the residual solution gap from the first phase. Numerical results show that only the bounding phase is necessary if loose optimality tolerances are acceptable. Attaining tight solution tolerances, however, requires utilization of the decomposition phase, which performs much better in terms of convergence speed than attempting to solve the problem using either algorithm, the bounding method or Benders decomposition, separately.

ABSTRACT

The main contributions of this dissertation include a better understanding of the interaction between different renewable energy policy designs and transmission investments, a new method to conduct transmission planning studies under gross economic and public policy uncertainties, and new algorithms to solve large-scale transmission and generation planning problems.

Academic Advisor and First Reader:

Benjamin F. Hobbs, Professor

Department of Geography and Environmental Engineering

The Johns Hopkins University

Second Reader:

Seth D. Guikema, Assistant Professor

Department of Geography and Environmental Engineering

The Johns Hopkins University

Third Reader:

Daniel Robinson, Assistant Professor

Department of Applied Mathematics and Statistics

The Johns Hopkins University

Acknowledgments

Completing this dissertation has been, by far, the longest and most challenging mountain I have ever climbed. Attaining the summit of it wouldn't have been possible without the enormous support from my advisor, colleagues, family, and friends. Working with Ben Hobbs has been an honor. His contagious motivation for doing research and curiosity are truly inspirational to me. He is the one that prevented me from going off route in my research endeavors and helped me get my ideas onto paper. I am enormously thankful for his continuous support and guidance.

I would like to thank my parents, sister, and friends in Chile for their constant support in this seemingly never-ending journey. They somehow made me feel like they were always sitting next to me, cheering me up, even though they are more than 10,000 miles away from Baltimore. I'm also grateful for the friendship of Anya Castillo, Saamrat Kasina, Venkat Prava, Stefanie Falconi, and Javier Iñon. My pass through DoGEE wouldn't have been the same if it wasn't for them. I would also like to thank Andrea Staid for all her love and patience with me in this last year of the Ph.D. program. I'm also thankful for insightful discussions with Seth Guikema and Enzo Sauma, the second of whom participated intensively in the development of the second chapter of this dissertation while visiting our department. I also want to thank Jonathan Ho for his help collecting and sorting all the data that I needed for chapters 3 and 4.

Finally, I would like to thank John Birge, from the University of Chicago, and Mihai Anitescu, from Argonne National Laboratories, for useful comments on the convergence of the batch-means method for stochastic optimization problems. I also thank Suvrajeet Sen, from the University of Southern California, for the explanation of the use of the expected-value problem to stabilize the cuts in the implementation of the stochastic decomposition algorithm in the NEOS solver. I want to thank Jean-Paul Watson and his group at Sandia National Laboratories for their guidance on the use of the Pyomo modeling package. I would also like to acknowledge the financial support from the CERTS Reliability and Markets program and the Fulbright Foundation.

Contents

Abstract **ii**

Acknowledgments **v**

List of Tables **xii**

List of Figures **xiv**

1 Introduction **1**

1.1 Approximations in Power Transmission Planning 3

1.2 Transmission Planning Under Uncertainty 6

1.3 New Computational Methods to Solve Large-Scale Planning Problems 9

1.4 Scope 12

2 Approximations in Power Transmission Planning: Implications for the Cost and Performance of Renewable Portfolio Standards **15**

2.1 Introduction 17

2.2 Comparative Statics for a Two-Node Example 25
2.3 Meshed Models 32
2.3.1 Single-Stage Models 34
2.3.2 Dynamic Model 37
2.4 Theoretical Results 40
2.5 Case Study and Results 42
2.5.1 The Effects of Using Simplified Transmission Representations 45
2.5.2 Effects if Noncompliance is Allowed 58
2.5.3 Dynamic Analysis: Benefits of Banking and Borrowing 61
2.6 Conclusions 70

3 An Engineering-Economic Approach to Transmission Planning Under Market and Regulatory Uncertainties: WECC Case Study 73

3.1 Introduction 74
3.2 Literature Review 80
3.3 Model Description 82
Nomenclature 84
3.4 Case Study: WECC 240 90
3.4.1 Generation Assumptions 91
3.4.2 Transmission Assumptions 93
3.4.3 Scenarios 94
3.5 Results 98

3.5.1 Planning Based on Deterministic Scenario Models 99
3.5.2 Optimal Stochastic Planning 105
3.6 Conclusions 108

4 New Bounding and Decomposition Approaches for Multi-Area Transmission and Generation Planning With Large Amounts of Intermittent Generation 110

4.1 Introduction 112
4.2 Stylized Planning Model 117
4.2.1 Notation 117
4.2.2 Investment Model 119
4.2.3 Operations Model 120
4.3 Phase One: The Bounding Algorithm 121
4.3.1 New Lower Bounds 122
4.3.2 Upper Bounds 126
4.3.3 Updating the Upper and Lower Bounds 131
4.4 Phase Two: Enhanced Benders Decomposition 133
4.5 Numerical Example 136
4.5.1 Description of the WECC 240-bus System 137
4.5.2 Analysis of Upper Bound Estimates 138
4.5.3 Clustering Algorithm 141
4.5.4 Phase One: Performance of the Bounding Algorithm 143

4.5.5 Can the Lower-Bound Problem Be Used for Planning? 147
4.5.6 Phase Two: Enhanced Benders Decomposition 151
4.6 Conclusions 160

5 Conclusions 163
5.1 Summary 163
5.2 Future Research 168

Appendix A Chapter 2 Additional Material 171

Appendix B Chapter 3 Additional Material 174
B.1 Generation Investment Alternatives 174
B.1.1 California Renewable Energy Zones (CREZ) 175
B.1.2 Western Renewable Energy Zones (WREZ) 177
B.1.3 Conventional Generation 180
B.1.4 Characteristics of Load and Intermittent Generation Data . . 182
B.2 Backbone Transmission Investment Alternatives 184
B.3 First Stage Transmission and Generation Investments 189
B.4 Second Stage Transmission and Generation Investments 195

Appendix C Chapter 4 Additional Material 206
C.1 Sampling Methodology 206
C.2 Upper and Lower Bounds of Bounding Algorithm 208

C.3 Investments Bounding Algorithm 211

C.3.1 Linear Problem 213

C.3.2 Mixed-Integer Linear Problem 215

C.4 Upper and Lower Bounds of Regular and Enhanced Benders Decomposition 218

C.5 Investments of Regular and Enhanced Benders Decomposition 222

C.5.1 Regular Benders Decomposition 224

C.5.2 Enhanced BD LP - 1 Cluster 227

C.5.3 Enhanced BD LP - 10 Clusters 230

C.5.4 Enhanced BD LP - 33 Clusters 233

C.5.5 Enhanced BD MILP - 1 Cluster 236

C.5.6 Enhanced BD MILP - 1 Cluster + 400 Pre-Computed Cuts . . 239

Vita **270**

List of Tables

2.1 System characteristics and generation costs. 43
2.2 Compliance, Transmission Investments, and Incremental Costs for each case. 68

3.1 Candidate Generation 92
3.2 Summary of Scenarios 97
3.3 First-stage Investments in Radial Interconnections to renewable hubs 100
3.4 First-stage Investments in Transmission Backbones 101
3.5 First-Stage Transmission Investments Costs and Economic Performance of Planning Strategies. All costs in Billion USD. 102

4.1 Summary of results for 100 random and stratified samples for different sub-sample sizes. 139
4.2 Number of cuts and total computation time for different optimality gaps and auxiliary lower bounds of the linear relaxation. 153
4.3 Resulting solution gap and solution time to solve mixed-integer master problem using pre-computed cuts from its linear relaxation. 157

A.1 Correlations, means and standard deviations of load and capacity factors. 171
A.2 Garver network lines characteristics and investment costs. 172
A.3 Load and renewable generator capacity factors for the 20 time blocks. 173

B.1 Biomass resource potentials from CREZ study. 175
B.2 Solar resource potentials from CREZ study. 176
B.3 Wind resource potentials from CREZ study. 176
B.4 WREZ distances to nearest bus in WECC 240-bus test-case and interconnection costs per circuit ($2.88M per mile). 178
B.5 WREZ resource potentials and average capacity factors. 179
B.6 Maximum installed generation capacity per technology and state. . . 181
B.7 Means, standard deviations, and correlations for a sample of load, wind, and solar profiles. 183

B.8 List of Backbone Transmission Investment Alternatives ($2.88M per mile). 184
B.9 Second stage investments in transmission backbones. 197
B.10 Second stage investments in interconnections to renewable hubs. . . . 198

List of Figures

2.1 Renewable goal as a percentage of the total electricity demand by year for three states. . . . 19
2.2 Two-node network example. . . . 26
2.3 Optimal total cost as a function of renewable target. . . . 29
2.4 Investments and total cost curves for a) Copper-plate, b) Continuous, and c) Discrete approaches. . . . 30
2.5 Garver's six-bus initial topology. . . . 44
2.6 Transmission investments in circuits linking buses a) 2-6 (line 9), b) 3-5 (line 11), and c) 4-6 (line 14). . . . 47
2.7 Transmission topologies for different renewable supply ranges. a) Optimal network topologies for the Discrete-KVL. b) Optimal network topologies for the Discrete-Transportation model. . . . 48
2.8 Generation investments: a) Total aggregate, b) Conventional (aggregate), c) Wind 1, d) Wind 4, e) Wind 6 and f) Solar (aggregate). . . . 52
2.9 Total spillage per year as a percentage of the supplied demand. . . . 53
2.10 a) Total system costs versus RPS goal, noncompliance prohibited. b) Marginal system costs versus RPS goal under full compliance. . . . 55
2.11 Total costs of meeting the RPS target, noncompliance prohibited. . . . 57
2.12 Renewable energy supply versus RPS goal for a 100 $/MWh noncompliance penalty. . . . 59
2.13 Renewable energy supply versus RPS goal for different penalty levels using the Discrete-KVL approach. . . . 60
2.14 Timeline of the dynamic simulations. . . . 61
2.15 Network topologies by the end of period 4 for a) Case 1, b) Case 2, and c) Case 5. . . . 69

3.1 Timeline 82
3.2 WECC 240-Bus System 91

4.1 Sub-sample standard error versus sub-sample size for 100 replications of random and stratified samples ($N = 100$). 140
4.2 Solution gap for the linear relaxation and percentage of variance captured as a function of the number of clusters. Upper and lower bounds are in Figure C.2 in Appendix C.2. 142
4.3 Solution gap versus the number of clusters for different MIP gaps and the linear relaxation. Upper and lower bounds are in Figure C.3 in Appendix C.2. 145
4.4 Solution time (log) of the lower-bound problem versus the number of clusters for different MIP gaps and the linear relaxation. 147
4.5 Optimal objective function value of the lower-bound problems as a function of the number of clusters for different MILP gaps and the linear relaxation. 148
4.6 New transmission capacity and transmission investment costs as a function of the number of clusters for the linear relaxation. 149
4.7 Penalties from upper-bound problem as a function of the number of clusters. 150
4.8 Solution gap versus the number of iterations for different Benders decomposition schemes of the linear relaxation. Upper and lower bounds are in Figure C.13 in Appendix C.4. 152
4.9 Dual multiplier on auxiliary lower bound versus number of iterations of Benders decomposition for the linear relaxation. 154
4.10 Solution gap for enhanced Benders decomposition applied to the mixed-integer linear problem, using one cluster as auxiliary lower bound, as a function of the number of iterations. Effect of using pre-computed cuts from the linear relaxation. Upper and lower bounds are in Figure C.14 in Appendix C.4. 159

B.1 Map of first stage transmission and generation investments for the deterministic WECC 33% scenario (D-33% WECC) (map made by Jonathan Ho). 190
B.2 Map of first stage transmission and generation investments for the deterministic Carbon scenario (D-Carbon) (map made by Jonathan Ho). 191
B.3 Map of first stage transmission and generation investments for the deterministic State RPS scenario (D-State RPS) (map made by Jonathan Ho). 192
B.4 Map of first stage transmission investments for all deterministic scenarios and the stochastic solution (map made by Jonathan Ho). . . . 193
B.5 First stage generation investments per state for the three deterministic investment strategies and the stochastic plan. 194
B.6 Second stage generation investments for the D-State RPS approach. . 199
B.7 Second stage generation investments for the D-33% WECC approach. 200

B.8 Second stage generation investments for the D-Carbon approach. . . . 201
B.9 Second stage generation investments for Heuristic I. 202
B.10 Second stage generation investments for Heuristic II. 203
B.11 Second stage generation investments for Heuristic III. 204
B.12 Second stage generation investments for the Stochastic approach. . . 205

C.1 Metric W_N as a function of the sample size N. 207
C.2 Upper and lower bounds for the bounding algorithm (phase one) applied to the linear relaxation. 209
C.3 Upper and lower bounds for the bounding algorithm (phase one) applied to the mixed-integer linear problem. 210
C.4 Total new generation capacity per technology as a function of the number of clusters. Results from the application of the bounding algorithm (phase one) to the linear relaxation. 213
C.5 New CCGT generation capacity per state as a function of the number of clusters. Results from the application of the bounding algorithm (phase one) to the linear relaxation. 213
C.6 New CT generation capacity per state as a function of the number of clusters. Results from the application of the bounding algorithm (phase one) to the linear relaxation. 214
C.7 New wind generation capacity per state as a function of the number of clusters. Results from the application of the bounding algorithm (phase one) to the linear relaxation. 214
C.8 Total new generation capacity per technology as a function of the number of clusters. Results from the application of the bounding algorithm (phase one) to the mixed-integer linear problem (MILP gap 1%). . . . 215
C.9 New CCGT generation capacity per state as a function of the number of clusters. Results from the application of the bounding algorithm (phase one) to the mixed-integer linear problem (MILP gap 1%). . . . 215
C.10 New CT generation capacity per state as a function of the number of clusters. Results from the application of the bounding algorithm (phase one) to the mixed-integer linear problem (MILP gap 1%). . . . 216
C.11 New wind generation capacity per state as a function of the number of clusters. Results from the application of the bounding algorithm (phase one) to the mixed-integer linear problem (MILP gap 1%). . . . 216
C.12 New transmission generation capacity as a function of the number of clusters. Results from the application of the bounding algorithm (phase one) to the mixed-integer linear problems for MILP gaps of 5%, 3%, and 1%. 217
C.13 Upper and lower bounds for regular and enhanced Benders decomposition (phase two) applied to the linear relaxation. 219

C.14 Upper and lower bounds for enhanced Benders decomposition (phase two) applied to the mixed-integer linear problem (0.5% MILP gap). . 221
C.15 Total new transmission capacity and transmission investment cost as a function of the number of iterations. Results from the application of regular Benders decomposition to the linear problem. 224
C.16 Total new generation capacity and generation investment cost as a function of the number of iterations. Results from the application of regular Benders decomposition to the linear problem. 224
C.17 Total new generation capacity per technology as a function of the number of iterations. Results from the application of regular Benders decomposition to the linear problem. 225
C.18 New CCGT generation capacity per state as a function of the number of iterations. Results from the application of regular Benders decomposition to the linear problem. 225
C.19 New CT generation capacity per state as a function of the number of iterations. Results from the application of regular Benders decomposition to the linear problem. 226
C.20 New Wind generation capacity per state as a function of the number of iterations. Results from the application of regular Benders decomposition to the linear problem. 226
C.21 Total new transmission capacity and transmission investment cost as a function of the number of iterations. Results from the application of the enhanced Benders decomposition algorithm (phase two) to the single-cluster linear problem. 227
C.22 Total new generation capacity and generation investment cost as a function of the number of iterations. Results from the application of the enhanced Benders decomposition algorithm (phase two) to the single-cluster linear problem. 227
C.23 Total new generation capacity per technology as a function of the number of iterations. Results from the application of the enhanced Benders decomposition algorithm (phase two) to the single-cluster linear problem. 228
C.24 New CCGT generation capacity per state as a function of the number of iterations. Results from the application of the enhanced Benders decomposition algorithm (phase two) to the single-cluster linear problem. 228
C.25 New CT generation capacity per state as a function of the number of iterations. Results from the application of the enhanced Benders decomposition algorithm (phase two) to the single-cluster linear problem. 229
C.26 New Wind generation capacity per state as a function of the number of iterations. Results from the application of the enhanced Benders decomposition algorithm (phase two) to the single-cluster linear problem. 229

C.27 Total new transmission capacity and transmission investment cost as a function of the number of iterations. Results from the application of the enhanced Benders decomposition algorithm (phase two) to the 10-cluster linear problem. 230
C.28 Total new generation capacity and generation investment cost as a function of the number of iterations. Results from the application of the enhanced Benders decomposition algorithm (phase two) to the 10-cluster linear problem. 230
C.29 Total new generation capacity per technology as a function of the number of iterations. Results from the application of the enhanced Benders decomposition algorithm (phase two) to the 10-cluster linear problem. 231
C.30 New CCGT generation capacity per state as a function of the number of iterations. Results from the application of the enhanced Benders decomposition algorithm (phase two) to the 10-cluster linear problem. 231
C.31 New CT generation capacity per state as a function of the number of iterations. Results from the application of the enhanced Benders decomposition algorithm (phase two) to the 10-cluster linear problem. 232
C.32 New Wind generation capacity per state as a function of the number of iterations. Results from the application of the enhanced Benders decomposition algorithm (phase two) to the 10-cluster linear problem. 232
C.33 Total new transmission capacity and transmission investment cost as a function of the number of iterations. Results from the application of the enhanced Benders decomposition algorithm (phase two) to the 33-cluster linear problem. 233
C.34 Total new generation capacity and generation investment cost as a function of the number of iterations. Results from the application of the enhanced Benders decomposition algorithm (phase two) to the 33-cluster linear problem. 233
C.35 Total new generation capacity per technology as a function of the number of iterations. Results from the application of the enhanced Benders decomposition algorithm (phase two) to the 33-cluster linear problem. 234
C.36 New CCGT generation capacity per state as a function of the number of iterations. Results from the application of the enhanced Benders decomposition algorithm (phase two) to the 33-cluster linear problem. 234
C.37 New CT generation capacity per state as a function of the number of iterations. Results from the application of the enhanced Benders decomposition algorithm (phase two) to the 33-cluster linear problem. 235
C.38 New Wind generation capacity per state as a function of the number of iterations. Results from the application of the enhanced Benders decomposition algorithm (phase two) to the 33-cluster linear problem. 235

C.39 Total new transmission capacity and transmission investment cost as a function of the number of iterations. Results from the application of the enhanced Benders decomposition algorithm (phase two) to the single-cluster mixed-integer linear problem. 236
C.40 Total new generation capacity and generation investment cost as a function of the number of iterations. Results from the application of the enhanced Benders decomposition algorithm (phase two) to the single-cluster mixed-integer linear problem. 236
C.41 Total new generation capacity per technology as a function of the number of iterations. Results from the application of the enhanced Benders decomposition algorithm (phase two) to the single-cluster mixed-integer linear problem. 237
C.42 New CCGT generation capacity per state as a function of the number of iterations. Results from the application of the enhanced Benders decomposition algorithm (phase two) to the single-cluster mixed-integer linear problem. 237
C.43 New CT generation capacity per state as a function of the number of iterations. Results from the application of the enhanced Benders decomposition algorithm (phase two) to the single-cluster mixed-integer linear problem. 238
C.44 New Wind generation capacity per state as a function of the number of iterations. Results from the application of the enhanced Benders decomposition algorithm (phase two) to the single-cluster linear problem. 238
C.45 Total new transmission capacity and transmission investment cost as a function of the number of iterations. Results from the application of the enhanced Benders decomposition algorithm (phase two) to the single-cluster mixed-integer linear problem with 400 pre-computed cuts. 239
C.46 Total new generation capacity and generation investment cost as a function of the number of iterations. Results from the application of the enhanced Benders decomposition algorithm (phase two) to the single-cluster mixed-integer linear problem with 400 pre-computed cuts. 240
C.47 Total new generation capacity per technology as a function of the number of iterations. Results from the application of the enhanced Benders decomposition algorithm (phase two) to the single-cluster mixed-integer linear problem with 400 pre-computed cuts. 240
C.48 New CCGT generation capacity per state as a function of the number of iterations. Results from the application of the enhanced Benders decomposition algorithm (phase two) to the single-cluster mixed-integer linear problem with 400 pre-computed cuts. 241

C.49 New CT generation capacity per state as a function of the number of iterations. Results from the application of the enhanced Benders decomposition algorithm (phase two) to the single-cluster mixed-integer linear problem with 400 pre-computed cuts. 241
C.50 New Wind generation capacity per state as a function of the number of iterations. Results from the application of the enhanced Benders decomposition algorithm (phase two) to the single-cluster linear problem with pre-computed cuts. 242

Chapter 1

Introduction

The U.S. electric grid is the world's largest machine (DOE, 2013). The socio-economic implications of this system are so large that the National Academy of Engineering recently selected "electrification" as the greatest engineering achievement of the 20th century (GEA, 2012). In 2012, the U.S. transmission system allowed the exchange of 4,281 TWh of electricity between generators and consumers (EIA, 2013) through 211,000 miles of high-voltage transmission assets worth more than $100 billion—a result of more than a century of infrastructure additions to maintain a reliable and economic operation of the electric power system (DOE, 2003).

Today, this system is under stress. Meeting tomorrow's demand will require significant investments to replace aging infrastructure, reduce congestion, and maintain reliability. A new important consideration for transmission planning organizations is meeting environmental goals at minimum cost for consumers (FERC, 2013). Rising environmental concerns have driven regulatory changes that aim at promoting increasing amounts of generation from renewable resources and at reducing the reliance on carbon-intensive conventional generation (Fischer and Newell, 2008). These renewable resources are highly variable, locationally-constrained, and often far from the existing grid, which complicates both transmission and generation planning practices.

In this dissertation I utilize methods from economics, operations research, and electrical engineering to analyze and address some of the current and future challenges of power transmission planning. Through three essays, included here as chapters 2, 3, and 4, this thesis contributes to a better understanding of the policy, economic, and engineering aspects of this problem. Chapter 2 focuses on the effects of ignoring some of the nonlinearities of power transmission networks on the conclusions about the performance of renewable goals enforced through Renewable Portfolio Standards. This chapter also contains an assessment of the benefits of coordinating the design of these policies with transmission investments from a multi-stage perspective. In the second essay, included as Chapter 3, I propose a new decision-support tool for adaptive transmission planning under market and regulatory uncertainties. I utilize methods from economics, stochastic programming, and decision analysis to study the effect of uncertainty on investment decisions and to compare the performance of different investment decision rules currently used by practitioners. In the fourth chapter I develop new computational algorithms to solve large-scale planning problems. The main goal of Chapter 4 is to provide new practical tools for transmission and generation planning considering fine-grained representations of the variability of load and intermittent generation resources.

The next sections of this chapter introduce the three essays of this dissertation. Section 1.1 discusses some of the limitations of high-level electricity-market models for policy analysis. The research presented in the second chapter is introduced in Section 1.2, which outlines some of the basics of transmission planning under uncertainty. In Section 1.3 I describe the challenges of large-scale transmission and generation planning with high amounts of intermittent generation.

1.1 Approximations in Power Transmission Planning

Environmental regulations, such as Renewable Portfolio Standards (RPSs) or carbon cap-and-trade policies, seek to incentivize increasing amounts of generation from renewable resources and to deter production from carbon-intensive technologies (Fischer and Newell, 2008). Studying the effects of these policies on transmission and generation investments, as well as on operations, requires consideration of the physical laws that govern the electric power system, but this results in extremely complex models that lack practicality for long-term economic analysis. To overcome this difficulty, policy and planning studies rely on high-level optimization-based electricity market models, such as Haiku (Paul and Burtraw, 2002), ReEDS (Short et al., 2011), NEMS (Gabriel et al., 2001), and IPM (ICF, 2013) that simplify some of these physical characteristics that would otherwise result in nonlinear or nonconvex optimization problems.

Two common assumptions regarding the transmission system are ignoring the indivisibilities of transmission investments and relaxing Kirchhoff's Voltage Laws. These are important oversights, since it is widely recognized that large transmission investments are needed to access the most attractive renewable resources. Kahn (2010) estimates that the transmission costs associated with renewables are 10 times larger than the costs of providing ancillary services needed as backup resources. Despite this, the latter issue has received a huge amount of attention in the literature; the former issue has received much less. California, for example, estimates that $15.7 billion of investments in transmission infrastructure will be needed to meet the 33% renewable target by 2020—this is 30% of the cost of the renewable investments themselves (CPUC, 2009). However, there is no previous study that has quantified the distortion caused by simplifications of transmission nonlinearities in the results of these high-level policy analysis models.

In Chapter 2, I study how consideration of transmission constraints affect the ability of a power market to comply with policy targets for renewable energy investment. I use a six-bus network to illustrate how simplified resource planning models result in incorrect cost, compliance, and capacity estimates when used to predict the effect of a

Renewable Portfolio Standard. Furthermore, I discuss the importance of using multi-stage transmission planning models to find the most cost-effective infrastructure to meet renewable targets that increase over time, or flexible RPS designs.

First, using a single stage model, I study how disregarding transmission constraints or assuming that grid expansions can take place smoothly can result in overestimation of RPS compliance and underestimation of costs. Lumpy investments can result in decreasing (long-run) marginal system costs and consequently, they could cause the market to fall into noncompliance for intermediate RPS targets, but to fulfill the targets for higher renewable obligations. Interestingly, I find that under static planning, investments in infrastructure that are optimal for low RPS goals might not be included in the optimal solution for higher RPS targets.

Second, I use a dynamic model to study different flexible RPS designs where banking & borrowing of Renewable Energy Certificates is allowed. I find that the more flexible the RPS design, the lower total system costs. However, schemes with full flexibility (i.e., without boundary conditions) could result in underachievement of long-term renewable goals.

1.2 Transmission Planning Under Uncertainty[1]

In the last two decades, the electricity sector underwent two main changes. First, many markets migrated from integrated resource planning towards more decentralized structures in which market participants decide where and how much to invest (Sioshansi and Pfaffenberger, 2006). Second, increasing environmental concerns continue to lead authorities to implement regulations that aim to reduce emissions and increase the amount of power that is generated from renewables (Jaccard, 1995). The liberalization and subsequent implementation of stricter environmental regulation, including renewable mandates, have resulted in debate about which are the best regulations and technologies to direct the market toward sustainable and low carbon supplies of power at minimum cost for consumers.

One planning responsibility that has been particularly challenged by these changes is transmission planning. In the past, a centralized regulated or publicly owned monopoly would plan for both transmission and generation, dealing with a restricted set of uncertainties such as demand growth and fuel costs, using sensitivity analysis. Today, transmission planning and generation investment are the responsibilities of separate organizations (Sauma and Oren, 2006). Both the transmission planner and generators have to make decisions without knowing for certain what the other

[1] An earlier version of this introduction was published in Munoz et al. (2012).

market participants will do, and with the additional risks of unknown future technological changes and environmental regulation. Demand growth, fuel prices, efficiency measures, pollution control, technology costs, Renewable Portfolio Standards, demand response, plant retirements and Plug-in Electric vehicles—among many other factors—give investors uncertain and conflicting signals and incentives when deciding the size, location and timing of future generation investments.

Up until recently, most transmission planning has been done in a reactive manner. As a consequence of more ambitious environmental policies and renewable targets, the Federal Energy Regulatory Commission (FERC) has defined a new type of upgrade: policy upgrades. These new type of transmission upgrades are investments needed to harness the energy coming from the new generation mandated from the current renewable goals (FERC, 2013). An absence of or delay in the appropriate policy upgrades could prevent achievement of the goals of current and future environmental regulation. Alternatively, renewable goals may be met with less efficient resources due to the lack of transmission infrastructure, increasing costs for the consumers.

Transmission planners in the U.S. are aware of the need for new transmission capacity to accommodate new generation from renewable sources; however, there is still no unified view of how environmental and renewable policies and transmission planning should be harmonized (Puga and Lesser, 2009). The FERC policy upgrade order, along with the FERC powers to designate national interest electric transmission corridors under the Energy Policy Act of 2005, is only an incomplete federal response.

Consequently, some states and interregional organizations, concerned with the growing renewable requirements, have taken the lead, performing a variety of studies that consider the transmission upgrades required to have a grid that will meet the future needs (Schumacher et al., 2009). Elements common to all the studies are the need to plan for transmission to accommodate renewable generation in the most economic manner and the idea that transmission planning should be done proactively, in advance of generation (AESO, 2012; CAISO, 2012; MISO, 2010). Studies that attempt to make single recommendations for today consider uncertainty by defining several scenarios; optimal transmission configurations are then proposed for each scenario. The resulting configurations are then aggregated, assuming that upgrades that are required for all or most of the scenarios should be prioritized.

However, theoretical results from stochastic programming show that the best plan to hedge against uncertainty (in an expected value sense) might not look like any of the optimal decisions for individual scenarios (i.e., developed assuming perfect information) (Wallace, 2000). Consequently, there is no theory supporting the idea that the common features among the deterministic solutions provide a robust or least-regret recommendation for today.

In Chapter 3 I propose a new decision-support tool for adaptive transmission planning under market and regulatory uncertainties, considering both generators' response and Kirchhoff's Voltage Law. The model also accounts for recourse (or corrective) decisions, since some investments could be delayed until there is more information about the future. I present a numerical example using a 240-bus representation of the Western Electricity Coordinating Council and three different scenarios of exogenous market conditions. I find that the cost of ignoring uncertainty, which is the cost of using naive deterministic planning methods relative to explicitly modeling uncertainty, is on the same order of magnitude as the cost of first-stage transmission investments. Finally, I conclude that heuristic rules for constructing transmission plans using the overlapping solutions from the deterministic scenarios could actually yield higher expected costs than the naive approach of ignoring uncertainty altogether.

1.3 New Computational Methods to Solve Large-Scale Planning Problems

The electric power industry has been one of the main areas for applications of optimization algorithms and a test-bed for engineering-economic concepts to operate complex financial markets subject to physical constraints (Hobbs, 1995). One of the initial applications of optimization algorithms in electric utilities was linear programming (Turvey and Anderson, 1977). Known as economic dispatch models, these tools were used to find the output levels of generation fleets to meet demand at minimum cost for consumers. Computational limitations forced operators to ignore the non-convex characteristics of the generators, such as start-up costs, which are better represented using discrete instead of continuous variables. Economic dispatch models eventually evolved into unit commitment models, taking into account these non-convexities. However, unit commitment problems were only solved approximately using Lagrangian relaxation techniques, which often resulted in infeasible schedules (Hobbs et al., 2001). Today, many markets around the world use advanced mixed-integer programming techniques to solve unit commitment problems close to optimality and, most importantly, within time frames compatible with current market designs. The estimated savings from these advances in the U.S. alone are of USD 300 million per year (FERC, 2011).

Optimization models have been also used for long-term investment planning (Masse and Gibrat, 1957; Anderson, 1972; Bloom et al., 1984), but unlike short-term unit commitment models, there is no publicly available information regarding the cost savings that resulted from their utilization. From an electric utility's perspective, an optimal investment plan corresponds to a set of investment decisions that would minimize the sum of capital costs and the present worth of operating costs for the planning horizon to meet forecasted demand and environmental goals. The need for optimization algorithms stems from the complexity of evaluating different transmission and generation investment alternatives on a system-wide basis. To achieve computational tractability, long-term planning tools often approximate short-term operations by relaxing unit commitment variables and constraints, and by utilizing a few number of representative states of the future system load (e.g., peak, shoulder, and off-peak conditions) in economic dispatch models (Palmintier and Webster, 2011;

Shortt et al., 2013). Although these approximations have been often considered as "reasonable" for long-term investment planning purposes, they will require significant improvements to capture the true economic value of transmission and generation assets in future electric power systems with large amounts of variable and unpredictable generation from renewable energy technologies (Joskow, 2011).

In the third essay of this dissertation, included as Chapter 4, I propose a new computationally-tractable solution method to find optimal, or near-optimal, solutions for large-scale generation and transmission investment planning problems considering fine-grained representations of variability from demand and intermittent generation resources. The proposed algorithm is divided into two phases: a bounding phase and a decomposition phase. In the new bounding phase I exploit Jensen's inequality (Jensen, 1906) to define a new lower bound for planning problems with policy constraints designed to incentivize investments in intermittent generation from renewable resources. The decomposition phase corresponds to an enhancement of the traditional Benders' decomposition algorithm (Benders, 1962; Geoffrion, 1972), which includes an auxiliary lower bound in the master problem from the bounding phase. Calculation of upper bounds requires solving a large operations problem, which I instead estimate using a sub-sampling methodology that allows me to distribute the computational load among multiple independent computer nodes. I find that just the bounding phase of my algorithm is needed for planning applications that only require near-optimal solutions (e.g., 5% optimality gaps), which is often the case in real-world planning studies. However, attaining tight solution gaps requires utilization of the enhanced Benders decomposition phase, which converges faster than either algorithm, the bounding approach or regular Benders decomposition, separately.

1.4 Scope

This dissertation is structured as follows. The first essay is included as Chapter 2, which I titled *Approximations in Power Transmission Planning: Implications for the Cost and Performance of Renewable Portfolio Standards*. Within Chapter 2, Section 2.1 introduces the essay and provides an overview of the literature on high-level planning models for policy analysis. In Section 2.2, I utilize a stylized two-level model to illustrate the effects of indivisibilities in transmission investments on the cost and location of generation investments to meet renewable goals. Section 2.3 describes single- and multi-stage investment planning models that I later use for numerical analyses. In Section 2.4, I derive some theoretical results for a general case. Section 2.5 describes the case study and results.

The second essay is included in Chapter 3, titled *An Engineering-Economic Approach to Transmission Planning Under Market and Regulatory Uncertainties*. Sections 3.1 and 3.2 describe the challenges of transmission planning under uncertainty, and review relevant academic literature, as well as industry practices, on the topic. In Section 3.3, I formulate the new two-stage stochastic transmission investment model.

Section 3.4 describes the case study and assumptions, such as candidate renewable resources and scenarios. In Section 3.5 I present the results and compare the performance of my proposed stochastic model versus current approaches based on scenario analysis.

Chapter 4 includes the third essay, entitled *New Bounding and Decomposition Methods for Multi-Area Generation and Transmission Planning with Large Amounts of Intermittent Generation*. Section 4.1 introduces the problem and provides a general overview of the limitations of current planning algorithms. Section 4.2 describes a stylized planning model formulated as a mixed-integer linear problem with per scenario and expected-value constraints. In Section 4.3, I derive a new lower bound upon the optimal objective function value of stochastic problems with expected-value constraints and propose a statistical method to estimate upper bounds that take advantage of parallel computer systems. In Section 4.4, I describe the implementation of Benders decomposition and the introduction of auxiliary bounds in the master problem to accelerate its convergence. Section 4.5 illustrates the performance of the proposed algorithm through a numerical example.

I also include multiple appendices with supporting information for the three chapters of this dissertation. In Appendix A, I include all the network, load, wind, and solar data utilized for the numerical simulations in Chapter 2. Appendix B describes some of the renewable generation investment alternatives utilized in the numerical simulations of Chapters 3 and 4 and extends the discussion on first stage transmission and generation investments of Chapter 3. Finally, Appendix C includes supporting material of Chapter 4.

Chapter 2

Approximations in Power Transmission Planning: Implications for the Cost and Performance of Renewable Portfolio Standards[1]

Renewable Portfolio Standards (RPSs) are popular market-based mechanisms for promoting development of renewable power generation. However, they are usually implemented without considering the capabilities and cost of transmission infras-

[1]An earlier version of this research was published in Munoz et al. (2013b).

tructure. I use single- and multi-stage planning approaches to find cost-effective transmission and generation investments to meet single and multi-year RPS goals, respectively. Using a six-node network and assuming a linearized DC power flow, I examine how the lumpy nature of network reinforcements and Kirchhoff's Voltage Law can affect the performance of RPSs. First, I show how simplified planning approaches that ignore transmission constraints, transmission lumpiness, or Kirchhoff's Voltage Law yield distorted estimates of the type and location of infrastructure, as well as inaccurate compliance costs to meet the renewable goals. Second, I illustrate how lumpy transmission investments and Kirchhoff's Voltage Law result in compliance costs that are nonconvex with respect to the RPS targets, in the sense that the marginal costs of meeting the RPS may decrease rather than increase as the target is raised. Thus, the value of Renewable Energy Certificates (RECs) also depends on the network topology, as does the amount of noncompliance with the RPS, if noncompliance is penalized but not prohibited. Finally, I use a multi-stage planning model to determine the optimal generation and transmission infrastructure for RPS designs that set multiyear goals. I find that the optimal infrastructure to meet RPS policies that are enforced year-by-year differ from the optimal infrastructure if banking and borrowing is allowed in the REC market.

2.1 Introduction

Since the 1990s, electricity markets have experienced major changes worldwide, including restructuring to promote competition and increasingly stringent environmental rules. Public demand for environmental improvement together with a desire to diversify fuel sources have led to ambitious targets for development of renewable electricity generation, along with policies designed to encourage investment to achieve those targets. Specific policies used to promote renewable electricity vary from country to country. They include feed-in tariffs, taxes, subsidies and standards, as well as combinations of these policies (Wiser et al., 2007; Fouquet and Johansson, 2008).

One type of regulation that has become popular in the U.S. is the Renewable Portfolio Standard (RPS), which is a policy that seeks to create more demand for electricity supplied from renewable energy technologies. The RPS promotes demand for green electricity by obligating utilities, retailers, or other load-serving entities (LSEs) to provide a specified fraction of their sales from qualifying renewable technologies. Usually, a tradable credit system is implemented so that entities that have too little renewable production can buy surplus credits from entities that have more than the required minimum. These credits are generally called Renewable Energy Certificates (RECs), which are financial instruments created from the production of one unit of energy from a qualifying renewable energy source. Accordingly, RPSs with tradable RECs are described as market-driven regulations, because the policies specify neither which firm should invest nor which type of renewable technology should be used to fulfill the requirement (e.g., wind or solar). The aim is to promote competition among potential clean energy producers and adoption of the most cost-efficient technologies (Wiser et al., 2007). These mechanisms require specification of certain market features such as target definitions over time, resource eligibility, resource-specific requirements (tiers), who is responsible for compliance, geographic restrictions, and treatment of power imports, among others (Berry and Jaccard, 2001).

The flexibility provided by tradable RECs is important for minimizing the social cost of meeting the portfolio standard. Allowing banking and/or borrowing of the RECs also enhances flexibility. Banking allows firms to use excess RECs from past years for future compliance. If borrowing is allowed, then LSEs can compensate for a shortfall of RECs in a current period by using RECs from future years. If an LSE cannot acquire sufficient credits by trade, withdrawal of banked allowances, or borrowing, then they will usually pay a non-compliance penalty. In most cases, this penalty is proportional to the amount of the shortfall of renewable energy.

To date in the U.S., 30 states and the District of Columbia have implemented various versions of RPSs (AEO, 2011). California, for example, set a 20% obligation by 2013, 25% by 2016, and a 33% requirement by 2020 (SB2, 2011), with intermediate values for other years; however, compliance is enforced only for multi-year periods [2]. Hawaii, on the other hand, set specific, and increasing, goals for every year from 2010 until 2030. While in Hawaii there is no banking or borrowing, LSEs in California

[2]For example, California utilities are required at the end of 2016 to report an equivalent renewable generation of 21.7% of 2014 energy retail sales, with these percentages increasing to 23.3% in 2015, and 25% in 2016.

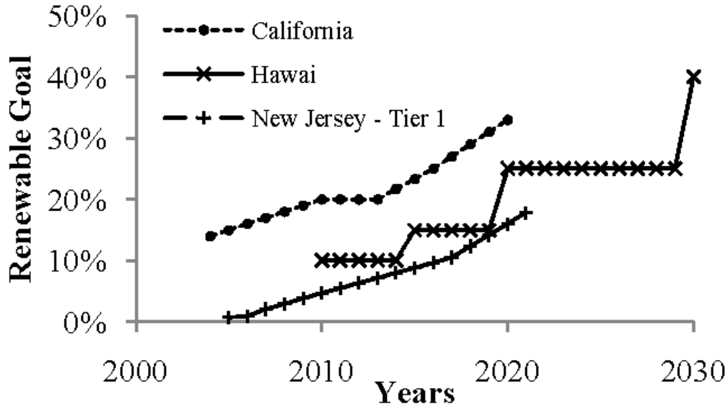

Figure 2.1: Renewable goal as a percentage of the total electricity demand by year for three states.

utilities have flexibility to shift production among years within a multiyear-compliance period. Moreover, in California, banking of RECs is allowed both within a compliance period and for future compliance periods, although borrowing is only allowed within a compliance period. Figure 2.1 shows the evolution of renewable goals in California, Hawaii, and New Jersey[3].

RPS policies have been established in the U.S. in order to induce renewable investments, to promote technology change and jobs, and to reduce emissions. However, in most cases, the renewable energy targets have been chosen without detailed analyses of either the benefits that would result, or their costs. Several authors have performed theoretical economic analyses of the effects of imposing different levels of RPSs (Amundsen and Mortensen, 2001; Palmer and Burtraw, 2005; Fischer, 2010); however, all these studies disregard transmission constraints and the need for transmission

[3]Tier 1 includes solar, PV, wind, geothermal, tidal, and biomass energy. The non-compliance penalty is 50 \$/MWh.

reinforcements to access renewable resources. One main difference between renewable and conventional generation is that the former is geographically constrained. Conventional generation can be built strategically near existing high-voltage transmission corridors, water supplies, and fuel networks, whereas the highest quality renewables are only available at certain specific sites that may be located hundreds of miles from the closest interconnection point. Large transmission investments are needed to access the most attractive renewable resources. California, for example, estimates that \$16 billion of investment in transmission infrastructure will be needed to meet the 33% renewable target by 2020 (CPUC, 2009), twice the \$8.2 billion annual cost of wholesale power in the California ISO market in 2011. More generally, Kahn (2010) estimates that the transmission costs associated with renewables are at least four times the costs of providing frequency regulation and other ancillary services needed to back up variable renewables, even though the expense of such services has received much more attention in the literature than have transmission costs. Hence, disregarding transmission constraints when assessing the cost and feasibility of renewable targets can be a problematic oversight.

Historically, transmission planning has been considered a challenging problem for several reasons. First, transmission investments present important economies of scale; therefore, investments in network infrastructure normally come in large lumps (Joskow and Tirole, 2005). Although some thermal generation technologies still have significant economies of scale, many renewable generation technologies are modular and tend to have more constant returns to scale[4]. Second, power flows on electricity networks obey Kirchhoff's Voltage Law (KVL), which causes what is known as loop-flow externalities (Chao and Peck, 1996). A transmission-planning model that ignores KVL can result in investment recommendations that could actually be detrimental for the system (e.g., by increasing rather than decreasing operating costs) (Wu et al., 1996). Third, changes in the topology or capacity of the existing grid have direct implications for the economics of future generation investments of any kind. This can cause inefficiencies in unbundled electricity markets, in which transmission and generation assets are no longer planned by the same authority (Sauma and Oren, 2006).

In the U.S., stringent state Renewable Portfolio Standards and, more recently FERC Order 1000, have motivated Regional Transmission Operators (RTOs), Independent System Operators (ISOs), and research organizations to perform transmission planning studies to identify cost-effective strategies to meet renewable goals (Schumacher et al., 2009). Studies by Ela et al. (2009), Hecker et al. (2009), and Gentile et al. (2010), for example, fit in the category of regional studies that develop indicative transmission plans for various scenarios of generation configurations. Others adopt the concept of Competitive Renewable Energy Zones (CREZ), first used in Texas (Lasher, 2008) and now applied in California (RETI, 2010) and the Western Elec-

[4]In an empirical study, Wiser and Bolinger (2011) found that wind projects do not present important economies of scale. The California Solar Statistics webpage also reports moderate economics of scale for solar projects smaller than 1 MW (CSS, 2012). Combined- and single-cycle power plants investment costs are generally larger than those from renewable power plants, but they are still small compared to the investment costs of some new high voltage transmission lines.

tricity Coordinating Council (WECC) (Pletka and Finn, 2009). CREZ-based transmission planning in California and the WECC operates under the assumption that renewable resources can be characterized, or ranked, using levelized or bus-bar costs, the latter including a pro-rata share of the transmission costs needed to deliver the power to the grid (Mills et al., 2011). Although some of these transmission-planning studies use detailed production cost simulations, they do not use formal optimization algorithms to identify the optimal (least-cost) set of generation and transmission investments. Moreover, in contrast to the models proposed in Sauma and Oren (2006), and Sauma and Oren (2007), they ignore the response of generation investors to the location of transmission expansions.

There are other examples of resource planning tools and transmission planning studies for renewable integration in the academic literature. In NREL's Regional Energy Deployment System (ReEDS), for example, Kirchhoff's Voltage Laws are enforced on existing lines (constant PTDF matrix), but transmission investments are assumed continuous (Short et al., 2011). Olson et al. (2009), focused on the integration of long HVDC transmission lines across the WECC for different scenarios, without using formal optimization approaches. Pozo et al. (2013) computed the optimal (least-cost) set of generation and transmission investments, but using a static model and assuming that transmission investments are continuous. Morales et al. (2012) also present a static model, but of a more complex Stackelberg game between a risk-averse transmission planner and remote wind developers. Munoz et al. (2012)

proposed a lumpy and dynamic transmission planning model for different levels of penetration of renewable generation, but taking generation investments as exogenous variables. While most of the previous works use static (i.e., single-decision stage) and/or deterministic models, van der Weijde and Hobbs (2012) and Munoz et al. (2012) propose multi-stage stochastic methodologies to find here and now investments to hedge against market uncertainties, while also taking into account generators' response. However, in all these studies, renewable goals are exogenously specified inputs, and no further analysis of renewable policy design was undertaken, nor were the economic and environmental benefits and costs of different renewable goals quantified.

To my knowledge, the only existing study focusing on the interaction between RPS design and transmission planning is Vajjhala et al. (2008). The authors compared the impacts of state and federal RPSs in the U.S. in terms of costs and infrastructure, concluding that the location of new transmission infrastructure will affect both the location and type of renewable generation investments. However, Kirchhoff's Voltage Law was ignored and new transmission capacity was exogenously imposed on the generation market using an iterative heuristic until most interregional congestion was eliminated. There are no studies that analyze the interaction between transmission planning and RPS performance using models that optimize transmission expansion taking into account the lumpiness of transmission investments, their effect on generation investments, Kirchhoff's Voltage Law, and the dynamic nature of investment decisions.

CHAPTER 2. APPROXIMATIONS IN POWER TRANSMISSION PLANNING: IMPLICATIONS FOR THE COST AND PERFORMANCE OF RENEWABLE PORTFOLIO STANDARDS

In this article I have three objectives. First, I ask: how do simplified transmission models that ignore transmission constraints, transmission lumpiness, or Kirchhoff's Voltage Law distort conclusions regarding the costs, investments, and degree of compliance with RPS targets? Second, I consider the question: how does the level of noncompliance penalties affect the amount by which renewable generation falls short of RPS targets, accounting for transmission costs? Third, I consider how answers to these questions are affected if I consider the dynamic interaction of transmission investments on renewable policies that change over time. Interactions between flexibility (in terms of both non-compliance penalties and the existence of banking & borrowing policies) and the discrete characteristics of transmission upgrades can have a significant impact on the performance of RPSs. Although many features of RPSs must be considered when designing them, I focus on RPS target levels, noncompliance penalties and banking/borrowing flexibility, and their interactions with lumpy transmission investments.

The rest of this article is organized as follows. In Section 2.2, I draw some basic results for simple radial networks to provide the basic economic intuition of transmission planning for renewables and the effects of ignoring transmission indivisibilities. In Section 2.3, I describe the single- and multi-stage models I use for my analyses, generalizing them to meshed networks, including the situation of growing renewable goals over time and the possibility of banking and borrowing RECs. In Section 2.4, I derive some theoretical results for the more general model. In Section 2.5 I describe my case study and results. In Section 2.5.1 I compare the effects of ignoring transmission constraints, lumpiness and KVL; in Section 2.5.2 I study the effects of noncompliance penalties; and in Section 2.5.3 I study how REC banking and borrowing mechanisms interact with transmission planning. Section 2.6 concludes.

2.2 Comparative Statics for a Two-Node Example

In this section, I derive some general results regarding the effects of using models that disregard the discreteness of transmission investments upon the performance of RPS policies and total costs. I use a radial-network to compare the effects of three different assumptions. The first approach is the Copper-Plate model, which minimizes total generation costs while entirely ignoring power transmission constraints. Examples of an RPS analysis using copper-plate models are in Amundsen and Mortensen (2001), Palmer and Burtraw (2005), and Fischer (2010). Another approach, which I call the Continuous model, minimizes total costs subject to transmission capacity constraints, and assumes that transmission capacity can be gradually added. Examples of this transmission planning approach are Mills et al. (2011), Short et al. (2011), and Pozo et al. (2013). Finally, the third approach presented in this section minimizes total costs subject to transmission capacity constraints and considers the lumpiness of power transmission investments. I call this the Discrete model. Next, I

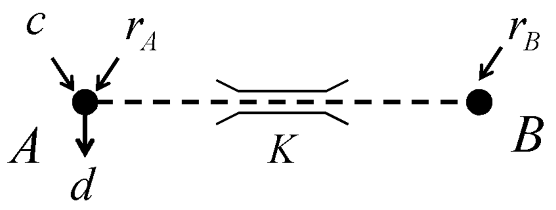

Figure 2.2: Two-node network example.

use a two-node network to illustrate the effects of these assumptions on the optimal combination of transmission and generation investments, as well as compliance costs. Thus, I disregard the complication of Kirchhoff's Voltage Law in this initial analysis, an assumption that I relax in subsequent sections.

Consider the situation of two isolated nodes, as displayed in Figure 2.2. Node A has perfectly inelastic demand d MW and there is no demand at node B. In node A, there is an existing conventional generator with cost c \$/MWh and a renewable generator with cost r_A \$/MWh. Node B is located far away from load A, but inexpensive renewable generation could be developed there at a cost of r_B \$/MWh. There is no line linking nodes A and B initially, but a line of maximum capacity K MW can be built at a cost of I \$. I assume that there are no capacity limits on any of the generators. The generation costs are such that the conventional generation at node A is cheaper than the renewable generation available at node B ($c \leq r_B$), and the renewable generation available at node A is more expensive than renewable generation at node B plus the pro-rata share of the line ($r_B + \frac{I}{K} \leq r_A$), if transmission capacity could be added in small increments.

Let me first assume that the penalty for noncompliance with the RPS is sufficiently high such that noncompliance is never economical. In the absence of an RPS, the total cost of meeting demand is cd, under the assumption that demand is met at the lowest possible cost which, in this case, is with the conventional generation. If instead an RPS is established that imposes a minimum proportion of the demand to be supplied from renewable sources, then the minimum amount of renewable generation is αd MWh. Ignoring transmission constraints (as in the Copper-Plate model), both demand and RPS goals are met at production cost $cd(1-\alpha) + r_B \alpha d$. However, since there is actually no transmission capacity available between node A and B, the only means of actually meeting the RPS target if no transmission capacity is built is to use local (and more costly) renewable sources, yielding a production cost of $cd(1-\alpha) + r_A \alpha d$. The Continuous model assumes that a line could be expanded in small increments. If the assumed transmission costs were proportional to the capacity of the line, then the least-cost way to meet demand and the RPS obligation would be to develop remote renewable generation before the local renewable generation. The resulting total cost would then be $cd(1-\alpha) + (r_B + \frac{I}{K})\alpha d$ for $\alpha d \leq K$ (i.e., when it is optimal to build a line with less than K capacity) and $cd(1-\alpha) + (r_B + \frac{I}{K})K + r_A(\alpha d - K)$ for $\alpha d \geq K$ (i.e., when it is optimal to build a line with capacity K).

However, in reality, the transmission investment is all-or-nothing, which is the Discrete model. In that case, the total costs of meeting both RPS and demand would be given by: $cd(1-\alpha) + r_A \alpha d$ for $0 \leq \alpha \leq \frac{I}{d(r_A - r_B)}$ (when it is optimal not to build the line), $cd(1-\alpha)+I+r_B\alpha d$ for $\frac{I}{d(r_A-r_B)} \leq \alpha \leq \frac{K}{d}$ (when it is optimal to build the line and the renewable target is met without using the entire capacity of the line), and $cd(1-\alpha)+I+r_BK+r_A(\alpha d-K)$ for $\alpha \geq \frac{K}{d}$ (when it is optimal to build the line and use all its capacity).

I now show the relationships among the costs of the three models. Defining TC_{C-P} as the total cost obtained in the optimal solution of the Copper-Plate model, TC_{Cont} as the total cost of the Continuous model solution, and TC_{Disc} as the total cost for the optimal solution of the Discrete model, I have:

$$TC_{C-P} = cd(1-\alpha)+r_B\alpha d = cd+\alpha d(r_B-c) \tag{2.1}$$

$$TC_{Cont} = \begin{cases} cd(1-\alpha)+(r_B+\frac{I}{K})\alpha d = cd+\alpha d(r_B+\frac{I}{K}-c) & : \text{if } 0 \leq \alpha \leq \frac{K}{d} \\ cd(1-\alpha)+(r_B+\frac{I}{K})K+r_A(\alpha d-K) = & \\ cd+I-(r_A-r_B)K+\alpha d(r_A-c) & : \text{if } \alpha \geq \frac{K}{d} \end{cases} \tag{2.2}$$

$$TC_{Disc} = \begin{cases} cd(1-\alpha)+r_A\alpha d = cd+\alpha d(r_A-c) & : \text{if } 0 \leq \alpha \leq \frac{I}{d(r_A-r_B)} \\ cd(1-\alpha)+I+r_B\alpha d = cd+I+\alpha d(r_B-c) & : \text{if } \frac{I}{d(r_A-r_B)} \leq \alpha \leq \frac{K}{d} \\ cd(1-\alpha)+I+r_BK+r_A(\alpha d-K) = & \\ cd+I+(r_B-r_A)K+\alpha d(r_A-c) & : \text{if } \alpha \geq \frac{K}{d} \end{cases} \tag{2.3}$$

Note that as I illustrate in Figure 2.3, the three cost functions are continuous and

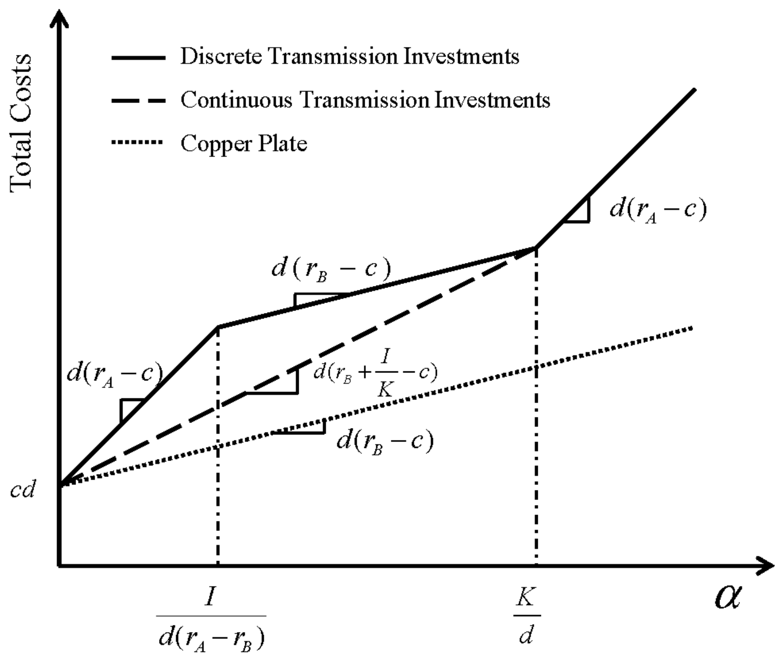

Figure 2.3: Optimal total cost as a function of renewable target.

strictly increasing in α. This result is generalized in Lemma 1, in Section 4, assuming RPS noncompliance is permitted. Also note that the optimal (least-cost) solution for the three transmission models always satisfies $TC_{C-P} \leq TC_{Cont} \leq TC_{Disc}$ for a given α. The rationale for this result is simply the fact that the optimal solution of the Discrete model is a feasible solution in the Continuous approach; thus, the total cost obtained in the optimal solution of the Discrete model cannot be less than the total cost obtained in the optimal solution of the Continuous one. Similarly, the optimal solution of the Continuous approach is a feasible solution in the Copper-Plate model and, thus, the total cost obtained in the optimal solution of the Continuous approach cannot be less than the total cost obtained in the optimal solution of the Copper-Plate model. These results are generalized for more complex networks in proposition

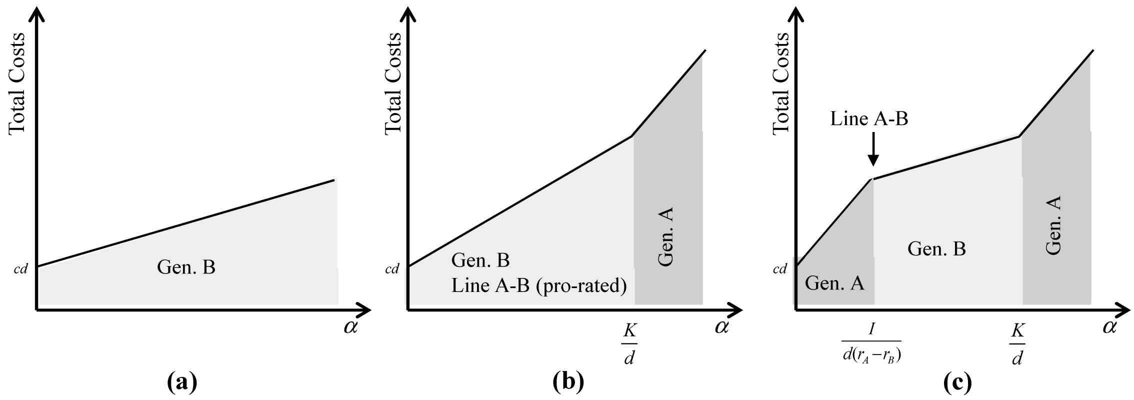

Figure 2.4: Investments and total cost curves for a) Copper-plate, b) Continuous, and c) Discrete approaches.

1, in Section 2.4.

In Figure 2.4 (a), (b), and (c) I illustrate the three cost functions as a function of the RPS goal, also indicating the investment decision that is in the margin for each range of renewable targets. Since transmission constraints are ignored in the Copper-Plate model, there is no need for transmission investments for any level of renewable obligation and, as indicated in Figure 2.4 (a), all the renewable supply is provided with resources from node B. Consequently, the marginal cost of enforcing an extra percentage of RPS goal is constant and equal to $d(r_B - c)$. If, instead, I assume that transmission capacity can be added in small increments, as in the Continuous approach, the costs of network-constrained renewable resources can be adjusted by adding a pro-rata share of the transmission costs, as in Mills et al. (2011), and compared directly to the costs of local resources. Given my cost assumptions, the Continuous model also finds it economic to first use all the renewable resources from node B, at marginal cost $d(r_B + \frac{I}{K} - c)$. For renewable targets higher than $\frac{K}{d}$, the remaining RPS target is met using resources from node A at a higher marginal cost $d(r_A - c)$. However, if I take into account the lumpiness of transmission investments, for small RPS requirements it is most economic to use the local renewable generation at marginal cost $d(r_A - c)$, but then to switch to using renewable resources from node B at marginal cost $d(r_B - c)$, after building the link $A - B$ for $\frac{I}{d(r_A - r_B)} \leq \alpha$. Note that in this case the later marginal cost is lower than the initial marginal cost, so that total cost is a non-convex function of the renewable target (Figure 2.4 (c)). One counterintuitive result from this nonconvexity is that there will exist values of the noncompliance penalty for the RPS system such that the market will choose partial noncompliance for some values of RPS goal, but to meet the renewable target for either low or high RPS requirements. In particular, if the penalty is larger per MWh than the slope of the middle section of Figure 2.4 (c), but smaller than the slope of the other two sections, this will occur. This result is illustrated in the case study presented in Section 5.

Note that my approach allows me to answer the question of what would be the optimal transmission infrastructure to develop, and its corresponding cost, in order to meet a given renewable target. Only the Discrete model's curve is accurate. The inaccuracy of the cost curves from the Copper-Plate and Continuous approaches can yield overly optimistic conclusions about the cost of meeting an RPS, and distorted renewable resource supply curves, defined as the marginal cost of adding renewable energy to the generation mix. The Copper-Plate model includes no costs of transmission, while the Continuous model includes a marginal transmission capacity cost for the left part of its range. In contrast, the actual cost function (Discrete) includes the fixed cost of transmission in its second and third segments, but no marginal transmission cost.

Another distortion in the Continuous model is that it tends to yield more monotonicity of investment. This means that transmission and renewable investments that are optimal for a given RPS goal α_1 are also part of the set of investments for $\alpha_2 \geq \alpha_1$. This is not true in the Discrete model, where it is optimal to first invest in renewable generation at node A for low values of α, but then it is suboptimal to use any of $A's$ renewable resources for RPS goals in the range $\frac{I}{d(r_A - r_B)} \leq \alpha \leq \frac{K}{d}$. Yet, transmission investment is monotonic in this Discrete model, as the line is added in the second and third segments, but not the first. However, in the more complex networks considered later in this article, nonmonotonicity in transmission investment occurs.

2.3 Meshed Models

Our more general models minimize total system costs for meshed networks. These costs include transmission- and generation-investment costs and energy market operational costs. Cost minimization is equivalent to a market equilibrium under the assumptions that: (i) the electricity generation market is perfectly competitive, (ii) the grid operator has an objective of maximizing total market surplus (i.e., market efficiency), and (iii) demand is perfectly inelastic (van der Weijde and Hobbs, 2012). My model accounts for transmission network constraints through a lossless DC approximation of Kirchhoff's laws. Nodal (or locational) power prices are given by the Lagrange multipliers of the energy balance constraint at every node.

In all models, renewable obligations are in the form of an RPS policy, where the renewable requirement is defined as a fraction of the served demand.[5] A noncompliance penalty is paid for every MWh of the renewable energy requirement that is not fulfilled. The representation of demand and generation is simplified, although not in ways that qualitatively affect my conclusions about the interaction of transmission costs and the RPS. Demand and intermittent generation variability are captured by considering a sample of operating hours with different loads as well as maximum wind capacity factors (i.e., maximum output in a given hour as a fraction of wind capacity). The distribution of operating levels accounts for quality of the wind resource at different locations, as well as correlations among locations. Marginal variable costs of thermal generation are constant, and generation capacity can be added in continuous amounts. The amount of generation that can be built at different nodes in the network is constrained, depending on the local availability of resources.

I first describe the static (single-year) models and then their dynamic generalizations.

[5] Although here I only focus on the integration of renewable generation into the system, my framework can also be used for studying the interaction of transmission planning with other market-based policies to put electricity production on a more sustainable footing, such as emissions trading programs.

2.3.1 Single-Stage Models

The static models minimize total system costs for a single year far enough in the future so that generation and transmission investments are also included as variables. In my model, B denotes the set of buses (or nodes, indexed by b), K the set of generation technologies (indexed by k), R the subset of K that are renewable generation technologies, L the set of lines (indexed by l), L_b the set of lines connecting bus b to other buses, N_l the set of circuits already built in corridor (or line) l (indexed by n), N_{lc} the set of candidate circuits to be built in corridor l, Ω_l the set (pair) of nodes connecting corridor l, and H is the set of hours per year (indexed by h).[6] The main decision variables of the models are $y_{b,k}$ MW for new generation investments, $x_{l,n}$ (dimensionless 0-1 variable) for transmission investments, $g_{b,k,h}$ MW for generation, and nonc MWh for the amount by which renewable generation falls short of the target. In hour h, variable $f_{l,n,h}$ denotes the MW power flow over corridor l and circuit n, and variable $\theta_{b,h}$ (in radians) corresponds to the voltage phase-angle at bus b.

With respect to the parameters used, new generation capacity of type k can be added at bus b at a capital cost $CY_{b,k}$ in \$/MW/yr and operated at marginal cost $MC_{b,k}$ \$/MWh. Parameters $Y^{max}_{b,k}$, $Y^0_{b,k}$, and $W_{b,k,h}$ represent the maximum generation capacity investment of type k allowed at bus b, the existing generation capacity of type k at bus b, and the capacity factor of generation of type k at bus b and hour h, respectively. The capital costs of adding a new circuit to corridor l are CX_l \$/yr.

[6]The model is stated as if H includes 8760 hours per year. If the sampled hours are fewer in number, then each sample hour's variables would be weighted by $\frac{8760}{|H|}$ in the objective function.

I assume that the cost of building n circuits in a given corridor is n times the cost of building a single circuit, although other assumptions could be made (reflecting, e.g., scale economies in line construction in a single corridor). Line capacities and susceptances are represented by parameters F_l^{max} and $_l$, respectively, and the non-compliance penalty is denoted as P_{nonc} \$/MWh. The demand at bus b and hour h is denoted as $D_{b,h}$. The renewable requirement is α, expressed as a fraction of the supplied energy.

The most realistic of the possible transmission models (referred as the Discrete-KVL model) recognizes the discreteness of transmission investments and Kirchhoff's Voltage Law, and is formulated as follows:

$$Min \sum_{b\in B}\sum_{k\in K} CY_{b,k}y_{b,k} + \sum_{l\in L}\sum_{n\in N_{lc}} CX_l x_{l,n} + \sum_{h\in H}\sum_{b\in B}\sum_{k\in K} MC_{b,k}g_{b,k,h} + P_{nonc}nonc \quad (2.4)$$

Subject to constraints:

$$y_{b,k} \leq Y_{b,k}^{max} \qquad \forall b,k \quad (2.5)$$

$$\sum_{l\in L_b}\sum_{n} f_{l,n,h} + \sum_{k\in K} g_{b,k,h} = D_{b,h} \qquad \forall b,k \quad (2.6)$$

$$f_{l,n,h} - \gamma_l(\theta_{b,h} - \theta_{p,h}) = 0 \qquad \forall (b,p)\in\Omega_l,\ \forall n\in N_l,\ \forall l,h \quad (2.7)$$

$$|f_{l,n,h} - \gamma_l(\theta_{b,h} - \theta_{p,h})| \leq M(1 - x_{l,n}) \qquad \forall (b,p)\in\Omega_l,\ \forall n\in N_{lc},\ \forall l,h \quad (2.8)$$

$$|f_{l,n,h}| \leq F_l^{max} \qquad \forall l, n, \ \forall n \in N_l \tag{2.9}$$

$$|f_{l,n,h}| \leq F_l^{max} x_{l,n} \qquad \forall l, n, \ \forall n \in N_{lc} \tag{2.10}$$

$$g_{b,k,h} \leq W_{b,k,h}(Y_{b,k}^0 + y_{b,k}) \qquad \forall b, k, h \tag{2.11}$$

$$\sum_{k \in R} \sum_{h \in H} \sum_{b \in B} g_{b,k,h} + nonc \geq \alpha \sum_{k \in K} \sum_{h \in H} \sum_{b \in B} g_{b,k,h} \tag{2.12}$$

$$y_{b,k} \geq 0 \quad g_{b,k,h} \geq 0 \quad x_{l,n} \in \{0, 1\}$$

The Discrete-KVL model minimizes total annualized system investment and operating costs (2.4), subject to generation build limits (2.5), Kirchhoff's Current Law (or nodal energy balances) (2.6), Kirchhoff's Voltage Law (2.7) and (2.8) for existing and new lines, respectively,[7] maximum power flow constraints (2.9), and (2.10), maximum generation constraints (2.11), and the RPS constraint (2.12). Note that, in this model, the right-hand side of (2.12) can be replaced by $\alpha \sum_{h \in H} \sum_{b \in B} D_{b,h}$, as I am ignoring transmission losses as well as the possibility of energy curtailments in which generation falls short of load.[8]

[7]See Schweppe et al. (1988) for a derivation of the linearized DC load flow model based upon explicit variables for bus voltage angles; this and other equivalent linear load flow models are widely used in power systems dispatch, planning, and market simulation models (Ventosa et al., 2005; Gabriel et al., 2012). Kirchhoff's Voltage Laws are written as disjunctive constraints for the candidate lines. That is, for $x_{l,n} = 1$, (2.8) becomes an equality constraint, equivalent to (2.7). For $x_{l,n} = 0$, (2.8) does not constrain the power flow variables in the left-hand side since M is a large positive number. This is a common way to represent the KVL constraints in transmission expansion models (Munoz et al., 2012).

[8]I use a simple deterministic model with a sufficiently high penalty for loss of load such that demand is always met. Modeling reliability requirements such as the "one day in ten years" loss of load expectation rule is beyond the scope of this article.

In addition to the Discrete-KVL model, I consider three simplifications: (i) Copper-Plate: Ignores all transmission constraints (equations (2.7)-(2.10)); (ii) Continuous-Transportation: Ignores Kirchhoff Voltage Law (KVL) constraints (equations (2.7) and (2.8)) and assumes that transmission capacity can be added in small increments ($x_{l,n}$ are continuous variables constrained to the interval $[0, 1]$); and (iii) Discrete-Transportation: Ignores KVL constraints (equations 2.7) and (2.8)), but assumes that transmission investments are lumpy ($x_{l,n}$ are binary variables).

2.3.2 Dynamic Model

By simulation tests (applied to the case study presented in Section 2.5), I verified that most of the results found by comparing the four static models remain qualitatively valid when incorporating the time dimension. Thus, I only extend the static Discrete-KVL model to a multi-year approach, which allows me to study the interactions among flexibility (in terms of banking & borrowing policies), growth in RPS requirements, and the discrete characteristics of transmission upgrades.[9]

Roughly, the dynamic model is the model described in (2.4) - (2.12) repeated every year of the considered time horizon, T, and adding a year index t to every parameter and decision variable. Now, transmission and generation investments can occur in any year t ($t \in \{1, .., T\}$), and their objective function coefficients are the full investment

[9]An important issue in the design of RPS systems is the ability to bank and borrow credits, which will dampen credit price volatility resulting from demand and wind output variations. Here I ignore this effect, as I do not model the inter-annual variability of wind production.

cost (in \$/yr) rather than the annualized capital cost. To avoid possible end effect distortions such as undervaluing of capital investments in later stages, I assumed that the last year represents operations for the last year plus $(T_e - 1)$ subsequent years. Accounting relationships are added to the constraint set so that capacity constructed in one year is also available in later years to generate or carry power (in the cases of generation and transmission capacity, respectively), and particular transmission lines can only be constructed once. Since my focus is on the dynamic interactions between RPS compliance and transmission investments, I assume no demand growth. Note that, to allow the study of banking and borrowing policies, now the renewable requirement varies over time. I denote the discount rate as δ.

Now, the dynamic Discrete-KVL model is as follows:

$$
\begin{aligned}
Min \ \sum_{t \in T} \delta^t \Bigg[\sum_{b \in B} \sum_{k \in K} CY_{b,k} y_{b,k} + \sum_{l \in L} \sum_{n \in N_{lc}} CX_l x_{l,n} \\
+ \sum_{h \in H} \sum_{b \in B} \sum_{k \in K} MC_{b,k} g_{b,k,h} + P_{nonc} nonc \Bigg]
\end{aligned} \tag{2.13}
$$

Subject to:

$$\sum_{t\in T} y_{b,k} \le Y_{b,k}^{max} \qquad \forall b,k \tag{2.14}$$

$$\sum_{l\in L_b}\sum_{n} f_{l,n,h,t} + \sum_{k\in K} g_{b,k,h,t} = D_{b,h,t} \qquad \forall b,k,t \tag{2.15}$$

$$f_{l,n,h,t} - \gamma_l(\theta_{b,h,t} - \theta_{p,h,t}) = 0 \qquad \forall (b,p)\in\Omega_l,\ \forall n\in N_l,\ \forall l,h,t \tag{2.16}$$

$$|f_{l,n,h,t} - \gamma_l(\theta_{b,h,t} - \theta_{p,h,t})| \le M(1 - \sum_{\tau\le t} x_{l,n,\tau}) \qquad \forall (b,p)\in\Omega_l,\ \forall n\in N_{lc},\ \forall l,h,t \tag{2.17}$$

$$|f_{l,n,h,t}| \le F_l^{max} \qquad \forall l,n,t,\ \forall n\in N_l \tag{2.18}$$

$$|f_{l,n,h,t}| \le F_l^{max}\sum_{\tau\le t} x_{l,n,\tau} \qquad \forall l,n,t,\ \forall n\in N_{lc} \tag{2.19}$$

$$g_{b,k,h,t} \le W_{b,k,h,t}(Y_{b,k}^0 + \sum_{\tau\le t} y_{b,k,\tau}) \qquad \forall b,k,h,t \tag{2.20}$$

$$\sum_{\tau\le t} x_{l,n,\tau} \le 1 \qquad \forall l,n,t \tag{2.21}$$

$$\sum_{k\in R}\sum_{h\in H}\sum_{b\in B} g_{b,k,h,t} + nonc_t \ge \alpha_t \sum_{k\in K}\sum_{h\in H}\sum_{b\in B} g_{b,k,h,t} \quad \forall t\in T \tag{2.22}$$

$$\sum_{t\in T}\sum_{k\in R}\sum_{h\in H}\sum_{b\in B} g_{b,k,h,t} + \sum_{t\in T} nonc_t \ge \sum_{t\in T}\alpha_t \sum_{k\in K}\sum_{h\in H}\sum_{b\in B} g_{b,k,h,t} \qquad \forall t\in T \tag{2.23}$$

$$y_{b,k,t} \ge 0 \quad g_{b,k,h,t} \ge 0 \quad x_{l,n,t} \in \{0,1\}$$

Different degrees of RPS flexibility are simulated by eliminating (2.23) if the RPS goals are going to be enforced year-by-year (YBY) without banking or borrowing, or by instead relaxing (2.22) if banking and borrowing (B&B) of RECs is allowed.

2.4 Theoretical Results

First, in Lemma 1, I point out that the optimal total cost of meeting RPS (under the four approaches considered here) is always continuously increasing in the RPS goal. Then in propositions 1, 2, and 3, I establish some results from comparing the different approaches (i.e., Copper-Plate, Continuous-Transportation, Discrete-Transportation and Discrete-KVL models).

Lemma 1: If RPS noncompliance with penalty P_{nonc} per unit is permitted, then the optimal cost of meeting an RPS is continuously increasing in α.

Proof: By contradiction, let's assume that the optimal cost jumps discretely by finite amount ΔTC when the RPS goal goes from α^* to $\alpha^*+\epsilon$, for an arbitrarily small $\epsilon > 0$. If noncompliance is allowed at finite penalty P_{nonc} \$/MWh, then the cost of meeting the goal $\alpha + \epsilon$, denoted $TC(\alpha^* + \epsilon)$, is upper bounded by the total cost of meeting α^*, denoted $TC(\alpha^*)$, plus the noncompliance cost for ϵ MWh of renewable generation, $P_{nonc}\epsilon \sum\limits_{h\in H} \sum\limits_{b\in B} D_{b,h}$. Then, for all $\epsilon < \frac{\Delta TC}{P_{nonc} \sum\limits_{h \ inH} \sum\limits_{b\in B} D_{b,h}}$, I have $TC(\alpha^*+\epsilon)-TC(\alpha^*) < \Delta TC$, which contradicts the initial assumption of a discontinuity.

Proposition 1: Assuming generation capacity can be added in small increments, the optimal (least-cost) solution for the four transmission models considered here always satisfies $TC_{C-P} \leq TC_{C-T} \leq TC_{D-T} \leq TC_{D-KVL}$ for a given value of α.

Proof: For the last inequality, as explained in Section 2.3, the optimal generation, flows, and investments of the Discrete-KVL model are a feasible solution in the Discrete-Transportation model because the latter simply omits the KVL constraints of the former, and so the latter cannot have a higher cost. Similarly, for the middle inequality, the optimal solution of the Discrete-Transportation model is a feasible solution in the Continuous-Transportation approach. This is because the two models differ only by the latter model's relaxation of the 0-1 constraints upon the $x_{l,n,t}$ variables, which means that the cost of the optimal solution to the latter model is no more than the former's cost. Finally, for the first inequality, the optimal solution of the Continuous-Transportation model is a feasible solution in the Copper-Plate model, because the latter omits the upper bound constraints on flows that are present in the former. Consequently, the optimal solution to the latter model cannot have a worse cost than the optimal solution of the former.

Proposition 2: The total costs obtained in the optimal solution of both the Copper-Plate and the Continuous-Transportation models are convex in α.

Proof: To prove this proposition, I use the fundamental result that the objective-function value of a minimization linear program (without binary variables) is a convex polyhedral function of the right-hand-side vector of the constraints (Bradley et al., 1977). Since both the Copper-Plate and the Continuous-Transportation models are minimization linear programs, the optimal total cost functions are convex functions of α (which is the right-hand side of the RPS-compliance constraint).

Proposition 3: The total cost obtained in the optimal solution of both the Discrete-Transportation and the Discrete-KVL models may be non-convex in α.

Proof: To prove this proposition, I only need an example of nonconvexity for these models, which is presented in Section 2.5.1.

2.5 Case Study and Results

I use a modified version of Garver 6-bus network to test my model. The system con-sists of 6 buses and 15 corridors, 6 of which initially have an existing line with a single circuit. The initial installed generation is 1110 MW, with a demand peak of 760 MW. All the initial installed generation was assumed to be thermal and non-intermittent and, therefore, could be dispatched at maximum capacity at any hour. Renewable capacity can be installed at certain locations, with limited availability. Wind generation is only available at three locations with different characteristics, while solar generation is available at all nodes and assumed to have the same characteristics everywhere.[10]

I distributed the total system load among the nodes using the original load distribution factors from Garver (1970), and based upon the variation of load over time of California ISO 2006 demand. Both wind and solar technologies have zero marginal costs. A sample of 20 hours is considered, representing a range of demand and solar conditions (see Table A.3 in Appendix A). Table 2.1 summarizes the peak demands, initial installed generation, total resource availability, and costs at each bus.[11] De-

[10]Note that since solar generation is available at all buses, it is an alternative to meet renewable goals instead of building new transmission capacity to access remote resources. The model will automatically recommend investments in solar generation at the load, instead of new transmission capacity if this configuration is more cost-effective than importing renewables from a distant bus, considering congestion effects.

[11]Here I am not considering the retirement of power generation units since it is not apparent that

Table 2.1: System characteristics and generation costs.

	Maximum Installed Capacity per bus [MW]						Capital Costs
	1	2	3	4	5	6	[$ 10^3/MW]
Conventional	500	500	500	500	-	-	1,000
Solar	200	200	200	200	200	200	5,000
Wind 6	-	-	-	-	-	300	2,500
Wind 4	-	-	-	100	-	-	2,500
Wind 1	50	-	-	-	-	-	2,500
Peak Demand [MW]	80	240	40	160	240	-	-
Initial Installed Thermal Generation [MW]	150	-	360	-	-	600	-
Thermal Marginal Costs [$/MWh]	80	60	60	60	-	50	-

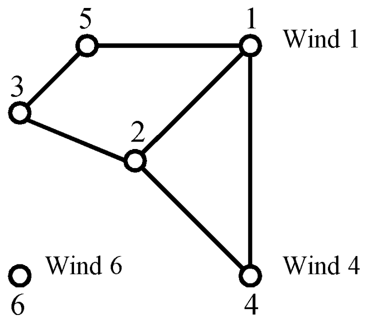

Figure 2.5: Garver's six-bus initial topology.

tails of the existing and candidate transmission lines are available in Table A.2 in the Appendix. Although I assume that scale economies in transmission investments are reflected as lumpy capacity additions, I assumed that the cost of building n circuits in a given corridor is n times the cost of building a single circuit. In my system, the capital costs of new transmission infrastructure are in the high end of what Mills et al. (2012) report for wind integration in the U.S.. As in Garver (1970), a maximum of 3 circuits can be built per corridor.

The capital costs of solar generation are twice the cost of wind generation, and solar generation has a lower capacity factor. Nodes 1 to 5 are initially interconnected (see Figure 2.5), but the initial installed conventional generation is not enough to meet the total demand. Therefore, even in the absence of a RPS target, the model will need to add either conventional generation within nodes 1 to 5 or a circuit to reach installed thermal generation at node 6, which can be thought of as a neighboring market with excess of thermal generation (e.g., node 6 could be Nevada, and nodes

this would materially affect my conclusions. However, a more refined model could explicitly include going-forward costs and decisions to retire.

1-5 could be a much larger market like California). Also, as shown in Table A.1 in Appendix A, node 6 has the wind with the best available characteristics (i.e., higher capacity factor and correlation with demand).

2.5.1 The Effects of Using Simplified Transmission Representations

In this section I study the effects of using models that ignore transmission constraints, Kirchhoff's Voltage Law, or the discrete nature of transmission investments. I solved the four versions of the single-stage models described in section 2.3.1 for RPS goals ranging from 0% to 50%, assuming full market compliance (noncompliance not permitted). I compare the results in terms of investments in generation and transmission infrastructure, generation spillage, and total system costs. As a sensitivity analysis, I also include results from a fifth approach, Continuous-KVL, assuming continuous transmission investments, but taking into account Kirchhoff's Voltage Law.[12] To my knowledge, this approximation has not been applied in policy studies since it involves solving a nonlinear problem and, therefore, I do not see it as a practical simplification of the reference Discrete-KVL approach. Yet, it illustrates how transmission non-linearities arise due to both transmission indivisibilities and Kirchhoff's

[12] In this case, Kirchhoff's Voltage Law cannot be written as linear disjunctive constraints (Equation (2.8)), since $x_{l,n}$ are defined as continuous instead of binary variables. I assume that suceptances are proportional to line capacities and enforce KVLs as nonlinear constraints: $f_{l,n,h} - {}_l x_{l,n}(\theta_{b,h} - \theta_{p,h}) = 0$. I find a local optimum using the nonlinear solver SNOPT 7.2 with the solution from the Continuous-Transportation approach as a starting point.

Voltage Law.

Differences in Transmission Infrastructure

I begin by comparing the transmission investments that the Discrete-KVL, Discrete-Transportation and Continuous-Transportation models find optimal for different RPS goals. Figures 2.6 (a)-(c) graph the amount of transmission capacity added for corridors connecting nodes 2-6, 3-5, and 4-6, respectively. Note that although the Continuous-Transportation approach provides accurate approximations of investments in corridors 2-6 and 4-6 for renewable targets up to 26% and 10%, it underestimates the capacity additions in corridor 3-5 by 60% with respect to the Discrete-KVL model for the entire range of simulated RPS goals (Figure 2.6 (b)). Moreover, for the maximum renewable target of 50%, it underestimates investments in corridor 2-6 by 61% (Figure 2.6 (a)) and overestimates the investments in corridor 4-6 by 180 MW, when the Discrete-KVL approach recommends no additions (Figure 2.6 (c)).

In contrast, the Discrete-Transportation approach provides accurate recommendations of transmission investments up to a 31% renewable target. However, for goals above 40%, ignoring Kirchhoff's Voltage Law but taking into account transmission lumpiness, results in an underestimation of 33% of the investments in corridor 2-6 (Figure 2.6 (a)) and an overestimation of 100 MW in corridor 4-6 (Figure 2.6 (c)).

Figures 2.7 (a) and (b) are an alternative portrayal of the differences in the evolution of the optimal network topologies that the Discrete-KVL and the simplified

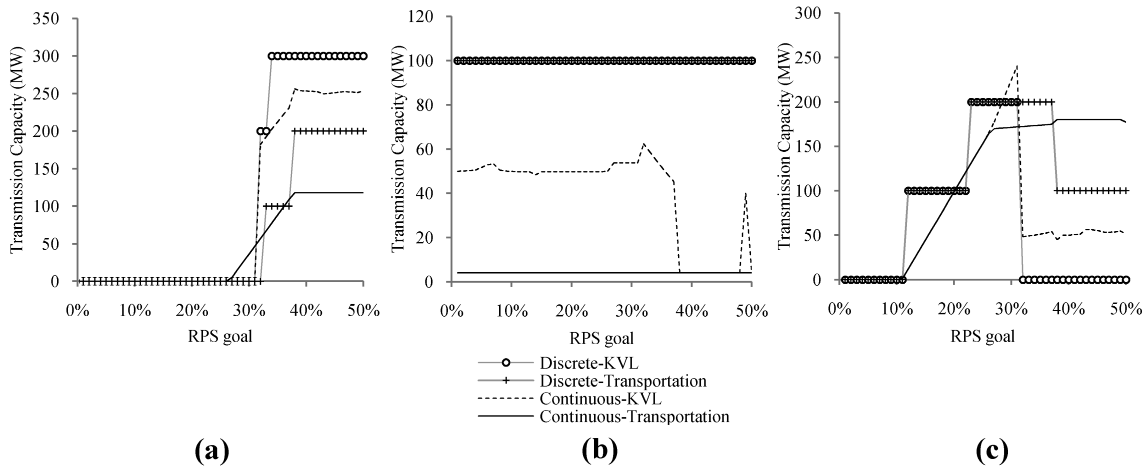

Figure 2.6: Transmission investments in circuits linking buses a) 2-6 (line 9), b) 3-5 (line 11), and c) 4-6 (line 14).

Discrete-Transportation model recommend for different ranges of renewable goals. For renewable goals between 33% and 50%, note that the Discrete-Transportation approximation recommends connecting node 6 to the rest of the network using 2-6 and 4-6 circuits, resulting in a new loop in the transmission network between nodes 2-4-6 (Figure 2.7 (b)). Since Kirchhoff's Voltage Law is relaxed in the Discrete-Transportation approach, this model does not account for the increased congestion or redispatch costs that result as a consequence of the new loop in the network. If that Law is instead enforced, as in the Discrete-KVL approach, it is then optimal to connect node 6 to the rest of the network only using radial circuits from nodes 2 or 4 (Figure 2.7 (a)).

Finally, observe in Figure 2.7 (a) that for renewable obligations above 32% (Topology 4), it would be optimal to send power from node 6 directly via a new line to node 2, instead of sending it to node 4, as done for renewable obligations between 12% and

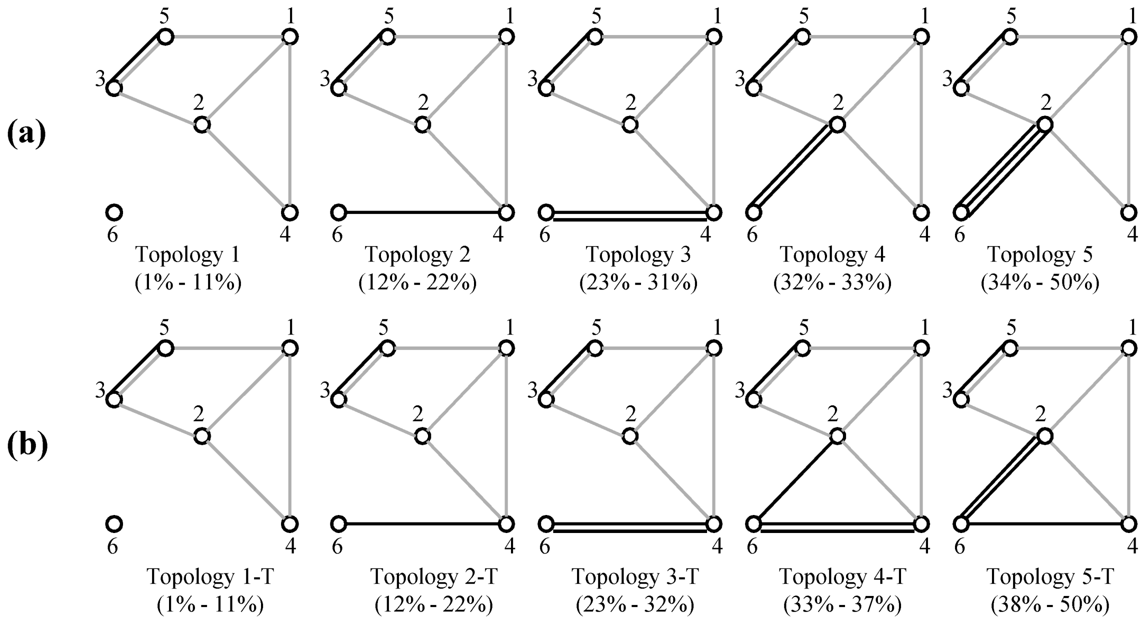

Figure 2.7: Transmission topologies for different renewable supply ranges. a) Optimal network topologies for the Discrete-KVL. b) Optimal network topologies for the Discrete-Transportation model.

31% (Topologies 2 and 3). As I already mentioned in the two-node example in Section 2.2, the optimal transmission and generation investment decisions are not necessarily monotonic in the RPS, in the sense that facilities built for low RPS targets will not necessarily be cost effective for higher renewable goals. Here I also observe that such nonmonotonicity also arises due to KVL in the auxiliary Continuous-KVL approach (Figure 2.6), where transmission investment variables are continuous.[13]

[13]Note that I am not stating that nonmonotonicity cannot occur in the Copper-Plate or Continuous-Transportation approaches; I am only highlighting how nonmonotonicity is enhanced by the lumpiness of transmission investments and Kirchhoff's Voltage Law.

Differences in Generation Investment

In Figure 2.8 (a), I graph the total amount of generation investment in both thermal and renewable technologies versus renewable goals, all under full RPS compliance. Figures 2.8 (b)-(f) correspond to the generation investments per technology, with Figures 2.8 (b) and (f) showing the total aggregated amount of investments for thermal and solar generation for the six buses, respectively. For all the models, the generation investment curves exhibit a knee at a 38% renewable target, the point at which all wind resources are depleted and costly solar resources are the sole remaining way to provide additional renewable energy (Figure 2.8 (f)). Under the Copper-Plate approach, the availability of conventional generation in node 6 and the assumption that there are no transmission constraints means that, if the RPS is zero, then existing installed generation is sufficient to meet the aggregate peak demand (Table 1) and no investment thus is needed (Figure 2.8 (b)). Therefore, the Copper-Plate model is the only approach that predicts that all investments in generation are renewable. In contrast, under the Discrete-KVL approach, as well as in the other two transmission-constrained approximations, I observe that it is optimal to also invest in some thermal generation until there is enough transmission capacity to access the installed thermal generation in node 6 (Figure 2.8 (b)).

Both discrete approaches present decreasing staircase curves of thermal generation investment as a function of the renewable goal (Figures 2.8 (b)), with each drop reflecting a change in the network topology (see Figures 2.7 (a) and (b)). Under the Continuous-Transportation approach, however, I miss these drastic changes. The absence of indivisibility (0-1) constraints for transmission investments enables the Continuous-Transportation model to compare investments in local generation versus investments of transmission capacity to access distant generation on a \$/MW basis, and to build small amounts of the latter if its marginal cost is lower. Figure 2.6 (c), for example, shows small increments in the capacity of the corridor 4-6 for renewable targets between 11% to 26%, correlated with generation investments in wind in node 6 (Figure 2.8 (e)), and negatively correlated with thermal generation investments (Figure 2.8 (b)).

Also note that the optimal amounts of investments in wind generation in node 1 oscillate with respect to the renewable target (Figure 2.8 (c)). As I show in Figure 2.7 (a), there are topology changes for the renewable targets of 11%, 22%, and 33%. In Figure 2.8 (c), I observe that generation investment in wind at node 1 falls to zero at these targets in the Discrete-KVL case, but as the target increases beyond any of those three levels, wind investment at node 1 then grows to the maximum capacity of the resource until the next transmission investment takes place. This is because each transmission addition increases the importing capacity of power from node 6, where wind resources have comparatively better characteristics (i.e., higher capacity factor, see Table A.3 in Appendix A) and where there is excess thermal capacity.

This is analogous to the two-node example in Section 2.2. In the case that remote resources have better characteristics than local resources, remote resources are utilized until the corridor becomes congested, after which local resources become attractive again. Consequently, the most cost-effective type, size, and location of generation investments can vary drastically in response to changes to the network when transmission investments are lumpy. As illustrated in Figure 2.8 (b) with the Continuous-KVL approach, Kirchhoff's Voltage Law can also cause drastic variations in the optimal generation portfolio, but to a lesser extent compared to transmission indivisibilities.

A direct implication of this conclusion is that selecting renewable energy developments using aggregate renewable resource supply curves, will, in general, provide sub-optimal recommendations for the development of renewable resources. Optimal transmission-renewable energy plans will, in general, include some more expensive (per MWh) renewable resources, while leaving out some cheaper ones. This is analogous to the effect of transmission constraints in economic dispatch problems, which results in out-of-merit-order dispatch of generation.

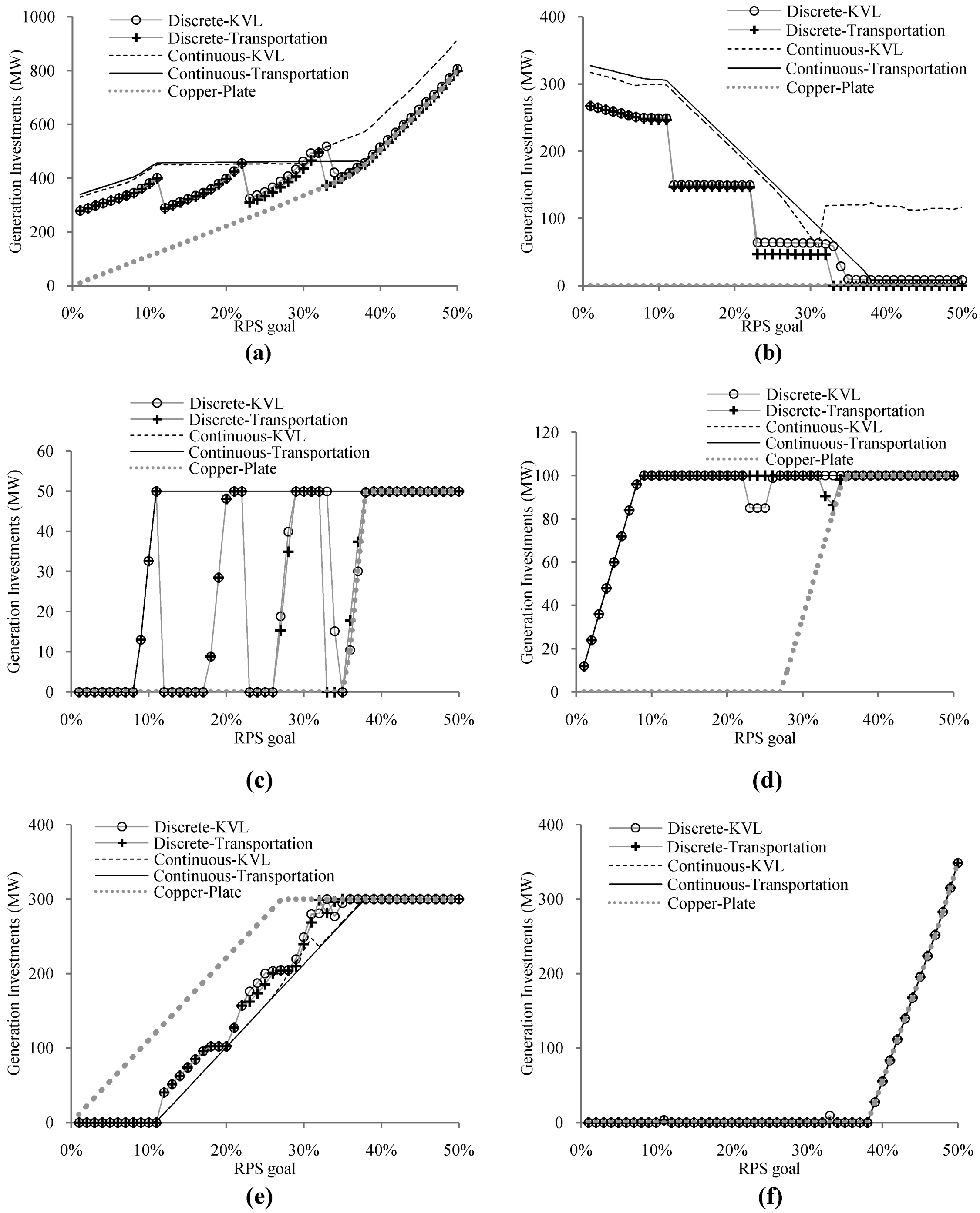

Figure 2.8: Generation investments: a) Total aggregate, b) Conventional (aggregate), c) Wind 1, d) Wind 4, e) Wind 6 and f) Solar (aggregate).

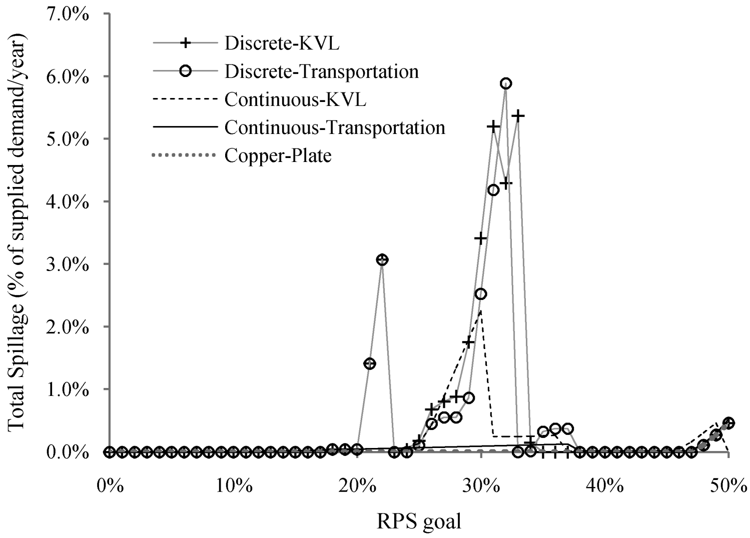

Figure 2.9: Total spillage per year as a percentage of the supplied demand.

Wind Spillage

In Figure 2.9, I show the total amount of spilled generation from renewables as a function of the renewable target. Spilled generation occurs when wind energy could be generated, but network congestion or other constraints prevent it all from being used. The discrete models show pronounced spikes in wind spillage (up to 6% of load and 20% of renewable generation) for some renewable targets because the cost of the next lumpy addition in transmission exceeds the value of the fuel savings that would occur if the line was built and spillage avoided. I observe a similar nonlinearity in the Continuous-KVL approximation, but with a spike of only 2.3% of load. In contrast, since both the Continuous-Transportation and Copper-Plate approximations assume that the infrastructure can be added in small increments and Kirchhoff's Voltage Law is relaxed, zero or negligible spillage occurs.

Biased Cost Estimates from Simplified Models

In Figure 2.10 (a), I plot the total system cost for each of the transmission modeling approaches, all of which increase as the renewable targets become more ambitious. As stated in Proposition 1, the Discrete-Transportation, Continuous-Transportation, and Copper-Plate models underestimate total system costs compared to the most accurate formulation, the Discrete-KVL model. The large cost gap between the Copper-Plate and the more complex models is a consequence of ignoring transmission constraints and, therefore, not accounting for congestion (out-of-merit generation operation and generation spill) or transmission investment costs. Figure 2.10 (a) illustrates Proposition 2, which states that since both the Copper-Plate and Continuous-Transportation models are linear programs, the total system costs are convex in the RPS targets for those models. This implies that the marginal cost of increasing the RPS is always nondecreasing. These marginal costs approximate what a competitive market would charge for the RECs.[14] However, this is not true for the discrete models; just as in my two-bus example in Section 2.2, the total costs of both discrete-transmission models are nonconvex in the RPS, which is a consequence of the lumpiness of transmission investments. This nonconvexity also arises in the Continuous-KVL approach which is, by construction, a nonlinear problem.

[14] Although there are issues about defining the marginal costs of RECs in the discrete cases, here I approximated them by finite-differences. Note that the price of RECs would not cover all incremental costs of meeting the RPS in those cases relative to a zero RPS target. This is an example of the duality gap phenomenon, which has been discussed extensively in the context of the use 0-1 unit commitment models to operate power systems (Hobbs et al., 2001).

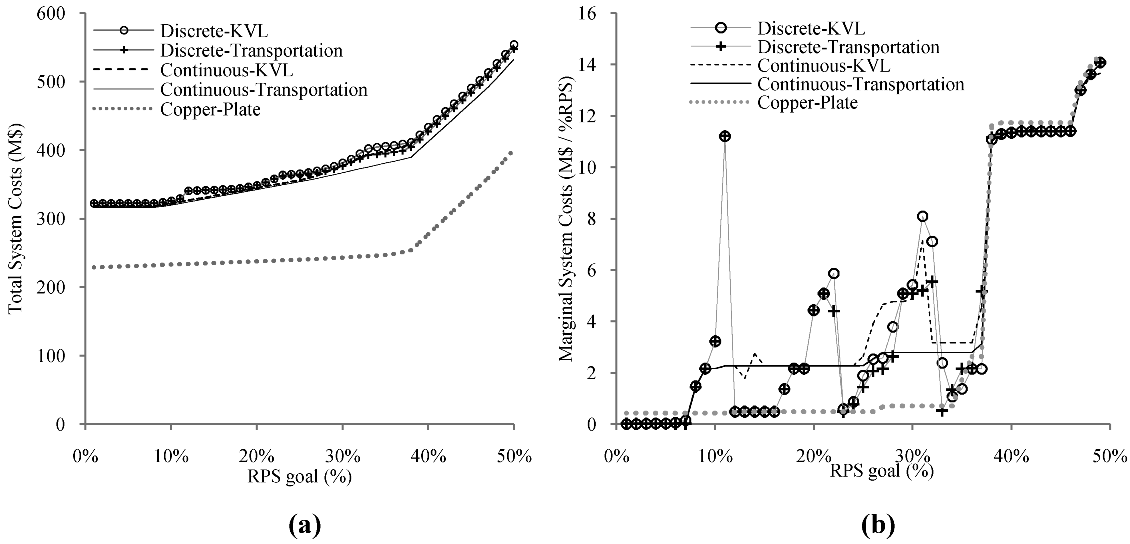

Figure 2.10: a) Total system costs versus RPS goal, noncompliance prohibited. b) Marginal system costs versus RPS goal under full compliance.

Note in Figure 2.10 (b) that the marginal costs of both Copper-Plate and Continuous

-Transportation models are increasing in the RPS goal, while this is not true for the Discrete-KVL and the Discrete-Transportation models. Since the latter two models consider lumpy network upgrades, it is not optimal to make transmission investments unless they can offset the additional costs of congestion and generation investments in local renewable resources, such as wind in node 4. As the graph in Figure 2.10 (b) shows, marginal costs are increasing for renewable targets from 8% to 11%, for both discrete models. This happens because, up to an 11% RPS goal, it is not justifiable to build new transmission capacity to access wind resources at node 6; thus, the renewable requirements are met using less effective, but more accessible local renewable resources. Furthermore, for an 11% goal, it is cost-effective to invest in a small amount of solar generation (Figure 2.8 (f)), which is the reason why marginal costs go up to similar levels reached for targets between 38% to 46% (Figure 2.10 (b)), when all the wind sites are used up to their maximum availability and investment in solar generation become necessary.

Also, note that the Copper-Plate model predicts higher marginal costs for RPS obligations below 8% and above 38%, although the total system costs are largely underestimated compared to the other models (see Figures 2.10 (a) and (b)). Since the Copper-Plate model ignores transmission constraints, for RPS goals below 8%, predicts that it is optimal to invest in wind generation located in node 6 and no conventional generation. In contrast, for the same RPS targets, the models that account for transmission constraints invest in wind generation at node 4 and some conventional generation. As shown Figures 2.8 (b) and 2.8 (c) for these models, investments in conventional generation decrease as investments in wind increase, which results in lower marginal enforcement costs compared to the costs predicted using the Copper-Plate approach.

In Figure 2.11, I show the incremental cost of meeting the RPS goal, which corresponds to cost curves plotted in Figure 2.10 (a) minus the costs of running the system without a renewable target. Contrary to what occurs with total system costs, the incremental cost of meeting the RPS is not necessarily lower with the Copper-Plate model. This can happen since under the Copper-Plate approach the total system costs without a renewable target are also grossly underestimated (Figure 2.10 (a)). But as

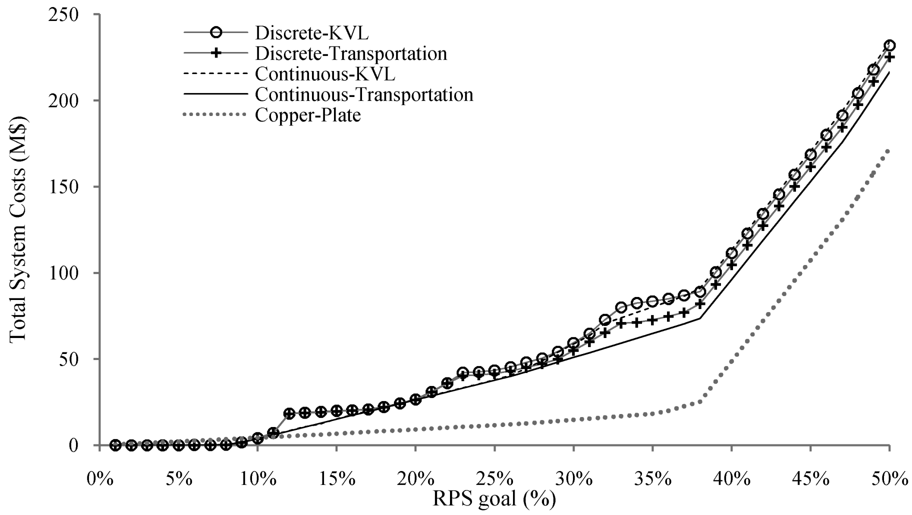

Figure 2.11: Total costs of meeting the RPS target, noncompliance prohibited.

the RPS target moves beyond 8%, I find that the simplified models underestimate the costs of meeting the renewable goal just as they underestimate the total system costs. The graph shows that the more accurate models also have the highest incremental cost beyond this point, although this is not a general result. I observe that, for this system, the impacts of the simplifications of the transmission costs of meeting the RPS depend on the renewable target. Above an RPS of 25%, the disregarding of transmission lumpiness causes cost distortions (Discrete-KVL vs. Continuous-Transportation) that are similar in magnitude to ignoring Kirchhoff's Voltage Law (Discrete-KVL vs. Discrete-Transportation); however between 11% and 24%, disregarding lumpiness is more important (as the Discrete-KVL and Discrete-Transportation lines coincide).

2.5.2 Effects if Noncompliance is Allowed

I have discussed the differences among the considered approaches in terms of costs and infrastructure, all assuming full RPS compliance. Here I examine how disregarding transmission lumpiness or Kirchhoff's Voltage Law can result in overestimation of compliance with renewable energy targets when noncompliance is allowed, but penalized. Such penalties provide an option for LSEs or generators to, in effect, buy RECs from the regulator at a pre-specified price, and which would count towards the RPS target just as if they were generated using renewable resources. They could also act as price caps on the price of RECs, ensuring that the RPS goals are met at reasonable costs for ratepayers. In theory, an efficient market would only support the integration of renewable generation until the marginal cost of an extra RPS percentage is equal to the noncompliance penalty. As I observed in Figure 2.10 (b), different approaches predict different marginal costs; thus, in general, they also present differences in terms of how much noncompliance with renewable targets occurs.

Figure 2.12, for instance, shows the different levels of renewable energy supply resulting for RPS goals ranging from 0% up to 50% if RECs can be bought from the regulator at 100 $/MWh. Both the Continuous-Transportation and Copper-Plate models predict full compliance up to an RPS goal of 38%, after which it becomes cheaper to pay the penalty fee than to build solar facilities to meet the RPS. But if transmission upgrades are assumed to be discrete, no more than 28% of the served demand will come from renewable generation. Counter-intuitively, there are ranges

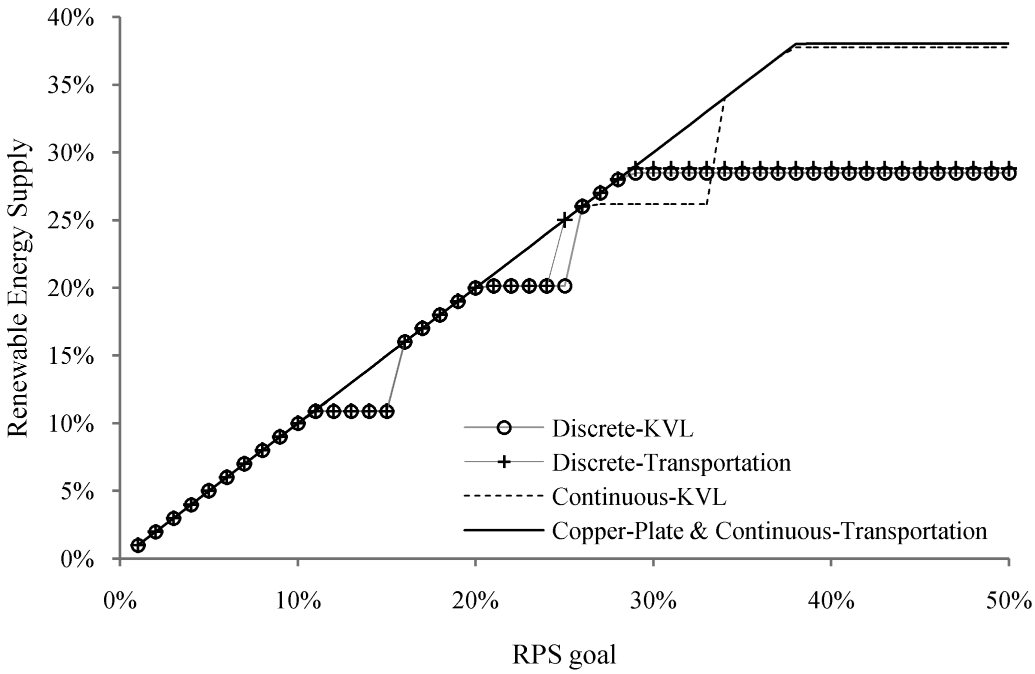

Figure 2.12: Renewable energy supply versus RPS goal for a 100 \$/MWh noncompliance penalty.

of RPS goals below 28% for which both discrete models find that partial attainment of renewable goals is optimal (provision of 11% renewable supply for RPS goals between 11% to 15%, and 20% renewables for goals between 20% and 25%). Thus, for example, enforcing a goal of 25%, instead of 20%, results in collecting more money from penalties, instead of incentivizing more investments in renewable generation. However, note that this is not only a consequence of transmission indivisibilities. The Continuous-KVL approach also predicts partial attainment of renewable mandates for RPS goals between 26% and 33%. These ranges correspond to regions with marginal costs spikes (Figure 2.10 (b)), which are a consequence of the nonlinearities caused by the lumpiness of transmission investments and Kirchhoff's Voltage Law.

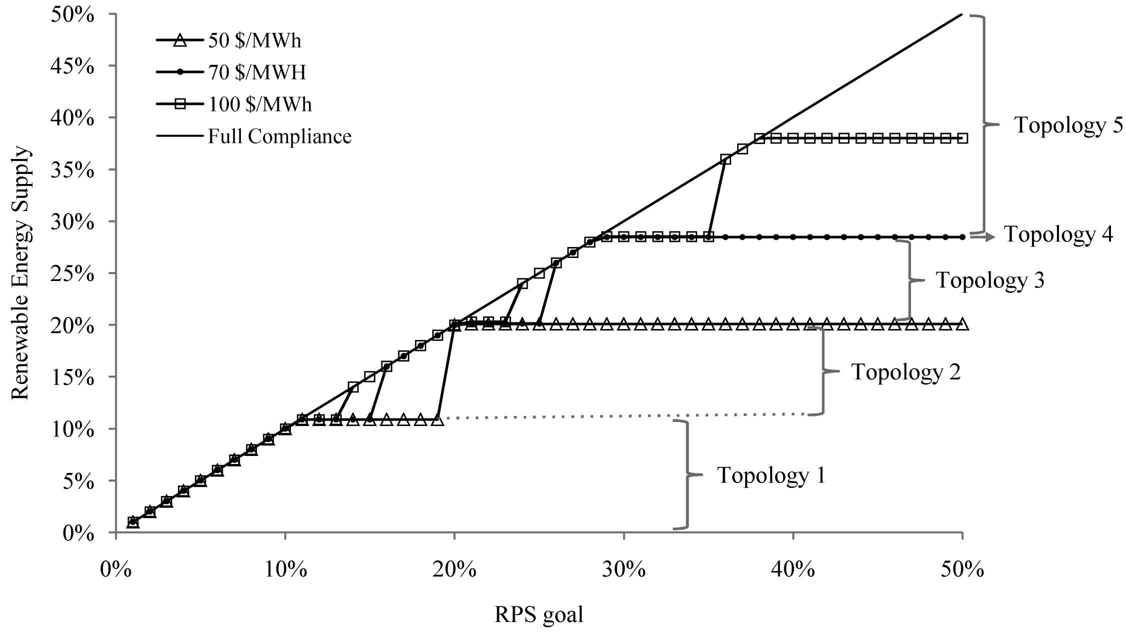

Figure 2.13: Renewable energy supply versus RPS goal for different penalty levels using the Discrete-KVL approach.

In Figure 2.13, I graph the total amount of renewable supply versus the RPS goal for four different penalty levels in the Discrete-KVL case. As illustrated, the lower the non-compliance penalty, the lower the amount of renewable supply that the market will support, and the larger the ranges of goals for which partial noncompliance is cost-effective. Each one of the vertical jumps observed in Figure 2.13 corresponds to a change in the network topology due to transmission investments (see Figure 2.7 (a)). In contrast, neither Copper-Plate nor Continuous-Transportation approaches present intermediate noncompliance steps for all these penalty values, thus yielding a distorted characterization of RPS costs and compliance.

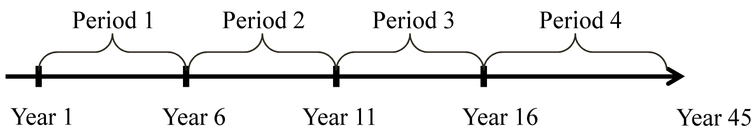

Figure 2.14: Timeline of the dynamic simulations.

2.5.3 Dynamic Analysis: Benefits of Banking and Borrowing

Here I focus on RPS designs that set multiple targets over time and that, in some cases, include REC banking and borrowing rules. Using the multi-stage model described in Section 2.3.2, I study the economic benefits of these features and how they affect the optimal investment strategy to meet the regulation. I assume a horizon of 45 years, divided into four decision periods, in which transmission and generation investments can only occur every five years, with year 16 the last year when they can take place (i.e., investments can occur in $t \in \{1, 6, 11, 16\}$) (Figure 2.14). In order to avoid possible end-effect distortions, I assume $T_e = 30$ years (i.e., the last decision year represents operations for the final 30 years).[15] I use an annual discount rate of 10%.

For simplicity, I assume no demand growth and intermediate RPS goals that are held constant for 5-year periods. Thus, I only model operations every five years, which I assume to be representative of the years in between. Relaxing the no-demand-growth assumption does not qualitatively change the conclusions. I assume the existence of an

[15] A more sophisticated model with additional 5-year stages did not yield qualitatively different results.

upward ramping RPS goal from period 1 to period 4, starting at 10% of the supplied demand per year, with 10% increments in every period, ultimately reaching a target of 40% of renewable supply in period 4. Renewable goals that are enforced year-by-year (YBY) are imposed with constraint (2.22), while constraint (2.23) enforces REC banking and borrowing rules (B&B) (if allowed) across different compliance periods. Using a combination of these two features, I perform five experiments that allow me to measure the benefits of giving the market flexibility to meet the targets. The first three cases are described as follows:(i) Case 1: RPS goals of 10%, 20%, 30%, and 40% are enforced year-by-year (YBY), representing the most stringent case; (ii) Case 2: REC banking and borrowing (B&B) rules between the four periods are applied, but a 40% RPS target is enforced in period four (i.e., constraint (2.22) is imposed for period 4 only); and (iii) Case 3: REC banking and borrowing (B&B) rules between the four periods are applied, without either YBY constraints or final RPS goals.

Although to my knowledge there are no RPS implementations that resemble Case 3 in the real world, I use it as a benchmark to contrast cases 1 and 2. I also perform experiments to study the effects of altering the optimal dynamic transmission investment strategy found in cases 1 and 3. The last two experiments are defined as: (iv) Case 4: REC banking and borrowing (B&B) rules between the four periods are applied, but Case 1's transmission plan is imposed (YBY RPS) and (v) Case 5: RPS goals of 10%, 20%, 30%, and 40% are enforced year-by-year (YBY), but I use the static model as a heuristic to generate a transmission plan for the dynamic model.

Dynamic Planning of Flexible RPS Designs: Cases 1, 2 and 3

Table 2.2 shows the renewable energy supply and transmission investments per period, as well as the incremental costs relative to no RPS policy for each of the five cases. Since Case 2 is a relaxed version of Case 1, under optimal dynamic planning the total system costs are going to be higher when RPS targets are enforced year-by-year. For my case study, the savings from allowing LSEs to bank and borrow RECs during the first three periods are \$35M, or 1% of the present worth of the costs relative to no RPS. These cost savings are a result of a better scheduling of transmission to support generation with renewable resources during the first three periods.

As shown in Table 2.2, when the market is given more flexibility, as in Case 2, it is more cost-effective to invest earlier in both renewable generation and transmission compared to Case 1, with Case 2 supplying 17.7% of demand with renewables during period 1 (7.7% more than the target for that period, which is the amount provided in Case 1), but only a 22.2% during period 3 (7.8% less than that period's target). In Case 1, LSEs are not allowed to bank and borrow RECs, therefore, the market will not invest more than what is strictly required to meet the RPS targets. In contrast, under Case 2, the market is given flexibility to bank and borrow RECs. Consequently, for my test case, it is more cost-effective to invest in two lines at the beginning of period 1 and take advantage of the new transmission infrastructure for as long as possible (periods 1 to 3), until new investments are required to meet the boundary condition during period 4 (40% goal). This result might seem counterintuitive, since discounting should provide an incentive to delay investment when possible. Although this is true, it turns out that the discounted savings from a 7.8% reduction in renewable supply in period 3 are actually higher than the extra costs of an extra (undiscounted) 7.7% renewable supply during period 1. In other words, requiring a moderate but constant amount of renewable energy over a multi-year time period, as opposed to a rapid ramping of the requirement from low to high in the middle years, results in a more efficient grid that is better utilized to transmit renewable power over the time horizon.

Much larger savings can be achieved under the hypothetical Case 3 (B&B), where there is no year-by-year RPS enforcement whatsoever, and the only renewable requirement is the B&B constraint (2.23). In that case, LSEs are allowed to bank and borrow RECs between periods 1 to 4. The total savings are of \$106M with respect to Case 2 (3.1% of costs relative to no RPS), and of \$141M with respect to Case 1 (4.1% of the costs relative to no RPS). However, note that in Case 3 (B&B), the maximum amount of renewable generation is only 29.8% of the supplied demand, reached during periods 3 and 4, well below the goal of 40% in the long term. Since the 40% target is not explicitly enforced in Case 3 (B&B), an optimal dynamic solution allocates investments and generation among the four periods, making a compromise between the advantages of delaying investment versus the higher incremental cost of renewable energy when penetrations are already high. Therefore, if reaching the final renewable target is more valuable than the total amount of renewable generation supplied while the RPS policy is in place, a final RPS goal may be needed on top of the B&B constraint, as in Case 2. In contrast, it may be the case that renewable energy supplied during the first period provides more environmental benefits than a unit of renewable energy generated at a later period. This would be the case if, for example, renewable energy was displacing polluting generation and emissions that were considered more harmful in the present, before the policy was enforced, than in the future, when lower levels of emissions have been already achieved. In that situation, the output from Case 3 (B&B) would become more valuable, since it achieves higher levels of renewable supply in the first two periods than in the first two RPS designs.

The Effect of Transmission Planning on Renewable Supply: Case 4

In the first three cases I saw the economic implications of giving the market flexibility to meet the RPS targets, assuming perfect coordination between both the transmission planner and generators to meet the goals at minimum cost. With Case 4 I want to illustrate how transmission investments affect generation investments and, thus, the final share of renewable supply. In Case 4 I used the same B&B constraint as in Case 3 (B&B), except that I imposed the transmission investments to be equal to the ones from Case 1, where renewable targets are enforced year-by-year. Interestingly, changing the type and timing of network reinforcements strongly affects the time profile of renewables in the system, without additional renewable constraints. The final share of renewables in Case 4 is 38% of the served demand, 8.2% higher than Case 3 (B&B), and only 2% lower than in Case 1 (YBY). This highlights the importance of transmission infrastructure to meet renewable goals, since the 40% goal is almost achieved by only changing the transmission investment strategy, without explicitly enforcing the final renewable target in period 4. This suggests that a proactive network planner can invest strategically in order to influence the timing and size of investments in renewable generation.

Short-Sighted Planning: Case 5

Case 5 is an example of a shortsighted network planner who builds infrastructure only considering shot-term goals using a static model, but where generators have foresight and plan over the entire time period. Unlike Cases 1 or 2, Case 5 is not an optimal dynamic transmission plan; however, by design, it reaches the final RPS target of a 40% of renewable supply by period 4. The costs of shortsighted transmission planning in this case are $26M higher than those in Case 1 (YBY), or 0.8% of the costs with respect to no RPS. By solving a series of static models, one circuit is added in every period, as in Case 1; however, note that in Case 5, node 6 is connected to the rest of the network with two circuits between nodes 4-6 and one between 3-6 (Table 2.2).

The present worth of $26M is the cost savings that could be achieved if transmission planning was done using a dynamic approach, taking into account the multi-year renewable goals, rather than solving a series of static optimization models focused only on the short-term renewable targets. The magnitude of these savings is similar to the savings resulting from implementing banking-and-borrowing of RECs (comparing Cases 1 and 2), and are thus important.

Path-Dependent Investments

In Section 2.5.1, when faced with a static RPS target, I showed that there are different optimal network topologies for different RPS targets and that infrastructure investments are nonmonotonic for the discrete models (Figure 2.7 (a)). Here I observe that under RPS designs with multi-year goals, the optimal final network topologies not only depend on the final renewable target, but also on how these goals are enforced over time. For example, under both cases 1 and 2, the market reaches renewable supply levels of 40% by period 4. However, the type and timing of the transmission investments differ. In Case 1, it is optimal to add one circuit in every period, while in Case 2, it is optimal to make transmission investments only at the beginning of periods 1 and 4. As I discussed before, since Case 2 allows for banking and borrowing of RECs, it is more cost effective to make investments at the beginning of period 1 and maintain fixed levels of renewable generation during the first 3 periods, and leave the last big investments for period 4, when a 40% RPS target is enforced.

The final network topology for Case 1, illustrated in Figure 2.15 (a), is equivalent to the optimal network topology that the static model predicts for a 40% RPS target (see Figure 2.7 (a)). In contrast, the final network topology in Case 2 (Figure 2.15

Table 2.2: Compliance, Transmission Investments, and Incremental Costs for each case.

Case N	Description	Renewable energy supply per period (% of supplied demand)				Transmission investments per period (from node - to node)				Incremental costs relative to no RPS (M$)
		1	2	3	4	1	2	3	4	
1	RPS goals enforced year-by-year.	10.0%	20.0%	30.0%	40.0%	3-5	2-6	2-6	2-6	512 (14.9%)
2	Banking and borrowing allowed between the four periods. RPS goal of 40% enforced in period 4.	17.7%	20.1%	22.2%	40.0%	3-5, 4-6			2-6 (twice)	477 (13.9%)
3	Banking and borrowing allowed between the four periods.	20.1%	20.3%	29.8%	29.8%	3-5, 4-6		4-6		371 (10.8%)
4	Banking and borrowing allowed between the four periods. Transmission investments imposed from Case 1.	9.2%	20.1%	32.6%	38.0%	3-5	2-6	2-6	2-6	473 (13.7%)
5	RPS goals enforced year-by-year. Transmission investments imposed from sequential solutions of static model.	10.0%	20.0%	30.0%	40.0%	3-5	4-6	4-6	3-6	538 (15.6%)

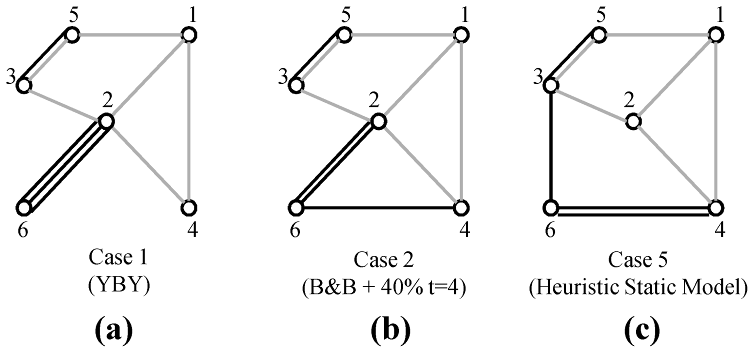

Figure 2.15: Network topologies by the end of period 4 for a) Case 1, b) Case 2, and c) Case 5.

(b)) involves one extra circuit linking nodes 4 and 6, but one less circuit linking nodes 2 and 6. Something similar occurs in Case 5, when I solve a series of static models as a heuristic to find a transmission plan for the four periods. In that case, the final network (Figure 2.15 (c)) differs from Cases 1 and Case 2, but in particular it includes a circuit linking buses 3 and 6 that was not added in any of the other cases. Also note that this line did not appear in any of the optimal static solutions either. The implication of this result is that transmission planning to accommodate renewables should be done not only looking at the final RPS goal, but also taking into account the intermediate goals over time and possible market responses to flexibility in the RPS designs, such as banking and borrowing.

2.6 Conclusions

In this article I studied the effects of transmission nonlinearities on the performance of Renewable Portfolio Standards both using static and dynamic planning models. Using a static model, I illustrated how ignoring transmission constraints or assuming that transmission investments can take place in small increments can generate significant errors in cost estimates and generation investments. Although it is not a general result, disregarding Kirchhoff's Voltage Law could distort optimal network investments and result in the creation of new loops in the network that, in reality, increase congestion and redispatch costs.

The most important effects of transmission lumpiness and Kirchhoff's Voltage Law on the performance of Renewable Portfolio Standards are threefold. First, under optimal static planning, the total system costs may be nonlinear and nonconvex as a function of the renewable targets and, therefore, the marginal system costs may decrease as the RPS goal increases. Second, optimal investments in infrastructure may be nonmonotonic in the renewable goals, in the sense that some generation and transmission investments that are cost-effective for low RPS targets might not be optimal for higher obligations. Third, as a consequence of the possibility of regions of decreasing marginal costs of meeting the RPS, if noncompliance is allowed with a financial penalty, partial noncompliance can be optimal for intermediate levels of an RPS, while compliance might be optimal for higher RPSs.

I used dynamic models to study the effects of using different RPS designs to reach a final, long-term goal of renewable supply. The models differed in the degree of flexibility that the policy gives the market to meet the obligation. My conclusions are that, first, there are cost savings that could be achieved by allowing LSEs to bank and borrow RECs between the compliance periods. Second, the optimal infrastructure to meet a final RPS target is path-dependent. The most cost-effective investments in transmission and generation depend on how flexible the RPS designs are, and not only on the long-term renewable goal. Third, under flexible RPS designs, where LSEs are allowed to bank and borrow RECs, a transmission planner can influence the installed amount of renewable generation in the long-term. Therefore, the long-term performance of renewable standards not only depends on how generators invest, but also on how transmission planning is done. Fourth, static single-shot models should not be used as proxies for long-term planning. Most RPS in place have become more stringent with time and incorporate different flexibility features; therefore, a proactive transmission planning approach to accommodate renewables should not only focus on short-term or final goals, but it should also take into account the specific design characteristics of the renewable standards in place, such as noncompliance penalties or REC banking-and-borrowing rules.

Throughout the article I have assumed that the market equilibrium is identical to the solution that minimizes total system costs. However, in reality, transmission planners and generators can have different and conflicting objectives such that they will fail to coordinate and achieve the least-cost solution (Sauma and Oren, 2007).

Since network expansions are lumpy, such investments cause non-marginal changes to the economics of generation investments depending on how transmission is priced, which can have important effects on the cost-effectiveness of RPS policies. Therefore, transmission planners should take into account their effects on the reactions of generators and the resulting costs of meeting RPS goals. This may be possible, for instance, in California, where the California Public Utilities Commission is responsible for both the implementation of the state Renewable Portfolio Standard as well as approval of transmission investments proposed by utilities. However, renewable mandates are not necessarily defined over regions that match the jurisdiction of transmission planning authorities. In the U.S., regional transmission organizations oversee multiple states, while renewable mandates are defined only at the state level. An analysis of the possible inefficiencies caused by this discrepancy is beyond the scope of this article and I leave it as a subject for future research.

Chapter 3

An Engineering-Economic Approach to Transmission Planning Under Market and Regulatory Uncertainties: WECC Case Study[1]

In this Chapter I propose a stochastic programming-based tool to support adaptive transmission planning under market and regulatory uncertainties. I model investments in two stages, differentiating between commitments that must be made now

[1]This study was published in Munoz et al. (2013a).

and corrective actions that can be undertaken as new information becomes available. The objective is to minimize expected transmission and generation costs over the time horizon. Nonlinear constraints resulting from Kirchhoff's voltage law are included. I apply the tool to a 240-bus representation of the Western Electricity Coordinating Council (WECC) and model uncertainty using three scenarios with distinct renewable electricity mandates, emissions policies, and fossil fuel prices. I conclude that the cost of ignoring uncertainty (the cost of using naive deterministic planning methods relative to explicitly modeling uncertainty) is on the same order of magnitude as the cost of first-stage transmission investments. Furthermore, I conclude that heuristic rules for constructing transmission plans based on scenario planning can be as suboptimal as deterministic plans.

3.1 Introduction

Electricity transmission networks are large interconnected systems used to ensure the reliable and economic delivery of power from generators to consumers. Recently, the National Academy of Engineering recognized electrification as *"the single most significant engineering achievement of the 20th Century"* (GEA, 2012). With an installed capacity of 1,100 GW and more than 160,000 miles of high-voltage transmission lines, the U.S. electricity system serves approximately 130 million customers with annual revenues totaling over $350 billion in 2010. Transmission comprises 10%

of the total system assets of $800 billion (DOE, 2003).

Historically, transmission investments were driven by load growth, remote siting of large thermal plants, and opportunities for inter-system exchanges of economic energy and reserves. Today, transmission is also seen as a key enabler of renewable energy integration, since the best renewable resources are often far from load centers and the existing grid. Considerable investment will be needed in the coming decade. WECC estimates that $20 billion in foundational transmission investments are needed by 2020 in the western U.S. to meet load projections and state Renewable Portfolio Standards (RPSs) (WECC, 2011). A similar study for California estimates that transmission investments to meet just that state's 33% RPS target by 2020 will cost approximately $16 billion (CPUC, 2009), which is double the annual cost of wholesale power in the CAISO market in 2011.

Complying with renewable goals at minimum cost to consumers will require careful consideration of trade-offs between the cost of transmission investments to remote resources and the quality and diversity of those resources. In vertically integrated markets, a central decision maker can, in theory, select the optimal combination of generation and transmission investments to meet demand and renewable mandates at minimum cost under the Integrated Resource Planning paradigm. But such coordination is a challenge in restructured markets where only transmission assets are centrally planned. Although transmission planning has been traditionally "reactive" to generation investments (i.e., generation investments first, transmission afterwards), transmission planning authorities increasingly recognize two facts. First, transmission investments influence the profitability of investment decisions concerning generation, demand-side management (DSM) and other resources, and therefore affect the siting and timing of those investments. Second, because large transmission projects can have longer lead-times than natural gas-fueled and renewable power plants and DSM, transmission commitments must be made before generation is constructed. Therefore, *"(c)apturing long-term benefits of transmission investments requires processes more akin to integrated resource planning in order to evaluate 'long-term resource cost' benefits (such as)...the ability to build new generation in lower-cost locations (and to)...find lower-cost (or higher-value) combination of transmission and generation investments to satisfy policy requirements, such as (renewable portfolio standards)"*(Pfeifenberger and Hou, 2012; Pfeifenberger, 2012). This has resulted in an "anticipative" or "proactive" philosophy being embodied in FERC Order 1000 (FERC, 2013) and a growing interest among planning authorities (such as the California ISO Awad et al. (2010)) to use transmission planning to steer the generation market towards potentially better social outcomes compared to the old reactive approach. For instance, the Eastern Interconnection States Planning Council has been sponsoring research on "Co-optimization models" (EISPC, 2012), which consider how generation investments react to transmission investment; examples of such models include Gu et al. (2012), Hobbs (1984), and Roh et al. (2007), as well as the model of this paper.

Proactive or anticipative planning doesn't come without challenges though. Planning for long-lived infrastructure before it is needed involves making assumptions about the timing, size and location of future generation investments that will depend strongly on network characteristics as well as on highly uncertain market and regulatory conditions (e.g., technology and fuel costs, environmental regulation, and renewable mandates). Disregarding any of these features can result in myopic plans and the risk of stranded transmission assets (Woolf, 2003; Sauma and Oren, 2006; Wong et al., 1999).

Methods now used in transmission planning studies have two limitations. First, planners usually rely on detailed production cost modeling tools and Monte Carlo simulation to assess the economic performance of a set of pre-defined transmission and generation configurations (e.g., PSS-E (SIEMENS, 2012), GridView (ABB, 2012), and PROMOD IV (VENTYX, 2012)). However, these commercial packages lack topology optimization capabilities and cannot suggest potentially better transmission configurations (O'Neill et al., 2013; Kahn, 2010). The few commercial packages that can optimize topology (e.g., NETPLAN (PSR, 2012)) account for neither the generators' responses to transmission investments nor uncertainties in market and regulatory conditions.

A second limitation arises from using scenario planning to cope with uncertainty. In scenario planning, several scenarios are defined that represent alternative future economic and regulatory conditions, and then a separate plan is developed separately for each scenario using either deterministic network optimization or a production costing-based comparison of pre-defined plans. Then investments that are attractive in all or most scenarios are identified as robust. Examples of such planning approaches are the Multi-Value Projects by the Midwestern ISO (MISO) (MISO, 2010), and the least-regret investments by California ISO (CAISO) (CAISO, 2012). The underlying assumption of these approaches is that investments needed for all or most scenarios provide a hedge against uncertainty and, thus, correspond to the projects that should be developed now. However, it has been proven theoretically that optimal stochastic investment strategies (i.e., ones that minimize probability-weighted costs across scenarios) cannot in general be constructed by such heuristics. Stochastic optima are rarely optimal for any individual scenario, and may include projects that would not be in the deterministic optimal plan for any particular scenario (Wallace, 2000) (an example is shown later in this paper for WECC.) For instance, a somewhat more expensive route for a circuit between two buses might keep more options open later for additional circuits in that corridor or connections to other circuits; the cost of this additional adaptability must be suboptimal for any particular scenario, but could be worthwhile under uncertainty. For these reasons, scenario planning and heuristics are limited for planning under uncertainty.

In this paper I propose a model for adaptive transmission planning that takes into account generators' response, Kirchhoff's Voltage Law (parallel flows), and uncertainty. I also include recourse or "wait-and-see" investment decisions, since in reality not all decisions must be made today, as some can be delayed until there is more information available. I apply my approach to a 240-bus representation of the WECC adapted from Price and Goodin (2011) to illustrate the insights that can be gained. Uncertainty is modeled with three scenarios with diverging environmental policies and fuel costs. I compare the economic performance of the optimal stochastic solution with deterministic investment strategies as well as heuristic rules used in current transmission planning studies. I also calculate the Expected Value of Perfect Information (EVPI) and the Expected Cost of Ignoring Uncertainty (ECIU, equal to the expected loss from using deterministic rather than stochastic programming). I find that in this case they both have the same order of magnitude for the WECC case study, and that the ECIU is approximately three times the cost of transmission investments in the first-stage.

The rest of the paper is organized as follows. In Section 3.2 I review the existing literature on multi-stage transmission planning under uncertainty, considering the response of generator investment and operations. My two-stage stochastic transmission planning model is formulated in Section 3.3. In Section 3.4 I describe my case study and assumptions regarding candidate renewable resources and scenarios. In Section 3.5 I present my results and discuss the limitations of the current approaches. Finally, I offer conclusions in Section 3.6.

3.2 Literature Review

Transmission planning using optimization is an active re-search area (Latorre et al., 2003). Initial approaches to finding cost-effective transmission plans were based on linear programming (Garver, 1970). However, due to scale economies, transmission capacity additions are better represented with discrete variables instead of continuous ones (Joskow and Tirole, 2005). This is an advantage if power flows are modeled using a linearized dc approximation (Schweppe et al., 1988), since Kirchhoff's Voltage Laws for candidate transmission lines can be enforced with linear disjunctive constraints instead of non-linear ones (Granville and Pereira, 1985; Munoz et al., 2012, 2013b). The resulting problem is formulated as a mixed integer linear problem and solved with commercial MIP solvers (Binato et al., 2001; Samarakoon et al., 2001; Bahiense et al., 2001; Alguacil et al., 2003).

There is also a broad literature on transmission planning under uncertainty (e.g., de la Torre et al. (1999), Buygi et al. (2004), Silva et al. (2006), Cedeño and Arora (2011)). However, most of it focuses on single-stage (or open loop) planning, assuming that all investment decisions must be made today, and ignoring the option of delaying commitments until more information is available. A number of studies have quantified option value by considering later decision (Hedman et al., 2005). But these studies have usually been of individual transmission investments, without considering alternatives elsewhere in the network. Multi-stage network planning models have been proposed in Akbari et al. (2011), Dehghan et al. (2011) and van der Weijde and Hobbs (2012), but the former studies take generation investments as exogenous, therefore ignoring interactions of transmission and generation investments. Game-theory approaches, on the other hand, can account for market power and generators' responses (Sauma and Oren, 2006), but network optimization based on such methods is computationally intractable for real-world applications.

Recently, van der Weijde and Hobbs (2012) proposed a two-stage stochastic transmission planning approach that takes into account generators' response, variable renewable, and long-run structural uncertainties. However, it was a radial network formulation applied to a seven zone representation of the Great Britain system, and only considered dc or radial ac links, thus ignoring the parallel flow impacts of Kirchhoff's Voltage Law. Here I improve van der Weijde and Hobbs (2012) by extending the formulation to include looped ac transmission networks as well as flowgate/nomogram-type constraints. I also model the effect of having differentiated state renewable mandates and the effect of the geographical definition of renewable certificate markets on the optimal configuration of transmission and generation investments. My model is applied to a network that is two orders of magnitude larger than the one in van der Weijde and Hobbs (2012). Besides applying the approach to a larger problem, the contribution of the present application is to compare the performance of heuristic rules that are commonly utilized in current transmission planning studies (e.g., MISO (MISO, 2010) and CAISO (CAISO, 2012)) with the optimal stochastic plan. No such comparison was made in van der Weijde and Hobbs (2012), even though heuristics are increasingly used in practice.

3.3 Model Description

I model transmission and generation investment decisions in two stages, each followed by market operations (see Figure 3.1). The two stages are divided into three periods, one before it is known which scenario will occur, and two after uncertainty is revealed. Investment decisions made in one period do not become available until the beginning of the following period.

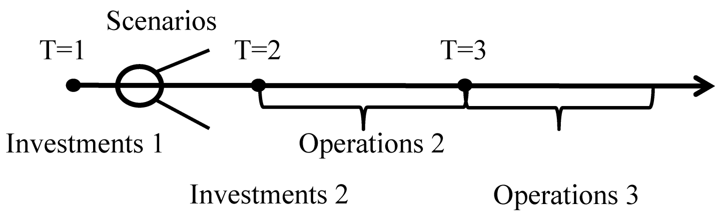

Figure 3.1: Timeline

Power flows are modeled using a linearized dc approximation (Schweppe et al., 1988). Generation intermittency and load variations are modeled by including a sample of hours chosen so that the averages, standard deviations, and correlations of wind and load across different locations are well approximated. As in van der Weijde and Hobbs (2012), I assume perfect competition and nodal pricing; as a result, the generation market equilibrium can be simulated by minimizing the present worth of total investment and operating costs, which is the same objective I assume for transmission planners. Because the objectives are consistent, the bilevel transmission planning-generation market planning problem can be reduced to a single combined transmission-generation optimization model.[2] Thus, my model is mathematically equivalent to an Integrated Resources Planning approach (Hobbs, 1995), except that in a deregulated market, generation investments represent the optimal market response to the transmission planner strategy, rather than a result of an integrated plan.

I assume that a cost penalty of $VOLL$ for failing to meet demand, but aside from deterministic derates of generation capacity, I do not explicitly model the possibility of lines or generation outages. Ideally, loss of load should instead be analyzed using a probabilistic production cost simulation. However, the focus of this paper is on transmission additions that are motivated by economics: savings in costs of investing in and operating resources, and the need to develop least-cost strategies to achieve renewable integration and other policy goals (as in FERC Order 1000 (FERC, 2013)). Although reliability is, and will remain, an important driver of some transmission additions, the economic factors considered in this paper are the primary drivers behind large interregional transmission proposals today.[3]

[2]The conditions for equivalence of market equilibria to the solution of a single optimization model are discussed in Gabriel et al. (2012).

[3]Transmission additions that are primarily motivated by improvements in reliability must be evaluated by a different set of techniques. When assessing the reliability implications of new transmission, reliability metrics such as the "one day in ten year" loss of load expectation (LOLP) or the expected energy not served (EENS) are relevant (Billinton and Allan, 2003). They are generally modeled in industry practice using probabilistic simulations considering, for instance, line outages, generator forced outages, the full distribution of load, and wind variability. Examples of such simulation models include Concorda MARS (MARS, 2013) and CRUSE (Lu et al., 2005). Such modeling has not yet been integrated in economic optimization models for transmission but is an important topic for future research.

Nomenclature

Sets and Indices:

B : Buses, indexed b, p;

B_j : Buses within reliability region j;

E : Regions with CO_2 limits, indexed e;

FG : Flowgates, indexed a;

G : Generators, indexed k;

G_b : Generators at bus b;

G_i : Generators at zone i;

G_R : Renewable generators;

G_C : Candidate generators;

G_I : Intermittent generators;

G_{NI} : Non-intermittent generators;

H : Hours, indexed h;

J : Reliability regions, indexed j;

L : Transmission lines, indexed l;

L_E : Existing lines;

L_C : Candidate lines;

R : Regions with renewable mandates, indexed i;

S : Scenarios, indexed s;

T : Periods, indexed t, u, and v;

Ω_l : Pair of nodes connected to line l;

Parameters:

$CAP^t_{e,s}$: Carbon emissions limit;

$CX^t_{l,s}$: Capital cost of line;

$CY^t_{k,s}$: Capital costs of generator;

$D^t_{b,h,s}$: Forecasted demand;

$ELCC_k$: Effective Load Carrying Capability factor;

EM_k : Carbon emissions rate;

$\overline{F_l}$: Line capacity;

$\overline{FG_a}$: Flowgate limit;

h^* : Peak demand hour;

M_l : Large positive number;

$MC^t_{k,s}$: Generation marginal cost;

NC^t_s : Noncompliance penalty;

p_s : Probability of scenario s;

RM_j : Reserve margin requirement;

$RPS^t_{i,s}$: Renewable obligation;

S_l : Line susceptance;

V_t : Period length;

$VOLL$: Value of loss load;

$W_{k,h}$: Hourly capacity factors for wind and solar;

$\overline{Y_k}$: Maximum resource potential;

Y^0_k : Installed generation;

YR^t_k : Retirement of generation capacity;

δ : Discount rate;

$\Phi_{b,l}$: Element of node-line incidence matrix;

$\Psi_{a,l}$: Element of flowgate-line incidence matrix;

Variables:

$f^t_{l,h,s}$	:	Power flow;
$g^t_{b,k,h,s}$	:	Generation;
$n^t_{i,s}$	:	Noncompliance of renewable target;
$r^t_{b,h,s}$	:	Load curtailment;
$x^t_{l,s}$	:	Transmission investment decision;
$y^t_{k,s}$	:	Generation new build;
$\theta^t_{b,h,s}$	:	Phase angle;

Objective Function: I define investment costs for a single scenario, before uncertainty is revealed, in $t = 1$ and for multiple scenarios, after uncertainty is revealed, in $t = 2$, as the sum of transmission and generation investments:

$$I^t_s = \sum_{l \in L_C} CX^t_{l,s} x^t_{l,s} + \sum_{k \in G_C} CY^t_{k,s} y^t_{k,s} \tag{3.1}$$

Operating costs O^t_s for periods $t = 2, 3$ and scenario s account for generators operating costs OC^t_s, and penalties OP^t_s for load curtailments and noncompliance with renewable targets. To maintain a manageable model size, I simulate market operations for a single year at the beginning of periods 2 and 3, and assume that they represent operations for the remaining years in each period.[4]

[4]Here I define the model for a full year (H=1..8760). A sample of hours can be used instead by weighting each sampled hour's variables by $\frac{|H|}{8760}$ in Equations 3.2, 3.3, 3.15, and 3.16.

$$OC_s^t = \sum_{v=1}^{V_t} \left(\frac{1}{1+\delta}\right)^{v-1} \sum_{h\in H}\sum_{k\in G} MC_{k,s}^t g_{k,h,s}^t \tag{3.2}$$

$$OP_s^t = \sum_{v=1}^{V_t} \left(\frac{1}{1+\delta}\right)^{v-1} \left[\sum_{b\in B} VOLL\ r_{b,h,s}^t + \sum_{i\in R} NC_s^t n_{i,s}^t\right] \tag{3.3}$$

$$O_s^t = OC_s^t + OP_s^t \tag{3.4}$$

The cost-minimization problem is then defined as:

$$min\ I^1 + \sum_{s\in S} p_s \left[\left(\frac{1}{1+\delta}\right)^{V_1} (I_s^2 + O_s^2) + \left(\frac{1}{1+\delta}\right)^{V_1+V_2} O_s^3\right] \tag{3.5}$$

Constraints. The above objective is optimized subject to:

Kirchhoff's Current Law:

$$\sum_{l\in L} \Phi_{b,l} f_{l,h,s}^t + \sum_{k\in G_b} g_{k,h,s}^t + r_{b,h,s}^t = D_{b,h,s}^t \quad \forall b,h,s \tag{3.6}$$

Kirchhoff's Voltage Law for existing and candidate lines, respectively:[5]

[5] An ideal choice of M_l is equal the maximum angle difference times the susceptance of candidate line l. Thus, if the line is not built, the left-hand-side of equation (3.8) is unconstrained. Values of M above this minimum would still enforce constraint (3.8), but can cause numerical difficulties in branch-and-bound algorithms (Bahiense et al., 2001). Here I only consider reinforcements to the trunk transmission system and radial interconnections, therefore, the maximum angle difference is bounded by the maximum power flow in any line connecting buses b and p. Bounds for candidate lines that create new loops in the system, or that interconnect initially disconnected systems, can be computed by solving shortest- or longest-path problems, respectively (Binato et al., 2001).

$$f^t_{l,h,s} = S_l(\theta^t_{b,h,s} - \theta^t_{p,h,s}) \quad \forall (b,p) \in \Omega_l, l \in L_E, h, s, t \tag{3.7}$$

$$|f^t_{l,h,s} - S_l(\theta^t_{b,h,s} - \theta^t_{p,h,s})| \leq M_l(1 - \sum_{u=1}^{t} x^u_{l,s}) \quad \forall (b,p) \in \Omega_l, l \in L_C, h, s, t \tag{3.8}$$

Note that the right hand side is equal to zero if a line is built, but otherwise is a very high number so that the constraint doesn't bind (Granville and Pereira, 1985; Binato et al., 2001).

Thermal limits on existing and candidate lines:

$$|f^t_{l,h,s}| \leq \overline{F_l} \qquad \forall l \in L_E, h, s, t \tag{3.9}$$

$$|f^t_{l,h,s}| \leq \overline{F_l} \sum_{u=1}^{t} x^u_{l,s} \quad \forall l \in L_C, h, s, t \tag{3.10}$$

Flowgates. I assume that the capacity of interfaces be-tween neighboring systems are defined as a fraction of the aggregated capacity of the lines, so the constraints can be updated depending on reinforcements to existing corridors:

$$\sum_{l \in L} \Psi_{a,l} f^t_{l,h,s} \leq \overline{FG_a} \left[\sum_{l \in L_E} |\Psi_{a,l}| \overline{F_l} + \sum_{l \in L_C} \sum_{u=1}^{t} |\Psi_{a,l}| \overline{F_l} \; x^u_{l,s} \right] \quad \forall a, h, s, t \tag{3.11}$$

Maximum generation:

$$g_{k,h,s}^{t} \leq W_{k,h}(Y_{k}^{0} + \sum_{u=1}^{t}[y_{k,s}^{u} - YR_{k}^{u}]) \quad \forall k,h,s,t \tag{3.12}$$

Installed reserve margins: I enforce installed reserve margins in predefined reliability areas. Intermittent generators are included using Effective Load Carrying Capability Factors (ELCCs).

$$\begin{aligned} &\sum_{k \in G_{NI} \cap G_j} (Y_k^0 + \sum_{u=1}^{t} y_{k,s}^{u}) + \sum_{k \in G_I \cap G_j} ELCC_k (Y_k^0 + \sum_{u=1}^{t} y_{k,s}^{u}) \\ &\qquad \geq (1 + RM_j) \sum_{b \in B_j} D_{b,h,s}^{t} \quad h = h^* \ \ \forall j,s,t \end{aligned} \tag{3.13}$$

Generation resource constraints that limit construction in each region:

$$\sum_{u=1}^{t} y_{k,s}^{t} \leq \overline{Y_k} \quad \forall k \in G_C, s \tag{3.14}$$

Renewable Portfolio Standards that place a lower bound on renewable energy output in a defined region, accounting for credits that are allowed to be imported from other regions:

$$\sum_{k \in G_R \cap G_i} \sum_{h \in H} g_{k,h,s}^{t} + n_{i,s}^{t} \geq RPS_{i,s}^{t} \sum_{k \in G_i} \sum_{h \in H} g_{k,h,s}^{t} \ \ \forall i,s,t \tag{3.15}$$

Emissions constraints that limit total emissions of CO_2 within defined areas:

$$\sum_{k\in G_e}\sum_{h\in H} g^t_{k,h,s} EM_k \leq CAP^t_{e,s} \quad \forall e,s,t \tag{3.16}$$

Nonnegativity and integrality:

$$g^t_{k,h,s}, y^t_{k,s}, n^t_{i,s}, r^t_{b,h,s} \geq 0 \qquad \forall k,b,h,i,s,t \tag{3.17}$$

$$x^t_{l,s} \in \{0,1\} \qquad \forall l,s,t \tag{3.18}$$

3.4 Case Study: WECC 240

The WECC 240-bus test-case is a network reduction of the synchronized western North American interconnection (Price and Goodin, 2011). It consists of 240 buses, 448 transmission elements, and 157 aggregated generators with a total installed capacity of 224 GW. The model also includes limits for 28 flowgates that are normally enforced during operations in the WECC. Since the original WECC 240 test-case was created to replicate present market operations, it lacks information about candidate renewable resources or transmission alternatives that is necessary to test my transmission-planning approach.

For this example, I assume a ten-year lag between decisions to build transmission and generation, and project completion. Therefore, I model investment decisions at the beginning of years 2013 and 2023 (period 1, $V_1 = 10$). Market operations are

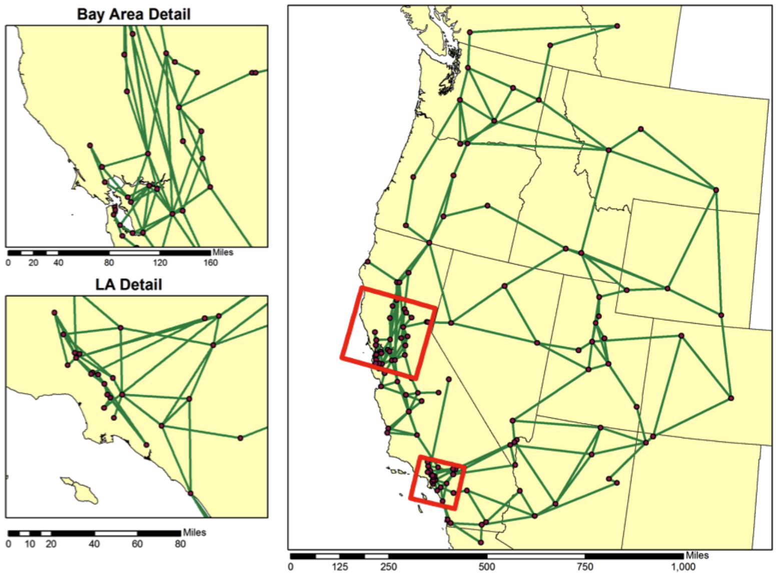

Figure 3.2: WECC 240-Bus System

modeled between years 2023 and 2033 (period 2, $V_2 = 10$), and between years 2033 and 2063 (period 3, $V_3 = 30$).

Here I describe my main assumptions in adapting this test-case for the long-term transmission planning study.

3.4.1 Generation Assumptions

I use projections of both capital and fuel cost data from the Energy Information Administration (EIA) (EIA, 2012). Capital costs of new generation (CX) include both overnight capital costs and the sum of the discounted fixed operation and maintenance costs. I use a geographic information system (GIS) to spatially analyze renewable resource potential from the Western Renewable Energy Zones study (WREZ,

Table 3.1: Candidate Generation

Technology	Overnight Capital Cost [$/kW]	Fixed O&M Cost [$/kW]	Variable O&M Cost [$/MWh]	Heat Rate [MMBtu /MWh]
Coal CCS	4,579	63.21	9.05	12.0
CCGT	978	14.39	3.40	7.1
CCGT CCS	2,060	30.25	6.45	7.5
CTGT	665	6.70	9.87	9.8
Hydro	3,500	15	6	-
Wind	2,438	28	0	-
Solar PV	5,400	22	0	-
Biomass	3,860	103	5	12.5
Geothermal	4,141	84	9	-

2012) and the Renewable Energy Transmission Initiative in California (RETI, 2010). Wind generation variability is represented using 54 spatially aggregated hourly profiles from NREL's Western Wind Resources Database (NREL, 2012b). Similarly, solar intermittency is included in 29 regions with hourly profiles generated using NREL's PVWatts tool (NREL, 2012a). In terms of conventional generation, I assume that no new nuclear or large hydroelectric power plants are going to be built in the WECC. EPA's new carbon pollution standard makes it difficult to build new conventional coal power plants (EPA, 2012), so I only allow for new coal generation that has CCS technologies. I retire 11,752 MW of once-through cooling power plants in California and 1,572 MW in the rest of the WECC, as projected in the WECC 10-Year Regional Transmission Plan (WECC, 2011). Table 3.1 summarizes the costs for candidate generators. Appendix B includes a more detailed description of generation investment alternatives.

I impose installed reserve margins of 12% within 8 different regions of the WECC. Intermittent generators are included in reserve margins with derated capacities using typical ELCC values. Finally, I assume that hydroelectric operations will be consistent with those in the WECC 240 profiles for the year 2004. Operations of hydroelectric power plants are constrained by both the technical characteristics of the power plants and by environmental constraints specific to each basin. Flexible dispatch of hydropower, as well the introduction of other energy storage technologies, can be used to provide energy, capacity, and ancillary services (Hu et al., 2012; Jewell and Hu, 2012), all of which could result in potential savings in transmission and generation infrastructure and improve the economics of renewable generation. Capturing these benefits, however, would require chronological simulation of operations and consideration of multiple scenarios of hydrological conditions (Gorenstin et al., 1993; Nordlund et al., 1987), both of which are beyond the scope of this chapter, but should be the subject of future research.

3.4.2 Transmission Assumptions

The original WECC-240 test case does not include ratings for all transmission elements. For unconstrained lines, I approximate thermal limits based on line lengths, voltage levels, and St. Clair line loadability curves (Gutman et al., 1979). However, I assume that all transformers are unconstrained, since their capital costs are relatively low compared to transmission upgrades. Based on the Western Renewable Zones Study, I group candidate resources into 31 renewable hubs distributed throughout the WECC that require new transmission capacity to deliver power to the existing grid. Consequently, I consider two types of transmission upgrades: backbones and interconnections. Backbone reinforcements are capacity additions parallel to existing corridors, while interconnections are radial links from initially disconnected renewable hubs to the nearest existing high voltage buses. For illustration purposes, I limit the availability of rights-of-way to a maximum of two new 500 kV circuits for the trunk system, and four for interconnections. This assumption can be relaxed to include more alternatives of different voltage levels, but at the expense of a larger model. The full list of candidate interconnections to renewable hubs and transmission backbone alternatives are in Tables B.4 and B.8 in Appendix B.

3.4.3 Scenarios

Environmental policies and renewable mandates in the U.S. vary greatly among states. While California, for example, has a stringent renewable goal of 33% by 2020, neither Wyoming nor Idaho now have renewable mandates (DSIRE, 2012). Furthermore, some states allow Load Serving Entities (LSEs) to meet a fraction of the state mandates using out-of-state renewable generation through Renewable Energy Certificates (RECs), which are tradable financial instruments created from electricity generated from qualifying renewable resources (Wiser et al., 2007). Although there is currently neither a national nor a WECC-wide REC markets, their implementation would relax the geographic heterogeneity between state RPS goals and result in renewable generation investments in the most cost-effective locations (Holt and Bird, 2005). In contrast, a shift in the focus of future environmental regulation from state renewable mandates towards carbon emissions limits would give generators fewer incentives to invest in renewables and would, instead, promote the use of clean conventional generators, especially in my scenario of low natural fuel prices.

For illustration purposes, I develop three scenarios that represent uncertainty in regulatory and market conditions.[6] Although load growth and technology costs are also important sources of uncertainty, here I assume they are the same in all scenarios. I also assume that load patterns will be the same as in 2004, although changes in load shapes, due to, e.g., demand response and electric vehicles, can affect the optimal transmission and generation investment plans (Kazerooni and Mutale, 2010b,a; Prabhakar et al., 2012; De Jonghe et al., 2012). Multiple scenarios for load growth and load shapes can be included in additional scenarios as in van der Weijde and Hobbs (2012), while demand management can be included as a resource and decision variable in the model, but at the expense of computational efficiency. The

[6]The scenarios defined in my study are only used to illustrate an application of my methodology and do not constitute an attempt to represent the full range of scenarios that might be used in an actual application (e.g., as in the MISO (MISO, 2010) and CAISO (CAISO, 2012) studies), which is the reason why I treat parameters independently. In real-world studies, scenarios can be defined by managers and stakeholders using techniques for expert elicitation. Since Royal Dutch Shell's pioneering use of scenarios in 1960's, a number of systematic approaches have been proposed and applied to define sets of scenarios (Mahmoud et al., 2009).

three scenarios, assumed equally likely, are defined as follows (Table 3.2):

- **State RPS**: This is the reference case. I assume that renewable goals remain as projected and differentiated by state (DSIRE, 2012), but allow 25% of each state's RPS to be met with out-of-state resources. The fuel prices I use are average projections from the EIA.

- **33% WECC**: This is an analog to the scenario modeled in Mills et al. (2011). In this case there is a strong pressure on renewables with a 33% WECC-wide RPS goal together with high fuel prices. Unlike the State RPS scenario, here I assume the existence of an efficient WECC-wide REC market allowing renewable generation to be built in the most cost-effective locations.

- **Carbon**: In this scenario, environmental regulation focuses on carbon emissions reductions instead of renewable mandates, and fuel prices are lower than average projections. I set emissions limits based on the Waxman/Markey bill that passed the U.S. House of Representatives in 2009, which sets carbon reduction targets of 17% below 2005 levels by 2020 and of 42% below 2005 levels by 2040 (ACESA, 2012).

Table 3.2: Summary of Scenarios

	Scenarios		
	State RPS	33% WECC	Carbon
Probability	1/3	1/3	1/3
Natural Gas prices [$/MMBtu]			
2023	5.01	6.81	3.96
2033	6.06	7.82	4.81
Coal prices [$/MMBtu]			
2023	1.89	2.38	1.51
2033	2.02	3.14	1.34
Total renewable goals [$TWh/Year$]			
2023	229	336	0
2033	290	417	0
Emissions limits [$MMTCO_2/Year$]			
2023	No limit	No limit	292
2033	No limit	No limit	183
Certificate trading	≤25% of state goals	Yes	Yes

3.5 Results

All model runs reported in this chapter were done in the AIMMS 3.12 modeling language using the CPLEX 12.4 solver on a 32-core workstation with 112 GB of RAM. In order to keep the model size small, I simulated market operations using a sample of only 10 hours and ignored ramping limits, which resulted in a model with 110,000 variables (2,040 binary variables for transmission investments) and 240,000 constraints for the stochastic case. The solution time to solve the deterministic equivalent of the stochastic formulation of the problem was 2.5 hours, and 1 hour for the deterministic cases. Larger transmission networks, more scenarios, or more granular representation of operations, however, will increase the size of the problem significantly, and the approach of solving a single deterministic equivalent might then be computationally prohibitive. Decomposition might then be the most practical approach to solving these problems. Examples of alternative decomposition-based solution methods include Benders decomposition (Binato et al., 2001), which divides the problem into a master or investment problem and subproblems, and Progressive Hedging (Rockafellar and Wets, 1991), which relies on scenario decomposition instead. These alternative methods were, however, unnecessary for the WECC model described here. As in Binato et al. (2001), I first relaxed all the disjunctive constraints and used that solution as a starting point for the full formulation. I stopped computation once I reached a MIP gap of 1%. To ensure electricity load and renewable energy targets are met, I used a high noncompliance penalty of 500 $/MWh.

3.5.1 Planning Based on Deterministic Scenario Models

Scenario planning is a common practice in industry when important investment decisions must be made under uncertainty. By developing a set of scenarios that represent the uncertain future, decision makers can analyze different investment strategies for each scenario, and also assess the performance of other investment strategies resulting from heuristic planning procedures. Here I find the optimal deterministic plan for each scenario s^* by setting its probability p_s^* to 1 and removing all constraints for $s \neq s^*$. Tables 3.3 and 3.4 summarize the optimal first-stage transmission investment strategies for different planning approaches. Second stage transmission and generation investments are discussed in Appendix B.4.Note that for the 33% WECC scenario, it is optimal to build multiple lines to access distant renewable hubs, while for the Carbon scenario it is cost-effective to build only one such line and instead meet emissions targets using a combination of near-load renewable resources and natural gas generators. The minimum system costs for each deterministic scenario (CPI_{s*}) are \$565.5 Billion for State RPS, \$711.9 Billion for 33% WECC, and \$495.0 Billion for the Carbon scenario. I refer to the probability-weighted sum of these costs as the Expected System Costs under Perfect Information ($EC|PI$), which provides a lower bound upon the expected cost under uncertainty for any actual strategy:

Table 3.3: First-stage Investments in Radial Interconnections to renewable hubs

Approach / Corridor N	I2	I5	I6	I8	I9	I10	I11	I14	I20	I23	I24	I25	I26
D-Carbon												1	
D-33% WECC	1	4	1	3	1	1	2	1	1	1	1	1	
D-State RPS		2		2	1				1		1	1	1
Heuristic I												1	
Heuristic II		2		2	1				1		1	1	
Heuristic III	1	4	1	3	1	1	2	1	1	1	1	1	1
Stochastic	1	4	1	3	1	1	2	1	1		1	1	1

Table 3.4: First-stage Investments in Transmission Backbones

Approach / Corridor N	19	37	56	68	72	73	74	92	95	125	133	136	137	143	151	157	168	169	201	202	218	222	237	238
D-Carbon				1					1	1	1		1	2								2	1	2
D-33% WECC		1			1	1	2		1								1	1	1		1	1	2	
D-State RPS	2	1	1					2		2		1								1		1		2
Heuristic I																						1		
Heuristic II		1							1	1												1	1	2
Heuristic III	2	1	1	1	1	1	2	2	1	2	1	1	1	2			1	1	1	1	1	2	2	2
Stochastic		1		1			2		1	2			1		1	1	1				1	1		2

Table 3.5: First-Stage Transmission Investments Costs and Economic Performance of Planning Strategies. All costs in Billion USD.

	First Stage Transmission Investments			Total Cost Under Each Scenario			Expected
Approach	Backbones	Interconnections	Total	Carbon	33% WECC	State RPS	System Costs
D-Carbon	4.0	0.1	4.1	553.1	1,000.4	631.1	728.2
D-33% WECC	6.1	9.3	15.4	598.7	724.6	637.4	653.6
D-State RPS	7.2	4.1	11.3	558.6	857.0	585.4	667.0
Heuristic I	0.3	0.1	0.4	777.0	1,217.7	859.3	951.3
Heuristic II	2.4	3.9	6.3	574.0	853.8	609.8	679.1
Heuristic III	14.7	9.5	24.2	590.5	721.2	621.9	644.5
Stochastic	5.6	9.2	14.8	575.2	716.9	616.5	636.2
System Costs Under Perfect Information (CPI_s) (Both transmission and generation have perfect information)				495.0	711.9	565.5	590.8

$$EC|PI = \sum_{s \in S} p_s CPI_{s*} = \$590.8 \text{ Billion} \tag{3.19}$$

However, the minimum cost under perfect information is overly optimistic, since, in reality, other scenarios for which the deterministic plans are suboptimal can still occur.

In Table 3.5 I summarize the costs of first-stage transmission investments in backbones and interconnections, as well as the performance of different first-stage transmission investment strategies. I estimate expected system costs for deterministic approaches ($ECDS_s$) by imposing their first-stage transmission investment decisions onto the stochastic model, which is then free to choose second-stage investments that differ among the scenarios, but assuming that generators still take uncertainty into account in the first-stage. Because the first stage decisions are constrained in this manner, the objective function must be no better than that for the full stochastic model, since the latter is free to choose the first stage decisions to minimize cost. Note that of the three deterministic alternatives, the D-33% WECC is the one requiring the highest investment in transmission in the first stage, but these are the investments that will result in the lowest expected system costs when tested against all scenarios (see Total Cost Under Each Scenario in Table 3.5). In contrast, planning the grid using the D-Carbon strategy yields high regrets, compared to the system costs under perfect information, if the resulting scenarios are 33% WECC or State RPS

A common practice today in transmission planning studies is to construct investment strategies by combining deterministic results using heuristic rules. For example, one approach used both at CAISO (CAISO, 2012) and MISO (MISO, 2010) is to recommend projects chosen by deterministic models in all or most scenarios. Here I emulate these approaches with two heuristic rules for choosing lines to build immediately.

- *Heuristic I:* Select lines that are built in the first stage in each and every scenario-specific deterministic model.
- *Heuristic II:* Select lines that are built in at least two out of the three scenario-specific deterministic models.

A more ambitious approach followed by the Alberta System Operator (ASO) is to plan for a congestion-free network so that any possible scenario of generation investment is accommodated (AESO, 2012). Therefore, as a proxy for the ASO's planning approach, I consider an additional heuristic:

- *Heuristic III:* Select any lines that are built in the first stage of any scenario-specific deterministic model.

Table 3.5 shows that the heuristics modeled after the procedures proposed by the CAISO and MISO actually do worse than most plans created using traditional deterministic methods. In particular, *Heuristic I* yields higher expected costs than planning myopically for any one deterministic scenario. This is evidently because the marginal value of new transmission is very high for the first few additions (because of avoided noncompliance penalties), and that heuristic constructs the fewest lines. Meanwhile, *Heuristic II* does better than planning using the deterministic Carbon scenario, but still is worse than the deterministic D-33% WECC and D-State RPS plans. In contrast, *Heuristic III* (build all lines identified in any scenario) gives lower expected system costs compared to any of the deterministic plans or other heuristics. Note that this advantage is not a necessary result, and depends on the data. But III requires nearly twice as much first-stage transmission investment as any other plan ($24.2B, Table 3.5) and therefore has a high risk of stranded assets. In sum, since scenario planning as well as heuristics based upon scenario plans do not attempt to identify network designs that optimize performance across all scenarios simultaneously, they are a weak approach for planning under uncertainty.

3.5.2 Optimal Stochastic Planning

In contrast, the model described in Section III provides a single recommendation for transmission investment commitments now (here, 2013, for implementation by 2023). My approach also models recourse (second-stage) decisions, which are investments that should not start until 2023 when there is more clarity about market and regulatory conditions. This is analogous to a Real Options approach, where the cost difference between the first-stage transmission investments of the stochastic plan and a reference strategy (e.g., a deterministic or heuristic-based plan) constitute the price of the option, which can be exercised later depending on the state of the system (Wang and Neufville, 2004).

By definition, the investment plan recommended using my two-stage stochastic approach yields the lowest expected system costs compared to both deterministic and heuristic approaches (see Table 3.5). The optimal stochastic solution recommends only \$14.8 Billion in transmission investments in the first-stage, \$9.4 Billion less than *Heuristic III*, and results in expected system costs of \$636.2 Billion ($ECSS$), or \$8.3 Billion less than *Heuristic III*. Note that the set of transmission investments recommended by the stochastic approach includes projects (B151 and B157) that would not be chosen for any scenario under perfect information. In other words, these two projects are suboptimal in retrospect for any of the three scenarios; however, they are optimal in an expected value sense since they are physical hedges that impart more flexibility to the system than projects selected under the deterministic approaches.[7]

Besides the optimal strategy, I can also use the stochastic approach to calculate two indices from the decision analysis literature (Birge and Louveaux, 1997) of the economic consequences of uncertainty, the Expected Value of Perfect Information ($EVPI$) and the Expected Cost of Ignoring Uncertainty ($ECIU$). The $EVPI$ provides an upper bound on the value of better forecasts for the uncertain parameters, and is calculated as:

[7]Please refer to Appendix B.3 for further discussion on first-stage transmission and generation investment plans.

$$\begin{aligned} EVPI &= ECSS - EC|PI \\ &= \$636.2B - \$590.8B = \$45.4 \text{ Billion} \end{aligned} \tag{3.20}$$

That is, this is the cost of the optimal stochastic solution $ECSS$ minus (the necessarily no worse) expected cost across scenarios if generation and transmission planners could perfectly foresee which scenario would occur ($EC|PI$).

The $ECIU$ is, on the other hand, a measure of the expected cost savings from using the stochastic approach for transmission planning instead of a naive deterministic one, but assuming that generators still consider all scenarios.[8] It is formally defined as the difference between the expected performance of the deterministic solutions minus the expected costs of the stochastic plan (Birge and Louveaux, 1997):

$$\begin{aligned} ECIU &= \sum_{s \in S} p_s ECDS_s - ECSS \\ &= \frac{1}{3}(728.2B + 653.6B + 667.0B) - 636.2B \\ &= \$46.7 \text{ Billion} \end{aligned} \tag{3.21}$$

[8]A more detailed description of how to calculate $EVPI$ and $ECIU$ for both transmission and generation, and transmission only is given in van der Weijde and Hobbs (2012).

3.6 Conclusions

In this essay I describe a tool for transmission planning under gross economic and policy uncertainty. It is formulated as a two-stage stochastic mixed-integer linear program, and I solve it with a commercial optimization package. It improves upon van der Weijde and Hobbs (2012) in that I model a system that is two orders of magnitude larger with a meshed network in which Kirchhoff's Voltage Law as well as interface (flowgate) constraints are considered. Using the WECC 240-bus test case and three scenarios representing carbon and renewable policy uncertainties, I compare the economic performance of transmission strategies based on deterministic scenario planning, heuristic combination of scenario plans, and stochastic optimization. The transmission investments recommended by my stochastic approach outperform the deterministic plans by \$46.7B in the expected value of the present worth of costs ($ECIU$), and by \$17.4B compared to the best deterministic solution (D-33% WECC), which is triple the cost of first-stage transmission investments in the stochastic solution. Thus, better transmission planning can yield cost savings exceeding the cost of the lines themselves.

Since deterministic approaches do not value flexibility (Wallace, 2000), heuristic rules that select lines based on the common elements of deterministic scenario plans may perform no better than deterministic strategies. Indeed, in my case study, they perform worse. However, investing in all the lines found in the deterministic solutions as a heuristic to hedge against uncertainty can, in turn, yield lower expected system costs compared to other heuristics, but requires nearly double the transmission investment in the first stage and thereby posing a higher risk of stranded transmission assets.

In contrast, stochastic planning explicitly considers the flexibility of a system to adapt to uncertain developments. Plans that incur extra costs for flexibility are unlikely to be found to be optimal for any individual scenario, and so would be overlooked in deterministic planning (O'Neill et al., 2013; Wallace, 2000). As my results illustrate, the optimal stochastic strategy not only differs from all deterministic and heuristic solutions, but also includes line additions not identified in any of the deterministic plans. Thus stochastic transmission planning that considers optionality and flexibility from the entire network's perspective are needed.

One potential direction of future work in this research would be the implementation of decomposition algorithms to solve large-scale problems with dozens of scenarios. A potentially efficient method that could leverage parallel computer systems is Progressive Hedging (Rockafellar and Wets, 1991). This algorithm could be used to decompose the stochastic transmission planning problem on a per-scenario basis by relaxing non-anticipativity constraints and, under such a scheme, the only limitation to the number of scenarios would be the number of independent computer nodes available.

Chapter 4

New Bounding and Decomposition Approaches for Multi-Area Transmission and Generation Planning With Large Amounts of Intermittent Generation

This chapter describes a two-phase bounding and decomposition approach to compute optimal or near-optimal solutions to large-scale transmission and generation planning problems in which policy constraints are designed to incentivize high amounts of intermittent generation in electric power systems. The bounding phase exploits Jensens inequality to define a new lower bound, which I also extend to the case of stochastic problems with expected-value constraints. The decomposition phase, in which I tighten the bounds, is an improvement of the regular Benders algorithm that I utilize to shrink the residual solution gap from the bounding phase. The lower bound is tightened by using the same Jensens inequality-based approach to introduce an auxiliary lower bound into the Benders master problem. Upper bounds for both phases are computed using statistical estimates of an operations problem that I calculate using a sub-sampling approach implemented in a parallel computer system. I illustrate my methodology using a realistic 240-bus representation of the Western Electricity Coordinating Council using one year of hourly demand, wind, solar, and hydro levels from historical data. Numerical results show that only the bounding phase is necessary if loose optimality tolerances are acceptable. Attaining tight solution tolerances, however, requires utilization of the decomposition phase, which performs much better in terms of convergence speed than attempting to solve the problem using either algorithm, the bounding method or Benders decomposition, separately. I also show that exploitation of Benders cuts that are derived from a relaxed (linear programming) version of the original mixed integer problem can greatly accelerate convergence of the Benders procedure for the original problem.

CHAPTER 4. NEW BOUNDING AND DECOMPOSITION APPROACHES FOR MULTI-AREA TRANSMISSION AND GENERATION PLANNING WITH LARGE AMOUNTS OF INTERMITTENT GENERATION

4.1 Introduction

The electric power industry has been one of the main areas of application of optimization algorithms (Hobbs, 1995). This sector comprises 2% of the U.S. economy, which provides strong economic incentives for electric utilities to plan and operate power infrastructure efficiently. Increasing amounts of generation from renewable resources challenge short- and long-term operations in the electric power industry and promote the development of new decision-support tools to account for their variability and unpredictability. For instance, new unit commitment models that explicitly factor in uncertainty in the availability of power supply from wind and solar generators often yield lower dispatch costs when compared to traditional deterministic unit commitment approaches, but these come at the expense of higher computational complexity (Bertsimas et al., 2013; Papavasiliou and Oren, 2013). Investment planning models, on the other hand, face the challenge of capturing the true economic value of these resources to meet forecasted demand as well as renewable and environmental goals at minimum cost for consumers. First, resource-specific characteristics, such as locational constraints and distance from load centers and the existing transmission grid, require analysis of both transmission and generation investment alternatives on a system-wide basis. Second, failure to capture the variability and spatial correlations among all intermittent resources will likely result in suboptimal investment recommendations (Joskow, 2011). In this chapter I focus on solution approaches that reduce the computational effort required to deal with these challenges in multi-area generation and transmission planning models, yielding practical methods to solve such models.

Because of computational limitations, as well as uncertainty in long-term forecasts of demand levels and capacity factors of intermittent resources, investment planning models have been traditionally disconnected from fine-grained operating planning models (Palmintier and Webster, 2011). To achieve computational tractability, these planning approaches instead utilize deterministic or probabilistic production cost models (Hobbs, 1995; Kahn, 1995) that a) approximate the load or net-load duration curves using a few number of steps (e.g., peak, shoulder and off-peak demand levels), b) ignore spatial correlations between demand zones and intermittent generation across multiple regions, and c) neglect the chronology of hours and thereby ramping constraints and start-up costs. Early planning models only considered single-area load duration curves based on time-series of historical and forecasted data (Anderson, 1972; Booth, 1972), but these were later improved, through the use of Gram-Charlier series for instance (Caramanis et al., 1982), to account for the effect of non-dispatchable technologies, such as wind and solar, on the optimal generation mix. A simpler approach that matches some of the moments of the dataset of demand, wind, solar, and hydro levels is the one used by van der Weijde and Hobbs (2012), where the sample of hours that best approximates the means, standard deviations and correlations of the state space is selected to determine the optimal portfolio of transmission and generation investments. Further refinements and analyses on the use of load-duration curves in planning models considering unit commitment variables and constraints are in Palmintier and Webster (2011), Shortt et al. (2013), and de Sisternes and Webster (2013), but only applied to generation and not transmission planning. None of these approximation methods, however, provide metrics (e.g., bounds) to quantify the effect of the quality of the approximations on the resulting investment plans and the total system costs and, therefore, they can only be deemed as heuristics.

Large-scale applications and computational limitations motivated researchers to solve generation and transmission planning models using Benders decomposition (Bloom, 1983; Bloom et al., 1984; Pereira et al., 1985; Sherali et al., 1987; Sherali and Staschus, 1990). This method separates the investment problem (i.e., master problem) from the probabilistic production cost problems (i.e., subproblems), which can then be solved independently taking advantage of parallel computer systems (Nielsen and Zenios, 1997). The quality of the investment plans proposed in the master problem is improved by iteratively evaluating their performance against the probabilistic production cost models, which also provide marginal cost information that is subsequently used in the master problem. Benders decomposition also provides bounds upon the optimal system costs for each candidate investment and their convergence is guaranteed under certain conditions (Geoffrion, 1972). These bounds cannot be guaranteed as valid, however, if only a few observations of load levels and capacity factors of intermittent resources are considered in the subproblems, as it is often done in planning studies. Furthermore, convergence of the algorithm is often slow, which has prevented its widespread utilization among practitioners, although acceleration techniques are an ongoing subject of research (Mcdaniel and Devine, 1977; Magnanti and Wong, 1981; Sahinidis and Grossmann, 1991). Finally, consideration of environmental constraints, such as minimum amounts of generation from renewable resources per year, impedes the parallel solution of the subproblems. This is because such constraints couple the solutions for different hours, thereby imposing a computational restriction on the level of granularity of the market operations representation.

In this chapter I develop a computationally-tractable methodology to find candidate transmission and generation investment plans for a given horizon of operating conditions, as well as bounds upon the minimum system costs. I focus on improvements to simplifications a) and b), and provide directions on how to extend my approach to account for c) in the Conclusions. I propose a two-phase approach that improves a bounding algorithm (Hobbs and Ji, 1999) and Benders decomposition, both of which provide bounds upon the expected system costs. In the first phase, a lower bound is computed by solving a low-resolution planning problem using clustered observations of demand, wind, solar, and hydro levels, based on an extension of Jensen's inequality for stochastic problems with expectation constraints. Upper bounds are estimated using a sub-sampling method to compute the operations costs for each candidate investment plan from the lower-bound planning problem. These bounds are progressively tightened by refining the partitioning of the space of time-dependent data. Due to asymptotic properties of this algorithm, however, tight convergence tolerances might only be achieved in the limit, for large cluster counts that result in computationally expensive lower-bound planning problems. To overcome this difficulty, I propose a second phase to the bounding approach that uses Benders decomposition with an auxiliary lower bound to close the remaining solution gap. Although I apply my methodology to a power system planning problem, my approach can be generalized to other stochastic problems with both per-scenario and expectation constraints.

The rest of the chapter is organized as follows. In Section 4.2 I describe a stylized planning model that I formulate as a stochastic mixed-integer linear problem with per-scenario and expectation constraints. In Section 4.3 I provide a proof on how to use Jensen's inequality to compute lower bounds for a stochastic problem with expected-value constraints and describe a statistical method to compute upper bounds that takes advantage of parallel computer systems. Section 4.4 describes the implementation of Benders decomposition and the introduction of auxiliary lower bounds in the master problem to accelerate its convergence. In Section 4.5 I illustrate the performance of the proposed bounding and decomposition approach using a modified version of the transmission and generation planning problem described in Chapter 3. Finally, in Section 4.6 I conclude.

4.2 Stylized Planning Model

Throughout this chapter I will focus on investment planning models that can be formulated as linear or mixed integer linear programs.[1] Examples of models that fit into this category are: Caramanis et al. (1982), Bloom (1983), and Sherali and Staschus (1990) for generation planning; Binato et al. (2001) for transmission planning; and Pereira et al. (1985), Dantzig et al. (1989), van der Weijde and Hobbs (2012), and Munoz et al. (2013a) for composite transmission and generation planning. Other examples of planning models that are commonly used for energy and environmental policy analysis are IPM (ICF, 2013), the Electricity Market Module of NEMS (Gabriel et al., 2001) , ReEDS (Short et al., 2011), Haiku (Paul and Burtraw, 2002), and MARKAL (EPA, 2013).

4.2.1 Notation

Here I define the main notation used in the following sections. More parameters and variables will be defined as needed.

Parameters:

[1]Modeling unit commitment variables and constraints or AC optimal power flows results in nonlinear and non-convex operations models. Their utilization in long-term investment models has been limited to research applications on small test-cases.

A	:	Coefficients matrix associated to investment constraints;
b	:	Right-hand-side vector of parameters on investment constraints;
c	:	Vector of marginal generation and curtailment costs;
d	:	Right-hand-side vector of parameters on expected-value constraints;
e	:	Vector of transmission and generation capital costs;
K	:	Fixed recourse matrix associated to expected-value constraints, known with certainty;
$T(\omega)$	:	Coefficients matrix associated with investment variables in operations problem, also known as transition matrix. This matrix includes some scenario- or time-dependent parameters such as hourly levels of wind, solar, and hydro;
(Ω, p)	:	Discrete probability space composed of the sample space Ω and the probability measure $p(\cdot)$ over Ω. For planning purposes, this space is commonly constructed using 8760 observations of hourly demand levels and capacity factors from historical time-series data (i.e., $\lvert\Omega\rvert = 8760$), each event ω_i with probability of occurrence $p(\omega_i) = 1/8760$, $\forall \omega_i \in \Omega$;
$r(\omega)$	:	Right-hand-side vector of parameters for scenario ω;
W	:	Fixed recourse matrix, known with certainty;

Decision variables:

x	:	Vector of generation and transmission investment variables;
$y(\omega)$	:	Vector of power generation levels, power flows, phase angles, and demand curtailment variables for each realization of ω;

4.2.2 Investment Model

Broadly, the goal of a planning tool is to provide a recommendation of where and when to invest in new transmission and/or generation infrastructure, given a forecast of operating conditions that I model with the probability space (Ω, p). These models are of the form:

$$TC((\Omega,p)) = \underset{x}{Min} \; e^T x + f(x,(\Omega,p)) \tag{4.1}$$

$$\text{s.t. } Ax = b \tag{4.2}$$

$$x \geq 0 \tag{4.3}$$

The function $f(x,(\Omega,p))$ denotes the minimum expected operating costs for a given set of investments x and scenarios described by (Ω,p) and $TC(\Omega,p)$ the minimum total system cost. The matrix A and vector b define investment constraints such as generation build limits, installed reserved margins per area, and limits on the maximum number of circuits per corridor. Some of the elements in the vector of investment variables x can be defined as discrete instead of continuous, as it is typically the case for transmission investment variables (Binato et al., 2001; van der

Weijde and Hobbs, 2012; Munoz et al., 2013b). Note that multi-stage planning models, such as the one described in Chapter 3 and in van der Weijde and Hobbs (2012) can be also written in the above format if all investment decisions are separated from operations.

4.2.3 Operations Model

The objective function of the operations problem is to minimize operating costs for a given horizon and a set of forecasted realizations of demand, wind, solar, and hydro levels, denoted (Ω, p).

$$f(x,(\Omega,p)) = f_c(x,(\Omega,p)) = \underset{y(\omega)}{Min}\ \mathbb{E}_\omega[c^T y(\omega)] \tag{4.4}$$

$$\text{s.t. } Wy(\omega) = r(\omega) - T(\omega)x \qquad \forall \omega \in \Omega \tag{4.5}$$

$$\mathbb{E}_\omega[Ky(\omega)] = d \tag{4.6}$$

$$y(\omega) \geq 0 \qquad \forall \omega \in \Omega \tag{4.7}$$

Per-scenario (e.g., hourly) constraints, (4.5), include Kirchhoff's first and second law, maximum generation limits for both conventional and intermittent units, maximum power flow limits, flowgate limits, and ramping constraints. Expectation constraints (4.6) (e.g., annual) are used to enforce policy objectives, such as renewable targets or emission limits on a per-year basis (Munoz et al., 2013a). The sub-index c in $f_c(x,(\Omega,p))$ will be utilized in the next section to develop proofs, but it will be omitted unless necessary.

4.3 Phase One: The Bounding Algorithm

One alternative to solving large-scale stochastic problems is using computationally-tractable approximations that provide lower and upper bounds upon the optimal objective function value. Traditional bounds for problems with stochastic right-hand-sides include Jensen's inequality for lower bounds (Jensen, 1906) and the Edmunson-Madansky inequality for upper bounds (Madansky, 1960). These bounds can be progressively tightened by refining the partitioning of the space Ω, until a certain tolerance is achieved (Huang et al., 1977; Birge and Louveaux, 1997; Hobbs and Ji, 1999). However, expectation constraints in my case limit the direct application of Jensen's lower bound, since standard results are only applicable to separable problems with per-scenario constraints. Upper bounds, on the other hand, could still involve the solution of large optimization problems, which are sometimes facilitated by the application of decomposition algorithms (Hobbs and Ji, 1999). In this section I provide an extension of Jensen's lower bound for problems with both per-scenario and expectation constraints (Section 4.3.1), and describe a sub-sampling method that provides a statistical estimate of the upper bound problem that I implement in a parallel computer system (Section 4.3.2).

4.3.1 New Lower Bounds

To develop the proofs in this section, I first define the function $g(x,(\Omega,p))$ as a relaxation of $f(x,(\Omega,p))$ that only includes per-scenario constraints (thus omitting (4.6)). This function is defined as:

$$g(x,(\Omega,p)) = g_c(x,(\Omega,p)) = \underset{y(\omega)}{Min}\ \mathbb{E}_\omega[c^T y(\omega)] \tag{4.8}$$

$$\text{s.t. } Wy(\omega) = r(\omega) - T(\omega)x \qquad \forall\omega \in \Omega \tag{4.9}$$

$$y(\omega) \geq 0 \qquad \forall\omega \in \Omega \tag{4.10}$$

Note that $g(x,(\Omega,p))$ is a function that involves solving a stochastic linear optimization program with stochastic right-hand-sides and per-scenario constraints. The standard lower bound based on Jensen's inequality can be used as stated in the following lemma.

Lemma 1: *Given a discrete sample space Ω with measure p, a partition $S_1,...,S_m$ of Ω, a sample space $\Psi^m = \{\xi_1,...,\xi_m\}$ is defined with measure q^m, such that the probability of each event ξ_i in Ψ^m equals the probability of each subset S_i as $q^m(\xi_i) = p(S_i)$, $\forall i \in 1,...,m$. If the right-hand-side vector of parameters $r(\cdot)$ and transition matrix $T(\cdot)$ are computed using the expected value of these parameters over the partitions, such that $r(\xi_i) = \mathbb{E}_\omega[r(\omega)|S_i]$, and $T(\xi_i) = \mathbb{E}_\omega[T(\omega)|S_i]$, $\forall\xi_i \in \Psi^m$, then for any vector of investments x, $g(x,(\Psi^m,q^m)) \leq g(x,(\Omega,p))$.*

Proof: The result follows from the convexity of the optimal objective function of linear programs on the right-hand-side vector of constraints and the application of Jensen's inequality (Huang et al., 1977; Birge and Louveaux, 1997)□

The interpretation of this result is that if the space Ω of realizations of demand, wind, solar, and hydro levels is partitioned or clustered into subsets, and if expected values of these parameters conditioned on each subset/cluster are used in the optimization problem and weighted in the objective function in proportion to the cluster sizes, then solving the operations problem $g(x,(\Psi^m,q^m))$ provides a lower bound upon the operations problem $g(x,(\Omega,p))$, which considers the full distribution of time-dependent parameters. Furthermore, if the sample space Ω is partitioned using a hierarchical clustering algorithm (i.e., Ψ^{m+1} is derived from Ψ^m by subdividing one (or more) of the subsets $S_1,...,S_m$ that define Ψ^m), then the bound always improves as the partitions get refined (i.e., $g(x,(\Psi^m,q_m)) \leq g(x,(\Psi^{m+1},q_{m+1}))\ \forall m$) (Birge and Louveaux, 1997). Convergence of the lower bounds $g(x,(\Psi^m,q^m)) \to g(x,(\Omega,p))$ is guaranteed as $m \to |\Omega|$ (Birge and Wallace, 1986; Kall and Mayer, 2010). Comparisons of the effect of different partitioning rules on the convergence speed are in Birge and Wallace (1986) and in Hobbs and Ji (1999). Unfortunately none of these properties are directly applicable to my operations problem $f(x,(\Omega,p))$ that has both per-scenario and expected-value constraints.

By definition, the relaxation $g(x,(\Omega,p))$ provides a lower bound upon $f(x,(\Omega,p))$,

$\forall x$, and thereby $f(x, (\Psi^m, q^m)) \leq f(x, (\Omega, p))$, $\forall x$, $\forall m \in 1, , |\Omega|$. However, these bounds, which relax the expectation constraints included in the problem $f(x, (\Omega, p))$, are likely to be loose if those constraints are active (and stringent) in the optimal solution of $f(x, (\Omega, p))$. In Munoz et al. (2013a), for instance, renewable goals and emissions limits, both formulated as expectation constraints, are the main drivers of transmission and generation investments in the model; their relaxation would therefore be expected to result in substantial underestimation of costs.

To develop tighter bounds I first define the partial Lagrange dual function $\phi(\lambda, x, (\Omega, p))$ of the minimization problem $f(x, (\Omega, p))$ as:

$$\phi(\lambda, x, (\Omega, p)) = \phi_c(\lambda, x, (\Omega, p)) = \underset{y(\omega)}{Min}\ \mathbb{E}_\omega[c^T y(\omega)] + \lambda^T(d - \mathbb{E}_\omega[Ky(\omega)]) \quad (4.11)$$

$$\text{s.t. } Wy(\omega) = r(\omega) - T(\omega)x \qquad \forall \omega \in \Omega \quad (4.12)$$

$$y(\omega) \geq 0 \qquad \forall \omega \in \Omega \quad (4.13)$$

The weak duality theorem states that $\forall \lambda$, $\phi(\lambda, x, (\Omega, p)) \leq f(x, (\Omega, p))$, while strong duality ensures that λ, $\phi(\lambda^*, x, (\Omega, p)) = f(x, (\Omega, p))$. Strong duality holds since the objective function and constraints are all affine functions (Bertsimas and Tsitsiklis, 1997). The following Proposition extends Lemma 1 to linear stochastic programs with both per-scenario and expectation constraints.

Proposition 1: *Given a discrete sample space Ω with measure p, a partition $S_1, ..., S_m$ of Ω, a sample space $\Psi^m = \{\xi_1, ..., \xi_m\}$ is defined with measure q^m, such that the prob-*

ability of each event ξ_i in Ψ^m equals the probability of each subset S_i as $q^m(\xi_i) = p(S_i)$, $\forall i \in \{1, ..., m\}$. If the right-hand-side vector of parameters $r(\cdot)$ and transition matrix $T(\cdot)$ are computed using the expected value of these parameters over the partitions, such that $r(\xi_i) = \mathbb{E}_\omega[r(\omega)|S_i]$, and $T(\xi_i) = \mathbb{E}_\omega[T(\omega)|S_i]$, $\forall \xi_i \in \Psi^m$, then for any vector of investments x, $f(x, (\Psi^m, q^m)) \leq f(x, (\Omega, p))$.

Proof: From the weak duality theorem it follows that $\phi_c(\lambda, x, (\Omega, p)) \leq f(x, (\Omega, p))$, $\forall \lambda$. Defining a new cost vector $c_\lambda^T = c^T + \lambda^T K$ and re-arranging terms in the objective function of $\phi_c(\lambda, x, (\Omega, p))$, I have that $g_{c^*}(x, (\Omega, p)) = \phi_c(\lambda, x, (\Omega, p))$. Now Lemma 1 (Jensen's lower bound) can be applied to $g_{c_\lambda}(x, (\Psi^m, q_m))$ implying that $g_{c_\lambda}(x, (\Psi^m, q_m)) \leq g_{c_\lambda}(x, (\Omega, p))$, $\forall m \in \{1, ..., m\}$. Replacing c_λ^T by $c^T + \lambda^T K$ in the objective function of $g_{c_\lambda}(x, (\Psi^m, q_m))$ and re-arranging terms, I have that $\phi_c(\lambda, x, (\Psi^m, q_m)) = g_{c_\lambda}(x, (\Psi^m, q_m))$. Using the strong duality theorem, I pick λ^{*m} such that $\phi(\lambda^{*m}, x, (\Psi^m, q_m)) = f(x, (\Psi^m, q_m))$ which implies:

$$f(x, (\Psi^m, q_m)) = \phi(\lambda^{*m}, x, (\Psi^m, q_m)) \leq \phi_c(\lambda^{*m}, x, (\Omega, p)) \leq f(x, (\Omega, p)) \qquad (4.14)$$

From left to right in (4.14), the equality results from the strong duality theorem, the first inequality follows from Jensen's inequality through Lemma 1, and last inequality derives from the weak duality theorem. Similar arguments were used in Kuhn (2009) to develop convergent bounds for multi-stage stochastic problems with expectation constraints, but my proof is much simpler. As in the case without expectation constraints, if a hierarchical clustering algorithm is used then the bound can be guaranteed to be nondecreasing (i.e., $f(x,(\Psi^m,q^m)) \leq f(x,(\Psi^{m+1},q^{m+1}))$, $\forall x$, $\forall m \in \{1,...,|\Omega|-1\}$) and convergent to $f(x,(\Omega,p))$. Finally, the following Proposition shows how this bound can be used to compute bounds upon the optimal total system costs $TC(\Omega,p)$.

Proposition 2: *Given the conditions described in Proposition 1, $TC((\Psi^m,q_m))$ is a lower bound on $TC((\Omega,p))$.*

Proof: Say x^* and x^{m*} are the investment plans that yield the minimum total system costs for the full-resolution problem $TC(\Omega,p)$, and for the partitioned/clustered one $TC(\Psi^m,q^m)$, respectively. From Proposition 1 I have that for x^*, $e^Tx^*+f(x^*,(\Psi^m,q^m)) \leq e^Tx^*+f(x^*,(\Omega,p)) = TC(\Omega,p)$, $\forall m \in \{1,...,|\Omega|\}$. From the definition of x^{m*} as a minimizer, $e^Tx^{*m}+f(x^{*m},(\Psi^m,q^m)) = TC(\Psi^m,q^m) \leq e^Tx^*+f(x^*,(\Psi^m,q^m))$, which implies that $TC(\Psi^m,q^m) \leq TC(\Omega,p)$, $\forall m \in \{1,...,|\Omega|\}$.

Once again, if a hierarchical clustering algorithm is used, such that $f(x,(\Psi^m,q^m)) \leq f(x,(\Psi^{m+1},q^{m+1}))$, $\forall x$, $\forall m \in \{1,...,|\Omega|-1\}$, then $TC(\Psi^m,q^m) \leq TC(\Psi^{m+1},q^{m+1})$, $\forall m \in \{1,...,|\Omega|-1\}$.

4.3.2 Upper Bounds

In the previous section I described a method to find trial investment solutions x^* using a using a low-resolution operations model $f(x^*,(\Psi^m,q^m))$. This operations model also provides a lower bound upon the true operating costs $f(x^*,(\Omega,p))$. By definition, $TC(\Omega, p)$ corresponds to the minimum total system cost and, therefore, for any feasible investment plan x^*, $e^T x^* + f(x^*, (\Omega, p))$ provides an upper bound upon $TC(\Omega, p)$. Computing $f(x^*, (\Omega, p))$, however, could be computationally prohibitive because of expectation constraints that link all scenarios within the operations problem and which impede a direct parallel implementation on a per-scenario basis, as it would be for $g(x^*, (\Omega, p))$. Relaxation of these constraints through Benders or Dantzig-Wolfe decomposition methods addresses this difficulty (O'Brien, 2004), but it comes at the expense of nested decomposition algorithms within my proposed approach. Future planning problems, however, might require consideration of multi-year time-series, sub-hourly resolution of intermittent data, and scenarios of component failures. These would result in extremely large sample spaces (Ω, p) and, therefore, large operations models that would be difficult to solve even in the absence of expectation constraints.

Other solution approaches that reduce the computational complexity of large-scale stochastic optimization problems involve the employment of samples of uncertain parameters, instead of their full distributions. Examples of their utilization to compute upper bounds within bounding approaches are in Birge and Louveaux (1997) and Pierre-Louis et al. (2011), and within a Benders decomposition in Infanger (1992) and Higle and Sen (1991). The quality of these approximations is progressively improved by increasing the sample size between iterations (Birge and Louveaux, 1997; Pierre-Louis et al., 2011) or by combining information from multiple independent samples through Benders' cuts (Higle and Sen, 1991; Infanger, 1992). In particular, convergence of the Sample Average Approximation method (SAA), which relies on large-sample results, is guaranteed for stochastic linear problems with per-scenario and expectation constraints (Anitescu and Birge, 2008), as it is in my case. The major drawback of these approximation methods is, however, the poor quality of the estimation during initial iterations as a consequence of their asymptotic convergence properties. Recent results from Birge (2011) show that, in some cases, a combination of sub-sample estimates, as in the batch-means method (Law and Carson, 1979; Schmeiser, 1982), can achieve earlier convergence and more robust results than considering a single large sample of equivalent size. In the spirit of Birge (2011), I implement a method to compute estimates of $f(x^*, (\Omega, p))$ utilizing a sub-sampling approach that is enhanced through stratified sampling to reduce the variance of the estimates.

Sub-Sample Estimation

The method relies on using the means of N independent groups, or batches, of M observations each, instead of using one large sample of equivalent size $N \times M$. I denote a random sample of M observations from the space Ω as Ω^M, and define the new probability measure $p^M(\cdot)$, such that all observed events have the same probability of occurrence $p^M(\omega_i) = 1/M$, $\forall i \in \{1, ..., M\}$. To approximate $f(x, (\Omega, p))$ I draw N independent samples of M observations each, denoted $\{\Omega_1^M, ..., \Omega_N^M\}$, and solve

N independent operations problems, denoted $f(x,(\Omega_1^M,p_1^M)),...,f(x,(\Omega_N^M,p_N^M))$. An estimate of $f(x,(\Omega,p))$ is then calculated as:

$$f(x,(\Omega,p)) \cong \frac{1}{N}\sum_{j=1}^{N} f(x,(\Omega_j^M,p_j^M)) \tag{4.15}$$

Using the sub-sample method to approximate $f(x,(\Omega,p))$, an upper bound upon $TC(\Omega,p)$ corresponds to $e^T x^* + \frac{1}{N}\sum\limits_{j=1}^{N} f(x,(\Omega_j^M,p_j^M))$. Convergence of this method as N is increased is assured for stochastic linear programs (Birge, 2011), as it is in my case, however, small biases might arise depending on the structure and stringency of the constraints within the optimization problem. Previous research on the traditional batch-means estimator shows that small batch sizes (i.e., small M) can be a source of biases on the sample-mean estimator (i.e., sample size), although normal distribution of errors is guaranteed for large samples and batch counts (Schmeiser, 1982; Chien et al., 1997; Steiger and Wilson, 2001; Sherman and Goldsman, 2002). An advantage of this method over other sampling approaches that rely on unique, large-sample results is that problems $f(x,(\Omega_1^M,p_1^M)),...,f(x,(\Omega_N^M,p_N^M))$ can be solved in parallel computer systems. Therefore, the extra computational load that results from increasing the sample size M or batch count N to reduce biases, and to ensure tight confidence intervals on the sample mean, can be efficiently distributed among multiple independent processors, instead of being given to a single optimization problem of comparable size (e.g., $f(x,(\Omega^{N\times M},p^{N\times M}))$.

Reducing the Variance through Stratified Sampling

To further reduce the computational cost of approximating $f(x, (\Omega, p))$ through sub-sample estimations, I propose the utilization of a stratification technique to select samples that would more accurately match the characteristics of Ω and, therefore, reduce the variance of the sub-samples $f(x, (\Omega_1^M, p_1^M)), ..., f(x, (\Omega_N^M, p_N^M))$. Stratified sampling has been used before for production cost modeling (Marnay and Strauss, 1991), but it has not been utilized yet in the context of the sub-sampling method proposed by Birge (2011). The stratified sampling algorithm proceeds as follows. For a given predetermined sample size M, the space Ω is partitioned into disjoint subsets (or stratums) $S_1, ..., S_M$, aiming to group the events into clusters of similar characteristics (e.g., observations are grouped based on load, wind, solar, and hydro levels or similar loads, included in $r(\omega)$ and $T(\omega)$). A stratified sample of M observations $\{\omega_1, ..., \omega_M\} \subset \Omega$ is such that $\omega_i \in S_i$, $\forall i \in \{1, ..., M\}$. To correct for the bias created using this sampling methodology, I define a new sample space $\Omega^N = \{\omega_1, ..., \omega_N\}$ with measure $p^N(\cdot)$, such that the probability of each sampled event in the operations problem is $p^N(\omega_i) = p(\omega_i)/p(\omega_i|S_i)$. This approach can be interpreted as a generalization of the discretization of load-duration curves, which consider multiple "steps" of different time duration (e.g., peak, shoulder, and off-peak).

4.3.3 Updating the Upper and Lower Bounds

Bounding methods that rely on clustering algorithms or sampling often require progressive refinement of the space partitioning, or increasing sample sizes, to decrease the solution gap and improve the accuracy of the upper bound estimation (Birge and Louveaux, 1997; Hobbs and Ji, 1999; Pierre-Louis et al., 2011). To avoid poor initial estimates of the upper bound, I propose selecting and fixing both the sample size M and batch count N prior to the initialization of the bounding or decomposition phases of my algorithm. A numerical analysis of the effects of sample sizes and sampling methodologies is given in Section 4.5.2. Throughout the rest this section and the following one, I assume that there is a computationally efficient method to approximate $f(x^*, (\Omega, p))$ for any candidate investment plan x^*.

The bounding algorithm, or phase one of my methodology, proceeds as follows. I initialize the iterations by setting $k = 0$, and the lower and upper bounds as $LB_0 = -\infty$ and $UB_0 = +\infty$, respectively. The incumbent solution is denoted x^*.

1. Set $k = k + 1$, solve the lower-bound planning problem using the partitioned space (Ψ^k, q^k), and find a trial investment plan x_k^*, and a lower bound on the optimal total system costs $TC(\Psi^k, q^k)$. If $TC(\Psi^k, q^k) > LB_{k-1}$, update the lower bound to $LB_k = TC(\Psi^k, q^k)$, otherwise, $LB_k = LB_{k-1}$.

2. Compute the operating costs $f(x_k^*, (\Omega, p))$. If $e^T x_k^* + f(x_k^*, (\Omega, p)) < UB_{k-1}$, update the upper bound to $UB_k = e^T x_k^* + f(x_k^*, (\Omega, p))$ and the incumbent

solution to $x^* = x_k^*$, otherwise, $UB_k = UB_{k-1}$.

3. Compute the solution gap, defined as $GAP_k = 100\% \times (UB_k - LB_k)/UB_k$. If GAP_k is less than or equal to a pre-determined solution tolerance, stop and use x^* as investment plan, otherwise, go to step 1.

Convergence of the algorithm follows from Birge and Wallace (1986) and Kall and Mayer (2010). It is often observed in clustering algorithms that only a few partitions explain a large fraction of the variance of the full dataset (the "elbow" criterion), but that the remaining fraction of variance converges asymptotically to 1 as the partitions are refined (Tibshirani et al., 2001). A potential implication of this for the bounding phase of my algorithm is that loose optimality gaps might be achieved using only small number of representative hours from the sample space (clustered load, wind, solar, and hydro levels), but that tight optimality gaps might be only attained for large values of k (Hobbs and Ji, 1999). This is particularly challenging for planning problems that consider binary decision variables (e.g., transmission investments), since solving the lower-bound planning problems $TC(\Psi^k, q^k)$ for large values of k can become increasingly difficult due to computational restrictions. In the following section I describe the use of Benders decomposition (phase two) to close the residual gap from the bounding phase through the addition of cuts into the lower-bound planning problem.

4.4 Phase Two: Enhanced Benders Decomposition

An alternative to the bounding approach described in the previous section is to take advantage of the decomposable structure of the planning problem and solve it iteratively using Benders decomposition (as in Bloom (1983)). The main drawback of this method is, however, its slow convergence speed and the growing size of the master problem as the algorithm iterates. Multiple techniques have been proposed to accelerate the convergence of the algorithm when applied to mixed-integer linear problems. Speed reductions can be achieved from tight mixed-integer formulations and the selection of Pareto optimal cuts for subproblems with degenerate solutions (Magnanti and Wong, 1981; Sahinidis and Grossmann, 1991). Other techniques address the computational challenge of solving multiple mixed-integer linear master problems by initially computing cuts from linear (Mcdaniel and Devine, 1977) and Lagrangian relaxations (Hoang Hai, 1980; van Roy, 1983; Cote and Laughton, 1984; Aardal and Larsson, 1990), as well as from feasible sub-optimal solutions found by prematurely stopping branch-and-bound type algorithms (Geoffrion and Graves, 1980). Trust regions combined with high-quality initial solutions have been proposed to reduce abrupt changes of the solutions found in the master problem (Sherali et al., 1987; Sherali and Staschus, 1990). However, approximate solution methods might prevent the master problem from generating essential cuts to ensure convergence of Benders decomposition (Holmberg, 1994).

Phase two of my algorithm consists of a modification of Benders decomposition that includes a valid polyhedral lower bound upon the optimal operating costs $f(x,(\Omega,p))$ based upon results from Section 4.3.1. This can be interpreted as a generalization of the stabilization scheme for the stochastic decomposition algorithm (Higle and Sen, 1991) currently implemented in the NEOS Solver (Sen, 2013), which utilizes the expected-value solution as an auxiliary lower bound in the master problem (i.e., expected value of all stochastic parameters).

The lower-bound planning problem of the bounding phase is now defined as the master problem, and is formulated as follows:

$$\underset{x,\theta}{Min} \; e^T x + \theta \tag{4.16}$$

$$\text{s.t.} \; Ax = b \tag{4.17}$$

$$\theta \geq f(x^*,(\Omega,p)) + \pi^T(x^*)(x - x^*) \tag{4.18}$$

$$\theta \geq f(x,(\Psi^m,q^m)) \tag{4.19}$$

$$x, \theta \geq 0 \tag{4.20}$$

Constraint (4.18) corresponds to the Benders' cuts which are computed using the sub-sampling method described in Section 3.2.1. The Lagrange multipliers $\pi(x^*)$ result from imposing $x = x^*$ in the calculation of $f(x^*,(\Omega,p))$. Constraint (4.19) involves consideration of the operations problem defined by Equations (4.4) - (4.7) for the sample space (Ψ^k, q^k). Unlike the traditional definition of the master problem for a Benders decomposition of capacity expansion problems that only considers investment variables (Bloom, 1983), the master problem in my case corresponds to a planning problem with an embedded low-resolution operations problem. The fidelity of the operations problem can be improved by increasing the number of clusters k used to approximate the sample space Ω. For $k = 0$, no constraints on the value of θ are imposed through constraint (4.19) and the problem defined by Equations (4.16)-(4.18) and (4.20) corresponds to the regular master problem used in Benders decomposition. For $k = |\Omega|$, all observations are considered and the master problem is equivalent to the original planning problem, which converges in a single iteration.

A second improvement upon the auxiliary lower bound is the utilization of the objective function value of $TC_{LP}(\Psi^k, q^k)$ for a large value of k as a tight, initial lower bound (LB_0) for the Benders' iterations. This is done to address the limitation of bounding algorithms that could potentially find high-quality solutions during initial iterations, but optimality cannot be proven until the difference between the upper and lower bounds is below a certain tolerance.[2]

Finally, as in the L-shaped method (Birge and Louveaux, 1997), I compute a single cut on each iteration using the expected value of the dual multipliers $\pi_1(x^*), ..., \pi_N(x^*)$ and operating costs $f(x^*, (\Omega_1^M, p_1^M)), ..., f(x^*, (\Omega_N^M, p_N^M))$ of the N sub-samples. An extension of this method, known as the multi-cut L-shaped algorithm, requires the

[2]This is often observed in branch-and-bound type of algorithms, where even if an optimal solution is found within the first iterations, optimality cannot be guaranteed until the algorithm has completed all the nodes.

addition of one cut per scenario, instead of a single "expected" cut, on each iteration (Birge and Louveaux, 1988). Improved convergence of the Benders' algorithm due to reduced information loss from the multi-cut method is, however, at least partially offset by the increased computational burden resulting from the growth in size of the master problem and I leave its implementation as a subject of future research.

In Section 4.5 I explore how intermediate values of k, within the range $(0, |\Omega|)$, can be used to close the residual solution gap from the bounding phase and can also accelerate the convergence of the traditional Benders algorithm.

4.5 Numerical Example

This section describes an application of my bounding and decomposition algorithms on a large-scale generation and transmission planning problem using a 240-bus representation of the Western Electricity Coordinating Council (WECC) in the U.S.. The clustering, bounding, and Benders decomposition algorithms were all implemented using the Pyomo algebraic modeling package (Hart et al., 2012). All optimization problems were solved with the CPLEX 12.4 solver and parallelized through the Message Passage Interface (MPI) on a 32-core computer system with 112 GB of RAM.

In the next subsection (Section 4.5.1) I summarize the main characteristics of the WECC-240 test-case and describe relevant modeling assumptions. In Section 4.5.2

I study the effect of different sampling methodologies and sub-sample sizes on the sub-sample estimates used to compute upper bounds. Section 4.5.3 describes the performance of the clustering algorithm used to compute lower bounds. In Section 4.5.4 I summarize the performance of the bounding algorithm (phase one) for both the linear and the mixed-integer linear cases. In Section 4.5.5 I discuss the potential value of the lower-bound problem for planning purposes. Section 4.5.5 describes the results of phase two of my algorithm (Benders decomposition) applied to the linear and mixed-integer linear cases.

4.5.1 Description of the WECC 240-bus System

I utilize a modified version of the WECC 240-bus test-case described in Chapter 3. The network consists of 240 existing buses, 448 transmission elements, and 157 aggregated generators. I model intermittent resources using 151 historical profiles of hourly demand, wind, solar, and hydro levels across multiple regions representing operating conditions for a typical year.[3] For illustration purposes, I assume that market and regulatory conditions are deterministic and focus instead on capturing the variability of intermittent resources. The planning model used to illustrate my algorithm is a single-scenario version of the two-stage stochastic model described in Chapter 3 without disjunctive constraints.[4] The application of the bounding and decomposition

[3]Table B.7 in Appendix B.1.4 describes means, standard deviations, and correlations among a sample of 18 profiles across regions.

[4]Disjunctive constraints are used to enforce Kirchhoff's Voltage Laws in candidate lines. In this chapter, Kirchhoff's Voltage Laws are only enforced in existing lines and relaxed for candidate ones.

algorithm to a stochastic transmission planning problem with disjunctive constraints, such as the one described in Chapter 3, is equivalent to the one described in this chapter for the deterministic case, however, their implementation is beyond the scope of this thesis. A single-scenario planning problem with 8736 hours[5] of intermittent data results in a mixed-integer linear program of 56 million constraints and 31 million variables (1020 integer). In order to make the operations problem feasible for any candidate investment plan, I allow for load curtailment at a cost of $1,000 per MWh, which is the price ceiling used in most electricity markets in the U.S., and noncompliance with annual renewable energy targets penalized at a rate of $500 per MWh.

4.5.2 Analysis of Upper Bound Estimates

A formulation of the operations problem $f(x, (\Omega, p))$ for 8,736 observations (i.e., $|\Omega| = 8,736$) of demand, wind, solar, and hydro data results in a linear program only a few thousand variables and constraints smaller than the original planning problem. Solving this problem with the available hardware is computationally infeasible due to memory limitations. To validate the sub-sample approximation method I use a large sample of intermittent data that minimizes the sum of the square difference of

As discussed in Chapter 3, disjunctive constraints can cause numerical difficulties in mixed-integer solvers. However, the bounding and decomposition procedures of this chapter are equally applicable to the formulation of the problem with disjunctive constraints.

[5] The sample is weighted by 8,760/8,736 in the objective function and expectation constraints of the operations problem. The sample size of 8,736 hours results from considering 52 weeks of hourly solar data for a typical year.

means, standard deviations, and correlations between the sample and the full dataset (van der Weijde and Hobbs, 2012). Figure C.1 in Appendix C.1 shows the fit of the best sample of 10,000 independent random samples for different sample sizes. A 5,000-hr operations problem is the largest manageable approximation of the 8,736-hr operations and the one that best matches the its statistical characteristics. As discussed in Section 4.3.2, decomposition approaches could be used to solve $f(x, (\Omega, p))$ exactly (e.g., Hobbs and Ji (1999) and O'Brien (2004)), but their implementation is beyond the scope of this chapter.

Table 4.1: Summary of results for 100 random and stratified samples for different sub-sample sizes.

Sub-Sample Size	Random Samples				Stratified Samples				5000-hr problem
	25	50	100	200	25	50	100	200	
Mean ($B)	543.9	526.3	535.7	526.3	527.0	532.6	528.2	529.7	527.7
Standard Deviation ($B)	100.2	70.9	52.2	37.5	59.3	43.5	27.8	16.6	-
Mean Solution Time (s)	23.4	48.3	103.1	208.6	23.4	48.7	104.3	211.5	8,814

The choice of the sub-sample size and sub-sample count was made taking into account the quality of the approximation and hardware restrictions. I first drew 100 independent samples of intermittent data, using both random and stratified sampling, for sub-samples considering 25, 50, 100, and 200 observations. This allowed me to

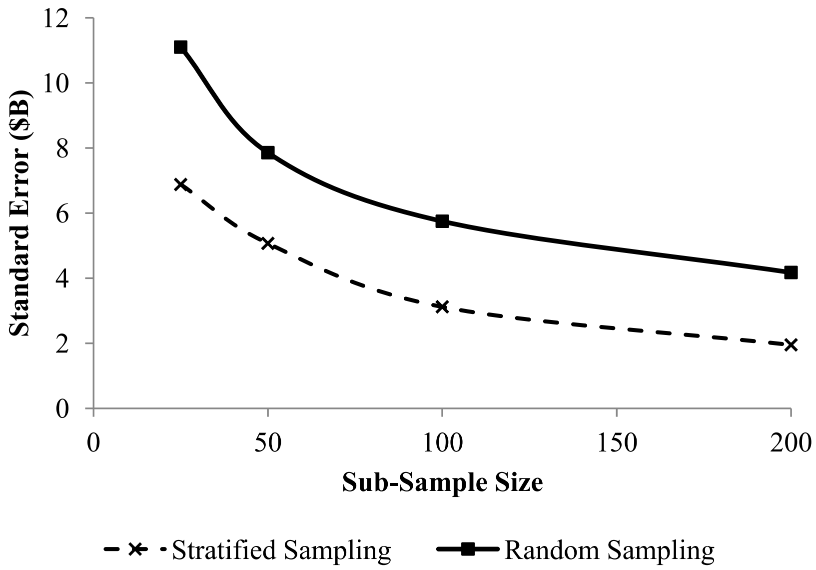

Figure 4.1: Sub-sample standard error versus sub-sample size for 100 replications of random and stratified samples ($N = 100$).

study the effect of the data stratification and sub-sample sizes on the quality of the estimator. All operations problems were run using the investment solution of the linearized expected value planning problem.

As shown in Table 4.1 and Figure 4.1, the sub-sample standard error[6] decreases dramatically with the number of sample hours in the operations problems for both random and stratified samples. The effect of data stratification using the K-Means clustering method, which is explained in the next section, yields approximately one half of the standard deviation observed in the random samples and is, in this case, more effective than doubling the sub-sample size.[7] Solution times also scale linearly.

[6]The standard error (SE) is defined as $SE = \frac{s}{\sqrt{N}}$, where s corresponds to the sample standard deviation and N is the sub-sample count.

[7]For instance, the standard error of the 50-hr random sub-samples is approximately \$8 B. Doubling the sample size to 100 hours reduces the standard error to approximately \$6 B. However, stratifying the sample space in the 50-hour sub-samples yields a standard error of approximately \$5 B.

The same investment plan yields \$527.7 B when tested against the 5,000-hr operations problem, but it requires nearly two and a half hours of computation time. In my implementation below I limit the sub-sample count to 20 ($N = 20$) in an attempt to balance computer resources for the estimation of the upper and lower bounds. Since the sub-sample count is rather small in comparison to the 100-sample analysis performed in this section, I choose to use sub-sample sizes of 200 stratified observations ($M = 200$), which yield the lowest sub-sample standard error among the four sub-sample sizes considered. Much larger sub-sample counts and sizes can be used to ensure tight confidence intervals on the optimal operating costs $f(x, (\Omega, p))$, but at the expense of higher computational complexity. Other potential extensions include re-sampling within the bounding phase (Pierre-Louis et al., 2011) or within the Benders phase (Higle and Sen, 1991; Infanger, 1992), but I leave them as subjects of future research in the context of my application.

4.5.3 Clustering Algorithm

The chosen algorithm to partition the intermittent data space is K-Means MacQueen (1967), although other partitioning schemes have been used in similar applications (Hobbs and Ji, 1999). K-Means is a nonhierarchical clustering algorithm, which implies that, in some cases, the total cost from the planning problem might decrease rather than increase as the partitions are refined (Birge and Louveaux, 1997). Despite this, Hobbs and Ji (1999) report that K-Means yielded the best clustering efficiency,

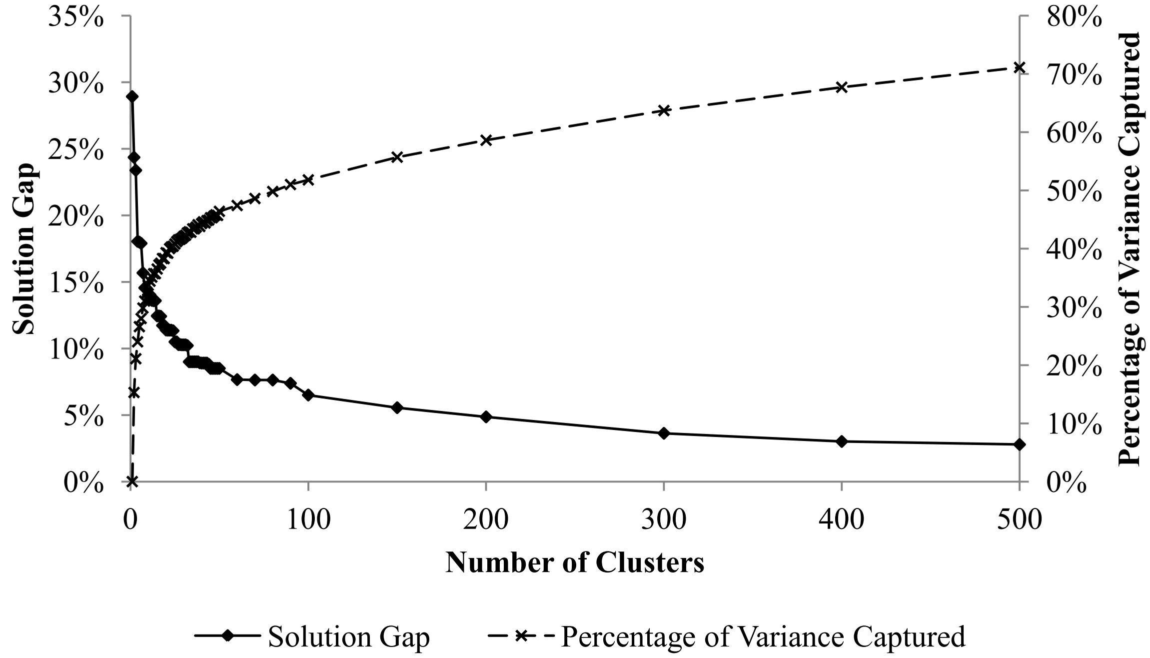

Figure 4.2: Solution gap for the linear relaxation and percentage of variance captured as a function of the number of clusters. Upper and lower bounds are in Figure C.2 in Appendix C.2.

measured as the fraction of variance captured from the full data set, compared to several other partitioning methods, including hierarchical methods. My implementation considered up to 500 clusters, which captured 71.1% of the variance of the 8,736-hr dataset (see Figure 4.1). The point of diminishing returns to scale (i.e., "elbow") is reached at approximately 50 clusters, representing 46.4% of variance. After this point, capturing an extra 10% of variance requires partitioning the space of intermittent data using 100 additional clusters.

4.5.4 Phase One: Performance of the Bounding Algorithm

4.5.4.1 Linear Problem (LP)

Figure 4.2 also shows the solution gap as a function of the number of clusters, calculated as the difference between the upper (UB) and lower (LB) bounds as a percentage of the upper bound ($100\% \times \frac{(UB-LB)}{UB}$) for the linear relaxation. The lower bound is computed solving the planning problem using the centroids of each of the subsets defined by the clustering of load, wind, solar, and hydro parameters. The upper bound equals the sum of the investment costs found from the lower-bound problem, plus a statistical estimate of the 8,736-hr operations problem $f(x,(\Omega,p))$ computed using the sample mean of 20 sub-samples ($N = 20$) of 200 stratified samples of load, wind, solar, and hydro levels each ($M = 200$). I find that, for this test-case, only 33 representative hours are needed to obtain a solution within 10% of the optimum, while more than 200 clusters are needed for solution gaps of less than 5%. Figure 4.2 shows that the "elbow" in the percentage of variance captured from the 8,736-hr dataset is a mirror image of the solution gap of the bounding algorithm, which decreases at a much slower rate after the first 39 clusters. The solution gap is reduced from 28.9%[8] to 8.9% with the first 39 clusters and increasing the number

[8]The solution gap for a single cluster, also known as the expected-value problem, provides an upper bound on the Value of the Stochastic Solution (VSS) as defined in Birge and Louveaux (1997). The VSS is a measure of the potential cost savings that could be achieved from considering the full distribution of hourly load levels and capacity factors of wind, solar, and hydro resources across all

of partitions to 500 only reduce the gap to 2.8%. This solution tolerance might be acceptable for high-level planning models formulated as linear programs (e.g., IPM (ICF, 2013), the Electricity Market Module of NEMS (Gabriel et al., 2001) , ReEDS (Short et al., 2011), Haiku (Paul and Burtraw, 2002), and MARKAL (EPA, 2013)).

4.5.4.2 Mixed-Integer Linear Problem (MILP)

As commented in Section 4.3.1, the linear relaxation of the planning problem provides a valid lower bound upon the optimal objective function value of mixed-integer linear formulation. However, the upper bound computed using the investment plan found with the linear relaxation is not an upper bound on the total system costs in the mixed-integer linear case, since investment costs are underestimated when discrete investments are assumed as continuous. For the mixed-integer linear case I estimate the solution gap as $100\% \times \frac{(UB-(1-\epsilon)LB)}{UB}$, where ϵ corresponds to the MILP gap. Note that $(1-\epsilon)LB$ provides a lower bound upon the optimal system costs for a zero MILP gap ($\epsilon = 0$), therefore, $100\% \times \frac{(UB-(1-\epsilon)LB)}{UB}$ is an upper bound on the solution gap that could be achieved if $\epsilon = 0$.

As I observe in Figure 4.3, the linear relaxation of the mixed-integer planning problem provides a computationally inexpensive alternative to assess the minimum number of clusters needed to approximate the operations problem with a pre-specified tolerance level and it also provides an approximate lower bound on the optimality

regions, instead of planning a system using the expected value of these parameters.

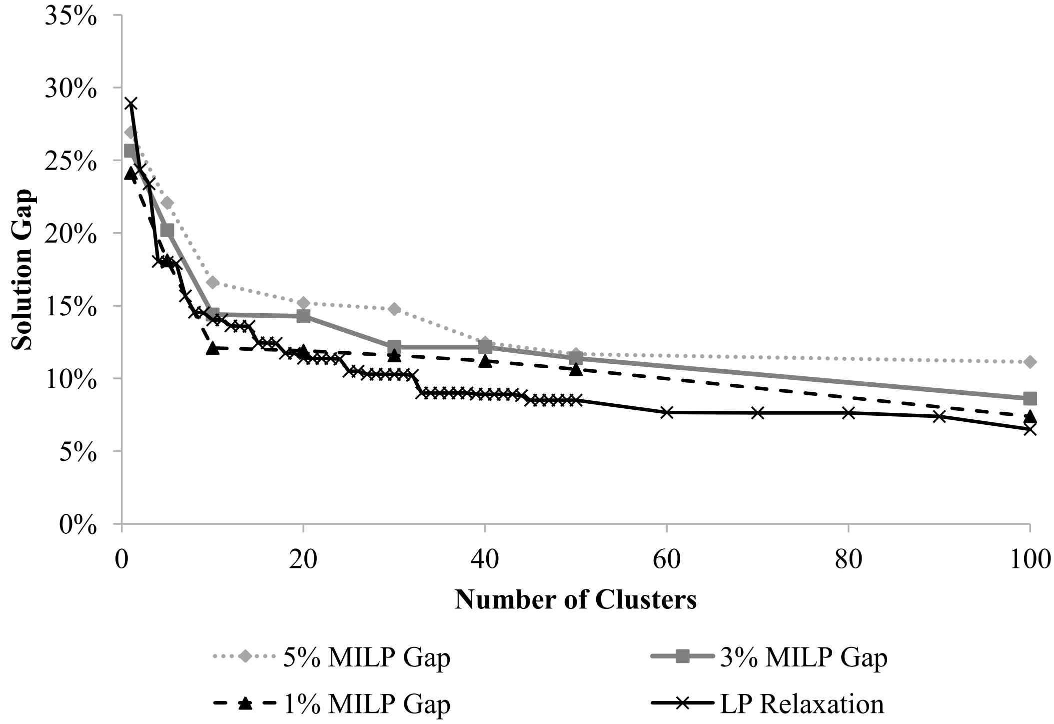

Figure 4.3: Solution gap versus the number of clusters for different MIP gaps and the linear relaxation. Upper and lower bounds are in Figure C.3 in Appendix C.2.

gap for the mixed-integer linear case for $\epsilon \ll 1$. As the MILP gap is relaxed, the total solution gap increases as a consequence of both the deterioration of the lower bound (the $(1-\epsilon)$ factor), and the suboptimality of the investment decisions, reflected as higher operating costs in the upper bound. I observe that 10 clusters are enough to achieve optimality gaps of 12.1% for a 1% MILP gap and that 90 additional clusters would only reduce the optimality gap to 7.4% (see results in Figure 4.3 for 100 clusters and 1% MILP gap).

As shown in Figure 4.4, solution times for the mixed-integer linear formulations are sensitive to the choice MILP gap and orders of magnitude larger than solution times for the linear relaxation. While the linear relaxation of the 100-cluster problem takes only 5 minutes to solve, the mixed-integer formulations require approximately 1.3, 6.6, and 6.8 hours to achieve 5%, 3%, and 1% MILP gaps, respectively. The reduction of 5.5 hours in solution time achieved from loosening the MILP gap from 1% to 5% is, however, contrasted with an increase in the total optimality gap from 7.4% to 11.1% (Figure 4.3). Further attempts to solve mixed-integer linear problems with 200 or more clusters and a MILP gap of 1% did not find a solution after more than 30 hours of computation time, and execution was stopped.

Finally, increasing the number of clusters in the linear relaxation tightened the lower bound upon the optimal system costs for the mixed-integer linear case more than reducing the MILP gap in the 100-hr problem. The 150-cluster linear relaxation, denoted $TC_{LP}(\Psi^{150}, q^{150})$, yielded a lower bound as tight as problems that considered 300 or more clusters, and required only 13 minutes of computing time. Recalculation of the optimality gaps for the 100-cluster mixed-integer linear problems using $TC_{LP}(\Psi^{150}, q^{150})$ as an initial lower bound (LB_0) reduced the tolerances from 11.1% and 8.6%, to 10.8% and 7.6% for the 5% and 3% MILP gaps, respectively.

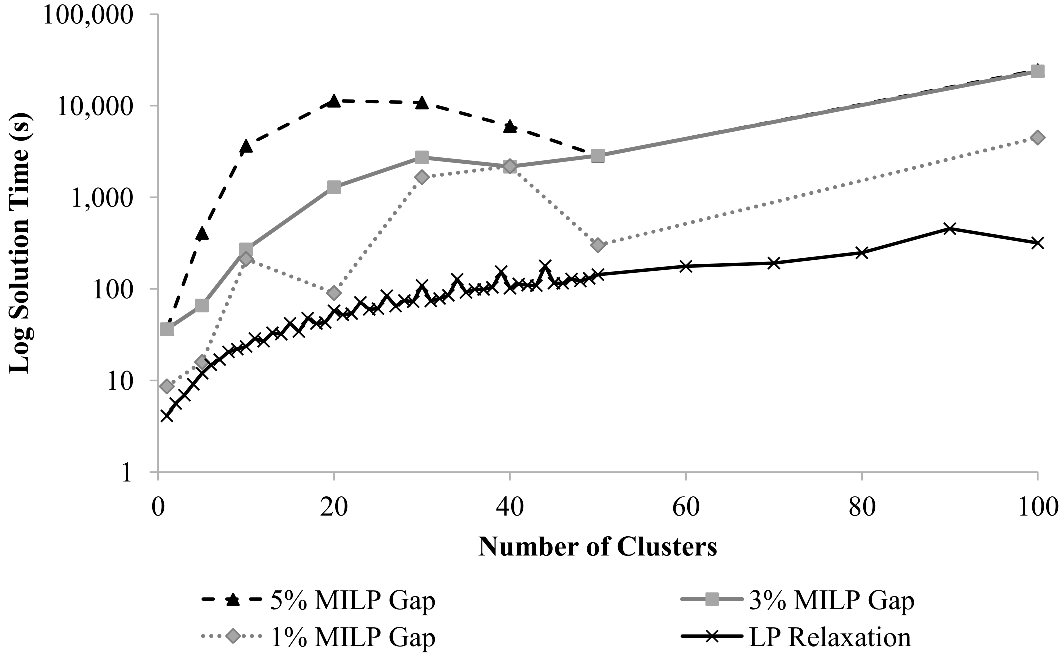

Figure 4.4: Solution time (log) of the lower-bound problem versus the number of clusters for different MIP gaps and the linear relaxation.

4.5.5 Can the Lower-Bound Problem Be Used for Planning?

As discussed in Hobbs and Ji (1999), the lower-bound investment planning problem can provide useful information about total and marginal system costs to meet forecasted demand and environmental goals, but these might be only meaningful for large cluster counts. Just using the lower bound as an indicator of convergence as in Heejung and Baldick (2013), however, can result in premature detention of the algorithm. Changes in the objective function value of the lower-bound planning problem only reflect improvements of the fidelity of the embedded operations problem that

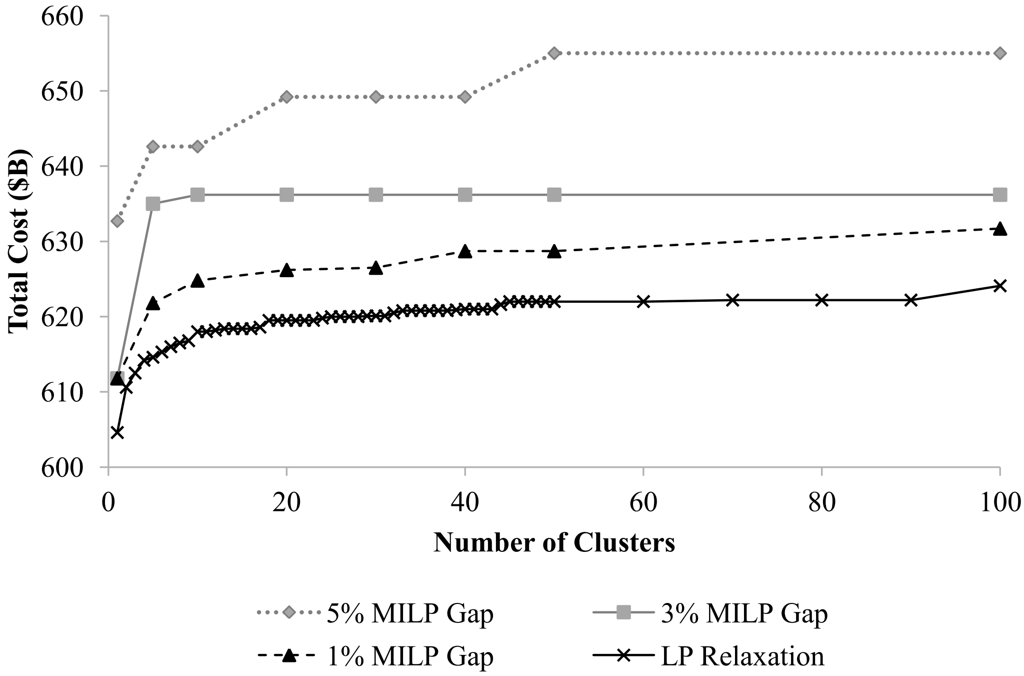

Figure 4.5: Optimal objective function value of the lower-bound problems as a function of the number of clusters for different MILP gaps and the linear relaxation.

utilizes clustered data, and they do not guarantee improvements on the quality of the investment plan when tested again the upper bound. As I observe in Figure 4.5, the rate of improvement of the lower bound deteriorates rapidly after the first 20 clusters, which could meet the convergence criterion described in Heejung and Baldick (2013), even though the solution gap is still above 10% (Figure 4.3).

I also observe that the lower-bound problem tends to underestimate transmission capacity for small cluster counts (see Figure 4.6), which is reflected as penalties due to curtailed load and noncompliance fines in the upper bound (see Figure 4.7).[9] Modifications to the clustering algorithm could potentially address this issue by weighting

[9]Additional information about changes in transmission and generation investments as a function of the number of clusters is included in Appendix C.3

(Tseng, 2007) or constraining (Wagstaff et al., 2001) K-Means to include peak-load hours as individual clusters. However, when I did a sensitivity analysis that included the peak-load hour as a single cluster, it only resulted on a marginal improvement for small cluster counts and did not change the solution quality compared to the regular K-Means algorithm, when more than 30 clusters were considered. A potentially better alternative to identify hours that drive transmission and generation investments is to first solve the planning problem for each hour independently, and use the resulting total cost vector to bias the hour-selection algorithm, as done in importance sampling (Infanger, 1992; Papavasiliou and Oren, 2013). However, these are all subjects of future research.

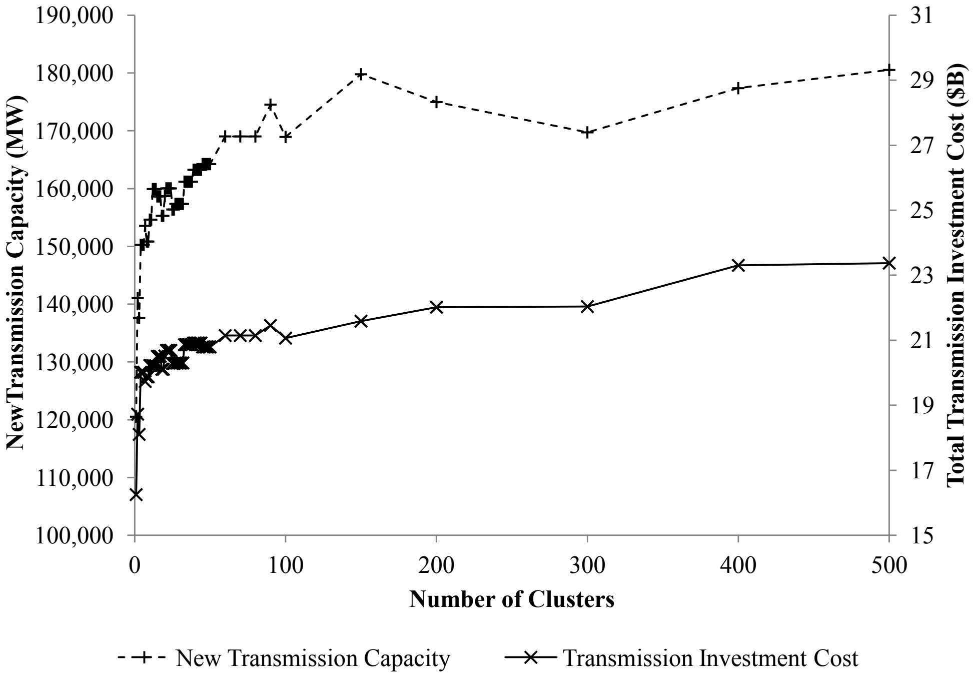

Figure 4.6: New transmission capacity and transmission investment costs as a function of the number of clusters for the linear relaxation.

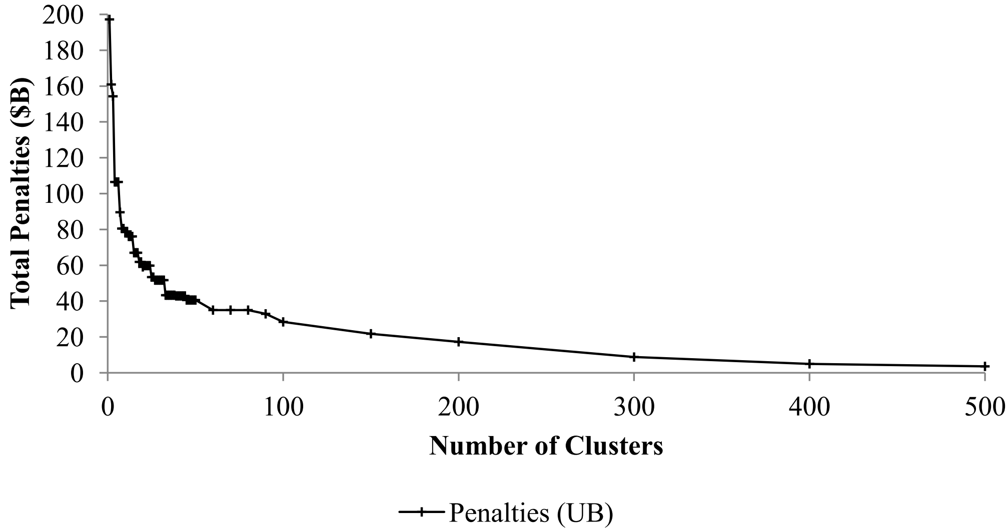

Figure 4.7: Penalties from upper-bound problem as a function of the number of clusters.

In summary, unless large cluster counts are considered, I do not recommend using the lower-bound planning problem to find investment plans without assessing their quality against the full resolution operations problem (upper bound). In the linear case, more than 200 clusters were needed to attain a solution gap below 5%, which could be considered as a reasonable precision tolerance for long-term planning purposes. Note that 200 clusters are nearly four times the number of clusters needed to achieve the "elbow" on the fraction of variance explained from the full dataset of load, wind, solar, and hydro levels (see Figure 4.1). The "elbow" criterion, often used to determine the number of clusters in a dataset (Tibshirani et al., 2001), can be used in my case to identify the point when the clustering algorithm becomes inefficient, and when it might be better to switch to phase two (Benders decomposition) of my proposed two-phase approach if tighter optimality gaps are needed. However, the "elbow" itself provides no information regarding the potential quality (i.e., optimality gap) of the investment plan that could be obtained just using the lower-bound planning problem.

4.5.6 Phase Two: Enhanced Benders Decomposition

4.5.6.1 Linear Problem (MILP)

The bounding algorithm successfully found investment solutions within a 2.8% optimality gap for the linear relaxation and within a 7.4% tolerance for the mixed-integer linear case. Achieving tighter tolerances, however, require significant refinements of the clustering due to the asymptotic convergence properties of the bounding method (Hobbs and Ji, 1999). To overcome this limitation, I utilized Benders' cuts to further reduce the optimality gap by iterating successively between the lower-bound investment planning problem (i.e., master problem) and the operations problems (i.e., subproblems). This procedure was outlined in Section 4.4 above.

Figure 4.8 shows the solution gap for the linear relaxation of Benders decomposition using different number of clusters as auxiliary lower bounds in the master problem. It also illustrates the convergence of the traditional Benders' algorithm without auxiliary bounds on the operations costs. The number of clusters for the experiments was selected based on changes in the convergence rate of the optimality

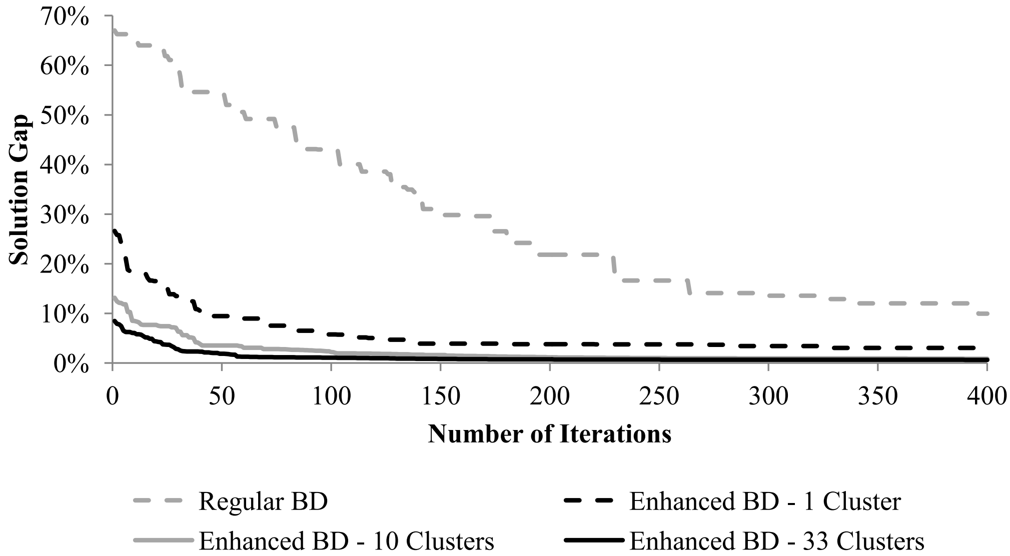

Figure 4.8: Solution gap versus the number of iterations for different Benders decomposition schemes of the linear relaxation. Upper and lower bounds are in Figure C.13 in Appendix C.4.

gap of the linear relaxation (see Figure 4.3). No experiments were considered beyond 33 clusters due to the significant decrease in the convergence rate of the bounding algorithm after that point. Although more clusters could further reduce the number of Benders' iterations required to achieve tight optimality gaps, their implementation would cause important increases in the time to solve the model in each iteration, particularly in the mixed-integer linear case (see Figure 4.4), and I leave it as a subject of future research. As in the previous section, I utilized the objective function value $TC_{LP}(\Psi^{150}, q^{150})$ to initialize the lower bound (LB_0). This is comparable to the method proposed by van Roy (1983) to compute auxiliary lower bounds for Benders decomposition using Lagrangian relaxation.

Table 4.2: Number of cuts and total computation time for different optimality gaps and auxiliary lower bounds of the linear relaxation.

Solution Gap LP Relaxation	Number of Clusters Used in the Auxiliary Lower Bound					
	1 Cluster		10 Clusters		33 Clusters	
	Number of Cuts	Total Time (s)	Number of Cuts	Total Time (s)	Number of Cuts	Total Time (s)
5.0%	117	31,140	38	11,307	17	6,026
3.0%	329	95,053	69	21,018	29	10,359
1.0%	>400	>117,332	246	78,917	116	44,001

In Figure 4.8 I observe that including the expected-value problem in the master problem, as done in Sen (2013), results in shrinkage of the solution gap to 3% in 329 iterations after 26.4 hours of computing time (Table 4.2). In contrast, the regular Benders decomposition implementation in which no such auxiliary constraint is included only yielded a 10.0% optimality gap after 400 iterations and 30 hours of computing time. Therefore, the regular Benders' implementation performed considerably worse than the bounding algorithm in terms of convergence time in the relaxed (LP) case. Including more clusters resulted in further reductions in the number of iterations and solution time to achieve small optimality gaps (Table 4.2). In this case, using 33 clusters reduced the solution time to achieve a 1% optimality gap in more than half (12.2 hours), compared to including the expected-value solution (1 cluster) in the master problem (more than 32.6 hours).

Including more clusters in the auxiliary lower bound of Benders decomposition yielded even larger speedups for looser solution tolerances, but the larger master

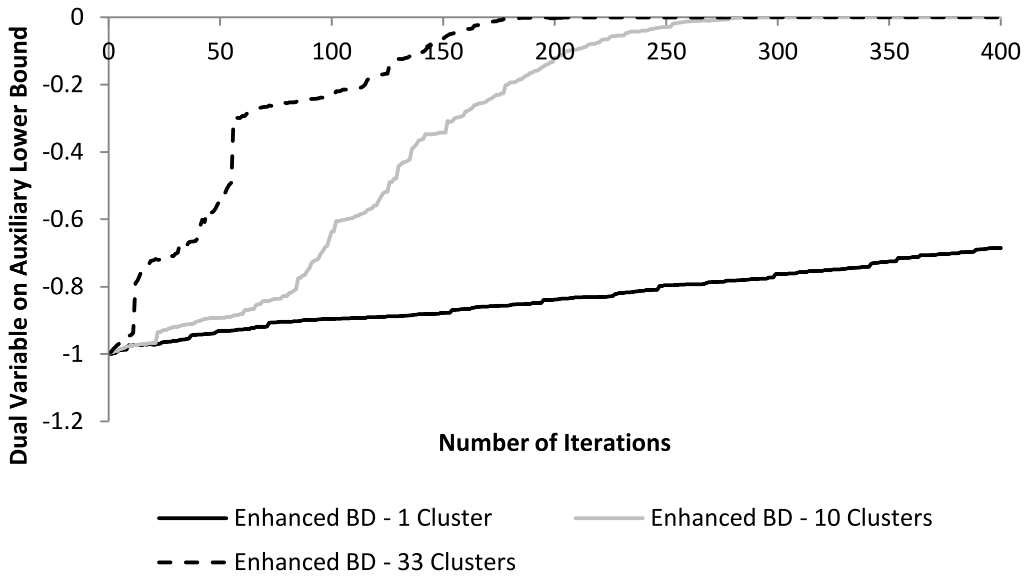

Figure 4.9: Dual multiplier on auxiliary lower bound versus number of iterations of Benders decomposition for the linear relaxation.

problem caused solution times to eventually become higher than those achieved by increasing the number of clusters using the bounding algorithm in the linear case. Attaining a 3% tolerance for the LP relaxation required 400 clusters (Figure 4.2) and 30 minutes of computation (Figure 4.4) through the bounding method, but 29 iterations (Figure 4.8) and 2.8 hours using the Benders approach with 33 clusters. Hence, the bounding method might be more efficient than the modified Benders' algorithm if loose optimality gaps for the linear relaxation are acceptable for planning purposes.

I also observe that the proposed auxiliary lower bound accelerated convergence of Benders decomposition throughout a large fraction of the iterations of the enhanced algorithm. Figure 4.9 shows the value of the dual variable on constraint (4.19) of the modified master problem. No cuts are available the first time the master problem is solved in the modified Benders decomposition and the only lower bound upon the operating costs is $f(x,(\Psi^k,q^k))$ with dual variable -1. As Benders' cuts are incorporated into the master problem, the contribution of the auxiliary lower bound $f(x,(\Psi^k,q^k))$ to the total system costs is progressively reduced, reflected in a smaller magnitude of its dual. In any case in which the Benders' cuts provide a tighter (i.e., higher) lower bound upon the operating costs than $f(x,(\Psi^k,q^k))$, the value of the dual variable for the auxiliary constraint (4.19) should be zero. This is the case for the 10- and 33-cluster experiments after 300 and 279 iterations, respectively. Note that in the 33-cluster experiment, the solution gap after 279 iterations is 0.67%; therefore, constraint (4.19) is still binding even when the Benders' algorithm has attained small optimality tolerances. In summary, as observed in Figure 4.9, the stringency of the auxiliary lower bound depends on the fidelity of the operations problem included in the master problem. More clusters result in higher values of the dual variables of (4.19) and result in less support from the Benders' cuts to approximate the operating costs.

4.5.6.2 Mixed-Integer Linear Problem (MILP)

For the mixed-integer linear case I followed the approach proposed by Mcdaniel and Devine (1977), and utilized the cuts computed using the linear relaxation for different optimality tolerances and imposed them in the mixed-integer master problem, in conjunction with the auxiliary lower bound (constraint (4.19)). I first considered the heuristic where I only use the cuts from the linear relaxation to shrink the optimality gap, without computing any cuts using the mixed-integer master problem. The second experiment considers both pre-computed cuts from the linear relaxation and iterations of the Benders' algorithm using the mixed-integer master problem.

Table 4.3 summarizes the results for the first set of experiments (heuristic) for different MILP gaps and numbers of clusters. The linear relaxation gap in the second column of Table 4.3 corresponds to the solution gap of the enhanced Benders decomposition; the number of cuts needed to attain such tolerances is listed in Table 4.2. Tightening the solution tolerance of the LP relaxation (i.e., adding more cuts) and the MILP gap often resulted in lower resulting gaps. However, in none of the experiments I was able obtain resulting gaps comparable to the solution tolerances attained using the Benders' cuts in the linear relaxation (second column of Table 4.3), even when considering a tight MILP gap of 0.5% (last three rows of Table 4.3). Counter intuitively, the addition of Benders' cuts resulted in looser solution tolerances in some cases. For instance, in the 10-cluster experiment with a 0.5% MILP gap, increasing the number of pre-computed cuts from the linear relaxation from 38 (5% LP gap) to 69 (3% LP gap) reduced the resulting gap from 7.9% to 5.9%. Yet, adding 177 more Benders' cuts (1% LP gap) resulted in a solution gap of 8.3%, higher than the one obtained with only 38 cuts, which illustrates the heuristic nature of this method.

The tightest solution tolerance, 4.3%, was obtained by including 116 Benders'

Table 4.3: Resulting solution gap and solution time to solve mixed-integer master problem using pre-computed cuts from its linear relaxation.

MILP Gap	Solution Gap LP Relaxation	Number of Clusters Used in the Auxiliary Lower Bound					
		1 Cluster		10 Clusters		33 Clusters	
		Resulting Gap	Solution Time MILP Master Problem (s)	Resulting Gap	Solution Time MILP Master Problem (s)	Resulting Gap	Solution Time MILP Master Problem (s)
5.0%	5.0%	16.1%	111	9.9%	56	9.8%	2,901
	3.0%	11.5%	554	13.3%	75	11.8%	192
	1.0%	-	-	12.1%	309	8.0%	294
3.0%	5.0%	16.1%	69	9.9%	58	8.8%	3,884
	3.0%	11.5%	421	12.4%	345	11.3%	1,619
	1.0%	-	-	11.7%	311	8.0%	291
1.0%	5.0%	9.4%	94	8.7%	1,529	7.0%	26,076
	3.0%	6.8%	546	7.6%	880	5.3%	2,467
	1.0%	-	-	7.1%	4,816	5.2%	6,624
0.5%	5.0%	8.8%	126	7.9%	5,998	6.2%	28,174
	3.0%	6.8%	541	5.9%	8,738	6.0%	11,625
	1.0%	-	-	8.3%	4,714	4.3%	35,045

cuts from the linear relaxation of the 33-cluster experiment with a 0.5% MILP gap, and is suitable for long-term planning purposes that do not require extremely tight solution gaps. Although this heuristic improved the solution tolerance of the MILP formulation from 7.4% (best solution found just using the bounding phase) to 4.3%, these are not general results and iterating with the mixed-integer master problem to compute tighter cuts might be needed to further reduce the solution gap.

Given the long solution times observed for the 10- and 33-cluster mixed-integer master problems for MILP gaps of 0.5%, I only considered further iterations of the enhanced Benders decomposition (second experiment) using the expected-value problem (1 cluster) and 400 pre-computed cuts from the linear relaxation. The solid gray line in Figure 4.10 illustrates the solution gap of the enhanced Benders decomposition without pre-computed cuts from the linear relaxation, whereas the solid black line shows the convergence of the same implementation with the 400 pre-computed cuts. The best investment plan found without pre-computed cuts resulted in a 7% optimality gap after 200 iterations and 43 hours of computation time. Computing the 400 cuts required 32.5 hours, but resulted in significant improvements in the solution gap in the mixed-integer linear problem. Only 11 iterations were needed to attain a 5% optimality gap (1.9 hours), and letting the algorithm run for 166 more iterations and 39.4 hours reduced the solution gap to 4.1%.

As in the previous experiments with the linear relaxation, I utilized the objective function value $TC_{LP}(\Psi^{150}, q^{150}) = 624.3$ to initialize the lower bound ($LB_0 = 624.3$). A tighter lower bound can be obtained from solving the linear relaxation close to optimality using the enhanced Benders decomposition. From my experiments, the 33-cluster implementation resulted in the tightest solution gap (0.64%) and in the highest lower bound (\$635.5 B) after 400 iterations and 44 hours of computation time (see Figure C.2 in Appendix C.2). If this value is used as an initial lower bound ($LB_0 = \$635.5$), the solution gaps of both experiments described in Figure 4.10 are reduced in approximately 1.7%. The solution tolerance of the investment plan found after 200 iterations is reduced from 4.1% (solid black line) to 2.4% (dotted black line), which is sufficient for long-term planning studies. Consequently, the auxiliary lower bound, pre-computed cuts, and a tight lower bound can be used to attain tight

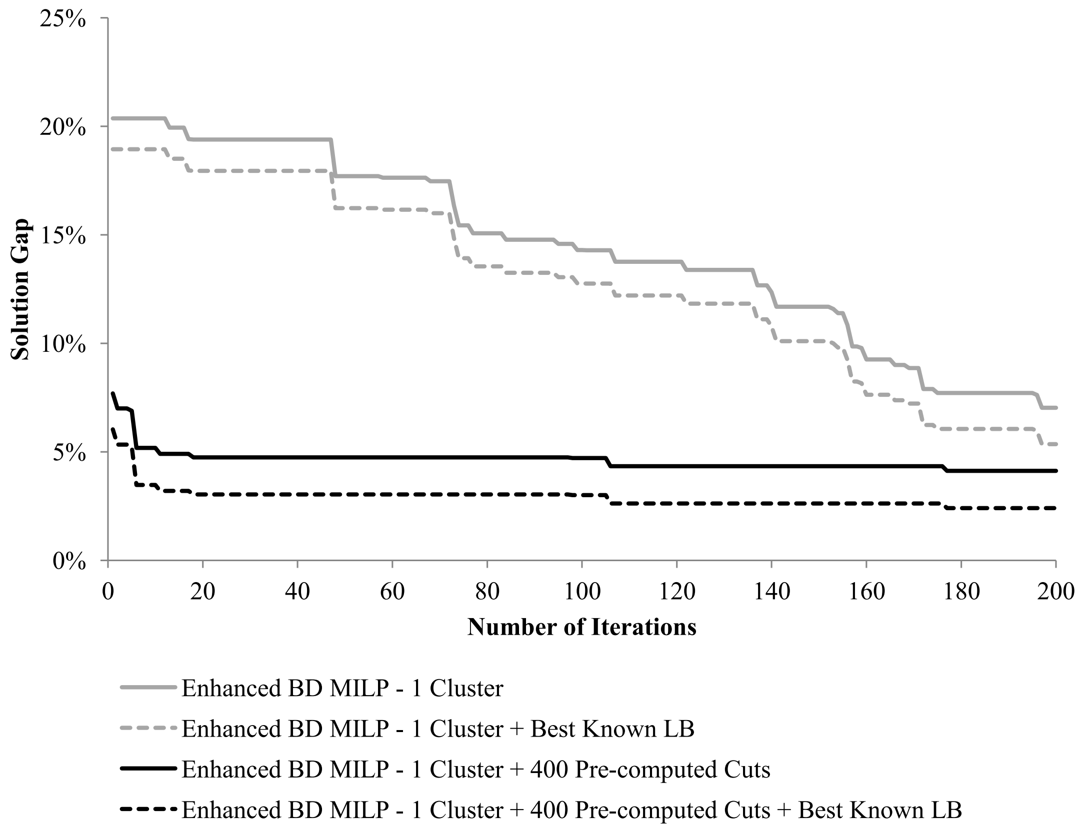

Figure 4.10: Solution gap for enhanced Benders decomposition applied to the mixed-integer linear problem, using one cluster as auxiliary lower bound, as a function of the number of iterations. Effect of using pre-computed cuts from the linear relaxation. Upper and lower bounds are in Figure C.14 in Appendix C.4.

solution gaps for large-scale planning problems with integer variables.

4.6 Conclusions

One of the challenges of increasing penetration of variable and unpredictable generation from renewables is capturing the true economic value of these resources in long-term investment planning models. Two aspects that complicate the proper selection of transmission and generation investments under scenarios of large renewable penetration are their variability and geographic distribution. The former can be addressed by refining the time resolution of operations models used within planning analyses, whereas the latter involves consideration of transmission and generation investment alternatives on a system-wide basis. While conventional planning models can be improved upon to address both complications, they will likely result in optimization problems of unmanageable sizes with current computer hardware.

In this chapter, I proposed a two-phase solution approach that improves existing bounding and decomposition algorithms to find investment plans with bounds upon the optimal system costs for large-scale transmission and generation planning problems. The bounding phase is an extension of approaches proposed in Hobbs and Ji (1999) for stochastic problems with environmental restrictions that I model with expectation constraints. The decomposition phase is a modification of Benders decomposition that includes a low-resolution operations problem in the master problem as an auxiliary lower bound upon the operating costs. I compute upper bounds for both algorithms using a sub-sample estimation of the true operating costs for a given investment plan implemented in a parallel computer system. From my numerical experiments, I find that the bounding phase can be more efficient than the traditional Benders decomposition to find investment plans within moderate optimality tolerances (i.e., 3% to 6% approximately) for both linear and mixed-integer cases. For implementation purposes, the bounding phase is far more practical than Benders decomposition since improving the quality of the investments only requires refining the clustering of the time-dependent data. However, for applications where the bounding method presents rapid deterioration of the convergence rate, a combination of the bounding algorithm with Benders decomposition, as demonstrated in phase two, can be used to attain tight optimality gaps, and is more efficient than using any of these two algorithms separately.

My enhancement to the Benders algorithm is based on a lower bound that could be progressively improved by refining the partitioning of the space of load, wind, solar, and hydro levels, but which requires the planning problem to have all stochasticity limited to the right-hand-side of the constraints so that I can apply Jensens' inequality. An interesting direction for future research would be to explore the effect of including other valid lower bounds in the master problem of Benders decomposition. This could be done, for example, by relaxing constraints that complicate the solution of the planning model and iterating between loosely constrained (lower bound) and highly constrained (upper bound) problems. Another potential extension of my algorithm is the inclusion of unit commitment variables and constraints in long-term planning model, an area of growing attention among operation researchers

(Palmintier and Webster, 2011; Nweke et al., 2012; Shortt et al., 2013). This would, however, require including binary variables in the operations problems which would then become nonconvex. My bounding algorithm would still be applicable by relaxing all binary variables to compute lower bounds; however, I would not be able to guarantee convergence of the bounds to the true optimal system costs. Baringo and Conejo (2012) and Kazempour and Conejo (2012) have recently implemented and shown convergence of Benders decomposition including integer variables in the subproblems. Their results are based on Bertsekas and Sandell (1982), who proved that for a certain class of stochastic mixed-integer optimization problems, the duality gap converges to zero as the number of scenarios and integer variables is increased to infinity. A future step in my research is to study the implications of this result for a planning problem with unit commitment variables and to verify convergence of the Benders' algorithm with nonconvex subproblems.

Chapter 5

Conclusions

5.1 Summary

This dissertation studies and addresses some of the challenges faced in the field of transmission planning with an emphasis on the complexities brought on by accommodating renewables in electric power systems. These challenges, and the resulting analyses, are presented in three independent essays. In the first essay I study the effects of transmission nonlinearities on the cost and performance of Renewable Portfolio Standards. The second essay describes a new methodology for adaptive transmission planning under market and regulatory uncertainties. In the third essay I propose novel bounding and decomposition methods for large-scale transmission and generation planning under policy constraints that incentivize high amounts of intermittent generation from renewable resources. Although the three essays are self-contained, they all utilize methods from operations research, economics, and electrical engineering to provide a better understanding of policy, economic, and engineering aspects of power transmission planning.

In the first essay, included as Chapter 2, I present a study of the effects of transmission nonlinearities in the cost and performance of Renewable Portfolio Standards. I find that ignoring transmission constraints or assuming that transmission investments can take place in small increments, as it is often done in high-level policy models, can result in significant biases on implementation cost estimates and distorted generation investment recommendations. As illustrated using a simple two-node example, the optimal development of new generation capacity as renewable goals get more stringent is, in general, non-monotonic. The inclusion of transmission lumpiness and Kirchhoff's Voltage Law often results in non-monotonic changes in the type and location of generation and transmission investments with respect to renewable targets. This means that those investments that are economically optimal for small renewable goals are not necessarily part of the set of investments for higher renewable targets.

A direct implication of the results from Chapter 2 is that neither generation nor transmission investments should be analyzed using renewable resource supply curves, which rank generation resources based on levelized costs as a function of the renewable targets. Furthermore, the marginal system costs as a function of the renewable targets might decrease rather than increase as the RPS goal increases. If noncompliance is allowed with a financial penalty, a decrease in marginal system costs can be reflected as noncompliance of renewable targets for intermediate RPS goals, but as full compliance for higher RPSs. I also utilize multi-stage models to study the effects of using different RPS designs to attain a final, long-term goal of renewable energy supply. I find that it is possible to attain cost-savings by allowing electric utilities to bank and borrow renewable energy certificates between compliance periods and by coordinating transmission investments with the design of the renewable energy policies.

The model described in the second essay is a novel approach to transmission planning under market and regulatory uncertainties. The model is formulated as a two-stage stochastic mixed-integer linear program that can be solved using commercial optimization packages, and considers generators' response to transmission investments, as well as Kirchhoff's Voltage Law through linear disjunctive constraints. Uncertainty is modeled using different scenarios that represent possible future policy, economic, and technological states of the world. I present a numerical application of the stochastic planning model using a 240-bus representation of the Western Electricity Coordinating Council and three distinct scenarios of carbon and renewable energy policies. I also compare the performance of different heuristic investment strategies based on scenario analysis, which are commonly used among practitioners in real-world transmission planning studies. I find that the stochastic solution yields significantly lower costs, in an expected value sense, than any of the optimal deterministic strategies for each scenario. This is reflected in the Expected Cost of Ignoring Uncertainty (ECIU), which is approximately three times the cost of first stage transmission investments of the optimal stochastic solution. Heuristic solutions, on the other hand, perform worse than the stochastic solution and, in some cases, could result in higher expected costs than the scenario-specific deterministic solutions. These results are consistent with Wallace (2000), in that scenario analysis, and heuristic approaches based on scenario analysis, are weak methods for finding investment plans to hedge against uncertainty. The stochastic investment model explicitly values flexibility and selects transmission investments that are sub-optimal and not part of the optimal solution for any of the three deterministic scenarios. Thus, stochastic transmission planning models that consider optionality and flexibility from the entire networks perspective are needed for investment planning under uncertainty.

Finally, the third essay, included as Chapter 4 in this dissertation, proposes new bounding and decomposition methods for solving large-scale transmission and generation planning problems under policy constraints. These restrictions, which I model as expectation constraints, are used to incentivize investments and generation from renewable resources (e.g., Renewable Portfolio Standards) or to limit emissions from carbon-intensive power plants (e.g., carbon cap-and-trade programs). The bounding phase of my algorithm corresponds to an improvement of the method proposed by Hobbs and Ji (1999), which I extend for stochastic optimization problems with expected-value constraints. I compute lower bounds using an investment problem that utilizes clustered load, wind, solar, and hydro data. Upper bounds are calculated using a parallelizable sub-sampling methodology to approximate the true operating costs for a given investment plan. The decomposition phase is an enhancement of Benders decomposition, which I improve by including an auxiliary lower bound from the bounding phase in the master problem. I find that the bounding phase is more efficient and practical than the decomposition phase at finding near-optimal investment plans (i.e. 3%-5% optimality gaps). However, for extremely large planning problems, attaining high-quality solutions using the bounding algorithm can be computationally prohibitive. For those cases, the decomposition phase, which combines Benders decomposition and an auxiliary lower bound from the bounding phase, is more efficient than using any of these two algorithms separately.

The new planning methods presented in chapters 3 and 4 of this dissertation are relevant for real-world transmission planning studies, while the analysis presented in chapter 2 contributes to a better understanding of the implications of ignoring some of the physical characteristics of power transmission networks in high level models for policy analysis. Today, uncertainty and variability are two of the main concerns for planning authorities that seek to optimize investment decisions for a future with a large share of renewables energy technologies. However, due to computational limitations, these two factors are often only considered in the sensitivity and/or scenario analysis stages of planning studies, after the selection of investment decisions has already been made. Chapters 3 and 4 describe new methods to explicitly account for these factors within planning models, and their inclusion could result in potentially better investment alternatives compared to analyses that ignore uncertainty or that use coarse representations of intermittent resources. Although the methods here are applied to power systems, they could be easily adapted to solve problems in other areas involving complex infrastructure systems, such as transportation, telecommunications, and manufacturing.

5.2 Future Research

The experiments conducted in this research address some of the challenges of power transmission planning under uncertainty and renewable resource policies. However, with any research project, there are limitations, and more research could be conducted to further improve the aforementioned models. One of the greatest limitations of the numerical results presented in the first essay (Chapter 2) is scale. The theoretical conclusions about the impact of relaxing the indivisibility of transmission investments and Kirchhoff's Voltage Law are model-independent, but the magnitude of the biases that result due to these simplifications in larger models is unknown. A direct extension of the research presented in Chapter 2 would be to study the effects of these approximation models in large energy-economic models, such as Haiku (Paul and Burtraw, 2002) and ReEDS (Short et al., 2011). New work in this direction would allow one to revise these high-level models in order to emulate the effect of the physical characteristics of power transmission networks on infrastructure investments under renewable resource policies.

Scale is also a limitation on the study presented in the second essay (Chapter 3). The application only considered a 240-bus network reduction of the Western Electricity Coordinating Council and 3 scenarios of distinct market and regulatory uncertainty. However, a real-world planning study could involve thousands of transmission investment alternatives and dozens of scenarios. For those cases, it is unlikely that the resulting mixed-integer stochastic program will be solvable directly using commercial solvers, as was done in Chapter 3. A next step in the research proposed in the second essay is to implement alternative solution techniques that could leverage parallel computer systems. A promising algorithm with such capabilities is Progressive Hedging (Rockafellar and Wets, 1991). This method could be used to decompose the stochastic transmission planning problem on a per-scenario basis by relaxing non-anticipativity constraints.

Finally, all models in this dissertation ignored ramping limits as wells as unit commitment variables and constraints. Although these relaxations have historically been considered reasonable in long-term investment planning studies, the large scale integration of highly variable and unpredictable generation from renewable resources will require careful consideration of extreme ramp events. Future work in this direction will require utilization of chronological optimization in probabilistic production cost models. This could be done by, for example, sampling representative weeks from historical time series of load, wind, solar, and hydro data (de Sisternes and Webster, 2013), and enforcing ramping limits between all hours within each week. A further refinement in this direction is modeling unit commitment variables and constraints, since, as discussed in Palmintier and Webster (2011), Nweke et al. (2012) and Shortt et al. (2013), their relaxation can bias the optimal generation mix in long-term investment models. Such improvement to the models proposed in this dissertation will, however, result in increased computational complexity due to the non-convexities that result from including binary unit commitment variables. As discussed at the end of Section 4.6 in Chapter 4, such complex planning problems could be solved using an extension of the enhanced Benders decomposition model that I propose in the third essay.

Appendix A

Chapter 2 Additional Material

This section describes all the network data for the Garver six-bus test-case as well as load, wind, and solar characteristics that I utilized to perform all analysis in Chapter 2.

Table A.1: Correlations, means and standard deviations of load and capacity factors.

	Demand	Solar	Wind 6	Wind 4	Wind 1
Demand	1	0.035	-0.08	-0.293	-0.34
Solar	0.035	1	0.017	0.207	0.597
Wind 6	-0.08	0.017	1	0.399	0.397
Wind 4	-0.293	0.207	0.399	1	0.778
Wind 1	-0.34	0.597	0.397	0.778	1
Mean	0.683	0.337	0.494	0.481	0.407
Standard deviation	0.124	0.239	0.377	0.382	0.463

Table A.2: Garver network lines characteristics and investment costs.

Line Number	From Node	To Node	Thermal Limit Per Circuit [MW]	Susceptance Per Circuit [p.u.]	Capital Costs Per Circuit [10^6 \$]
1	1	2	100	2.5	400
2	1	3	100	2.63	380
3	1	4	80	1.67	600
4	1	5	100	5	200
5	1	6	70	1.47	600
6	2	3	100	5	200
7	2	4	100	2.5	400
8	2	5	100	3.23	310
9	2	6	100	3.33	400
10	3	4	82	1.69	590
11	3	5	100	5	200
12	3	6	100	2.08	480
13	4	5	75	1.59	630
14	4	6	100	3.33	350
15	5	6	78	1.64	610

Table A.3: Load and renewable generator capacity factors for the 20 time blocks.

Time Block	Demand	Solar	Wind 6	Wind 4	Wind 1
1	0.5	0	0.933	0.98	0
2	0.651	0.151	0.994	0.974	0.988
3	0.658	0	0.615	0.51	0
4	0.528	0	0.11	0.003	0.011
5	0.7	0.068	0.085	0.076	0.02
6	0.551	0	0.148	0.638	0.777
7	0.715	0.004	0	0.072	0
8	0.967	0	0.977	0	0.003
9	0.685	0.538	0.971	0	0
10	0.702	0	0.049	0.53	0.038
11	0.6	0	0.252	0.729	0.004
12	0.687	0	1	0.993	1
13	1	0	0.066	0.229	0.009
14	0.594	0.504	0.981	0.025	0.474
15	0.634	0.048	0.581	0.149	0.005
16	0.651	0.612	0.18	0.983	0.978
17	0.747	0.669	0.33	0.136	0
18	0.609	0.354	0.603	0.992	0.981
19	0.747	0.306	0.175	0.249	0
20	0.729	0.451	0.335	0.383	0

Appendix B

Chapter 3 Additional Material

B.1 Generation Investment Alternatives

This section describes the candidate generation resources considered in Chapters 3 and 4 of this dissertation. The original WECC 240-bus test-case (Price and Goodin, 2011) does not include information about candidate resources, so it was necessary to include such data from various databases. Here I summarize some of the most important assumptions. Detailed information about intermittent resource profiles and specific locations can be found in the supporting electronic files of this dissertation.

For candidate renewable resources, I utilized the California Renewable Energy Zones (CREZ) (RETI, 2010) and the Western Renewable Energy Zones (WREZ) (WREZ, 2012) studies, both of which provide location and resource potentials in California and the rest of the regions that are part of the Western Electricity Coordinating Council (excluding California), respectively. Hourly resource profiles were retrieved from NREL's Western Wind Resources Dataset (NREL, 2012b) and NREL's PVWatts (NREL, 2012a) online tool for the year 2004, using the geographic locations listed in the CREZ and WREZ studies. A large fraction of this work was done by Jonathan Ho and Saamrat Kasina, who collaborated with me as research assistants from March 2011 until November 2013.

B.1.1 California Renewable Energy Zones (CREZ)

I assumed that, within California, the costs of interconnecting the resources listed in the CREZ study (RETI, 2010) to the existing grid were negligible and, therefore, all resources from the CREZ study were aggregated and made available at the nearest bus of the WECC 240-bus system. The following three tables summarize the resource potentials and assumed location of biomass (Table B.1), solar (Table B.2), and wind (Table B.3) resources in the WECC 240-bus system.

Table B.1: Biomass resource potentials from CREZ study.

Bus Number	Resource Potential (MW)
17	65
85	55
21	91
27	138
30	37
Total CREZ Biomass Potential	386

Table B.2: Solar resource potentials from CREZ study.

Bus Number	Average Capacity Factor 2004	Resource Potential (MW)
10	0.24	7,550
14	0.24	10,420
17	0.22	2,850
18	0.25	3,205
27	0.22	7,445
30	0.21	1,350
43	0.25	5,875
44	0.25	3,780
45	0.25	1,200
60	0.21	5,000
68	0.21	6,200
69	0.23	2,800
70	0.23	800
132	0.25	7,545
Total CREZ Solar Potential		66,020

Table B.3: Wind resource potentials from CREZ study.

Bus Number	Average Capacity Factor 2004	Resource Potential (MW)
15	0.23	338
18	0.21	51
27	0.36	582
30	0.37	855
43	0.33	86
67	0.34	329
85	0.28	132
Total CREZ Wind Potential		2,373

B.1.2 Western Renewable Energy Zones (WREZ)

For renewable resources outside of California, I utilized the potentials listed in the WREZ study (WREZ, 2012). Most renewable hubs (i.e. WREZ) are far from the existing buses listed in the WECC 240-bus test-case and interconnection costs are, therefore, not negligible. I assumed that all renewable hubs could be interconnected to the nearest bus of the WECC 240-bus system using up to four radial circuits of 500 kV each. Table B.4 lists all renewable hubs, number of nearest bus, distance, and transmission cost estimates per circuit. Table B.5 lists resource potentials and average capacity factors for the year 2004 for each renewable hub.

Table B.4: WREZ distances to nearest bus in WECC 240-bus test-case and interconnection costs per circuit ($2.88M per mile).

Renewable Hub ID	Nearest Bus	Distance (miles)	Capacity of 500 kV Single-Circuit Alternative (MW)	Cost of 500 kV Single-Circuit Alternative ($M)
1	45	22	3,479	63
2	1	28	3,275	79
3	9	100	2,168	287
5	127	349	1,088	1,004
6	113	398	973	1,147
8	3	166	1,726	479
9	107	47	2,810	136
10	108	82	2,333	237
11	110	136	1,898	392
14	2	135	1,906	388
19	115	192	1,601	554
20	117	191	1,605	551
21	4	59	2,624	169
23	99	86	2,291	248
24	95	32	3,150	92
25	103	50	2,757	145
26	124	72	2,442	209
27	94	33	3,116	95

Table B.5: WREZ resource potentials and average capacity factors.

Renewable Hub ID	Resource Potentials (MW)			Average Capacity Factor 2004	
	Geothermal	Solar	Wind	Solar	Wind
1		8,184	217	0.22	0.26
2		696	3,499	0.22	0.26
3		38,309		0.23	
5		4,943	11,461	0.21	0.32
6			19,071		0.32
8		183	11,290	0.22	0.34
9	125		696		0.25
10	154		907		0.22
11			10,058		0.31
14		32,156	1,894	0.23	0.31
19	24	17,382		0.22	
20	1,344	16,741	198	0.21	0.21
21		7,916	233	0.22	0.27
23			2,043		0.24
24	501		511		0.23
25	331		343		0.23
26	225	15,268	1,678	0.22	0.26
27			3,260		0.23
Total WREZ Potentials	2,704	141,778	67,359		

B.1.3 Conventional Generation

Unlike the CREZ and WREZ studies, I found no data available regarding the availability of sites for building new conventional generators. I made the assumption that up to 20,000 MW of new capacity per bus could be built of each of the following technologies: combined cycle gas turbines (CCGT), combined cycle gas turbines with carbon capture storage (CCGT CCS), and combustion turbines (CT). However, I did not allow for investments in new conventional generators in buses representing densely populated areas of the WECC, such as the city of San Francisco. For potentials of new coal power plants, I assumed that the existing generators listed in the WECC 240-bus test-case could be replaced by coal power plants with carbon capture storage technology (Coal CCS). Table B.6 summarizes maximum installed generation capacity per technology and state.

Table B.6: Maximum installed generation capacity per technology and state.

State	Maximum Installed Generation Capacity per Technology (MW)									Total per State (MW)
	Biomass	CCGT	CCGT CCS	Coal	CT	Geothermal	Hydro	Solar	Wind	
AB	269	20,000	20,000	5,275	20,000		1,890		1,959	69,393
AZ	489	40,000	40,000	2,685	40,000			74,361	8,363	205,898
BC	880	20,000	20,000		20,000	308	5,926			67,114
CA		340,000	340,000		340,000			62,569	14,777	1,097,346
CO	141	40,000	40,000	3,978	40,000			4,943	12,394	141,456
ID	358	20,000	20,000	13	20,000	279	8		1,603	62,261
MT	147	40,000	40,000	2,225	40,000				11,458	133,830
MX		20,000	20,000		20,000					60,000
NM	44	40,000	40,000	5,889	40,000			183	11,290	137,406
NV	318	60,000	60,000	1,037	60,000	1,368	2	56,303	1,228	240,256
OR	349	60,000	60,000	452	60,000	832	557		4,443	186,633
UT	3	20,000	20,000	5,091	20,000	225		15,868	1,678	82,865
WA	448	60,000	60,000	1,290	60,000	32	165		5,463	187,398
WY	29	20,000	20,000	4,675	20,000				22,093	86,797
Total per Technology (MW)	3,475	800,000	800,000	32,610	800,000	3,044	8,548	214,227	96,749	2,758,653

B.1.4 Characteristics of Load and Intermittent Generation Data

Table B.7 shows the population moments of a sample of 18 profiles of load, wind, and solar parameters. The full dataset is composed of 8,736 observations of 22 demand profiles, 67 wind profiles (18 existing + 49 candidate locations), 31 solar profiles (2 existing + 29 candidate), 29 hydro profiles (27 existing + 2 candidate), and 2 profiles of existing biomass powered generators. All hourly profiles are included in the supporting electronic files of this dissertation.

Table B.7: Means, standard deviations, and correlations for a sample of load, wind, and solar profiles.

		Demand profiles per region					Wind profiles per state							Solar profiles per state			
		SOUTHWST	BAYAREA	NORTHWST	CANADA	ROCKYMT	CA	AZ	NM	CO	NV	AZ	WA	CA	AZ	NM	CO
Demand	SOUTHWST	1.00															
	BAYAREA	0.71	1.00														
	NORTHWST	0.42	0.70	1.00													
	CANADA	0.25	0.68	0.91	1.00												
	ROCKYMT	0.67	0.82	0.86	0.79	1.00											
Wind	CA	-0.27	-0.28	-0.21	-0.21	-0.26	1.00										
	AZ	-0.21	-0.18	-0.15	-0.13	-0.18	0.49	1.00									
	NM	-0.27	-0.15	-0.01	0.06	-0.09	0.20	0.38	1.00								
	CO	-0.31	-0.19	-0.03	0.04	-0.14	0.23	0.41	0.77	1.00							
	NV	-0.30	-0.12	0.04	0.08	-0.04	0.46	0.37	0.20	0.20	1.00						
	AZ	-0.33	-0.16	-0.02	0.03	-0.11	0.48	0.55	0.22	0.26	0.83	1.00					
	WA	-0.16	-0.11	-0.03	0.06	-0.06	0.09	0.08	0.18	0.27	-0.03	0.03	1.00				
Solar	CA	0.23	0.40	0.32	0.32	0.36	-0.07	-0.10	0.02	-0.01	-0.01	-0.07	0.05	1.00			
	AZ	0.25	0.43	0.32	0.34	0.37	-0.08	-0.10	0.01	-0.02	-0.01	-0.07	0.03	0.96	1.00		
	NM	0.24	0.42	0.33	0.34	0.37	-0.07	-0.10	0.02	-0.01	-0.01	-0.07	0.04	0.96	0.98	1.00	
	CO	0.23	0.41	0.33	0.34	0.37	-0.06	-0.09	0.02	0.00	-0.01	-0.06	0.04	0.96	0.97	0.98	1.00
Mean		15,077	4,246	21,299	14,160	9,593	0.37	0.26	0.31	0.34	0.27	0.26	0.23	0.24	0.22	0.23	0.22
Std. Dev.		3,328	741	3,289	1,571	1,348	0.29	0.25	0.26	0.27	0.25	0.21	0.21	0.32	0.30	0.30	0.29

B.2 Backbone Transmission Investment Alternatives

Table B.8: List of Backbone Transmission Investment Alternatives ($2.88M per mile).

Branch Number	From Bus Number	To Bus Number	Length (miles)	Capacity of 500 kV Single-Circuit Alternative (MW)	Susceptance of 500 kV Single-Circuit Alternative (p.u.)	Cost of 500 kV Single-Circuit Alternative ($M)
1	52	64	60.0	2,817	53.7	172.8
2	52	71	57.1	2,866	60.0	164.3
3	52	78	6.3	3,895	628.9	18.2
4	156	189	142.0	1,948	375.0	1,469.2
5	157	211	219.1	1,522	10.4	631.0
6	127	128	43.8	6,660	259.9	453.3
7	127	238	24.7	3,654	80.9	255.2
8	127	152	36.0	6,660	259.9	373.0
9	196	200	66.8	2,559	677.7	290.2
10	196	214	115.2	1,976	945.4	500.2
11	196	223	49.5	2,831	995.6	215.0
12	158	156	229.5	1,587	375.0	2,375.6
13	158	161	0.9	22,650	6465.5	9.1
14	159	162	0.9	3,450	3333.3	2.5
15	159	187	111.1	2,133	122.0	320.0
16	224	210	271.1	1,614	77.7	2,806.0
17	224	218	149.8	1,889	77.7	1,550.0
18	225	196	121.3	1,919	33.4	526.6
19	225	198	238.0	1,425	489.1	1,033.4
20	199	212	152.9	1,867	77.7	1,582.4
21	199	218	104.1	2,319	101.4	1,077.9
22	128	145	28.5	6,660	259.9	295.5
23	160	228	227.2	1,732	37.2	654.2
24	86	92	22.4	8,400	590.6	231.5
25	86	93	37.9	8,400	590.6	392.7
26	86	152	23.9	6,660	259.9	246.9
27	86	154	30.4	8,400	590.6	314.2
28	200	209	109.2	2,035	41.9	474.1
29	200	214	48.4	2,850	945.4	210.3
30	200	222	44.6	2,915	130.8	193.7
31	200	223	18.7	3,412	2122.6	81.0
32	192	193	376.2	2,045	14.3	1,083.5
33	193	190	177.8	12,311	750.0	3,840.2
34	54	61	23.1	3,688	224.1	239.5
35	54	63	24.1	3,666	197.4	249.6
36	54	74	26.5	3,613	160.4	274.6
37	54	75	21.8	3,719	219.2	225.5
38	129	143	18.8	6,660	259.9	194.5
39	129	145	32.0	6,660	259.9	331.7
40	202	207	203.8	1,466	945.4	884.8

Branch Number	From Bus Number	To Bus Number	Length (miles)	Capacity of 500 kV Single-Circuit Alternative (MW)	Susceptance of 500 kV Single-Circuit Alternative (p.u.)	Cost of 500 kV Single-Circuit Alternative ($M)
41	204	199	280.6	1,636	101.4	2,903.8
42	204	212	319.6	1,782	101.4	3,307.8
43	204	216	246.9	1,584	101.4	2,555.4
44	205	211	292.4	1,591	71.2	842.0
45	3	1	22.7	7,922	154.1	147.4
46	3	17	225.7	1,514	47.4	650.0
47	130	132	93.7	6,285	44.3	969.6
48	130	154	54.6	6,285	74.3	565.2
49	132	235	521.7	3,955	80.9	5,399.2
50	132	133	45.8	5,603	80.9	474.3
51	132	137	62.9	6,285	65.9	650.9
52	132	147	34.2	5,640	112.9	354.0
53	132	154	147.0	5,603	27.4	1,521.9
54	235	238	366.5	2,071	54.7	3,793.1
55	235	240	344.5	1,920	27.4	3,565.1
56	164	157	72.7	2,619	50.0	209.3
57	164	175	97.1	2,291	48.3	279.7
58	164	183	125.7	1,989	122.0	362.2
59	33	49	34.5	3,600	110.5	99.3
60	111	114	77.1	2,555	51.6	221.9
61	111	118	76.0	2,570	47.9	219.0
62	34	39	9.2	17,400	290.7	94.8
63	34	43	30.5	8,700	106.6	315.9
64	35	42	52.7	3,600	70.7	151.7
65	79	81	6.2	8,400	590.6	64.2
66	209	214	70.4	2,507	64.5	305.6
67	209	219	130.8	1,838	25.6	568.0
68	209	221	52.7	2,778	60.5	229.1
69	209	222	66.2	2,569	57.4	287.3
70	6	1	131.9	1,829	113.2	572.6
71	6	220	94.2	2,198	51.6	409.1
72	6	19	23.6	3,310	424.5	102.6
73	7	13	141.5	1,858	31.6	407.7
74	7	14	121.5	2,029	10.4	349.9
75	106	135	32.9	6,660	259.9	340.5
76	106	136	20.3	6,660	259.9	210.0
77	210	216	98.6	2,387	77.7	1,020.1
78	113	126	67.7	6,660	259.9	700.4
79	114	139	81.4	2,450	50.4	234.5
80	55	70	3.0	4,173	1,037.3	31.6
81	55	73	5.2	4,117	1,399.3	54.3
82	133	154	101.2	5,603	36.7	1,047.6
83	134	145	26.3	3,618	259.9	272.1
84	134	238	22.9	3,693	80.9	237.2
85	134	152	72.6	6,660	259.9	750.9
86	229	221	147.5	1,715	23.3	640.7
87	98	113	52.6	6,660	259.9	543.9
88	98	100	53.0	6,660	259.9	548.1
89	98	103	31.1	6,660	259.9	322.3
90	98	104	41.2	6,660	259.9	426.6

Branch Number	From Bus Number	To Bus Number	Length (miles)	Capacity of 500 kV Single-Circuit Alternative (MW)	Susceptance of 500 kV Single-Circuit Alternative (p.u.)	Cost of 500 kV Single-Circuit Alternative ($M)
91	166	177	88.8	3,020	41.5	255.8
92	9	221	233.1	1,426	16.4	1,012.3
93	175	211	300.4	1,618	44.3	865.0
94	175	183	151.5	1,787	122.0	436.4
95	175	187	102.7	2,226	122.0	295.7
96	56	65	30.2	3,533	204.4	312.5
97	56	72	28.0	3,580	244.0	290.3
98	56	73	35.3	3,426	174.6	365.0
99	107	131	95.8	5,000	693.0	1,916.0
100	25	33	94.9	2,318	72.5	273.3
101	25	27	12.6	3,935	106.6	130.1
102	59	229	107.1	2,057	23.3	464.9
103	59	214	40.6	2,987	91.8	176.2
104	87	91	14.7	8,400	590.6	152.6
105	177	159	18.2	2,175	224.2	52.4
106	177	211	360.4	1,930	30.3	1,038.0
107	177	175	89.7	2,384	50.0	258.2
108	177	187	112.2	2,122	122.0	323.0
109	136	154	35.9	6,660	259.9	372.0
110	213	202	213.1	1,447	489.1	925.2
111	36	39	12.0	17,400	590.6	123.7
112	137	154	84.9	6,285	46.6	879.2
113	139	142	43.8	2,450	77.1	126.0
114	139	153	55.7	2,450	27.4	160.5
115	139	239	54.6	1,800	-75.1	157.3
116	37	35	163.8	3,600	36.0	471.9
117	37	41	28.3	3,600	133.3	81.5
118	37	42	160.0	3,600	32.3	460.9
119	37	47	45.5	3,600	78.1	130.9
120	37	78	14.4	3,705	243.9	41.6
121	37	51	41.7	3,600	88.9	120.2
122	179	231	211.7	1,450	33.4	919.3
123	180	170	182.4	3,020	66.6	525.4
124	180	173	182.4	3,020	70.8	525.4
125	180	182	74.3	2,595	418.4	214.0
126	180	236	130.0	1,951	77.3	374.5
127	80	82	4.0	17,760	693.0	80.8
128	81	87	19.1	8,400	590.6	197.3
129	81	85	10.1	8,400	590.6	104.1
130	102	113	42.4	6,660	259.9	439.3
131	102	103	43.7	6,660	259.9	452.3
132	12	35	13.3	3,731	10.4	38.3
133	12	10	54.8	2,904	47.4	157.9
134	12	78	166.1	1,699	39.6	478.4
135	12	21	188.5	1,598	14.9	542.9
136	39	40	29.8	3,541	138.9	308.8
137	39	46	23.1	6,660	259.9	239.3
138	39	50	32.7	17,400	189.9	339.0
139	89	91	18.6	8,400	590.6	192.9
140	89	141	35.4	6,660	259.9	366.2

Branch Number	From Bus Number	To Bus Number	Length (miles)	Capacity of 500 kV Single-Circuit Alternative (MW)	Susceptance of 500 kV Single-Circuit Alternative (p.u.)	Cost of 500 kV Single-Circuit Alternative ($M)
141	90	142	35.4	2,450	77.1	101.9
142	90	153	37.0	3,229	-132.5	106.6
143	23	27	46.0	6,660	138.9	475.7
144	23	29	92.2	6,660	138.9	954.3
145	227	225	40.8	2,983	97.2	177.1
146	227	198	278.6	1,468	489.1	1,209.6
147	227	233	182.9	1,531	33.4	794.2
148	117	126	75.1	6,660	259.9	776.8
149	118	115	64.3	2,450	-100.2	185.2
150	118	139	145.7	1,560	68.0	419.7
151	29	32	11.4	6,660	259.9	118.0
152	29	45	59.1	6,660	259.9	612.1
153	30	28	79.7	1,800	39.6	229.6
154	40	45	46.2	6,660	259.9	478.4
155	40	46	17.9	6,660	259.9	185.6
156	41	47	17.9	3,600	218.8	51.7
157	32	45	48.3	6,660	259.9	500.2
158	13	35	208.7	1,540	73.0	601.1
159	13	14	72.1	2,627	186.6	207.8
160	13	21	156.1	1,758	38.6	449.6
161	214	207	227.7	1,429	23.3	988.7
162	214	221	72.0	2,485	64.5	312.5
163	92	93	26.9	8,400	590.6	278.4
164	92	95	19.4	8,400	590.6	200.6
165	92	97	4.9	4,126	590.6	50.3
166	92	154	42.5	3,279	259.9	440.3
167	218	195	72.2	2,758	77.7	746.9
168	14	10	224.9	1,515	47.4	647.7
169	14	21	225.9	1,514	28.7	650.6
170	93	89	23.9	8,400	590.6	247.4
171	93	95	39.4	8,400	590.6	408.3
172	93	96	7.8	8,400	590.6	81.1
173	93	152	26.8	6,660	259.9	277.0
174	183	192	90.5	2,372	41.8	260.7
175	183	187	84.8	2,447	41.5	244.3
176	236	235	524.1	28,549	431.0	11,320.0
177	236	239	199.0	1,564	90.1	573.2
178	61	63	2.4	4,189	1,728.1	25.0
179	143	149	9.9	6,660	259.9	102.2
180	17	33	185.1	1,800	33.7	533.2
181	17	28	136.8	1,800	33.7	394.0
182	17	18	74.7	19,414	543.5	1,614.0
183	17	21	61.1	2,798	104.2	176.1
184	103	113	42.7	6,660	259.9	442.3
185	103	138	40.1	6,660	259.9	415.3
186	103	141	66.6	6,660	259.9	689.6
187	43	50	25.5	17,400	220.7	264.2
188	18	25	117.5	2,171	106.6	1,216.0
189	95	97	18.7	8,400	590.6	193.8
190	95	152	29.3	6,660	259.9	302.8

Branch Number	From Bus Number	To Bus Number	Length (miles)	Capacity of 500 kV Single-Circuit Alternative (MW)	Susceptance of 500 kV Single-Circuit Alternative (p.u.)	Cost of 500 kV Single-Circuit Alternative ($M)
191	96	152	33.7	6,660	259.9	348.6
192	63	70	10.4	3,988	473.8	107.7
193	63	74	5.2	4,118	772.4	53.6
194	63	75	2.4	4,190	1908.4	24.4
195	63	76	10.3	3,990	672.0	106.9
196	64	78	66.2	2,717	53.1	190.8
197	145	149	46.3	6,660	259.9	479.0
198	65	72	2.2	4,196	2049.2	22.4
199	65	73	5.4	4,113	1279.9	55.6
200	238	240	46.2	3,208	54.7	478.2
201	148	180	92.9	2,343	219.3	267.5
202	19	202	221.8	1,435	8.2	963.2
203	19	207	267.2	1,446	20.5	1,160.1
204	85	95	39.7	8,400	590.6	410.8
205	85	96	11.4	8,400	590.6	117.8
206	46	45	35.6	6,660	259.9	368.1
207	97	135	21.2	6,660	259.9	219.0
208	97	136	31.7	6,660	259.9	328.4
209	67	77	67.7	4,041	94.9	980.1
210	68	77	67.7	4,041	94.9	980.1
211	69	72	5.6	4,107	731.7	58.3
212	70	73	7.5	4,059	602.9	77.9
213	70	76	1.0	4,226	766.1	10.1
214	72	73	7.4	4,063	630.8	76.2
215	185	160	116.0	3,600	42.1	334.0
216	185	167	107.6	3,450	96.5	310.0
217	185	181	76.3	3,600	420.2	219.7
218	109	144	61.6	1,954	693.0	1,231.4
219	109	230	2.6	2,790	668.9	51.8
220	48	34	20.8	23,025	284.1	215.1
221	48	43	10.4	23,025	631.8	107.8
222	150	148	93.0	2,342	289.0	267.8
223	152	240	8.1	4,045	80.9	83.9
224	153	150	134.9	1,910	96.6	388.6
225	153	239	8.1	2,450	17.5	23.4
226	153	155	53.7	2,450	-91.1	154.8
227	231	229	225.6	1,431	23.3	979.5
228	231	230	59.1	23,789	668.9	2,280.4
229	231	233	166.0	1,606	33.4	720.8
230	155	150	85.4	2,667	81.4	245.9
231	49	47	35.3	3,600	107.5	101.6
232	233	229	167.7	1,598	33.4	728.1
233	78	35	153.0	1,777	39.6	440.7
234	51	120	98.1	2,134	-107.0	282.7
235	51	122	98.1	2,134	-107.0	282.7
236	51	124	98.1	2,100	-119.0	282.7
237	187	188	229.2	1,511	606.1	660.0
238	188	182	125.3	1,993	79.0	360.9
239	104	127	61.3	6,660	259.9	634.1

B.3 First Stage Transmission and Generation Investments

Figures B.1, B.2, and B.3 show first stage investments in transmission backbones and interconnections to renewable hubs for scenarios 33% WECC, Carbon, and State RPS, respectively. Figure B.5 shows optimal first stage generation investments per state, for each deterministic scenario and the stochastic solution. I observe that the optimal deterministic strategy for scenario 33% WECC is to invest heavily in interconnections to renewable hubs (WREZ) and to take advantage of the quality of the wind resources in the mountain states (see Figure B.1). Note that although the 33% WECC scenario is the most stringent one in terms of renewable requirements (33% requirement per state within the U.S.), generation investments in the D-33% WECC investment strategy are more evenly distributed among states compared to the less stringent D-State RPS, since the latter does not allow for trading of Renewable Energy Certificates (RECs) (see Figure B.5). Although I find no clear investment pattern in transmission backbones for the strategies D-State RPS and D-33% WECC, I observe that investments in the former tend to reinforce the northern and eastern transmission ties of California (see Figure B.3).

As noted in Figure B.5, there are relatively few new developments of new generation using renewable energy technologies in the D-Carbon strategy, compared to strategies D-State RPS and D-33% WECC. This is mainly because the annual car-

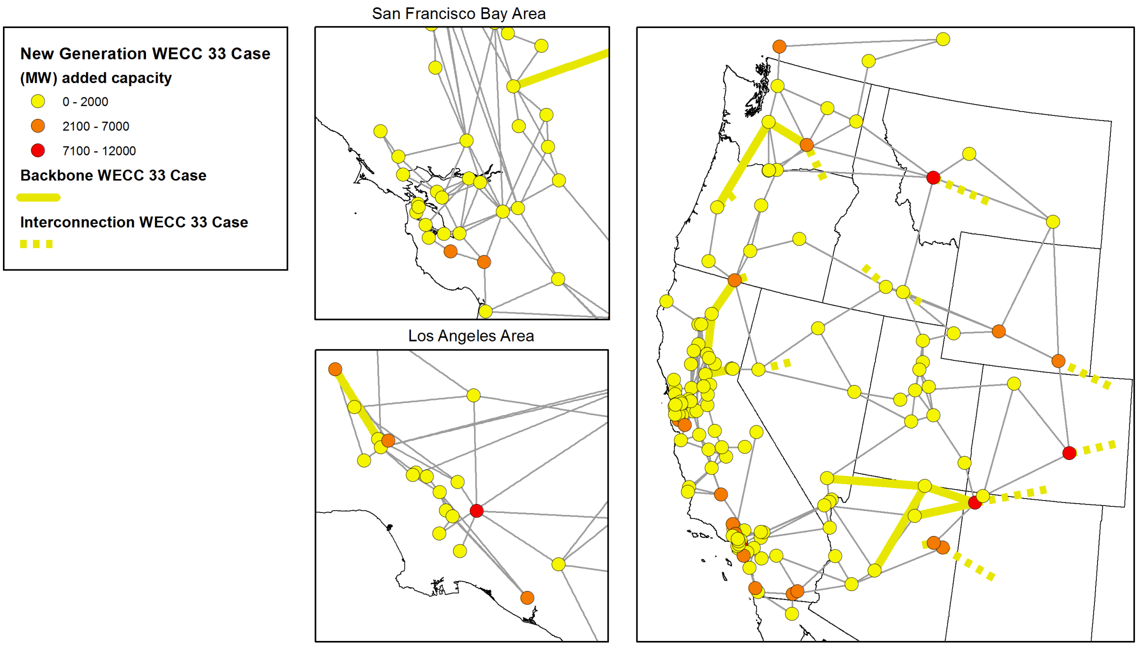

Figure B.1: Map of first stage transmission and generation investments for the deterministic WECC 33% scenario (D-33% WECC) (map made by Jonathan Ho).

bon emissions targets enforced in the Carbon scenario can be met using natural gas-powered generators (see investments in Arizona, Colorado, Montana, and Utah in Figure B.5) and renewable resources that are near the existing transmission grid (see California in Figure B.5). Also note that since environmental targets are not enforced in Mexico or Canada, it becomes optimal for the Carbon scenario to locate some of the new investments in conventional generation at those buses (see British Columbia and Mexico in Figure B.5) outside of the U.S. and to reinforce transmission ties to import power to northern Washington and southern California (see Figure B.2).

Figure B.4 describes the optimal stochastic investment strategy (in blue) and

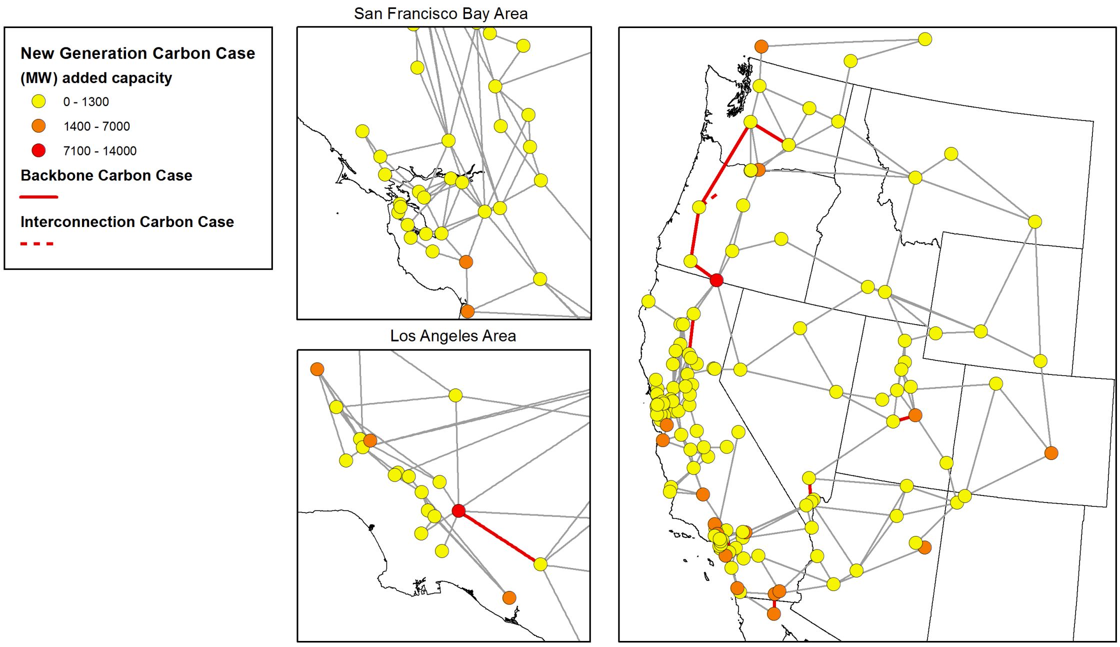

Figure B.2: Map of first stage transmission and generation investments for the deterministic Carbon scenario (D-Carbon) (map made by Jonathan Ho).

the three optimal deterministic strategies D-State RPS (in green), D-Carbon (in red), and D-33% WECC (in yellow). I observe that the stochastic plan includes all but one interconnections needed for the D-33% WECC strategy, but it only builds a small number of the transmission backbones shown in Figure B.3. Most of the investments in transmission backbones are, in fact, the corridors reinforced in all deterministic strategies (see Table 3.4 in Chapter 3). However, in the stochastic plan it is optimal to add two lines that interconnect the cities of San Diego and Los Angeles in southern California, which are not included in any optimal deterministic plan. As discussed in Chapter 3, this simple example disproves the heuristic investment rule currently used by transmission planners in the U.S., which is based on the analysis of

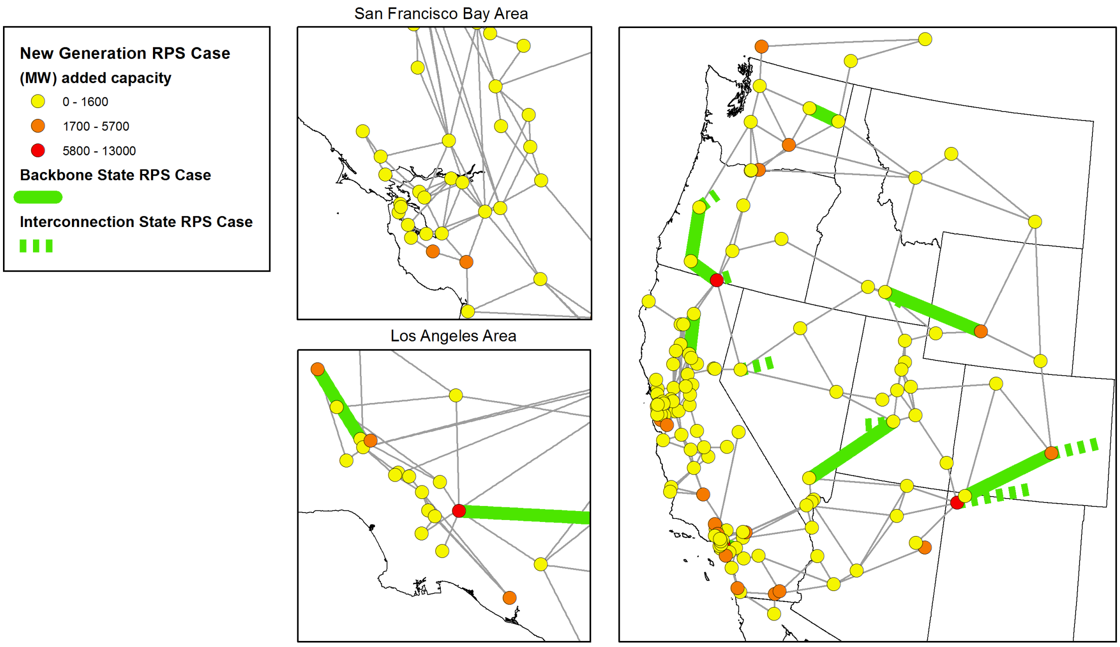

Figure B.3: Map of first stage transmission and generation investments for the deterministic State RPS scenario (D-State RPS) (map made by Jonathan Ho).

optimal transmission investments for individual scenarios (see discussion in Chapter 3). Similarly, generation investments in the stochastic case do not seem to follow any pattern that would allow one to approximate it using a deterministic model. While in the states of California, Colorado, Montana, and Wyoming the optimal stochastic strategy seems to be driven by the most stringent scenario (33% WECC), in other states I observe that the stochastic plan could be approximated by either the minimum (Mexico) or average generation investments of the three deterministic strategies (Oregon).

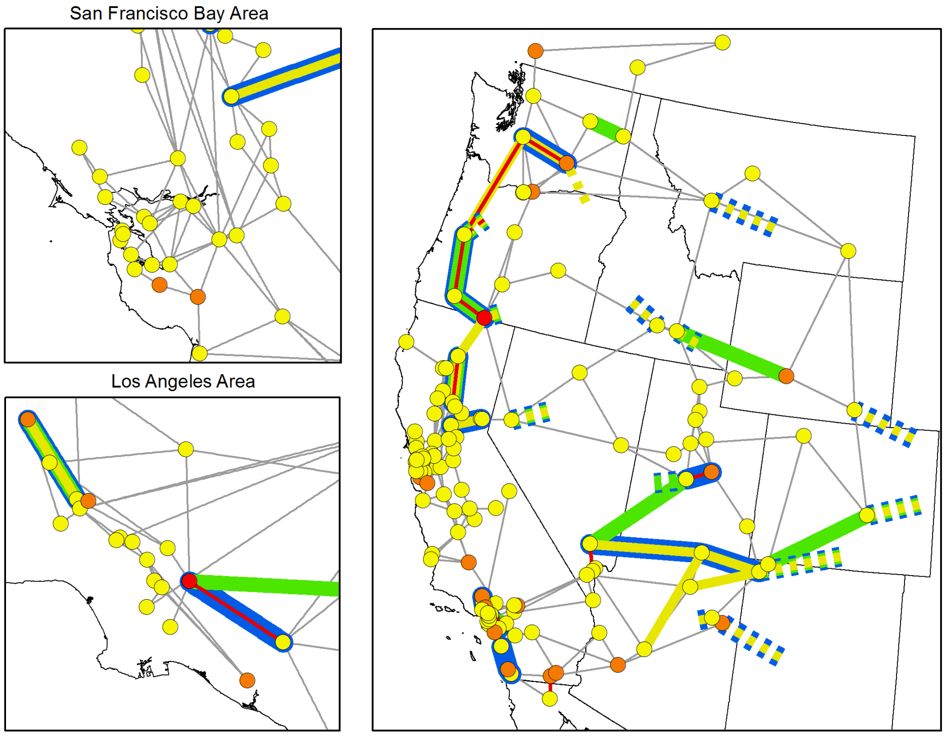

Figure B.4: Map of first stage transmission investments for all deterministic scenarios and the stochastic solution (map made by Jonathan Ho).

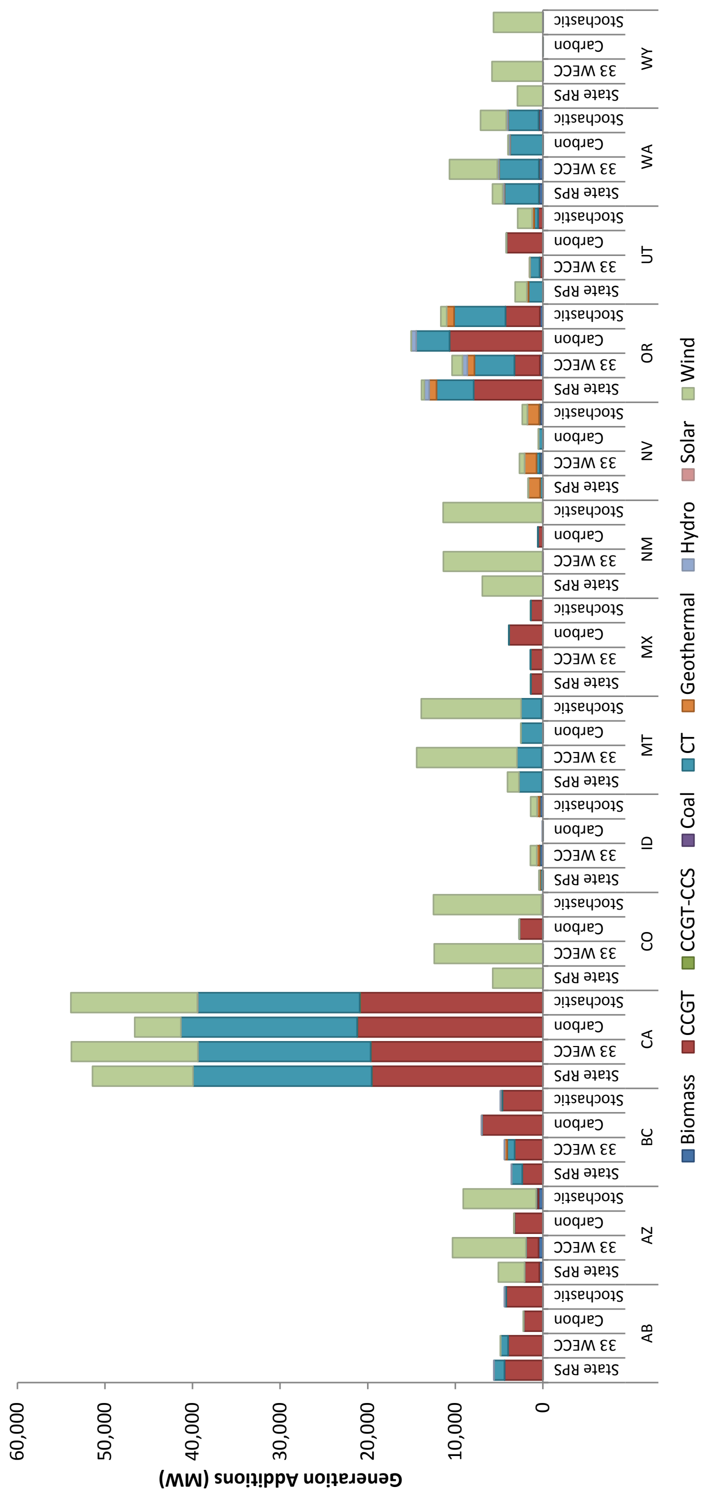

Figure B.5: First stage generation investments per state for the three deterministic investment strategies and the stochastic plan.

B.4 Second Stage Transmission and Generation Investments

Tables B.9 and B.10 show optimal second stage investments in transmission backbones and interconnections to renewable hubs for the three deterministic planning strategies (i.e., D-State RPS, D-33% WECC, and D-Carbon), the three heuristic planning approaches (i.e., Heuristic I, Heuristic II, and Heuristic III), and the stochastic plan. As expected, the two strategies that propose building the least number of transmission lines in the first stage, D-Carbon and Heuristic I, are the ones that face the largest regrets (i.e., highest expected costs, see Table 3.5 in Chapter 3), and the ones that require investing heavily in new transmission (see Tables B.9 and B.10) and generation capacity (see investments in new wind capacity in Colorado, New Mexico and Utah in Figures B.4 and B.4) in the second stage to meet each scenario's environmental goals. The Heuristic III approach, on the other hand, which invests heavily in transmission capacity in the first stage, requires significantly fewer transmission investments in the second stage in comparison to the deterministic and heuristic investment strategies. Fewer investments in the second stage, however, do not necessarily result in lower regrets (i.e., lower expected costs). The optimal stochastic strategy adds more transmission lines in the second stage than the D-33% WECC and Heuristic III approaches, which are the deterministic and heuristic plans that yield the lowest expected system costs.

As discussed in Section 3.5.2 of Chapter 3, the optimal stochastic strategy selects transmission backbones that are not optimal for any specific scenario in the first stage, but that impart flexibility to adjust the network in the second stage to any of the resulting market and regulatory conditions. As shown in Table B.9, the optimal reinforcements in transmission backbones in the second stage also include corridors that are not upgraded in any deterministic strategy (see corridors number 28, 100, and 111), which is consistent with Wallace (2000) and O'Neill et al. (2013) in that the optimal stochastic plan is the one that minimizes the expected total system costs, but it is sub-optimal in retrospective for all deterministic scenarios (i.e., final the total system costs are higher than the ones under perfect information).

Table B.9: Second stage investments in transmission backbones.

Transmission Planning Approach	Scenario	4	5	7	9	11	19	28	29	30	37	56	59	66	68	69	72	73	74	84	92	95	100	101	105	107	108	110	111	120
D-State RPS	State RPS														2															
	33% WECC																		2									1		
	Carbon																								2	2				
D-33% WECC	State RPS						1																				1			
	33% WECC																				1				1			2		
	Carbon				1									1																
D-Carbon	State RPS					1						1															1			
	33% WECC		1	1			1												2									2		
	Carbon	1							1															1	2	1				
Heuristic I	State RPS											1	1							1										
	33% WECC						1				1						1	2	2			1						2		1
	Carbon									2						1										2				
Heuristic II	State RPS																													
	33% WECC																		2									2		
	Carbon																								2					
Heuristic III	State RPS																													
	33% WECC																											1		
	Carbon																								2					
Stochastic	State RPS								1									1											1	
	33% WECC					1																						2	1	
	Carbon							1															1	1					1	

Transmission Planning Approach	Scenario	125	132	143	144	152	161	167	168	174	175	178	181	183	194	201	202	206	231	235	236	238
D-State RPS	State RPS																					
	33% WECC																					
	Carbon			2	2					2				1				2				
D-33% WECC	State RPS													1								
	33% WECC							1														
	Carbon		1	2	2	1				2								2				1
D-Carbon	State RPS		1				1										2					
	33% WECC								2			1			1	2						
	Carbon		1		2	1				2				1			2	2				
Heuristic I	State RPS	2												1					1		1	2
	33% WECC	2							2								2			2		2
	Carbon	1		2	2	1				2	1		1	1			2	2				1
Heuristic II	State RPS																					
	33% WECC								1								2					
	Carbon			2	2					2							2	2				
Heuristic III	State RPS																					
	33% WECC																					
	Carbon				2					2	2							2				
Stochastic	State RPS																1					
	33% WECC																					
	Carbon		1	2	2					2	1							2				

Table B.10: Second stage investments in interconnections to renewable hubs.

Transmission Planning Approach		Scenario	Corridor Number														
			I1	I2	I5	I6	I8	I9	I10	I11	I14	I20	I21	I23	I24	I26	I27
	D-State RPS	State RPS					1										
		33% WECC		1	2	4	1		1	2	1			1			1
		Carbon					1										
	D-33% WECC	State RPS														1	
		33% WECC				3	1									1	1
		Carbon															
	D-Carbon	State RPS			1		2	1	1			1			1	1	
		33% WECC		1	4	4	3	1	1	2	1	1		1	1	1	1
		Carbon						1				1					
	Heuristic I	State RPS			1		2	1	1			1			1	1	
		33% WECC		1	4	4	3	1	1	2	1	1		1	1	1	1
		Carbon															
	Heuristic II	State RPS														1	
		33% WECC		1	2	4	1		1	2	1			1		1	1
		Carbon															
	Heuristic III	State RPS															
		33% WECC				3	1										1
		Carbon															
	Stochastic	State RPS															
		33% WECC	1			3	1						1	1			1
		Carbon															

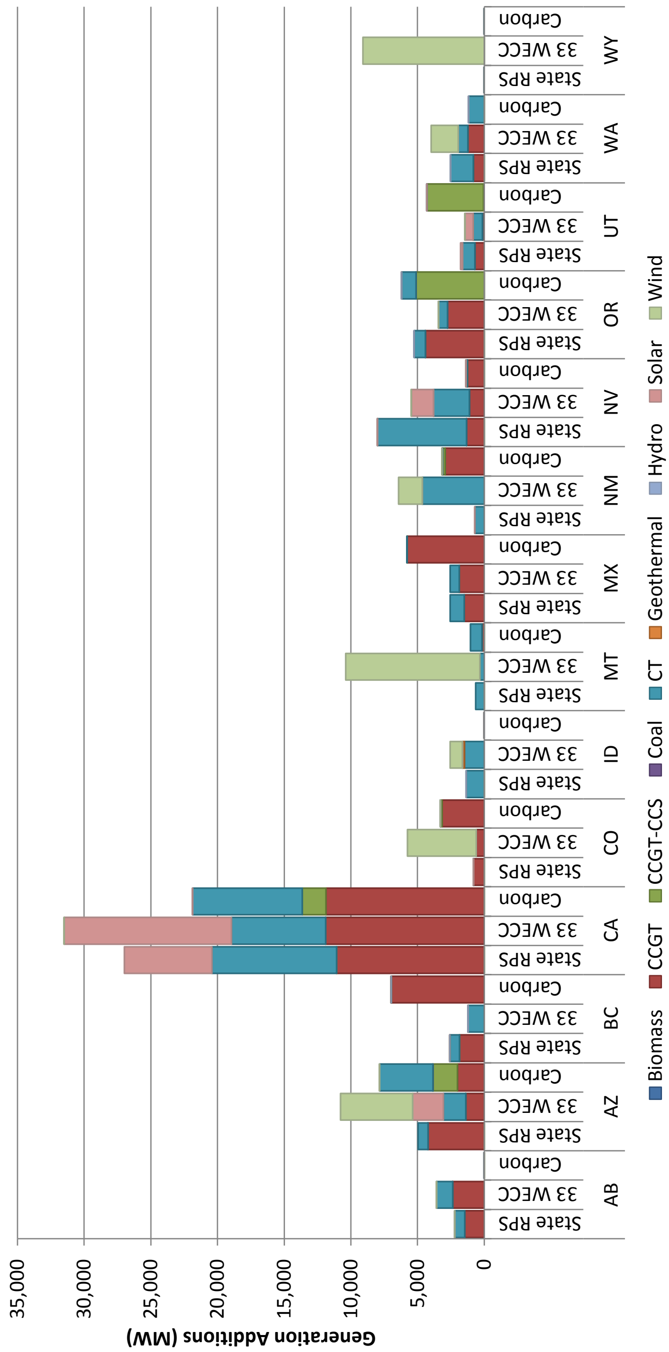

Figure B.6: Second stage generation investments for the D-State RPS approach.

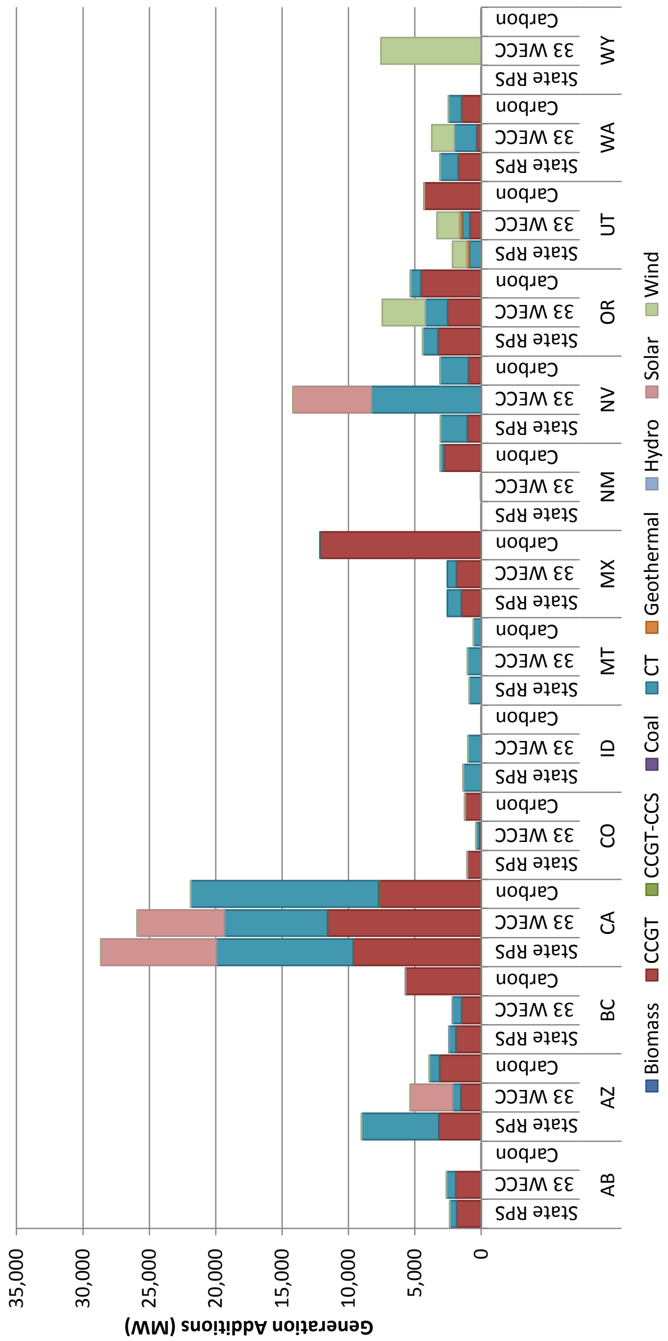

Figure B.7: Second stage generation investments for the D-33% WECC approach.

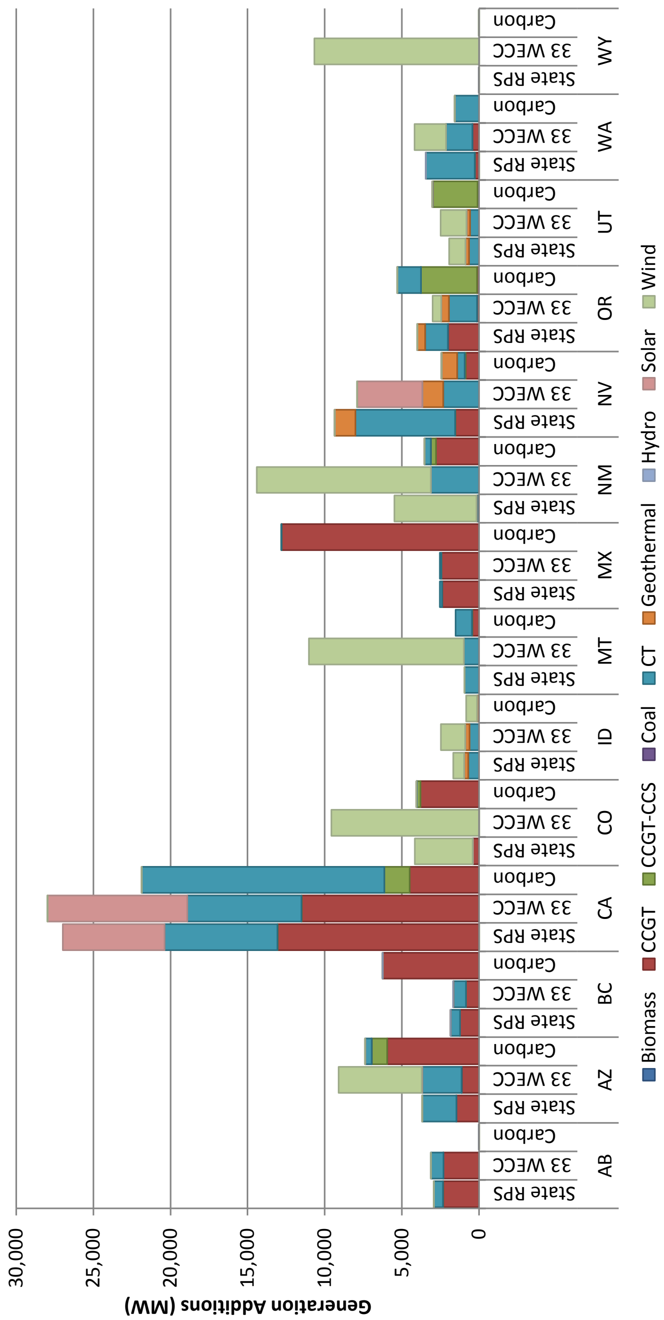

Figure B.8: Second stage generation investments for the D-Carbon approach.

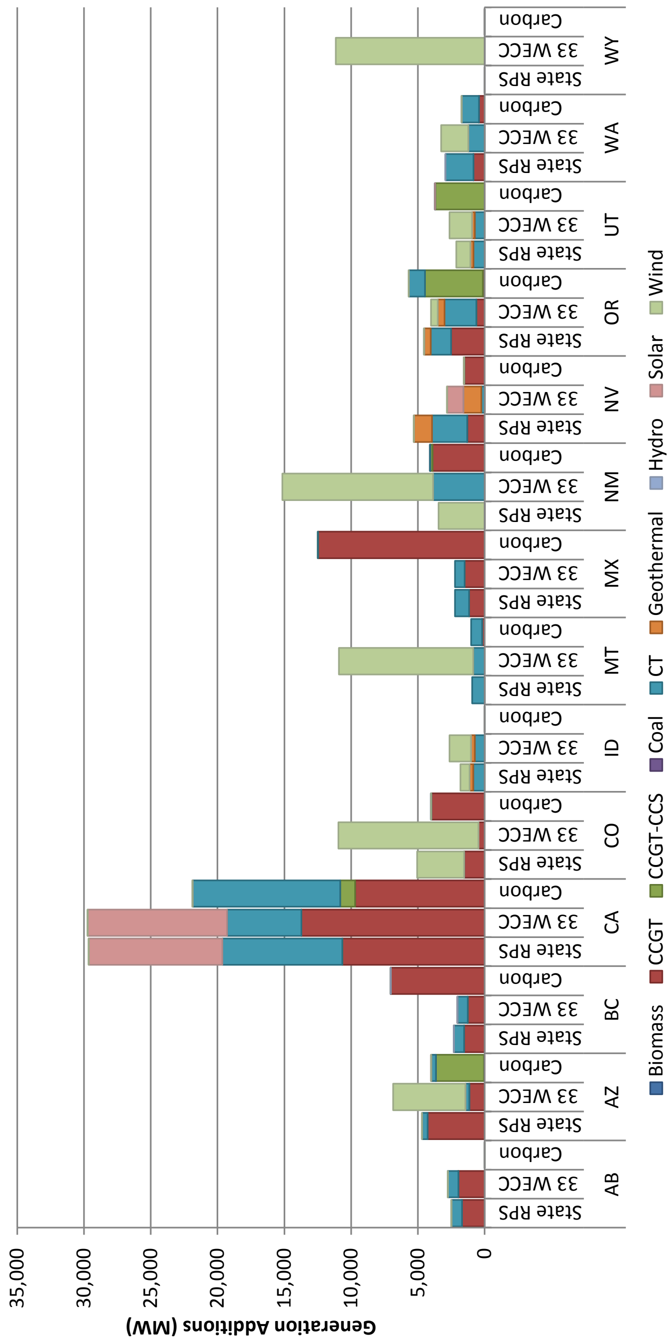

Figure B.9: Second stage generation investments for Heuristic I.

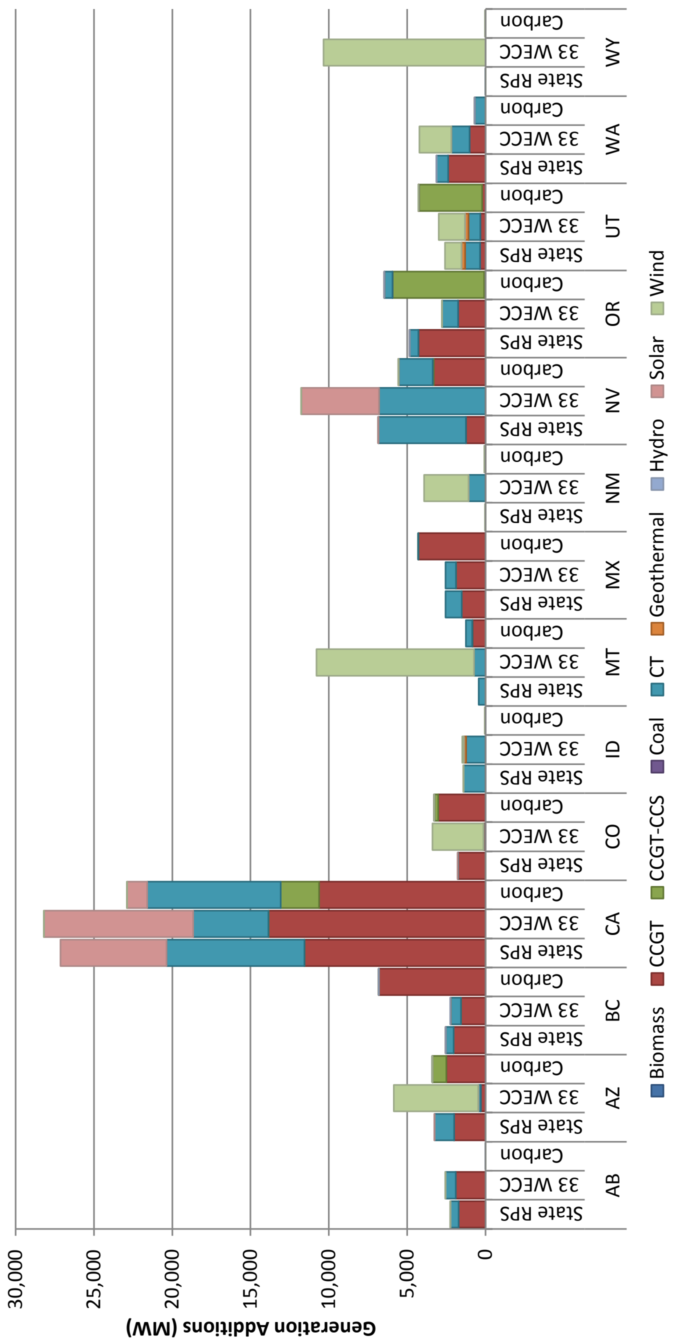

Figure B.10: Second stage generation investments for Heuristic II.

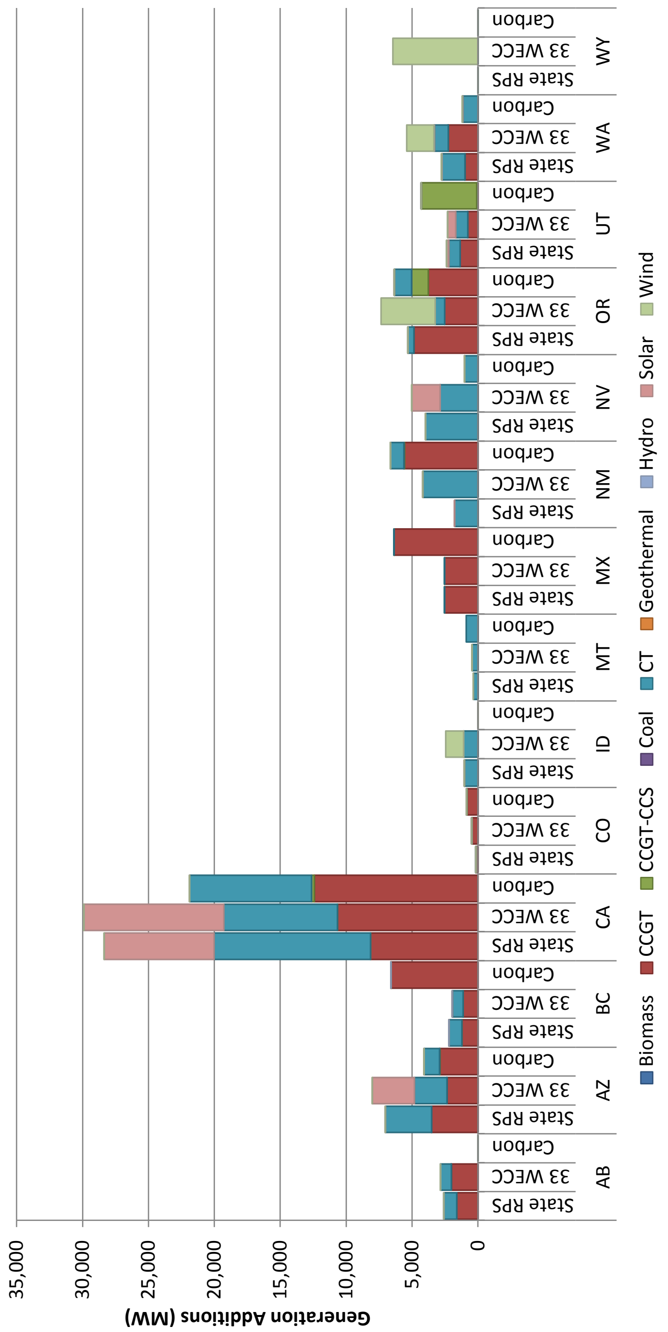

Figure B.11: Second stage generation investments for Heuristic III.

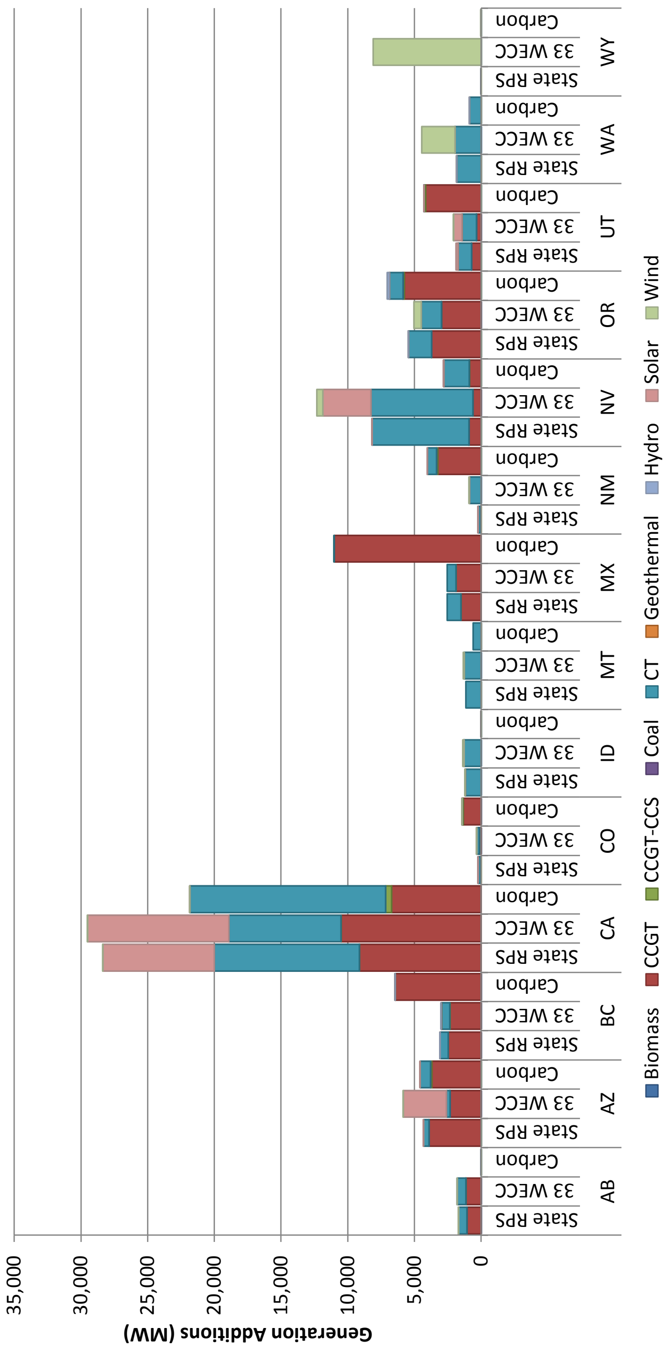

Figure B.12: Second stage generation investments for the Stochastic approach.

Appendix C

Chapter 4 Additional Material

C.1 Sampling Methodology

The sampling methodology to approximate the 8,736-hr problem is the one proposed by van der Weijde and Hobbs (2012). The method proceeds as follows. I consider 10,000 random samples each of N observations for load, wind, solar, and hydro levels, drawn from the state space Ω ($|\Omega| = 8,736$). I then select the sample that closely matches the means, standard deviations, and correlations of the full dataset. This is done by minimizing the following expression:

$$W_N = \sum_{i=1}^{I}\sum_{j=1}^{I}(cor_{i,j} - \overline{cor}_{i,j})^2 + \sum_{j=1}^{I}(\mu_i - \overline{\mu_i})^2 + \sum_{j=1}^{I}(sd_i - \overline{sd_i})^2 \tag{C.1}$$

In Equation C.1, $cor_{i,j}$ is the correlation between time-dependent variables i and j, and μ_i and sd_i correspond to the mean and standard deviation of time-dependent variable i, respectively. All parameters with bars are calculated using sampled data. I denote W_N as the minimum sum of square differences of means, standard deviations, and correlations of 10,000 random samples each of size N. Figure C.1 shows the value of the metric W_N as a function of the sample size. The 5,000-hr sample presents negligible differences in means, standard deviations, and correlations as compared to the full dataset of 8,736 observations.

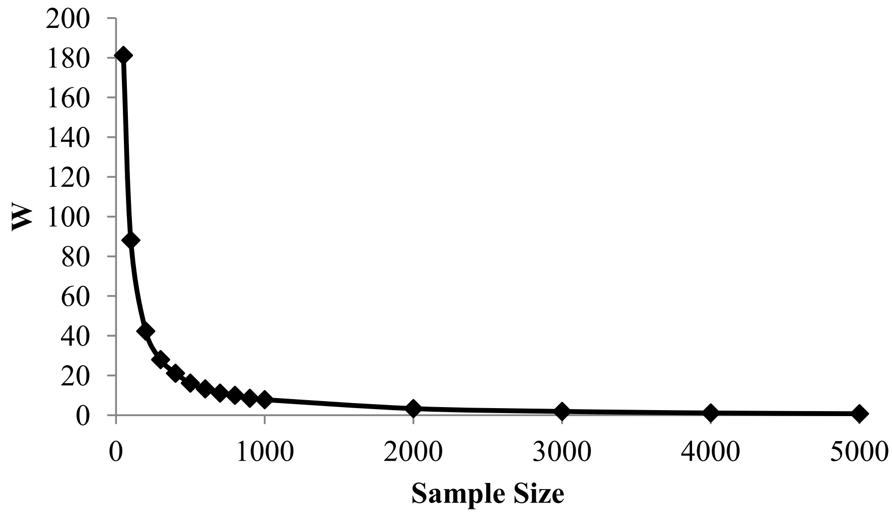

Figure C.1: Metric W_N as a function of the sample size N.

C.2 Upper and Lower Bounds of Bounding Algorithm

Figures C.2 and C.3 show the upper and lower bounds that resulted from applying the bounding algorithm to the linear relaxation and the mixed-integer linear problem, respectively. Note that the vertical axes of both figures have been scaled to highlight the differences between the upper and lower bounds. The resulting solution gap of the linear relaxation, calculated as $100\% \times \frac{UB-LB}{UB}$, is illustrated in Figure 4.2 of Chapter 4. The resulting solution gaps of the mixed-integer linear problems are calculated as $100\% \times \frac{UB-(1-\epsilon)LB}{UB}$, where ϵ corresponds to the MILP gap, and are plotted in Figure 4.3 of Chapter 4. Note that both the linear an mixed-integer linear cases present greater changes in the upper bounds (decrements) than in the lower bounds (increments) as the number of clusters is increased. As discussed in Section 4.5.5 of Chapter 4, approaches that only calculate the lower bound, as the one described in Heejung and Baldick (2013), can result in premature detention of the algorithm, when the upper bound is still significantly higher than the lower bound (i.e. large solution gap).

Also note that Figure C.3 includes the initial lower bound (LB_0) from the 150-cluster linear problem ($TC_{LP}(\Psi^{150}, q^{150}) = 624.3$), which I utilized to reduce the solution gaps of the mixed-integer problems. This initial bound was higher than the weighted objective function values of all lower-problems ($(1-\epsilon)LB$) for MILP gaps

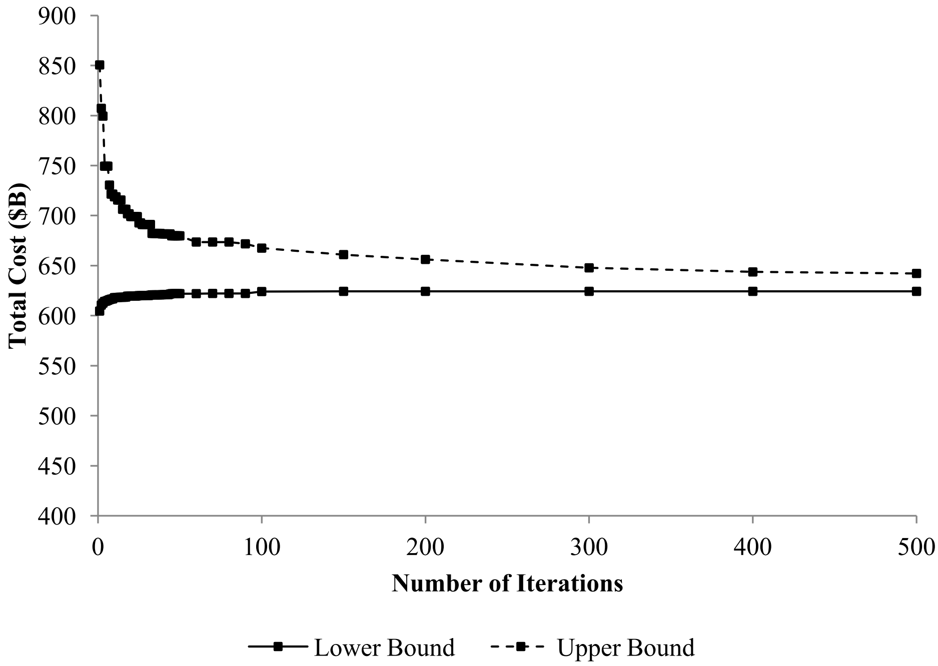

Figure C.2: Upper and lower bounds for the bounding algorithm (phase one) applied to the linear relaxation.

of 5% and 3% (see solid black and light blue lines in Figure C.3). With a tighter MILP gap of 1%, however, LB_0 was finally updated when I considered 100 clusters (see solid red line in Figure C.3).

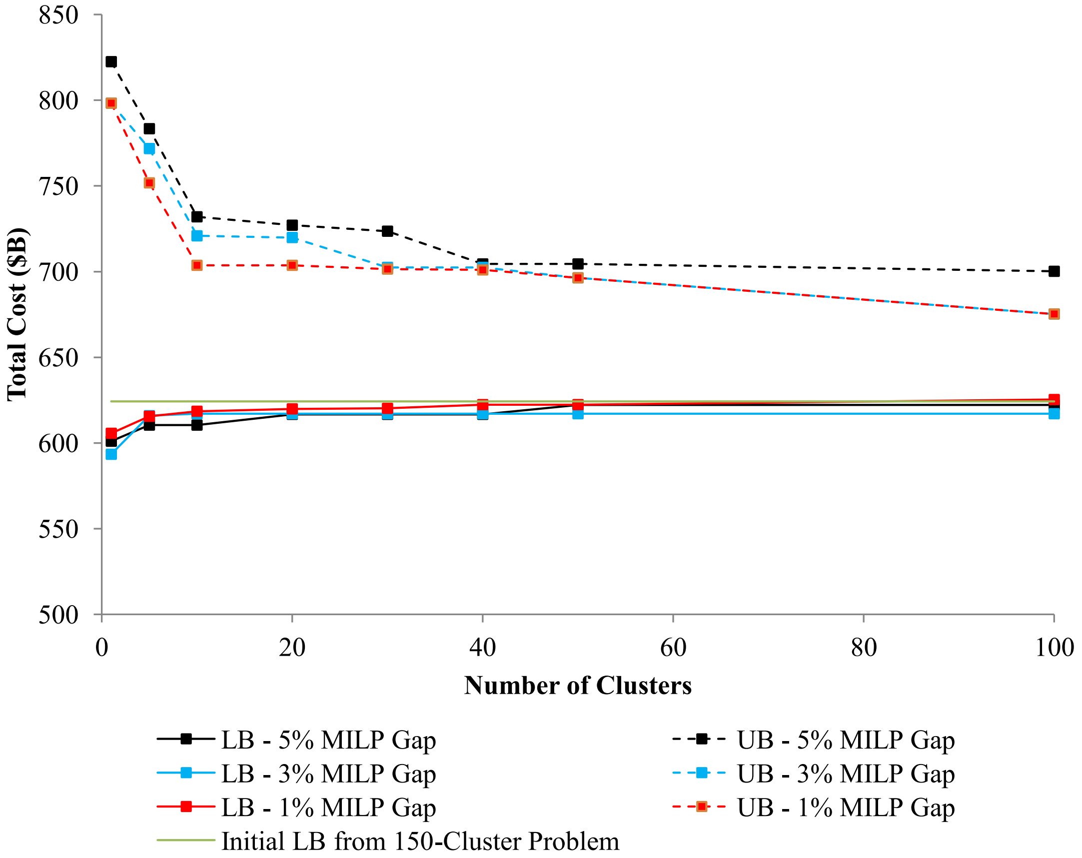

Figure C.3: Upper and lower bounds for the bounding algorithm (phase one) applied to the mixed-integer linear problem.

C.3 Investments Bounding Algorithm

This section describes investments in transmission and generation capacity, as a function of the number of clusters for the bounding algorithm (phase one) applied to the linear (LP) and mixed-integer linear (MILP) problems. I observe that, in both cases, the total generation investments per technology remain roughly constant as the partitions are refined (see Figures C.4 and C.8). However, for small cluster counts, the lower-bound problem biases investments in combustion turbines (CTs), combined cycle gas turbines (CCGTs), and wind with respect to the optimal levels found for 500 clusters. The expected-value problem (one cluster) underestimates investments in CCGT and wind capacity by 10.1% and 5.2%, respectively, and overestimates investments in CT by 4.2%. Similar trends are observed in the mixed-integer linear case (see Figure C.8). The major differences are, however, in transmission investments. As shown in Figure 4.6 of Chapter 4, the linear expected-value problem underestimates transmission capacity by 33.2% with respect to the 500-cluster problem. In the mixed-integer linear case (see Figure C.12), relaxing the MILP gap can also result in significant underestimation of transmission capacity. Loosening the MILP gap to 5%, for instance, yields 40.9% less transmission capacity than the levels found for a 1% MILP gap for 100 clusters (compare dotted red and black lines in Figure C.12).

Note that although the total generation investments per technology are roughly constant as the cluster count is increased, certain technologies present differences in their geographic location as the partitions are refined. I observe that the optimal location of new CCGT capacity, as well as CT and wind to a lesser degree, is sensitive to the number of partitions for small cluster counts. Investments in new CCGTs in the states of California, Oregon, and Arizona, for example, present an oscillatory pattern as the partitions are refined from 1 to 100; this behavior is, however, not observed for larger cluster counts.

The most important changes in the location of new generation investments as the partitions are refined are in new wind capacity. As shown in Figure C.7, the lower-bound planning problem overestimates investments in the state of Colorado (teal line) and underestimates the value of wind resources in the state of Washington (red line). Unlike the initial oscillatory pattern observed for wind additions in the states of Arizona and Wyoming, wind investments in California and Washington do not present stabilization points for large cluster counts. Although investments in these two states only correspond to a small fraction of the total wind additions throughout the WECC, this result highlights the importance of using fine-grained representations of variability within investment planning models to capture the true value of renewable resources.

For a more detailed description of generation (per bus) and transmission (per corridor) investments, please refer to the supporting electronic files of this dissertation.

C.3.1 Linear Problem

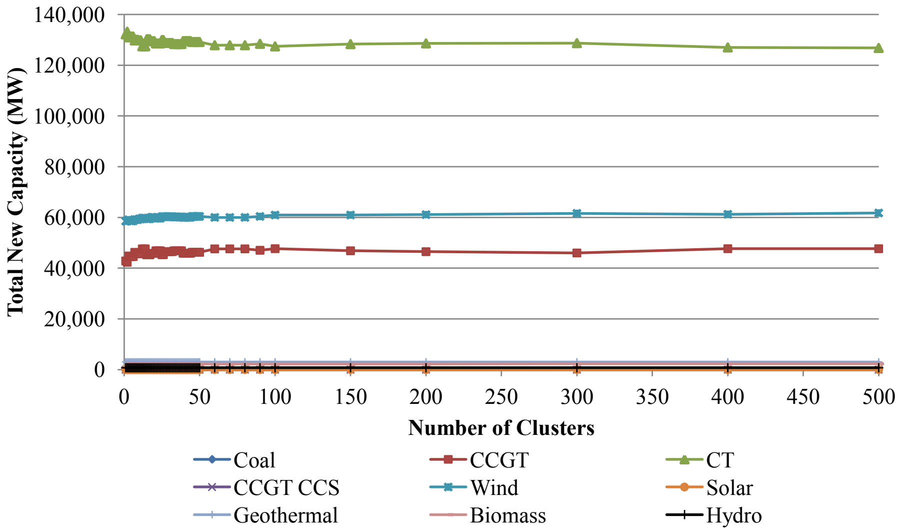

Figure C.4: Total new generation capacity per technology as a function of the number of clusters. Results from the application of the bounding algorithm (phase one) to the linear relaxation.

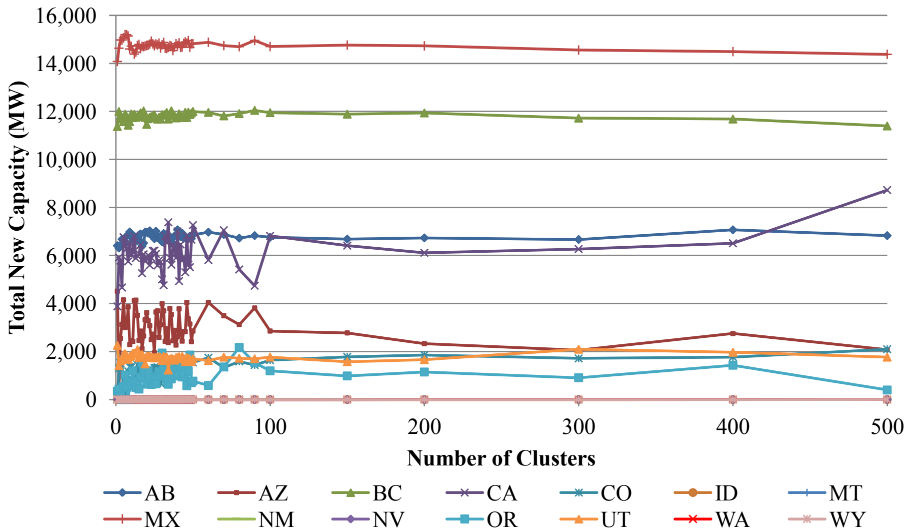

Figure C.5: New CCGT generation capacity per state as a function of the number of clusters. Results from the application of the bounding algorithm (phase one) to the linear relaxation.

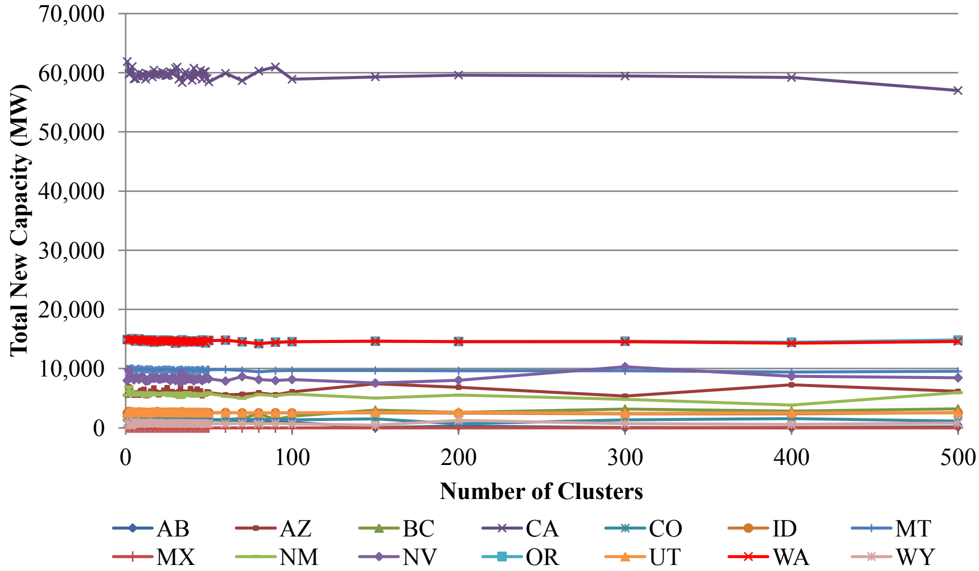

Figure C.6: New CT generation capacity per state as a function of the number of clusters. Results from the application of the bounding algorithm (phase one) to the linear relaxation.

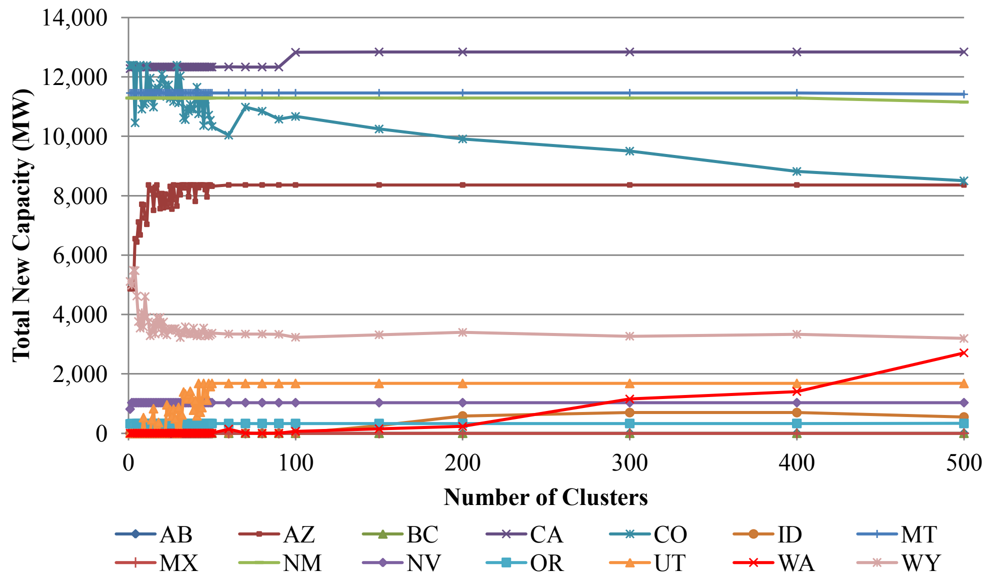

Figure C.7: New wind generation capacity per state as a function of the number of clusters. Results from the application of the bounding algorithm (phase one) to the linear relaxation.

C.3.2 Mixed-Integer Linear Problem

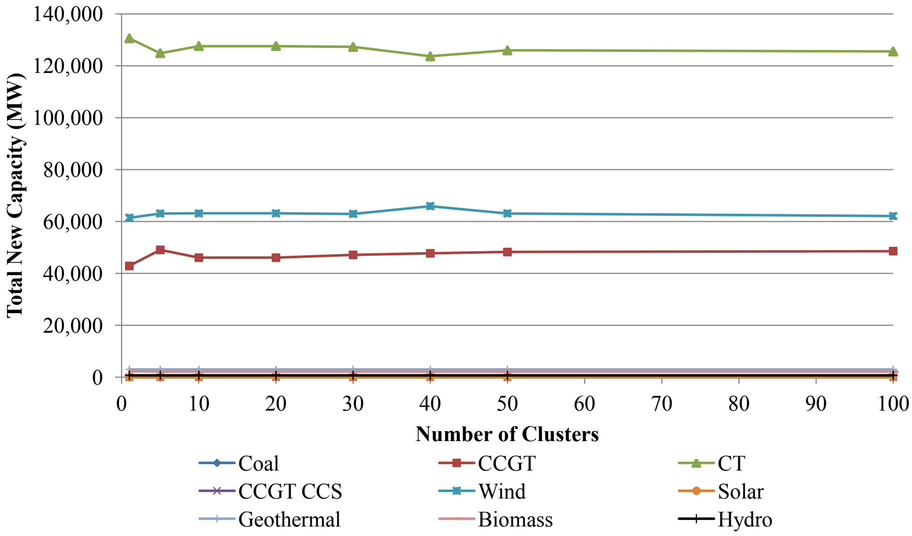

Figure C.8: Total new generation capacity per technology as a function of the number of clusters. Results from the application of the bounding algorithm (phase one) to the mixed-integer linear problem (MILP gap 1%).

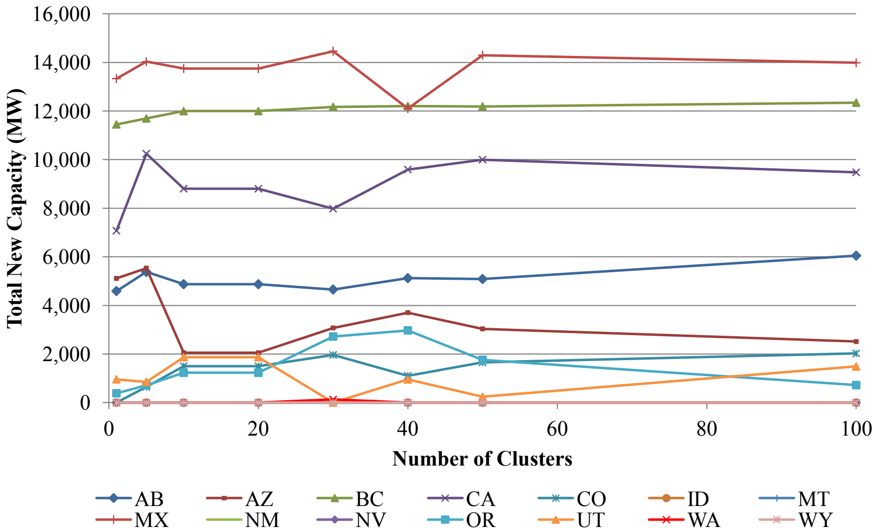

Figure C.9: New CCGT generation capacity per state as a function of the number of clusters. Results from the application of the bounding algorithm (phase one) to the mixed-integer linear problem (MILP gap 1%).

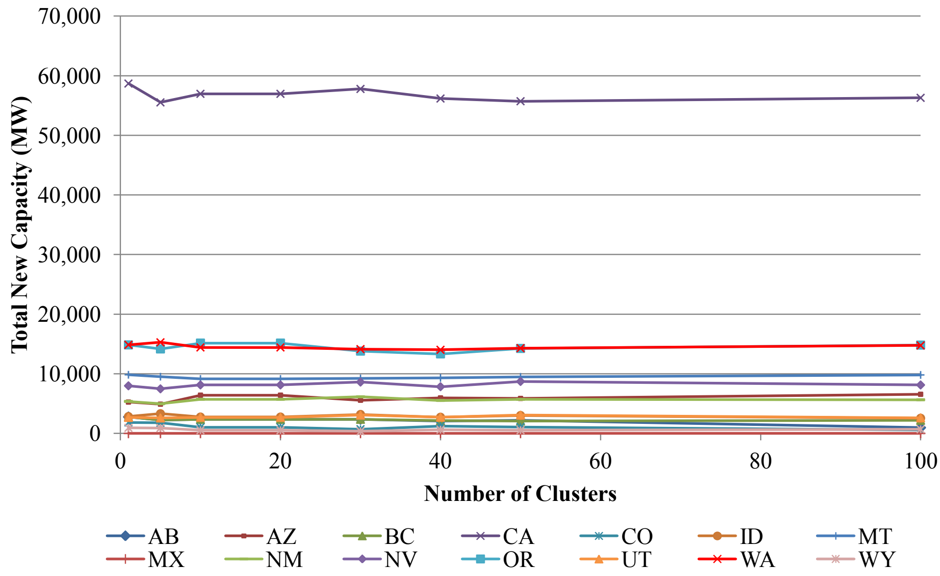

Figure C.10: New CT generation capacity per state as a function of the number of clusters. Results from the application of the bounding algorithm (phase one) to the mixed-integer linear problem (MILP gap 1%).

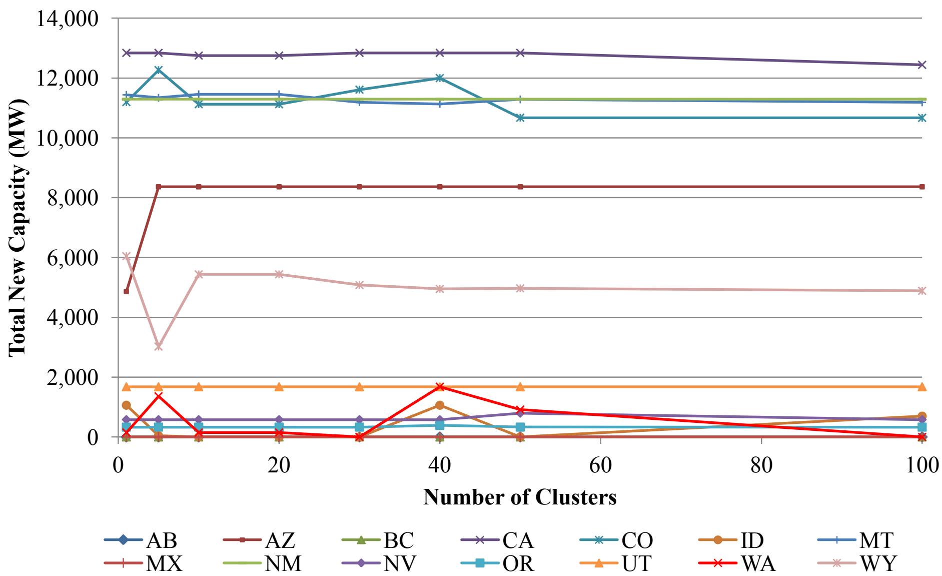

Figure C.11: New wind generation capacity per state as a function of the number of clusters. Results from the application of the bounding algorithm (phase one) to the mixed-integer linear problem (MILP gap 1%).

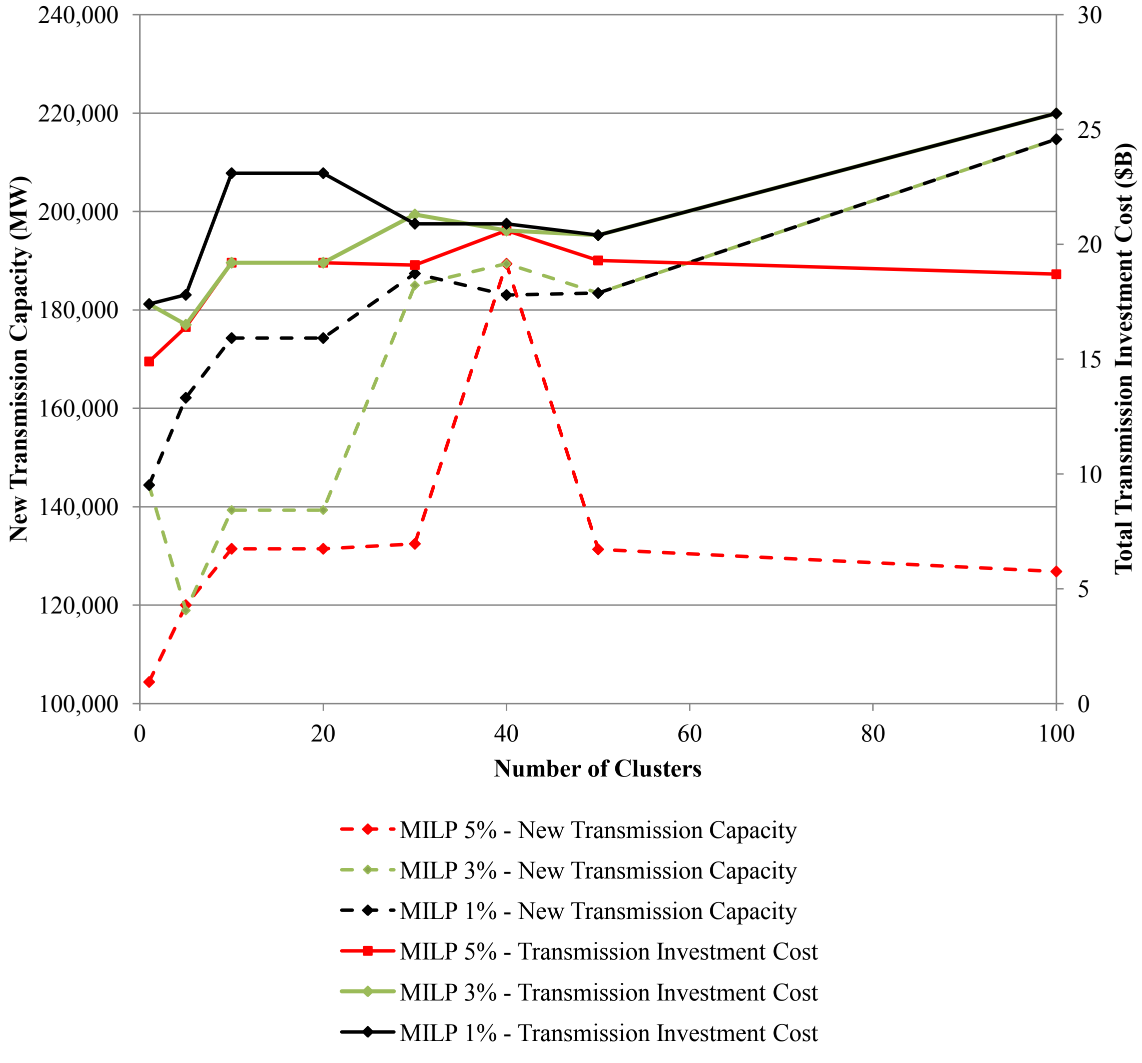

Figure C.12: New transmission generation capacity as a function of the number of clusters. Results from the application of the bounding algorithm (phase one) to the mixed-integer linear problems for MILP gaps of 5%, 3%, and 1%.

C.4 Upper and Lower Bounds of Regular and Enhanced Benders Decomposition

Figures C.13 and C.14 show the upper and lower bounds of the linear relaxation and the mixed-integer linear problem, respectively. Note that both figures plot the lower bounds that result from setting $LB_0 = -\infty$. However, the solution gaps described in 4.8 and 4.10 of Chapter 4 were calculated using the objective function value of the 150-cluster linear problem ($TC_{LP}(\Psi^{150}, q^{150}) = 624.3$) as an initial lower bound ($LB_0 = 624.3$). As illustrated in Figure C.13, including an auxiliary lower bound in the master problem from phase one results in significant improvements of upper and lower bounds. If the initial lower bound from the 150-cluster linear problem is disregarded (i.e. $LB_0 = -\infty$), the solution gap of the regular Benders decomposition after 400 iterations increases from 11.5% to 38.6%. However, the contribution of this initial lower bound for the experiments with auxiliary lower bounds is only marginal for large iteration counts. The single-cluster experiment is the only one in which $LB_0 = 624.3$ is not updated after 400 iterations; setting $LB_0 = 624.3$ results in a reduction of the solution gap from 3.5% to 3.0% with respect to the implementation in which $LB_0 = -\infty$. In the 10- and 33-cluster experiments this initial lower bound is updated after 70 and 17 iterations, respectively.

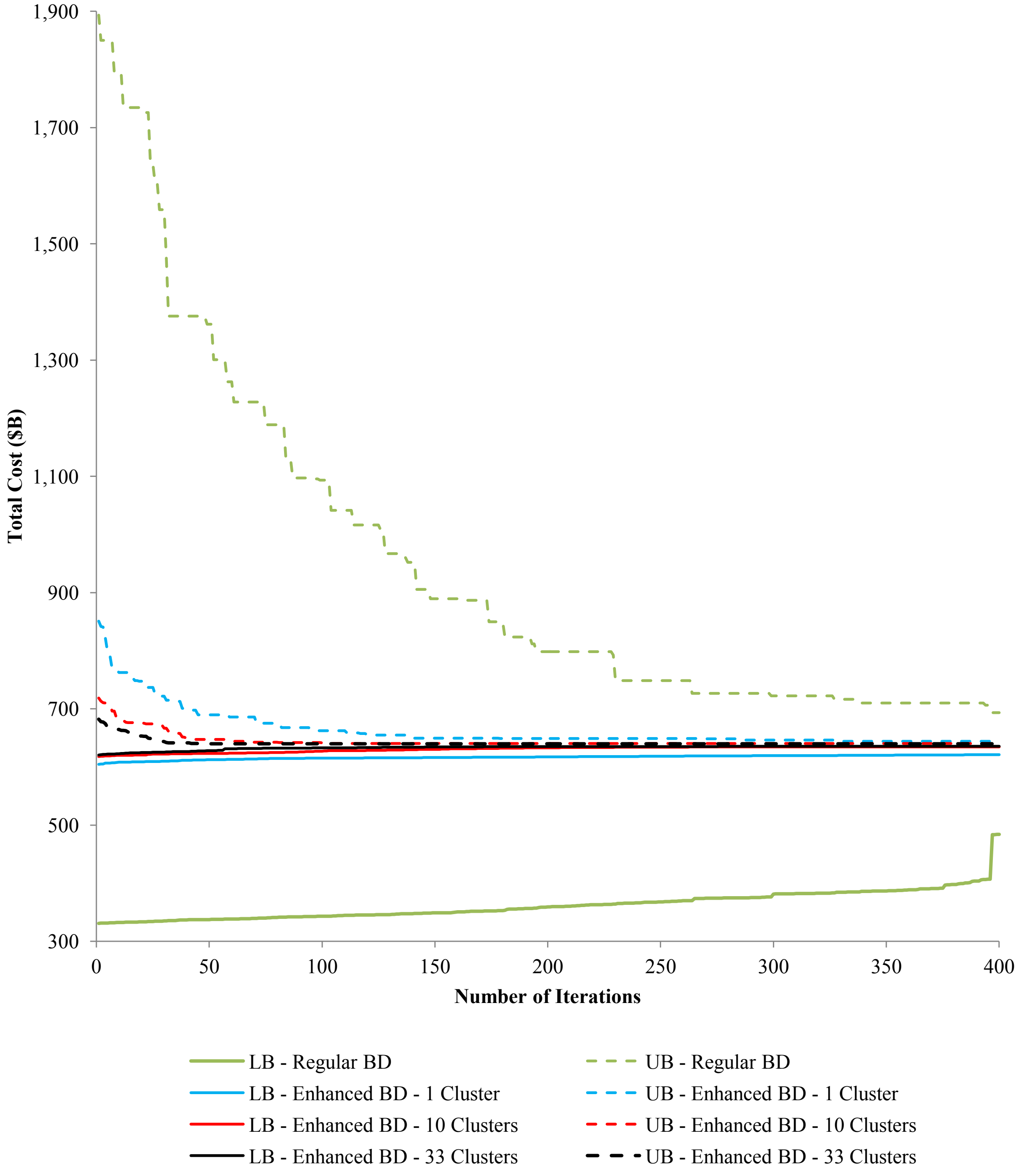

Figure C.13: Upper and lower bounds for regular and enhanced Benders decomposition (phase two) applied to the linear relaxation.

Figure C.14 illustrates the effect of including 400 pre-computed cuts from the linear relaxation in the mixed-integer master problem of the single-cluster experiment. Note that most of the improvements in the solution gap are a result of significantly tighter upper bounds (compare dotted gray and black lines in Figure C.14). Although the lower bounds are also improved (compare solid gray and black lines in Figure C.14), the initial lower bound from the 150-cluster linear problem (green solid line) is still higher than the objective function value of either lower-bound problems, with (solid black line) or without (solid gray line) pre-computed cuts. A much tighter lower bound is the one that resulted after 400 iterations of the enhanced Benders decomposition applied to the 33-cluster linear problem (solid black line in Figure C.13). This bound is plotted in Figure C.14 as a solid red line and, as discussed at the end of Section 4.5.6 of Chapter 4, yielded solution gaps that were 1.7% lower than the ones calculated without it (see Figure 4.10 in Chapter 4).

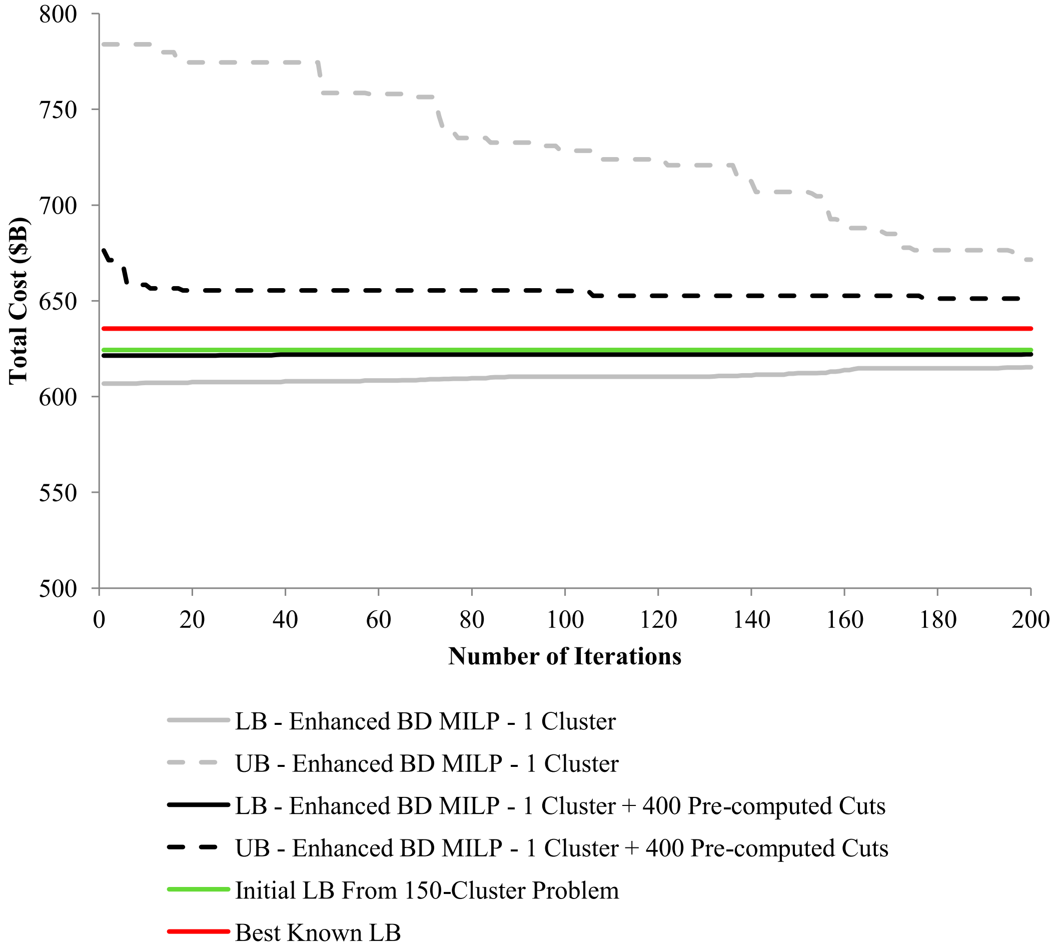

Figure C.14: Upper and lower bounds for enhanced Benders decomposition (phase two) applied to the mixed-integer linear problem (0.5% MILP gap).

C.5 Investments of Regular and Enhanced Benders Decomposition

This section summarizes generation and transmission investments that resulted from the application of the regular and enhanced Benders decomposition algorithms to the linear and mixed-integer linear problems. I find that the most important differences in investments are between the regular Benders algorithm and the enhanced method proposed in Chapter 4 (phase two). As shown in Figure C.15, the regular Benders algorithm significantly underestimates transmission investments during the first 200 iterations compared to the ones proposed by the enhanced implementations (see Figures C.21, C.27, and C.33). The traditional Benders algorithm then overestimates transmission capacity after 300 iterations by more than 30% with respect to the optimal levels found after 400 iterations of the enhanced Benders implementation using 33 clusters (Figure C.33), the latter of which corresponds to the best known solution for the linear problem (see Figure 4.8 in Chapter 4).

I also find that the total aggregate generation capacity level proposed by the regular Benders algorithm is roughly equivalent to the ones that result from the enhanced approaches (compare Figure C.16 to Figures C.22, C.28, and C.34). However, the generation mix and geographic distribution of investments present great discrepancies when compared to the enhanced implementations. For the first 330 iterations, the regular Benders algorithm (Figure C.17) overestimates CT and wind capacity by approximately 26% and 33%, respectively, with respect to the best known solution (Figure C.35), and it completely disregards investments in new CCGTs. Even though this bias in the generation mix of the regular Benders approach is largely reduced after 400 iterations, the geographic distribution of generation across the WECC still presents differences with respect to the best known solution (compare Figures C.18, C.19, and C.20 to Figures C.36, C.37, C.38).

Finally, among enhanced implementations, I find that the effect of increasing the number of clusters in the auxiliary lower bounds results in earlier stabilization of the primal investment solutions. This effect can be seen in the aggregate generation investments plotted in Figures C.22, C.28, and C.34; the oscillatory behavior of the total generation capacity additions is notoriously reduced after 329, 100, and 53 iterations for the single-, 10-, and 33-cluster implementations, respectively. However, this is not a general result. The total transmission capacity additions of the 10-cluster experiment present a significant drop after 390 iterations (see Figure C.27), which suggests the potential existence of alternate optima.

For a more detailed description of generation (per bus) and transmission (per corridor) investments, please refer to the supporting electronic files of this dissertation.

C.5.1 Regular Benders Decomposition

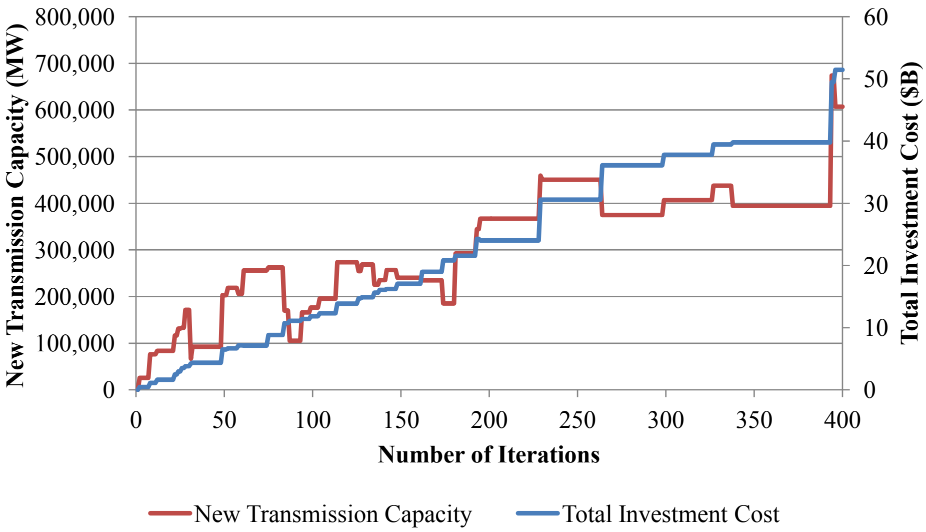

Figure C.15: Total new transmission capacity and transmission investment cost as a function of the number of iterations. Results from the application of regular Benders decomposition to the linear problem.

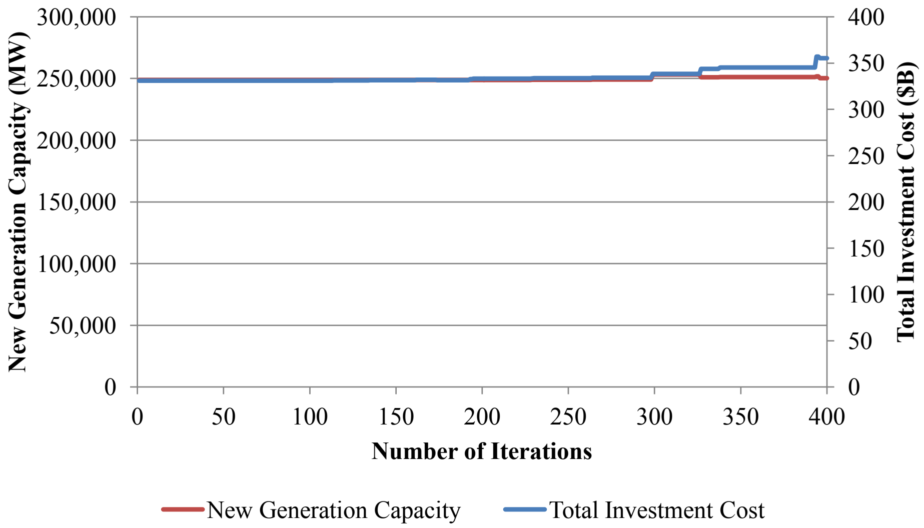

Figure C.16: Total new generation capacity and generation investment cost as a function of the number of iterations. Results from the application of regular Benders decomposition to the linear problem.

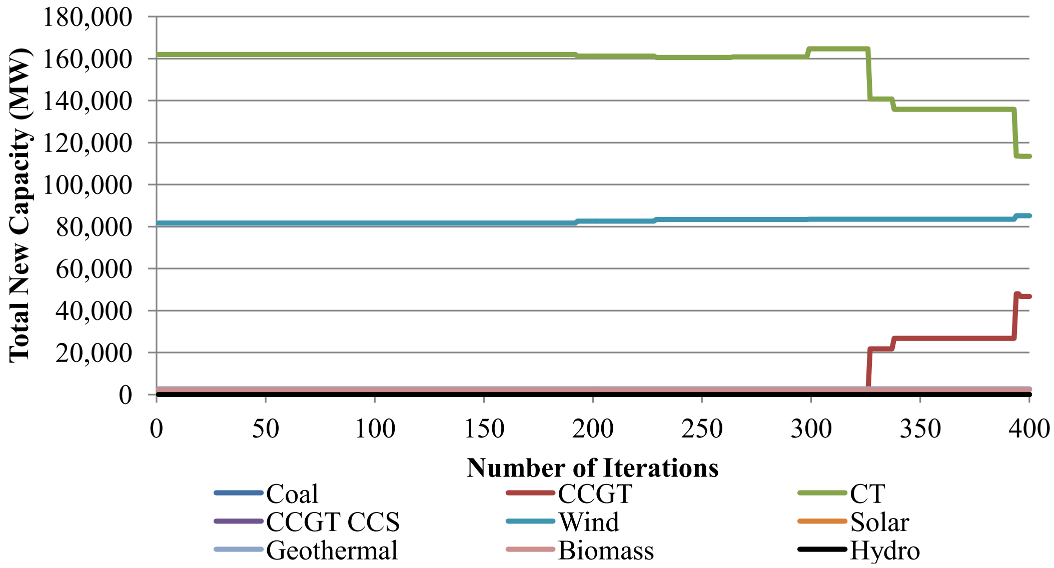

Figure C.17: Total new generation capacity per technology as a function of the number of iterations. Results from the application of regular Benders decomposition to the linear problem.

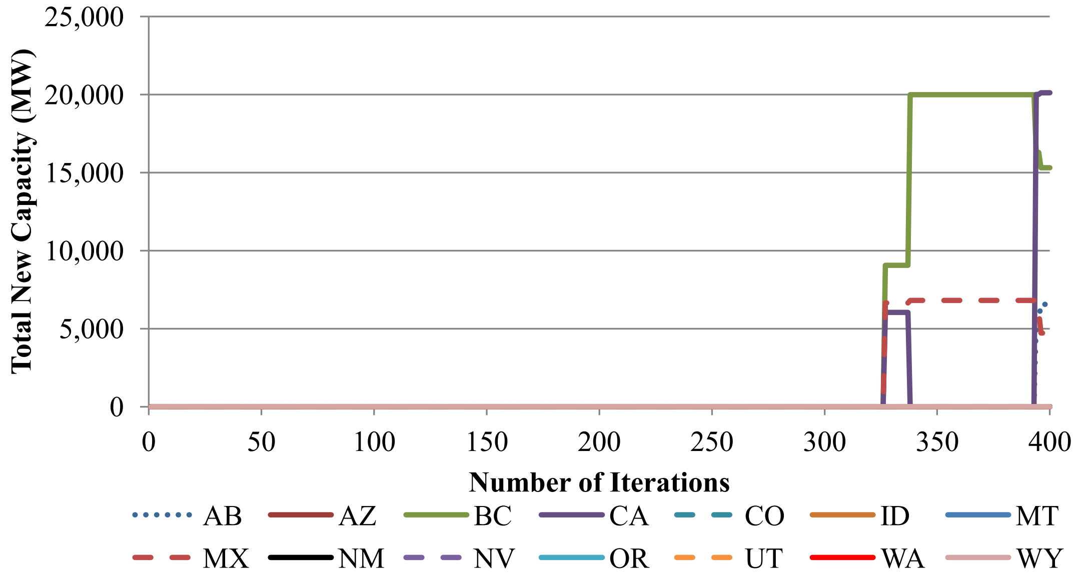

Figure C.18: New CCGT generation capacity per state as a function of the number of iterations. Results from the application of regular Benders decomposition to the linear problem.

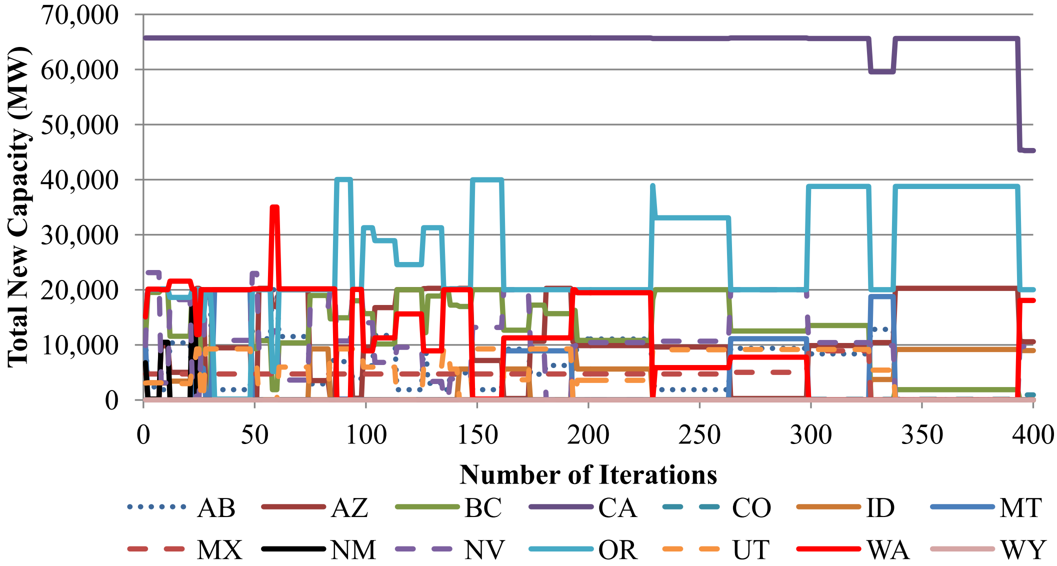

Figure C.19: New CT generation capacity per state as a function of the number of iterations. Results from the application of regular Benders decomposition to the linear problem.

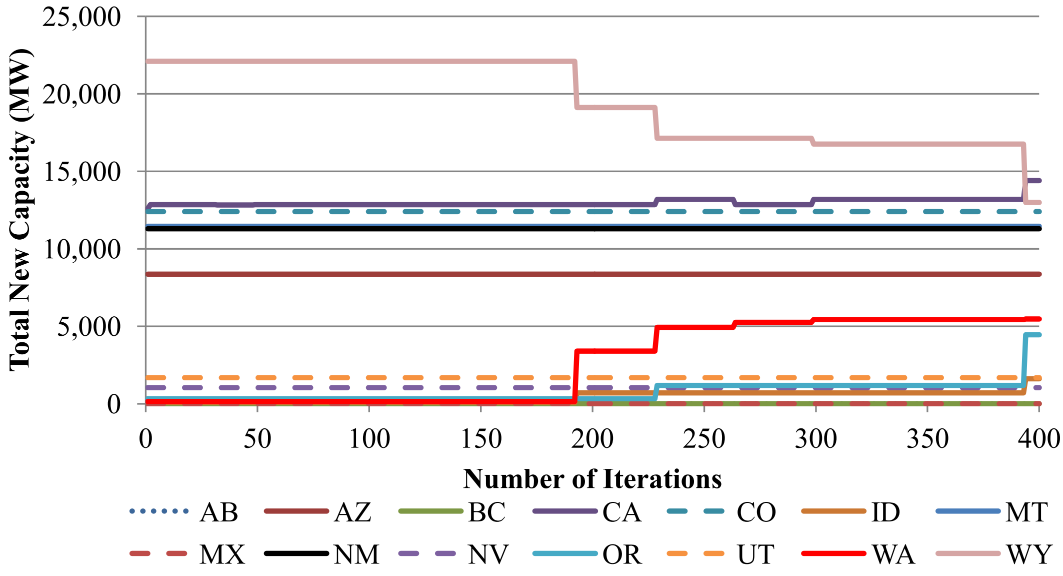

Figure C.20: New Wind generation capacity per state as a function of the number of iterations. Results from the application of regular Benders decomposition to the linear problem.

C.5.2 Enhanced BD LP - 1 Cluster

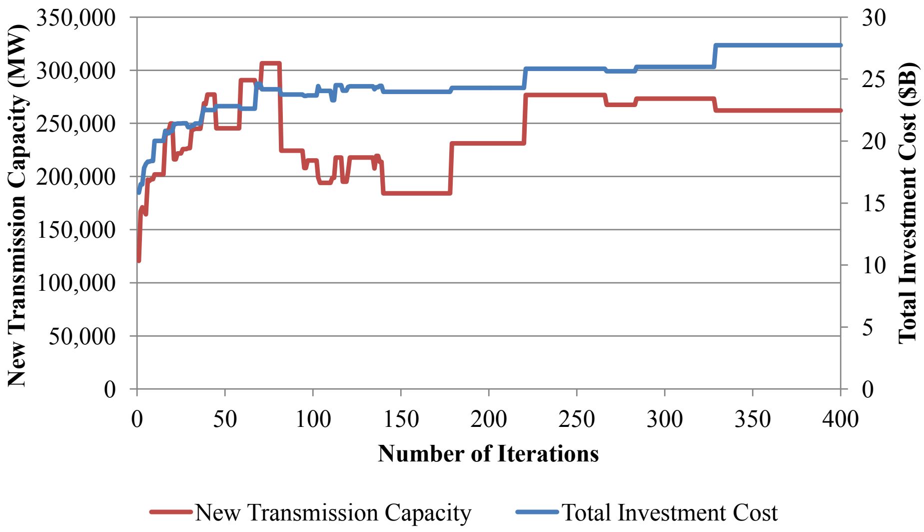

Figure C.21: Total new transmission capacity and transmission investment cost as a function of the number of iterations. Results from the application of the enhanced Benders decomposition algorithm (phase two) to the single-cluster linear problem.

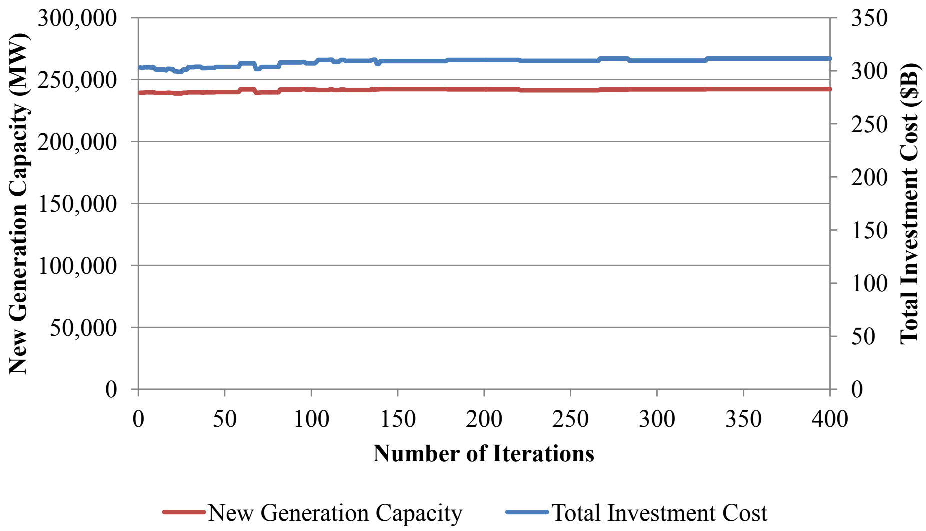

Figure C.22: Total new generation capacity and generation investment cost as a function of the number of iterations. Results from the application of the enhanced Benders decomposition algorithm (phase two) to the single-cluster linear problem.

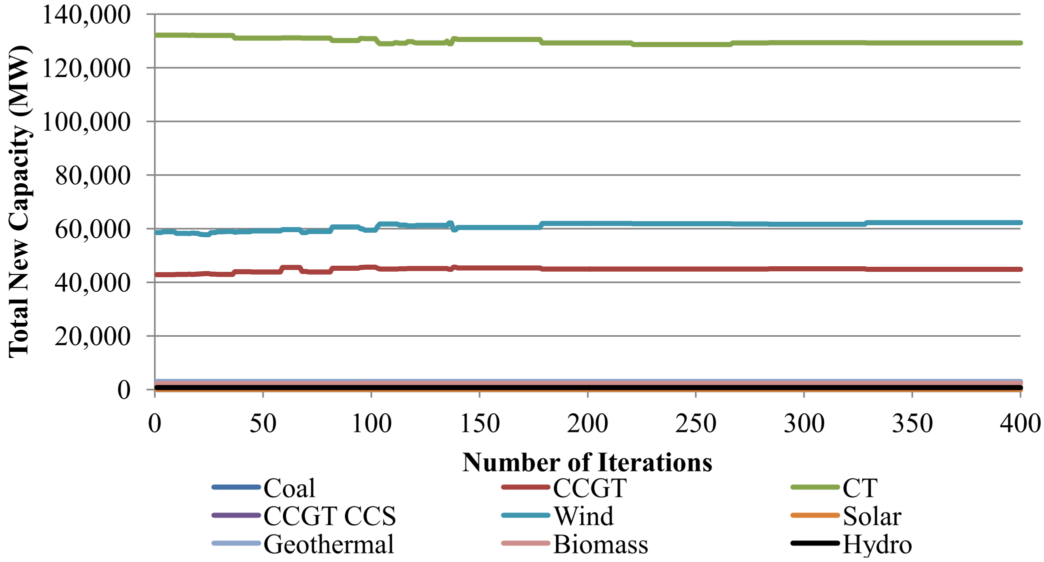

Figure C.23: Total new generation capacity per technology as a function of the number of iterations. Results from the application of the enhanced Benders decomposition algorithm (phase two) to the single-cluster linear problem.

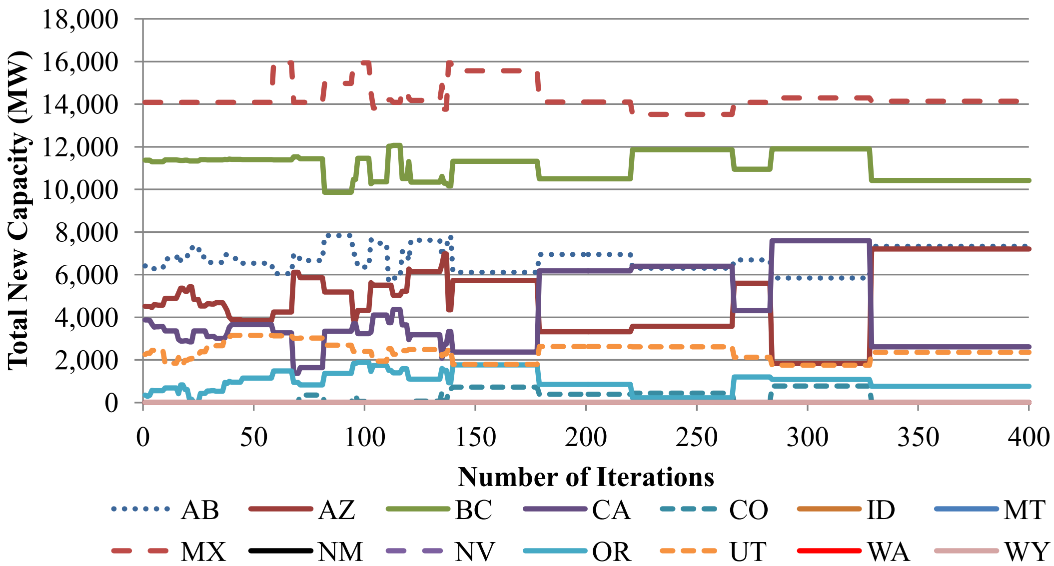

Figure C.24: New CCGT generation capacity per state as a function of the number of iterations. Results from the application of the enhanced Benders decomposition algorithm (phase two) to the single-cluster linear problem.

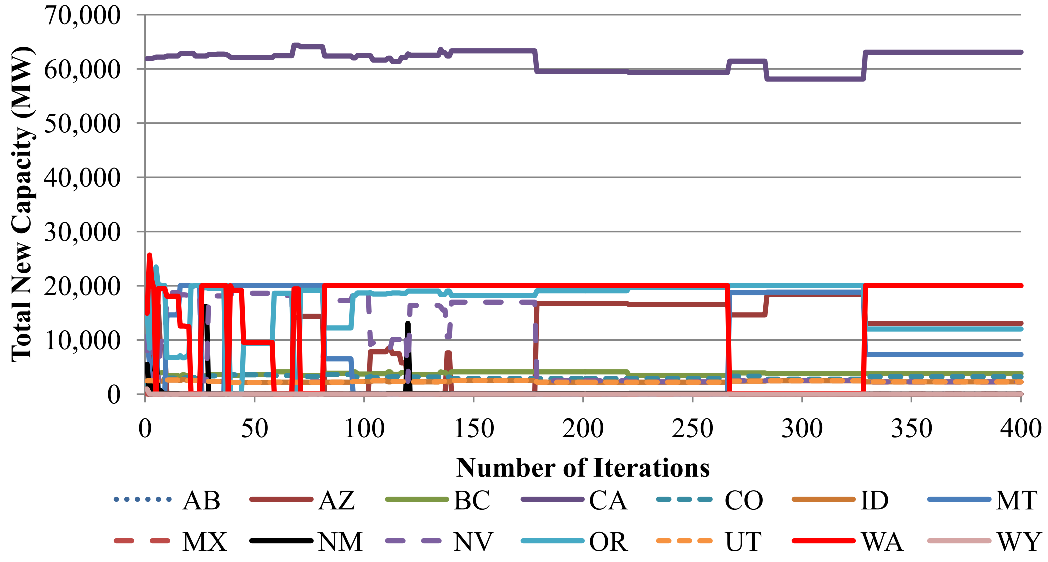

Figure C.25: New CT generation capacity per state as a function of the number of iterations. Results from the application of the enhanced Benders decomposition algorithm (phase two) to the single-cluster linear problem.

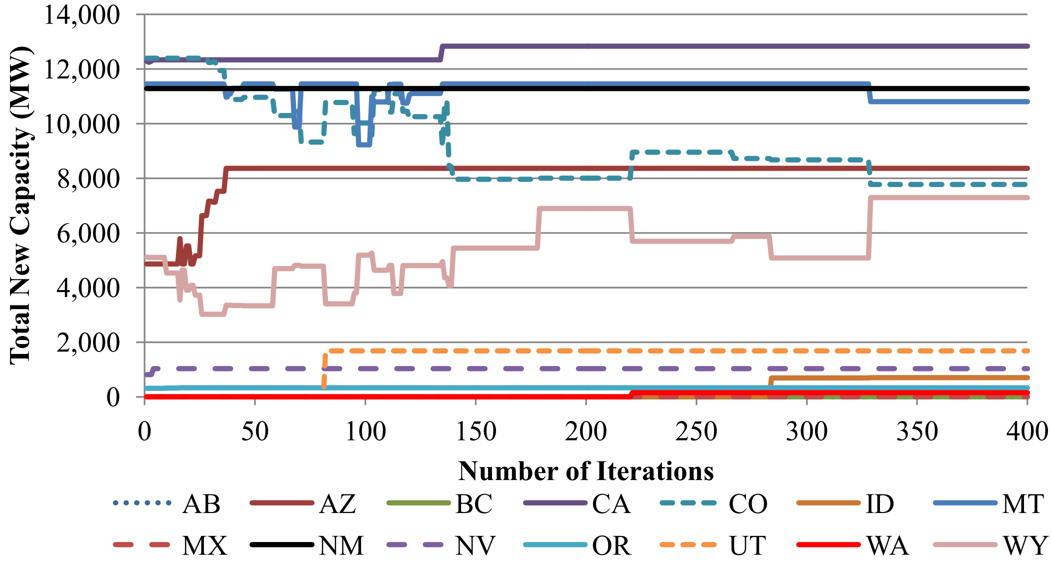

Figure C.26: New Wind generation capacity per state as a function of the number of iterations. Results from the application of the enhanced Benders decomposition algorithm (phase two) to the single-cluster linear problem.

C.5.3 Enhanced BD LP - 10 Clusters

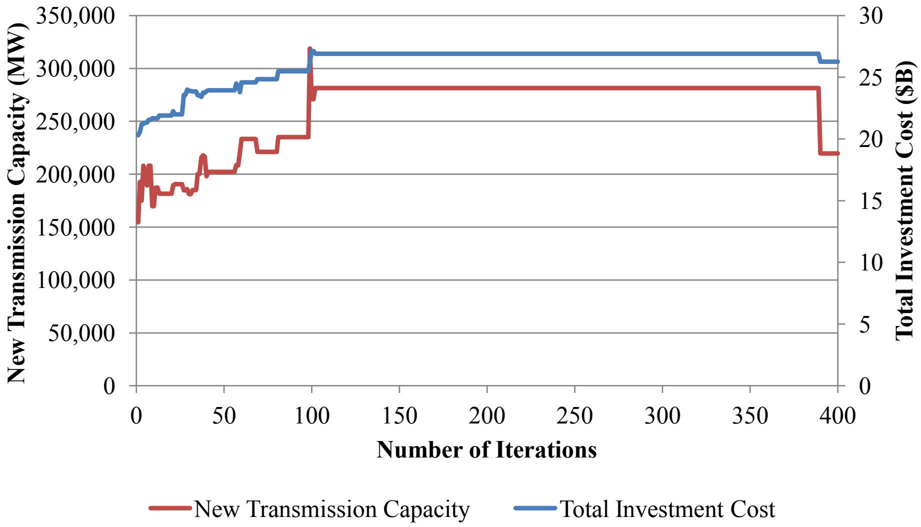

Figure C.27: Total new transmission capacity and transmission investment cost as a function of the number of iterations. Results from the application of the enhanced Benders decomposition algorithm (phase two) to the 10-cluster linear problem.

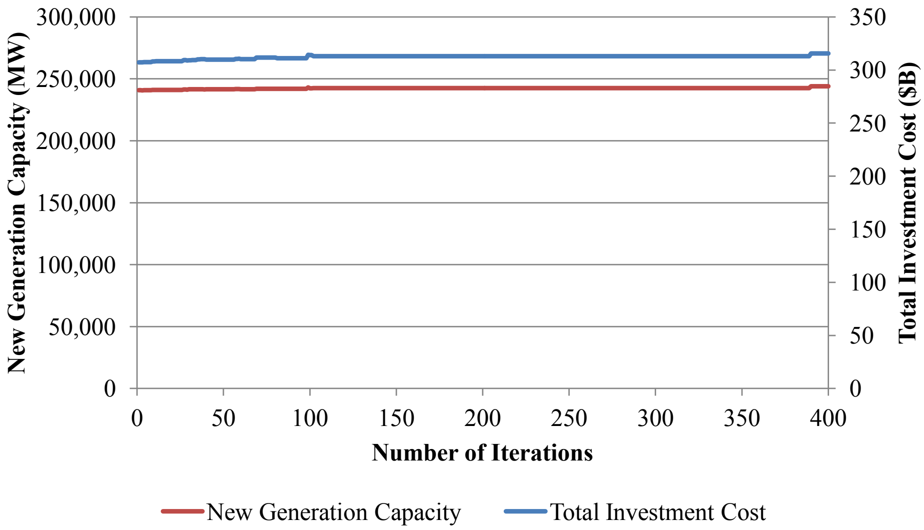

Figure C.28: Total new generation capacity and generation investment cost as a function of the number of iterations. Results from the application of the enhanced Benders decomposition algorithm (phase two) to the 10-cluster linear problem.

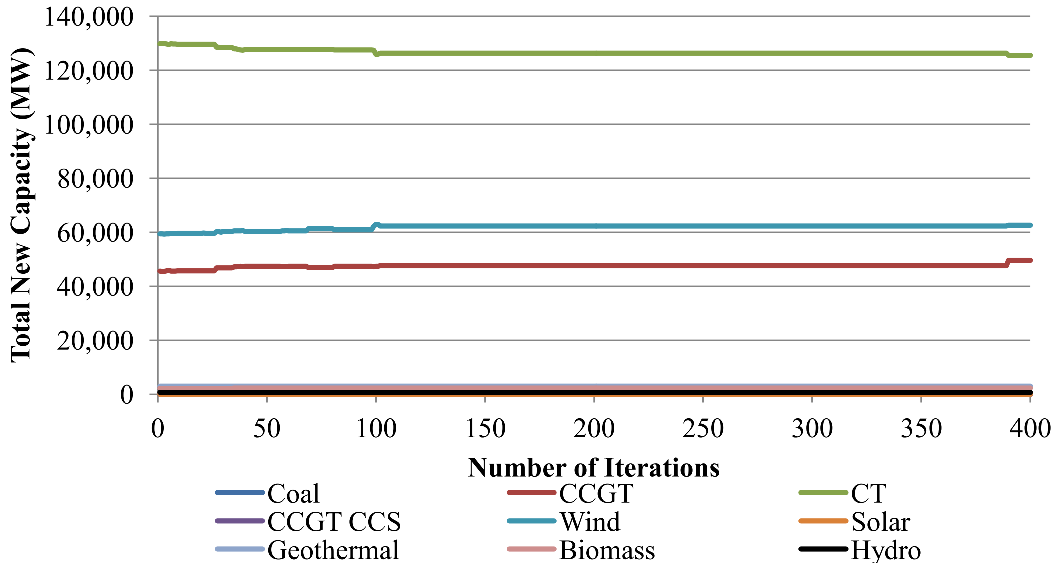

Figure C.29: Total new generation capacity per technology as a function of the number of iterations. Results from the application of the enhanced Benders decomposition algorithm (phase two) to the 10-cluster linear problem.

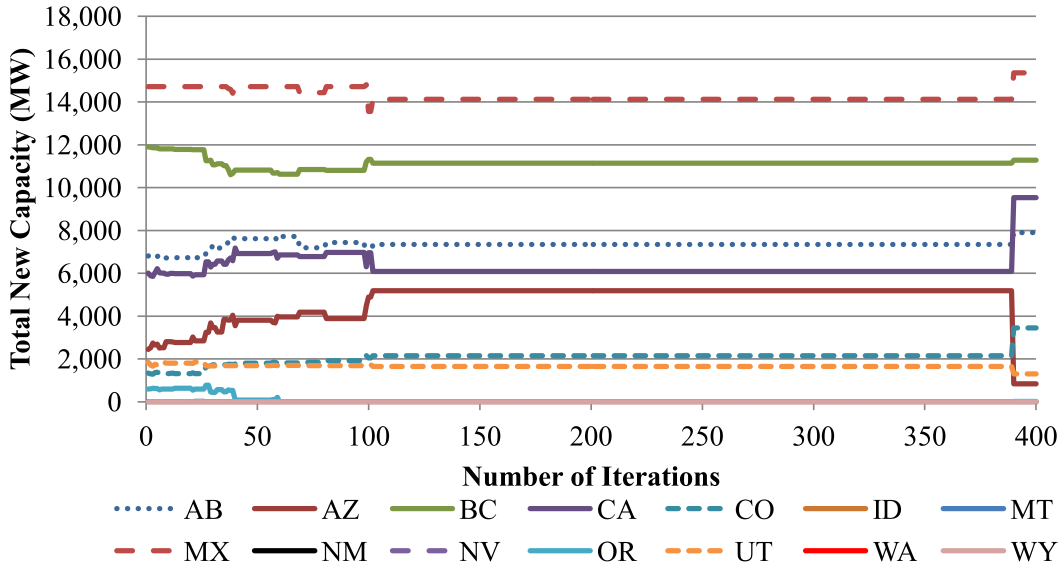

Figure C.30: New CCGT generation capacity per state as a function of the number of iterations. Results from the application of the enhanced Benders decomposition algorithm (phase two) to the 10-cluster linear problem.

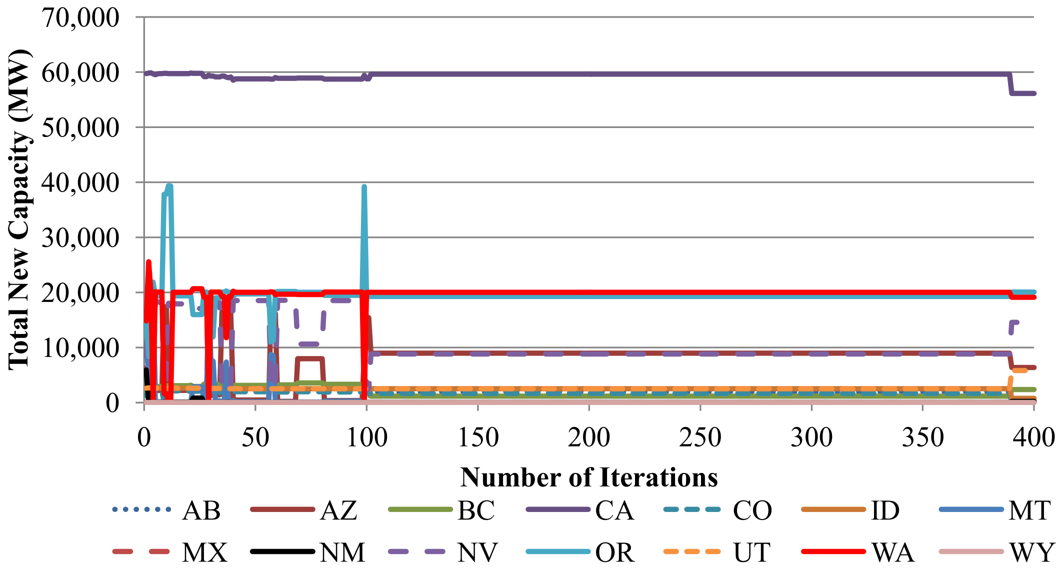

Figure C.31: New CT generation capacity per state as a function of the number of iterations. Results from the application of the enhanced Benders decomposition algorithm (phase two) to the 10-cluster linear problem.

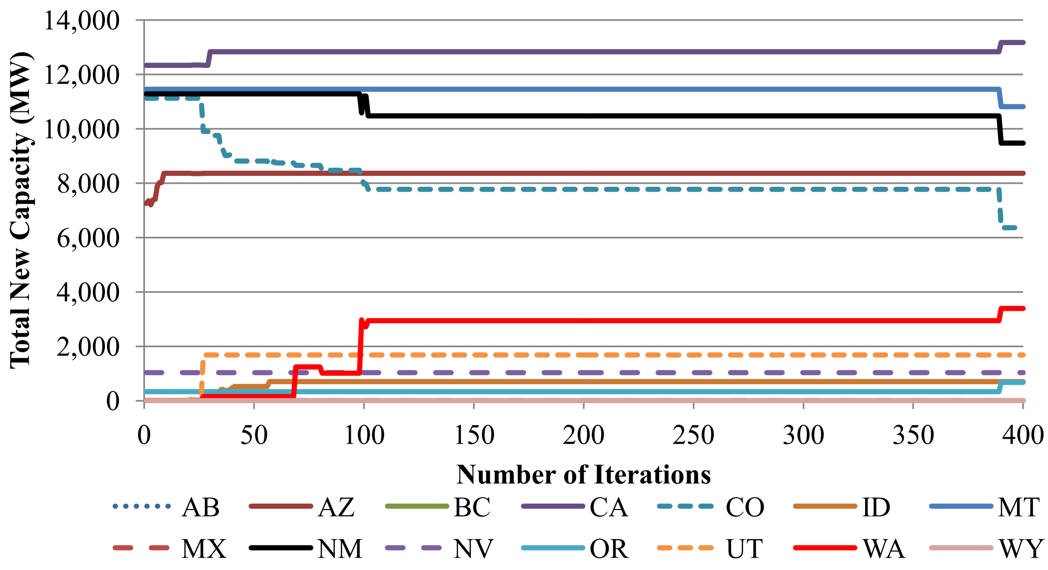

Figure C.32: New Wind generation capacity per state as a function of the number of iterations. Results from the application of the enhanced Benders decomposition algorithm (phase two) to the 10-cluster linear problem.

C.5.4 Enhanced BD LP - 33 Clusters

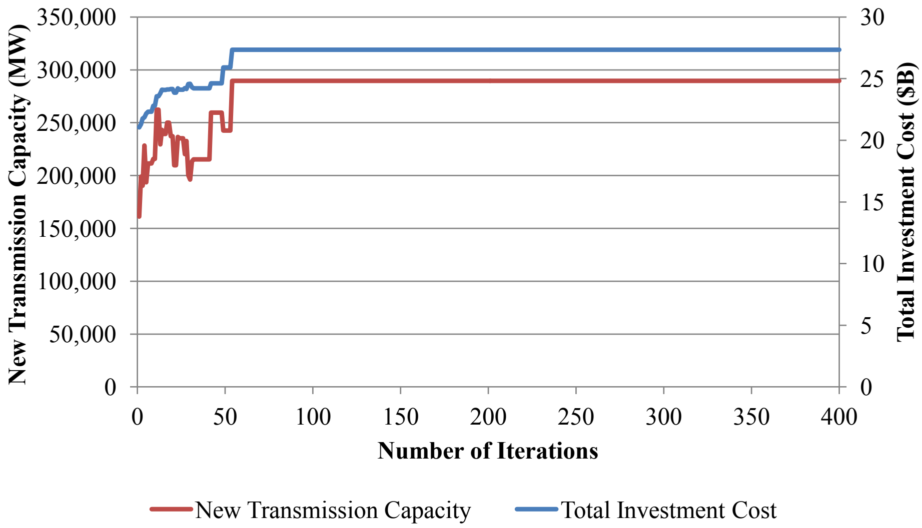

Figure C.33: Total new transmission capacity and transmission investment cost as a function of the number of iterations. Results from the application of the enhanced Benders decomposition algorithm (phase two) to the 33-cluster linear problem.

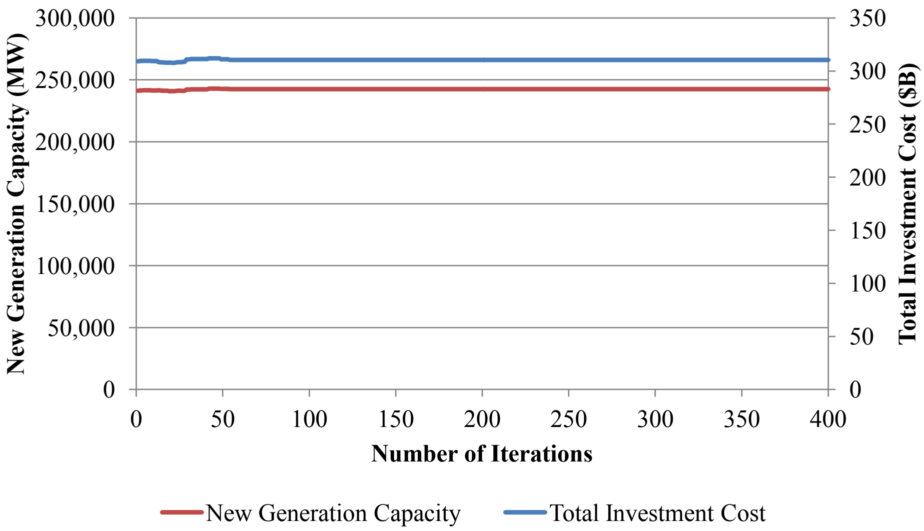

Figure C.34: Total new generation capacity and generation investment cost as a function of the number of iterations. Results from the application of the enhanced Benders decomposition algorithm (phase two) to the 33-cluster linear problem.

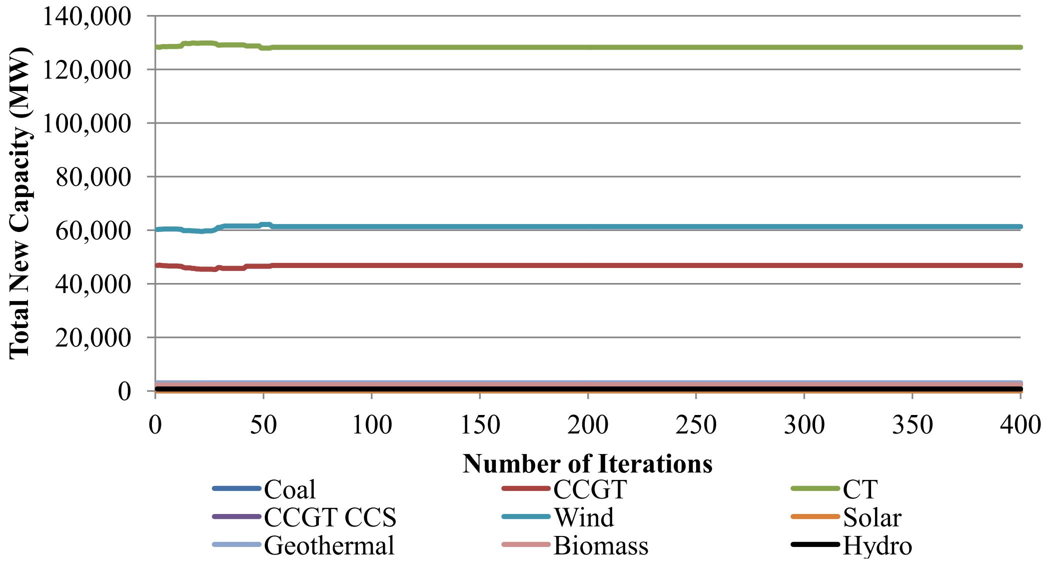

Figure C.35: Total new generation capacity per technology as a function of the number of iterations. Results from the application of the enhanced Benders decomposition algorithm (phase two) to the 33-cluster linear problem.

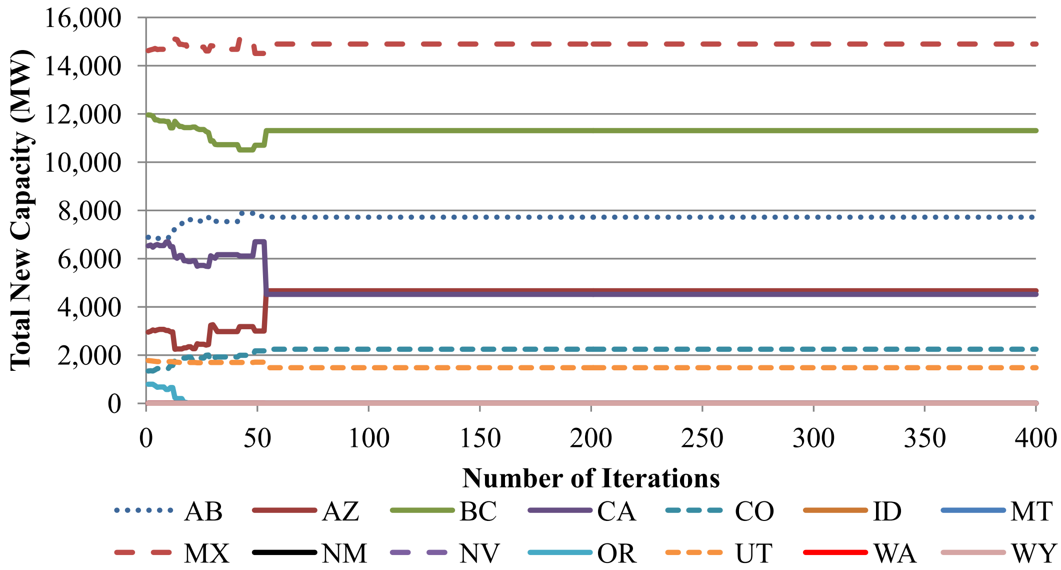

Figure C.36: New CCGT generation capacity per state as a function of the number of iterations. Results from the application of the enhanced Benders decomposition algorithm (phase two) to the 33-cluster linear problem.

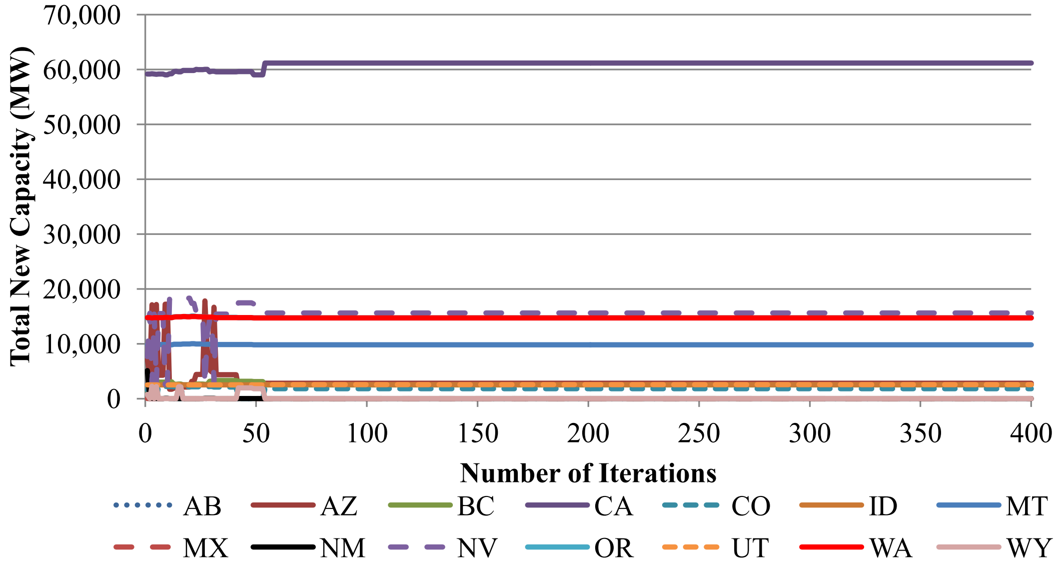

Figure C.37: New CT generation capacity per state as a function of the number of iterations. Results from the application of the enhanced Benders decomposition algorithm (phase two) to the 33-cluster linear problem.

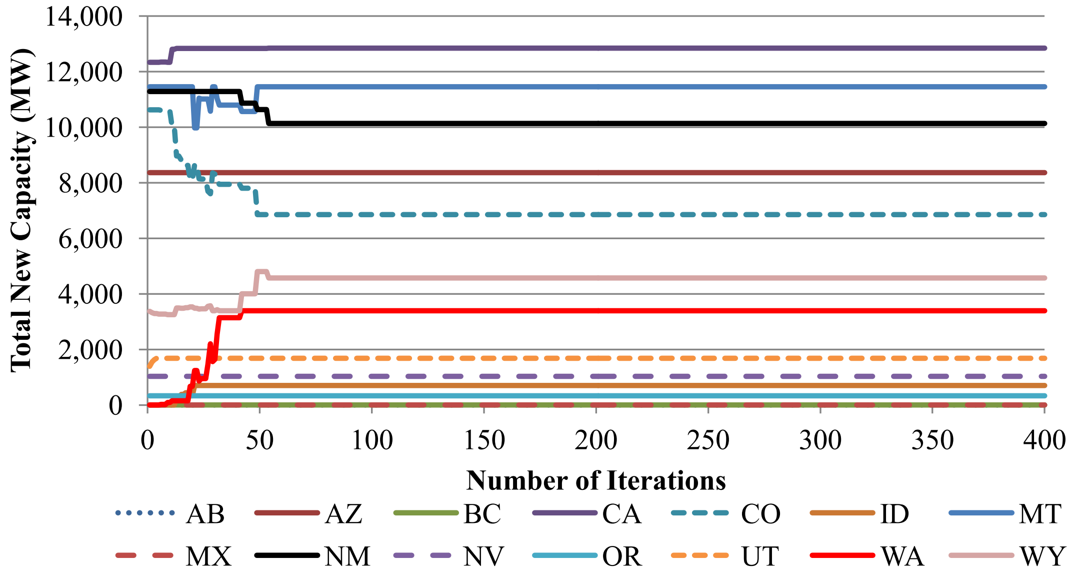

Figure C.38: New Wind generation capacity per state as a function of the number of iterations. Results from the application of the enhanced Benders decomposition algorithm (phase two) to the 33-cluster linear problem.

C.5.5 Enhanced BD MILP - 1 Cluster

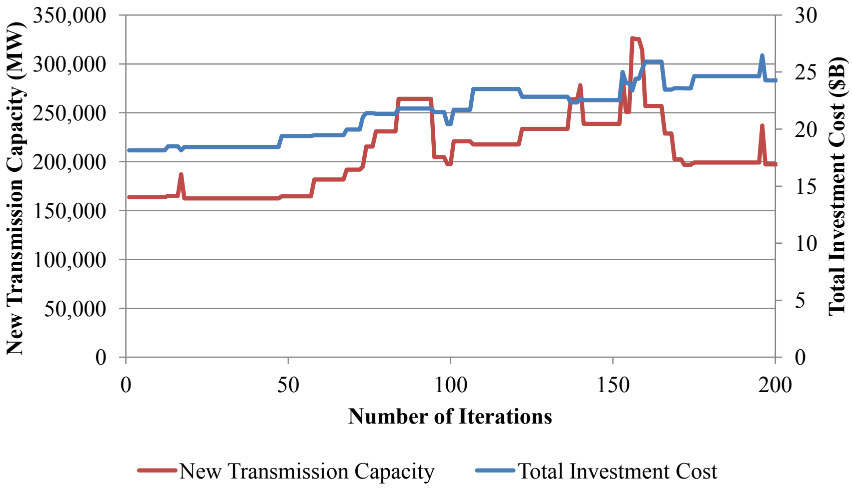

Figure C.39: Total new transmission capacity and transmission investment cost as a function of the number of iterations. Results from the application of the enhanced Benders decomposition algorithm (phase two) to the single-cluster mixed-integer linear problem.

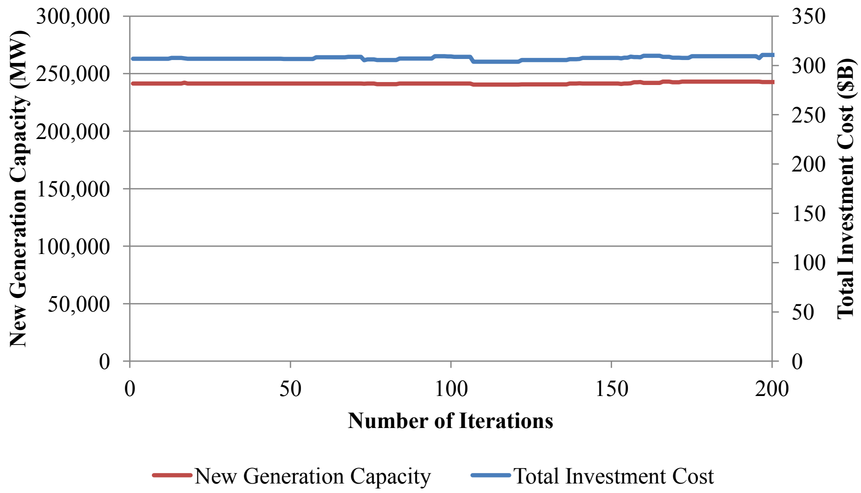

Figure C.40: Total new generation capacity and generation investment cost as a function of the number of iterations. Results from the application of the enhanced Benders decomposition algorithm (phase two) to the single-cluster mixed-integer linear problem.

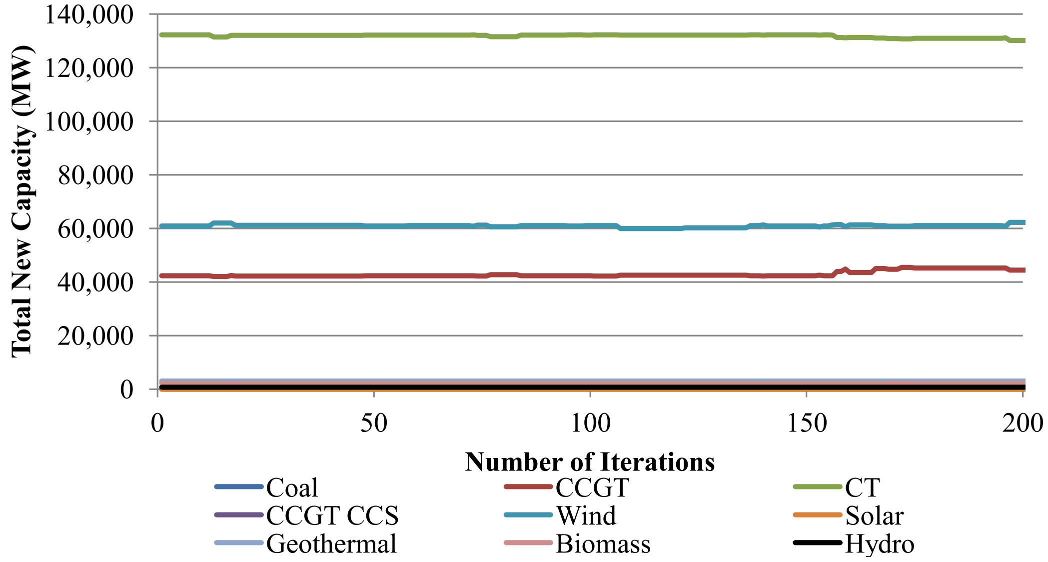

Figure C.41: Total new generation capacity per technology as a function of the number of iterations. Results from the application of the enhanced Benders decomposition algorithm (phase two) to the single-cluster mixed-integer linear problem.

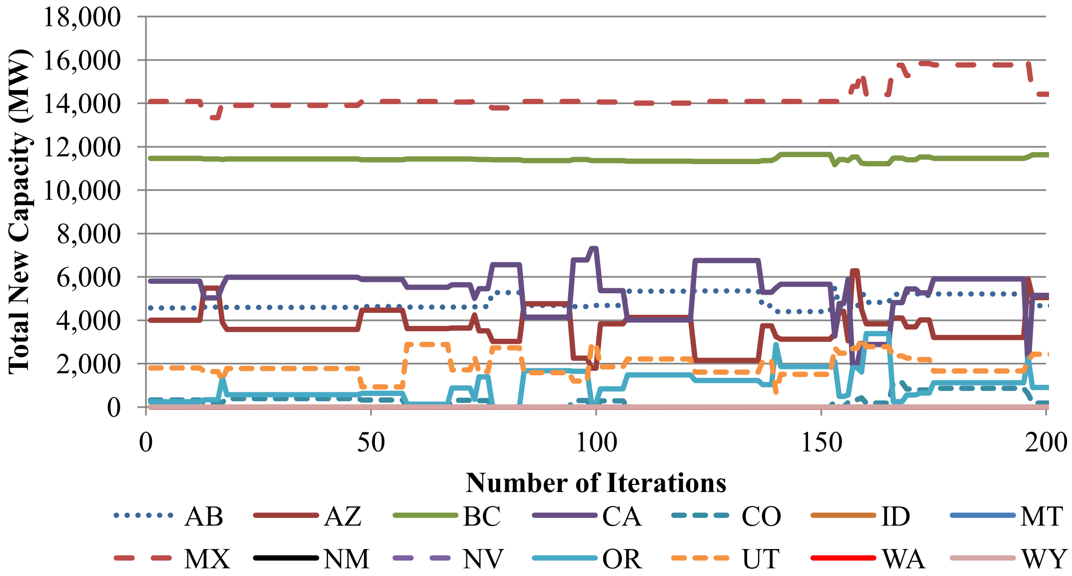

Figure C.42: New CCGT generation capacity per state as a function of the number of iterations. Results from the application of the enhanced Benders decomposition algorithm (phase two) to the single-cluster mixed-integer linear problem.

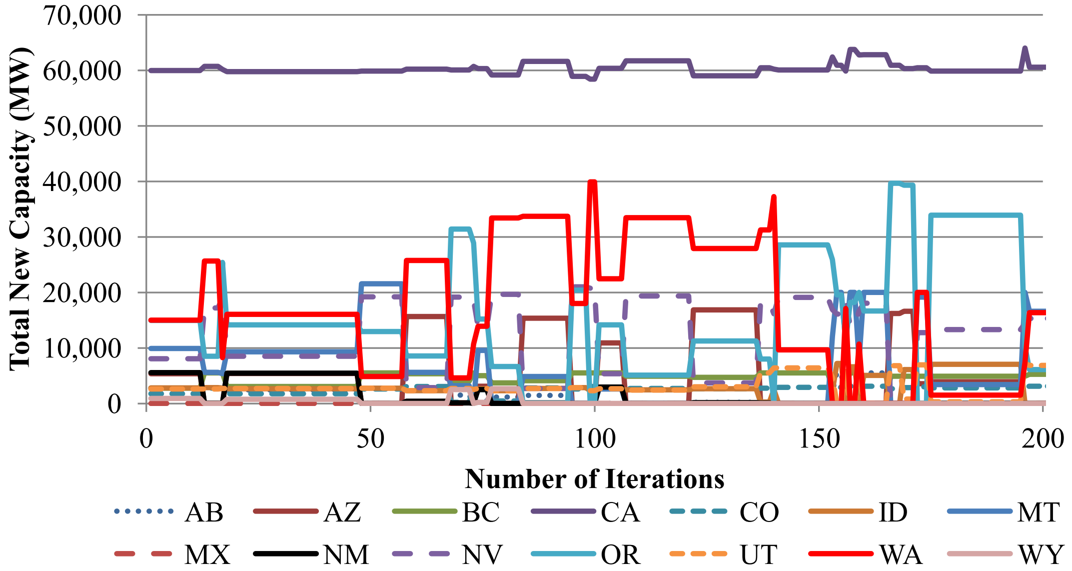

Figure C.43: New CT generation capacity per state as a function of the number of iterations. Results from the application of the enhanced Benders decomposition algorithm (phase two) to the single-cluster mixed-integer linear problem.

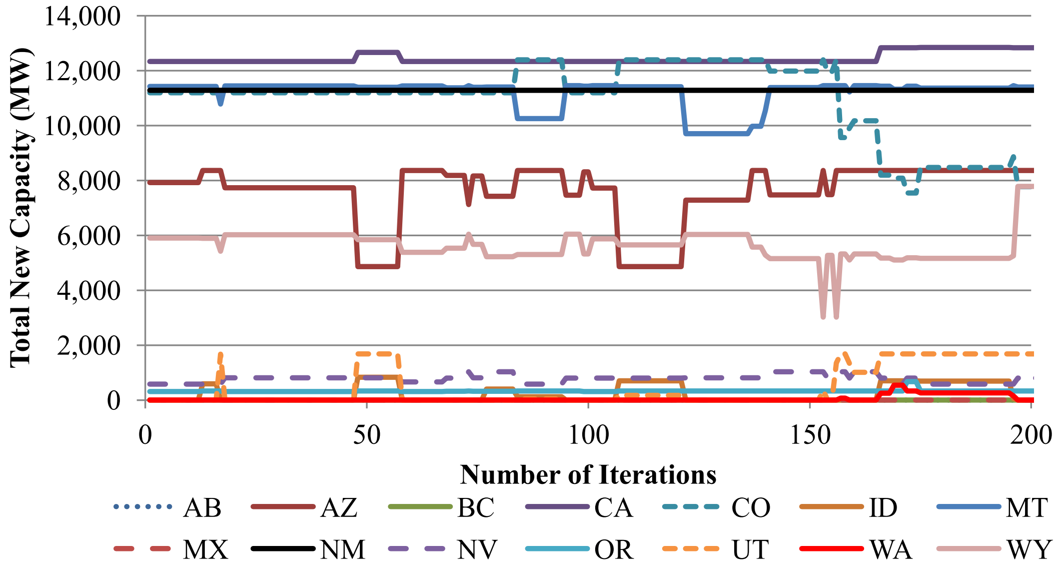

Figure C.44: New Wind generation capacity per state as a function of the number of iterations. Results from the application of the enhanced Benders decomposition algorithm (phase two) to the single-cluster linear problem.

C.5.6 Enhanced BD MILP - 1 Cluster + 400 Pre-Computed Cuts

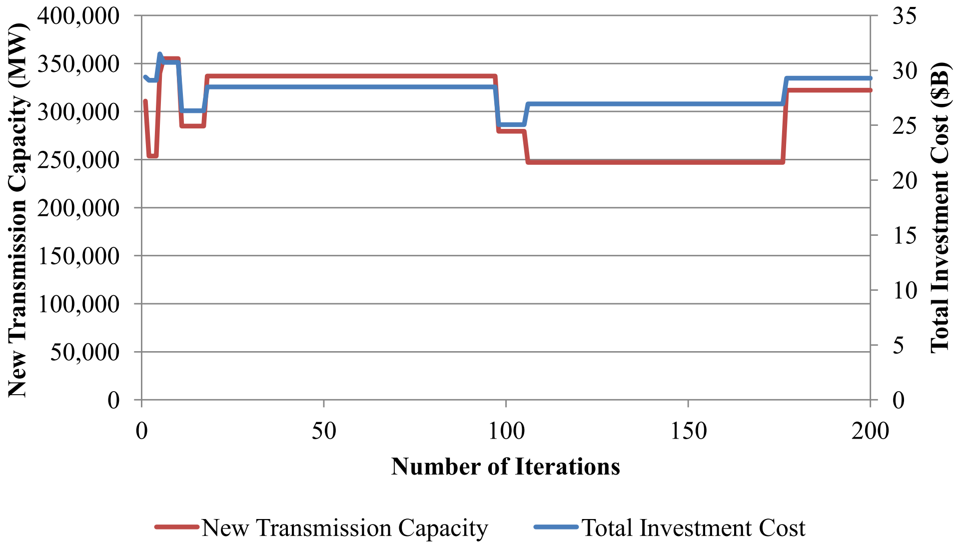

Figure C.45: Total new transmission capacity and transmission investment cost as a function of the number of iterations. Results from the application of the enhanced Benders decomposition algorithm (phase two) to the single-cluster mixed-integer linear problem with 400 pre-computed cuts.

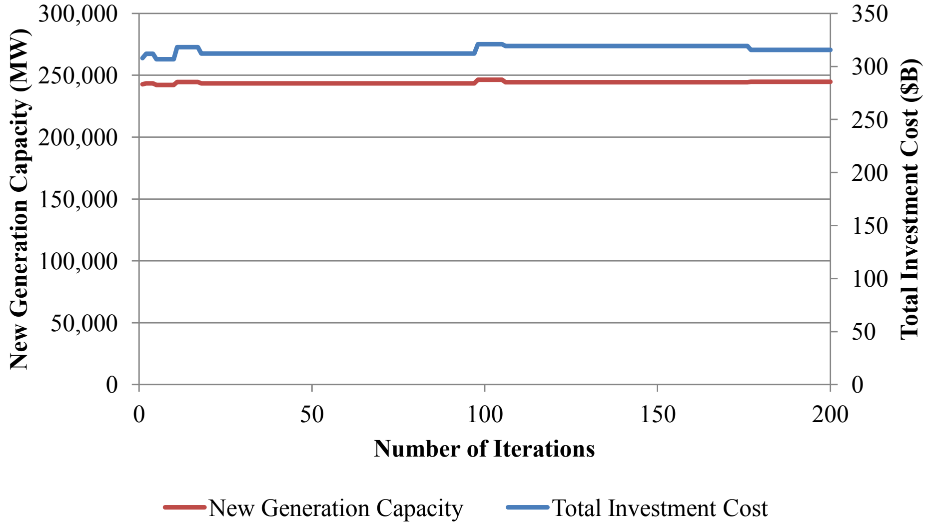

Figure C.46: Total new generation capacity and generation investment cost as a function of the number of iterations. Results from the application of the enhanced Benders decomposition algorithm (phase two) to the single-cluster mixed-integer linear problem with 400 pre-computed cuts.

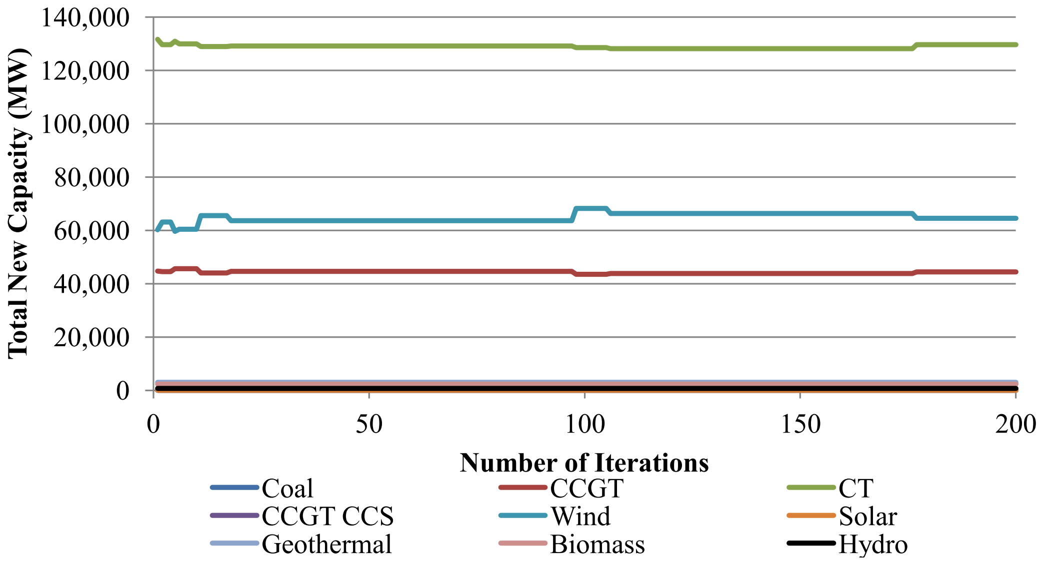

Figure C.47: Total new generation capacity per technology as a function of the number of iterations. Results from the application of the enhanced Benders decomposition algorithm (phase two) to the single-cluster mixed-integer linear problem with 400 pre-computed cuts.

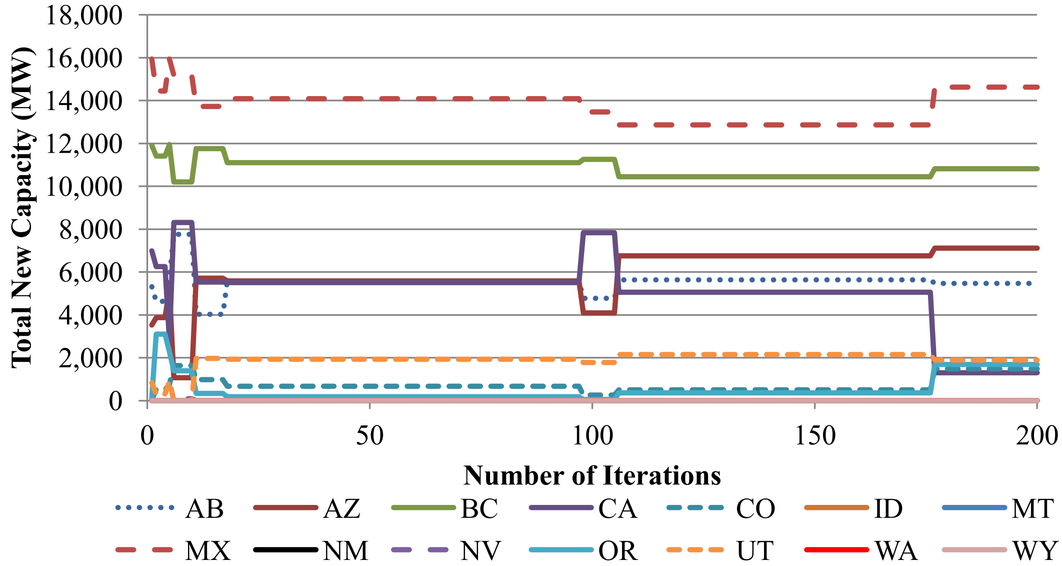

Figure C.48: New CCGT generation capacity per state as a function of the number of iterations. Results from the application of the enhanced Benders decomposition algorithm (phase two) to the single-cluster mixed-integer linear problem with 400 pre-computed cuts.

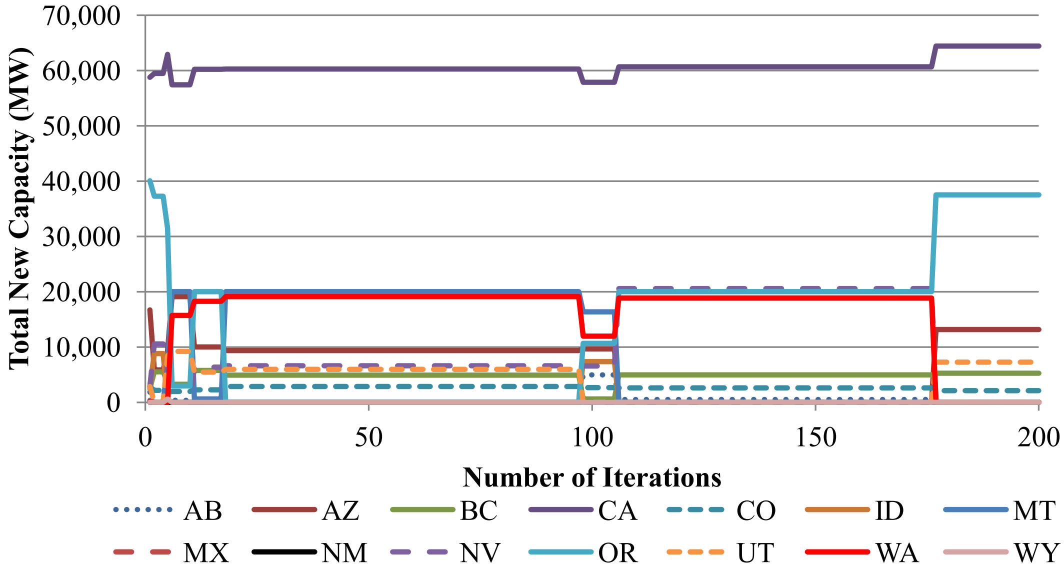

Figure C.49: New CT generation capacity per state as a function of the number of iterations. Results from the application of the enhanced Benders decomposition algorithm (phase two) to the single-cluster mixed-integer linear problem with 400 pre-computed cuts.

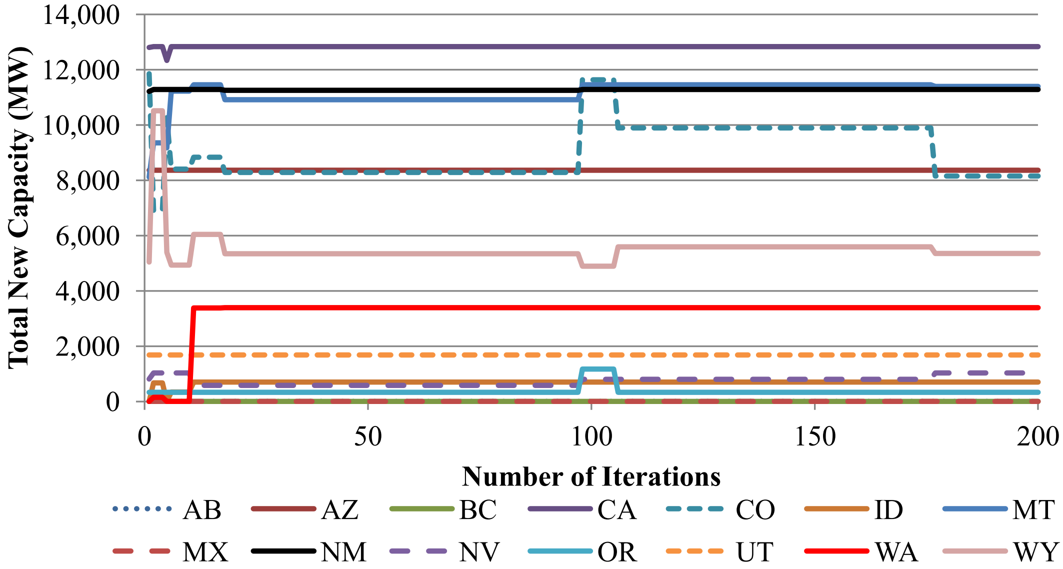

Figure C.50: New Wind generation capacity per state as a function of the number of iterations. Results from the application of the enhanced Benders decomposition algorithm (phase two) to the single-cluster linear problem with pre-computed cuts.

Bibliography

Aardal, K. and Larsson, T. (1990). A Benders Decomposition Based Heuristic for the Hierarchical Production Planning Problem. *European Journal of Operational Research*, 45(1):4–14.

ABB (2012). ABB GridView Software Brochure. Retrieved May 20, 2012, from http://www05.abb.com/global/scot/scot221.nsf/veritydisplay/581366a0c212c93ac 1256fda00488562/$file/Gridview%20Brochure.pdf.

ACESA (2012). H.R. 2454–111th Congress: American Clean Energy and Security Act of 2009. Retrieved April12, 2012, from http://www.govtrack.us/congress/bills/111/hr2454.

AEO (2011). Annual Energy Outlook 2011, U.S. Energy Information Administration. Report DOE/EIA-0383. Retrieved March 10, 2012, from http://www.eia.gov/forecasts/archive/aeo11/.

AESO (2012). AESO Long-term Transmission Plan. Retrieved July 5, 2012, from http://www.aeso.ca/downloads/AESO_2012_LTP_Sections_1.0_to_5.0.pdf.

Akbari, T., Rahimikian, A., and Kazemi, A. (2011). A Multi-Stage Stochastic Transmission Expansion Planning Method. *Energy Conversion and Management*, 52(8-9):2844–2853.

Alguacil, N., Motto, A., and Conejo, A. (2003). Transmission Expansion Planning: A Mixed-Integer LP Approach. *IEEE Transactions on Power Systems*, 18(3):1070–1077.

Amundsen, E. S. and Mortensen, J. B. (2001). The Danish Green Certificate System: Some Simple Analytical Results. *Energy Economics*, 23(5):489 – 509.

Anderson, D. (1972). Models for Determining Least-Cost Investments in Electricity Supply. *Bell Journal of Economics and Management Science*, 3(1):267–299.

Anitescu, M. and Birge, J. R. (2008). Convergence of Stochastic Average Approximation for Stochastic Optimization Problems with Mixed Expectation and Per-Scenario Constraints. Technical report, Argonne National Laboratory.

Awad, M. L., Casey, K. E., Geevarghese, A. S., Miller, J. C., Rahimi, A. F., Sheffrin, A. Y., Zhang, M., Toolson, E., Drayton, G., Hobbs, B. F., and Wolak, F. A. (2010). Using Market Simulations for Economic Assessment of Transmission Upgrades: Application of the California ISO Approach. In Zhang, X. P., editor, *Restructured Electric Power Systems*, pages 241–270. Hoboken, NJ:John Wiley & Sons, Inc.

Bahiense, L., Oliveira, G., Pereira, M., and Granville, S. (2001). A Mixed Integer Disjunctive Model for Transmission Network Expansion. *IEEE Transactions on Power Systems*, 16(3):560–565.

Baringo, L. and Conejo, A. J. (2012). Wind Power Investment: A Benders Decomposition Approach. *IEEE Transactions on Power Systems*, 27(1):433–441.

Benders, J. (1962). Partitioning Procedures for Solving Mixed-Variables Programming Problems. *Numerische Mathematik*, 4(1):238–252.

Berry, T. and Jaccard, M. (2001). The Renewable Portfolio Standard: Design Considerations and an Implementation Survey. *Energy Policy*, 29(4):263 – 277.

Bertsekas, D. P. and Sandell, N. R. (1982). Estimates of the Duality Gap for Large-Scale Separable Nonconvex Optimization Problems. In *21st IEEE Conference on Decision and Control*, volume 21, pages 782–785.

Bertsimas, D., Litvinov, E., Sun, X. A., Zhao, J., and Zheng, T. (2013). Adaptive Robust Optimization for the Security Constrained Unit Commitment Problem. *IEEE Transactions on Power Systems*, 28(1):52–63.

Bertsimas, D. and Tsitsiklis, J. (1997). *Introduction to Linear Optimization*. Nashua, NH:Athena Scientific.

Billinton, R. and Allan, R. N. (2003). Reliability of Electric Power Systems: An

Overview. In Pham, H., editor, *Handbook of Reliability Engineering*, pages 511–528. London:Springer.

Binato, S., Pereira, M. V. F., and Granville, S. (2001). A New Benders Decomposition Approach to Solve Power Transmission Network Design Problems. *IEEE Transactions on Power Systems*, 16(2):235–240.

Birge, J. and Louveaux, F. (1997). *Introduction to Stochastic Programming.* New York, NY:Springer.

Birge, J. R. (2011). Uses of Sub-sample Estimates in Stochastic Optimization Models. Working Paper, The University of Chicago.

Birge, J. R. and Louveaux, F. V. (1988). A Multicut Algorithm for 2-Stage Stochastic Linear-Programs. *European Journal of Operational Research*, 34(3):384–392.

Birge, J. R. and Wallace, S. W. (1986). Refining Bounds for Stochastic Linear-Programs with Linearly Transformed Independent Random-Variables. *Operations Research Letters*, 5(2):73–77.

Bloom, J. A. (1983). Solving an Electricity Generating Capacity Expansion Planning Problem by Generalized Benders Decomposition. *Operations Research*, 31(1):84–100.

Bloom, J. A., Caramanis, M., and Charny, L. (1984). Long-Range Generation

Planning Using Generalized Benders Decomposition - Implementation and Experience. *Operations Research*, 32(2):290–313.

Booth, R. R. (1972). Power-System Simulation Model Based on Probability Analysis. *IEEE Transactions on Power Apparatus and Systems*, Pa91(1):62–&.

Bradley, S. P., Hax, A. C., and Magnanti, T. L. (1977). *Applied Mathematical Programming*. Reading, MA: Addison-Wesley.

Buygi, M., Shahidehpour, M., Shanechi, H., and Balzer, G. (2004). Market Based Transmission Planning Under Uncertainties. In *International Conference on Probabilistic Methods Applied to Power Systems*, pages 563 –568.

CAISO (2012). 2011-2012 Transmission Plan. Retrieved April 5, 2012, from http://www.caiso.com/Documents/Board-approvedISO2011-2012-TransmissionPlan.pdf.

Caramanis, M. C., Tabors, R. D., Nochur, K. S., and Schweppe, F. C. (1982). The Introduction of Non-DIispatchable Technologies a Decision Variables in Long-Term Generation Expansion Models. *IEEE Transactions on Power Apparatus and Systems*, PAS-101(8):2658–2667.

Cedeño, E. B. and Arora, S. (2011). Performance Comparison of Transmission Network Expansion Planning Under Deterministic and Uncertain Conditions. *International Journal of Electrical Power & Energy Systems*, 33(7):1288–1295.

BIBLIOGRAPHY

Chao, H.-P. and Peck, S. (1996). A Market Mechanism for Electric Power Transmission. *Journal of Regulatory Economics*, 10(1):25–59.

Chien, C., Goldsman, D., and Melamed, B. (1997). Large-Sample Results for Batch Means. *Management Science*, 43(9):1288–1295.

Cote, G. and Laughton, M. A. (1984). Large-Scale Mixed Integer Programming - Benders-Type Heuristics. *European Journal of Operational Research*, 16(3):327–333.

CPUC (2009). 33% Renewables Portfolio Standard, Implementation Analysis and Preliminary Results. California Public Utilities Commission. Retrieved May 17, 2012, from http://www.cpuc.ca.gov/NR/rdonlyres/B123F7A9-17BD-461E-AC34-973B906CAE8E/0/ExecutiveSummary33percentRPSImplementationAnalysis.pdf.

CSS (2012). Costs by System Size, California Solar Statistics. Retrieved May 17, 2012, from http://www.californiasolarstatistics.ca.gov/reports/cost_vs_system_size/ on April 10, 2012.

Dantzig, G., Glynn, P. W., Avriel, M., Stone, J., Entriken, R., and Nakayama, M. (1989). Decomposition Techniques for Multi-area Generation and Transmission Planning Under Uncertainty: Final Report. Electric Power Research Institute.

De Jonghe, C., Hobbs, B. F., and Belmans, R. (2012). Optimal Generation Mix

With Short-Term Demand Response and Wind Penetration. *IEEE Transactions on Power Systems*, 27(2):830–839.

de la Torre, T., Feltes, J., Gomez San Roman, T., and Merrill, H. (1999). Deregulation, Privatization, and Competition: Transmission Planning Under Uncertainty. *IEEE Transactions on Power Systems*, 14(2):460–465.

de Sisternes, F. J. and Webster, M. (2013). Optimal Selection of Sample Weeks for Approximating the Net Load in Generation Planning Problems. Working paper ESD-WP-2013-03, Massachusetts Institute of Technology.

Dehghan, S., Kazemi, A., and Neyestani, N. (2011). Multistage Transmission Expansion Planning Alleviating the Level of Transmission Congestion. In *IEEE PowerTech, Trondheim*, pages 1–8.

DOE (2003). Grid 2030: A National Vision For Electricity's Second 100 Years. U.S. Department of Energy. Retrieved April 4, 2012, from http://energy.gov/sites/prod/files/oeprod/DocumentsandMedia/Electric_Vision_Document.pdf.

DOE (2013). Electricity Grid Basics. U.S. Department of Energy. Retrieved October 29, 2013, from http://www1.eere.energy.gov/tribalenergy/guide/electricity_grid_basics.html.

DSIRE (2012). DSIRE: Database of State Incentives for Renewables and Efficiency. Retrieved March 10, 2012, from http://www.dsireusa.org/.

EIA (2012). Capital Cost Estimates for Electricity Generation Plants. U. S. Energy Information Administration . Retrieved March 20, 2012, from http://www.eia.gov/oiaf/beck_plantcosts/.

EIA (2013). U.S. Energy Information Administration. Retrieved May 20, 2012, from http://www.eia.gov.

EISPC (2012). Eastern Interconnection States' Planning Council, Whitepaper: Co-Optimization of Transmission and other Supply Resources. Solicitation Number: NARUC-2012-RFP010-DE0316.

Ela, E., Milligan, M., Parsons, B., Lew, D., and Corbus, D. (2009). The Evolution of Wind Power Integration Studies: Past, Present, and Future. In *IEEE Power Energy Society General Meeting, 2009.*, pages 1–8.

EPA (2012). US EPA: Carbon Pollution Standard for New Power Plants. Retrieved Arpil 10, 2012, from http://epa.gov/carbonpollutionstandard/basic.html.

EPA (2013). MARKAL Technology Database and Model. Retrieved March 20, 2012, from http://www.epa.gov/nrmrl/appcd/climate_change/markal.htm.

FERC (2011). Recent ISO Software Enhancements and Future Software and

Modeling Plans. Retrieved October 29, 2013, from http://www.ferc.gov/industries/electric/indus-act/rto/rto-iso-soft-2011.pdf.

FERC (2013). FERC Order 1000 - Transmission Planning and Cost Allocation. Retrieved May 10,2013, from http://www.ferc.gov/industries/electric/indus-act/trans-plan.asp.

Fischer, C. (2010). Renewable Portfolio Standards: When Do They Lower Energy Prices? *The Energy Journal*, 0(Number 1):101–120.

Fischer, C. and Newell, R. G. (2008). Environmental and technology policies for climate mitigation. *Journal of Environmental Economics and Management*, 55(2):142 – 162.

Fouquet, D. and Johansson, T. B. (2008). European Renewable Energy Policy at Crossroads- Focus on Electricity Support Mechanisms. *Energy Policy*, 36(11):4079 – 4092.

Gabriel, S. A., Conejo, A. J., Fuller, J. D., Hobbs, B. F., and Ruiz, C. (2012). *Complementarity Modeling in Energy Markets*. New York, NY:Springer.

Gabriel, S. A., Kydes, A. S., and Whitman, P. (2001). The National Energy Modeling System: A Large-Scale Energy-Economic Equilibrium Model. *Operations Research*, 49(1):14–25.

Garver, L. L. (1970). Transmission Network Estimation Using Linear Programming. *IEEE Transactions on Power Apparatus and Systems,*, PAS-89(7):1688–1697.

GEA (2012). Greatest Engineering Achievements of the 20th Century. Retrieved June 10, 2012, from http://www.greatachievements.org/.

Gentile, T. J., Elizondo, D. C., and Ray, S. (2010). Strategic Midwest Area Renewable Transmission (SMARTransmission) Study, Phase 1 Report. Retrieved May 5, 2012, from http://www.aepsustainability.com/ourissues/energy/docs/Phase1SMARTReport_FINAL.pdf.

Geoffrion, A. M. (1972). Generalized Benders Decomposition. *Journal of Optimization Theory and Applications*, 10(4):237–260.

Geoffrion, A. M. and Graves, G. W. (1980). Multicommodity Distribution-System Design by Benders Decomposition. *Management Science*, 26(8):855–856.

Gorenstin, B. G., Campodonico, N. M., Costa, J. P., and Pereira, M. V. F. (1993). Power System Expansion Planning Under Uncertainty. *IEEE Transactions on Power Systems*, 8(1):129–136.

Granville, S. and Pereira, M. V. F. (1985). Analysis of the Linearized Power Flow Model in Benders Decomposition. *System Optimization Lab., Dept. of Operations Research, Stanford University.* Tech. Rep. SOL 85-04.

Gu, Y., McCalley, J., and Ni, M. (2012). Coordinating Large-Scale Wind Integration and Transmission Planning. *IEEE Transactions on Sustainable Energy*, 3(4):652–659.

Gutman, R., Marchenko, P. P., and Dunlop, R. D. (1979). Analytical Development of Loadability Characteristics for EHV and UHV Transmission Lines. *IEEE Transactions on Power Apparatus and Systems*, PAS-98(2):606–617.

Hart, W. E., Laird, C., Watson, J.-P., and Woodruff, D. L. (2012). *Pyomo - Optimization Modeling in Python*. New York, NY:Springer.

Hecker, L., Zhou, Z., Osborn, D., and Lawhorn, J. (2009). Value Based Transmission Planning Process for Joint Coordinated System Plan. In *IEEE Power Energy Society General Meeting, 2009.*, pages 1–6.

Hedman, K., Gao, F., and Sheble, G. (2005). Overview of Transmission Expansion Planning Using Real Options Analysis. In *Proceedings of the 37th Annual North American Power Symposium*, pages 497–502.

Heejung, P. and Baldick, R. (2013). Transmission Planning Under Uncertainties of Wind and Load: Sequential Approximation Approach. *IEEE Transactions on Power Systems*, 28(3):2395–2402.

Higle, J. L. and Sen, S. (1991). Stochastic Decomposition: An Algorithm for

Two-Stage Linear Programs with Recourse. *Mathematics of Operations Research*, 16(3):650–669.

Hoang Hai, H. (1980). Topological Optimization of Networks: A Nonlinear Mixed Integer Model Employing Generalized Benders Decomposition. In *19th IEEE Conference on Decision and Control including the Symposium on Adaptive Processes*, volume 19, pages 427–432.

Hobbs, B. F. (1984). Regional Energy Facility Location Models for Power System Planning and Policy Analysis. In B. Lev, F. Murphy, J. B. and Gleit, A., editors, *Analytic Techniques for Energy Planning*, pages 53–66. Amsterdam:North-Holland Press.

Hobbs, B. F. (1995). Optimization Methods for Electric Utility Resource Planning. *European Journal of Operational Research*, 83(1):1–20.

Hobbs, B. F. and Ji, Y. D. (1999). Stochastic Programming-Based Bounding of Expected Production Costs for Multiarea Electric Power Systems. *Operations Research*, 47(6):836–848.

Hobbs, B. F., Rothkopf, M. H., O'Neill, R. P., and Chao, H.-p. (2001). *The Next Generation of Electric Power Unit Commitment Models, International Series in Operations Research & Management Science*. Boston/Dordrecht/London: Kluwer Academic Publishers.

Holmberg, K. (1994). On Using Approximations of the Benders Master Problem. *European Journal of Operational Research*, 77(1):111–125.

Holt, E. and Bird, L. (2005). Emerging Markets for Renewable Energy Certificates: Opportunities and Challenges. Technical report, National Renewable Energy Laboratory.

Hu, Z., Zhang, F., and Li, B. (2012). Transmission Expansion Planning Considering the Deployment of Energy Storage Systems. In *2012 IEEE Power and Energy Society General Meeting*, pages 1–6.

Huang, C. C., Ziemba, W. T., and Ben-Tal, A. (1977). Bounds on the Expectation of a Convex Function of a Random Variable: With Applications to Stochastic Programming. *Operations Research*, 25(2):315–325.

ICF (2013). Integrated Planning Model brochure. Retrieved June 10, 2012, from http://www.icfi.com/insights/products-and-tools/ipm.

Infanger, G. (1992). Monte Carlo (Importance) Sampling within a Benders Decomposition Algorithm for Stochastic Linear Programs. *Annals of Operations Research*, 39(1):69–95.

Jaccard, M. (1995). Oscillating currents: The changing rationale for government intervention in the electricity industry. *Energy Policy*, 23(7):579 – 592.

Jensen, J. L. W. V. (1906). Sur les fonctions convexes et les ingalits entre les valeurs moyennes. *Acta Mathematica*, 30(1):175–193.

Jewell, W. and Hu, Z. (2012). The Role of Energy Storage in Transmission and Distribution Efficiency. In *2012 IEEE PES Transmission and Distribution Conference and Exposition (T D)*, pages 1–4.

Joskow, P. L. (2011). Comparing the Costs of Intermittent and Dispatchable Electricity Generating Technologies. *American Economic Review*, 101(3):238–241.

Joskow, P. L. and Tirole, J. (2005). Merchant Transmission Investment. *Journal of Industrial Economics*, 53:233–264.

Kahn, E. (1995). Regulation by Simulation - the Role of Production Cost Models in Electricity Planning and Pricing. *Operations Research*, 43(3):388–398.

Kahn, E. (2010). Wind Integration Studies: Optimization vs. Simulation. *The Electricity Journal*, 23(9):51–64.

Kall, P. and Mayer, J. (2010). *Stochastic Linear Programming: Models, Theory, and Computation*. New York, NY:Springer.

Kazempour, S. J. and Conejo, A. J. (2012). Strategic Generation Investment Under Uncertainty Via Benders Decomposition. *IEEE Transactions on Power Systems*, 27(1):424–432.

Kazerooni, A. K. and Mutale, J. (2010a). Network Investment Planning for High Penetration of Wind Energy Under Demand Response Program. In *2010 IEEE 11th International Conference on Probabilistic Methods Applied to Power Systems (PMAPS)*, pages 238–243.

Kazerooni, A. K. and Mutale, J. (2010b). Transmission Network Planning Under a Price-Based Demand Response Program. In *2010 IEEE PES Transmission and Distribution Conference and Exposition*, pages 1–7.

Kuhn, D. (2009). Convergent Bounds for Stochastic Programs with Expected Value Constraints. *Journal of Optimization Theory and Applications*, 141(3):597–618.

Lasher, W. P. (2008). The Development of Competitive Renewable Energy Zones in Texas. In *IEEE Power and Energy Society Transmission and Distribution Conference and Exposition*, pages 1–4.

Latorre, G., Cruz, R. D., Areiza, J. M., and Villegas, A. (2003). Classification of Publications and Models on Transmission Expansion Planning. *IEEE Transactions on Power Systems*, 18(2):938–946.

Law, A. M. and Carson, J. S. (1979). Sequential Procedure for Determining the Length of a Steady-State Simulation. *Operations Research*, 27(5):1011–1025.

Lu, M., Dong, Z. Y., and Saha, T. K. (2005). A Framework for Transmission

Planning in a Competitive Electricity Market. In *2005 IEEE/PES Transmission and Distribution Conference and Exhibition: Asia and Pacific*, pages 1–6.

MacQueen, J. (1967). Some Methods for Classification and Analysis of Multivariate Observations. In *Proceedings of the Fifth Berkeley Symposium on Mathematical Statistics and Probability*, volume 1, pages 281–297. University of California Press.

Madansky, A. (1960). Inequalities for Stochastic Linear-Programming Problems. *Management Science*, 6(2):197–204.

Magnanti, T. L. and Wong, R. T. (1981). Accelerating Benders Decomposition - Algorithmic Enhancement and Model Selection Criteria. *Operations Research*, 29(3):464–484.

Mahmoud, M., Liu, Y., Hartmann, H., Stewart, S., Wagener, T., Semmens, D., Stewart, R., Gupta, H., Dominguez, D., Dominguez, F., Hulse, D., Letcher, R., Rashleigh, B., Smith, C., Street, R., Ticehurst, J., Twery, M., van Delden, H., Waldick, R., White, D., and Winter, L. (2009). A Formal Framework for Scenario Development in Support of Environmental Decision-Making. *Environmental Modelling & Software*, 24(7):798 – 808.

Marnay, C. and Strauss, T. (1991). Effectiveness of Antithetic Sampling and Stratified Sampling in Monte Carlo Chronological Production Cost Modeling [Power Systems]. *IEEE Transactions on Power Systems*, 6(2):669–675.

MARS (2013). Concorda MARS. Retrieved July 10, 2012, from http://geenergyconsulting.com/practice-area/software-products/mars.

Masse, P. and Gibrat, R. (1957). Application of linear programming to investments in the electric power industry. *Management Science*, 3(2):149–166.

Mcdaniel, D. and Devine, M. (1977). Modified Benders Partitioning Algorithm for Mixed Integer Programming. *Management Science*, 24(3):312–319.

Mills, A., Phadke, A., and Wiser, R. (2011). Exploration of Resource and Transmission Expansion Decisions in the Western Renewable Energy Zone initiative. *Energy Policy*, 39(3):1732 – 1745.

Mills, A., Wiser, R., and Porter, K. (2012). The Cost of Transmission for Wind Energy in the United States: A Review of Transmission Planning Studies. *Renewable and Sustainable Energy Reviews*, 16(1):1 – 19.

MISO (2010). Regional Generation Outlet Study. Retrieved June 3, 2012, from https://www.midwestiso.org/Library/Repository/Study/RGOS/Regional%20Generation%20Outlet%20Study.pdf.

Morales, J. M., Pinson, P., and Madsen, H. (2012). A Transmission-Cost-Based Model to Estimate the Amount of Market-Integrable Wind Resources. *IEEE Transactions on Power Systems*, 27(2):1060–1069.

Munoz, C., Sauma, E., Contreras, J., Aguado, J., and de la Torre, S. (2012). Impact of High Wind Power Penetration on Transmission Network Expansion Planning. *Generation, Transmission Distribution, IET*, 6(12):1281–1291.

Munoz, F. D., Hobbs, B. F., Ho, J., and Kasina, S. (2013a). An Engineering-Economic Approach to Transmission Planning Under Market and Regulatory Uncertainties: WECC Case Study. *IEEE Transactions on Power Systems*.

Munoz, F. D., Hobbs, B. F., and Kasina, S. (2012). Efficient Proactive Planning to Accommodate Renewables. In *IEEE Power and Energy Society General Meeting*, pages 1–7.

Munoz, F. D., Sauma, E. E., and Hobbs, B. F. (2013b). Approximations in Power Transmission Planning: Implications for the Cost and Performance of Renewable Portfolio Standards. *Journal of Regulatory Economics*, 43(3):305–338.

Nielsen, S. S. and Zenios, S. A. (1997). Scalable Parallel Benders Decomposition for Stochastic Linear Programming. *Parallel Computing*, 23(8):1069–1088.

Nordlund, P., Sjelvgren, D., Pereira, M. V. F., and Bubenko, J. A. (1987). Generation Expansion Planning for Systems with a High Share of Hydro Power. *IEEE Transactions on Power Systems*, 2(1):161–167.

NREL (2012a). NREL: Renewable Resources Data Center - PVWatts. Retrieved April 10, 2012, from http://www.nrel.gov/rredc/pvwatts/.

NREL (2012b). NREL: Western Wind Resources Dataset. Retrieved April 13, 2012, from http://wind.nrel.gov/Web_nrel/.

Nweke, C. I., Leanez, F., Drayton, G. R., and Kolhe, M. (2012). Benefits of Chronological Optimization in Capacity Planning for Electricity Markets. In *IEEE International Conference on Power System Technology (POWERCON)*, pages 1–6.

O'Brien, M. (2004). Techniques for Incorporating Expected Value Constraints Into Stochastic Programs. Ph.D. thesis, Stanford University.

Olson, A., Orans, R., A., D., Moore, J., and Woo, C. K. (2009). Renewable Portfolio Standards, Greenhouse Gas Reduction, and Long-Line Transmission Investments in the WECC. *The Electricity Journal*, 22(9):38 – 46.

O'Neill, R. P., Krall, E. A., Hedman, K. W., and Oren, S. S. (2013). A Model and Approach to the Challenge Posed by Optimal Power Systems Planning. *Mathematical Programming*, 140(2):239–266.

Palmer, K. and Burtraw, D. (2005). Cost-Effectiveness of Renewable Electricity Policies. *Energy Economics*, 27(6):873 – 894.

Palmintier, B. and Webster, M. (2011). Impact of Unit Commitment Constraints on Generation Expansion Planning with Renewables. *IEEE Power and Energy Society General Meeting*.

Papavasiliou, A. and Oren, S. S. (2013). Multiarea Stochastic Unit Commitment for High Wind Penetration in a Transmission Constrained Network. *Operations Research*, 61(3):578–592.

Paul, A. and Burtraw, D. (2002). The RFF Haiku Electricity Market Model. Resources for the Future. Retrieved March 10, 2012, from http://www.rff.org/RFF/Documents/RFF-Rpt-Haiku.v2.0.pdf.

Pereira, M. V. F., Pinto, L. M. V. G., Cunha, S. H. F., and Oliveira, G. C. (1985). A Decomposition Approach to Automated Generation Transmission Expansion Planning. *IEEE Transactions on Power Apparatus and Systems*, 104(11):3074–3083.

Pfeifenberger, J. P. (2012). Transmission Investment Trends and Planning Challenges. Retrieved March 10, 2013, from http://www.brattle.com/_documents/UploadLibrary/Upload1073.pdf.

Pfeifenberger, J. P. and Hou, D. (2012). Transmission's True Value: Adding up the Benefits of Infrastructure Investments. *Public Utilities Fortnightly*, pages 44–50.

Pierre-Louis, P., Bayraksan, G., and Morton, D. P. (2011). A Combined Deterministic and Sampling-Based Sequential Bounding Method for Stochastic Programming. *Proceedings of the 2011 Winter Simulation Conference (Wsc)*, pages 4167–4178.

Pletka, R. and Finn, J. (2009). Western Renewable Energy Zones, Phase 1: QRA Identification Technical Report, National Renewable Energy Laboratory. Subcontract Report, NREL/SR-6A2-46877. Retrieved May 24, 2012, http://www.nrel.gov/docs/fy10osti/46877.pdf.

Pozo, D., Sauma, E. E., and Contreras, J. (2013). A Three-Level Static MILP Model for Generation and Transmission Expansion Planning. *IEEE Transactions on Power Systems*, 28(1):202–210.

Prabhakar, A. J., Van Beek, D., Konidena, R., Lawhorn, J., and Ng, W. S. (2012). Integrating Demand Response and Energy Efficiency Resources into MISO's Value-Based Transmission Planning Process. In *2012 IEEE Power and Energy Society General Meeting*, pages 1–7.

Price, J. E. and Goodin, J. (2011). Reduced Network Modeling of WECC as a Market Design Prototype. In *IEEE Power and Energy Society General Meeting*, pages 1–6.

PSR (2012). PSR NETPLAN Software. Retrieved May 22, 2012, from http://www.psr-inc.com.br/portal/psr/servicos/modelos_de_apoio_a_decisao/studio_plan/netplan/.

Puga, J. N. and Lesser, J. A. (2009). Public Policy and Private Interests: Why Transmission Planning and Cost-Allocation Methods Continue to Stifle Renewable Energy Policy Goals . *The Electricity Journal*, 22(10):7 – 19.

RETI (2010). Renewable Energy Transmission Initiative Phase 2B, Final Report. Retrieved May 1, 2012, from http://www.energy.ca.gov/2010publications/RETI-1000-2010-002/RETI-1000-2010-002-F.PDF.

Rockafellar, R. T. and Wets, R. J.-B. (1991). Scenarios and Policy Aggregation in Optimization under Uncertainty. *Mathematics of Operations Research*, 16(1):119–147.

Roh, J. H., Shahidehpour, M., and Fu, Y. (2007). Market-Based Coordination of Transmission and Generation Capacity Planning. *IEEE Transactions on Power Systems*, 22(4):1406–1419.

Sahinidis, N. V. and Grossmann, I. E. (1991). Convergence Properties of Generalized Benders Decomposition. *Computers & Chemical Engineering*, 15(7):481–491.

Samarakoon, H., Shrestha, R., and Fujiwara, O. (2001). A Mixed Integer Linear Programming Model for Transmission Expansion Planning with Generation Location Selection. *International Journal of Electrical Power & Energy Systems*, 23(4):285–293.

Sauma, E. E. and Oren, S. S. (2006). Proactive Planning and Valuation of Transmission Investments in Restructured Electricity Markets. *Journal of Regulatory Economics*, 30:261–290.

Sauma, E. E. and Oren, S. S. (2007). Economic Criteria for Planning Transmission Investment in Restructured Electricity Markets. *IEEE Transactions on Power Systems*, 22(4):1394–1405.

SB2 (2011). California Senate Bill No. 2, Chapter 1. Retrieved February 20, 2012, from http://leginfo.ca.gov/pub/11-12/bill/sen/sb_0001-0050/sbx1_2_bill_20110412_chaptered.pdf.

Schmeiser, B. (1982). Batch Size Effects in the Analysis of Simulation Output. *Operations Research*, 30(3):556–568.

Schumacher, A., Fink, S., and Porter, K. (2009). Moving Beyond Paralysis: How States and Regions Are Creating Innovative Transmission Policies for Renewable Energy Projects . *The Electricity Journal*, 22(7):27 – 36.

Schweppe, F. C., Caramanis, M. C., Tabors, R. D., and Bohn, R. E. (1988). *Spot Pricing of Electricity.* Norwell, MA: Kluwer.

Sen, S. (2013). Discussion About the Use of Stabilization Techniques for the Stochastic Decomposition Algorithm in the NEOS Solver, Personal Communication.

Sherali, H. D. and Staschus, K. (1990). A 2-Phase Decomposition Approach for Electric Utility Capacity Expansion Planning Including Nondispatchable Technologies. *Operations Research*, 38(5):773–791.

Sherali, H. D., Staschus, K., and Huacuz, J. M. (1987). An Integer Programming Approach and Implementation for an Electric Utility Capacity Planning Problem with Renewable Energy-Sources. *Management Science*, 33(7):831–845.

Sherman, M. and Goldsman, D. (2002). Large-Sample Normality of the Batch-Means Variance Estimator. *Operations Research Letters*, 30(5):319–326.

Short, W., Sullivan, P., Mai, T., Mowers, M., Uriarte, C., Blair, N., Heimiller, D., and Martinez, A. (2011). Regional Energy Deployment System (ReEDS). NREL/TP-6A2- 46534. Golden, CO: National Renewable Energy Laboratory.

Shortt, A., Kiviluoma, J., and O'Malley, M. (2013). Accommodating Variability in Generation Planning. *IEEE Transactions on Power Systems*, 28(1):158–169.

SIEMENS (2012). SIEMENS PSS-E Software. Retrieved May 25, 2012, from http://www.energy.siemens.com/hq/en/services/power-transmission-distribution/power-technologies-international/software-solutions/pss-e.htm.

Silva, I., Rider, M., Romero, R., and Murari, C. (2006). Transmission Network Expansion Planning Considering Uncertainty in Demand. *IEEE Transactions on Power Systems*, 21(4):1565–1573.

Sioshansi, F. and Pfaffenberger, W. (2006). *Electricity Market Reform: An International Perspective*. Elsevier Science.

Steiger, N. M. and Wilson, J. R. (2001). Convergence Properties of the Batch

Means Method for Simulation Output Analysis. *Informs Journal on Computing*, 13(4):277–293.

Tibshirani, R., Walther, G., and Hastie, T. (2001). Estimating the Number of Clusters in a Data Set Via the Gap Statistic. *Journal of the Royal Statistical Society Series B-Statistical Methodology*, 63:411–423.

Tseng, G. C. (2007). Penalized and Weighted K-means for Clustering With Scattered Objects and Prior Information in High-Throughput Biological Data. *Bioinformatics*, 23(17):2247–2255.

Turvey, R. and Anderson, D. (1977). *Electricity Economics: Essays and Case Studies*. World Bank Research Publication. Washington, DC:World Bank.

Vajjhala, S. P., Paul, A., Sweeney, R., and Palmer, K. (2008). Green Corridors: Linking Interregional Transmission Expansion and Renewable Energy Policies. Discussion Paper 08-06. Washington, DC: Resources for the Future.

van der Weijde, A. H. and Hobbs, B. F. (2012). The Economics of Planning Electricity Transmission to Accommodate Renewables: Using Two-Stage Optimisation to Evaluate Flexibility and the Cost of Disregarding Uncertainty. *Energy Economics*, 34(6):2089–2101.

van Roy, T. J. (1983). Cross Decomposition for Mixed Integer Programming. *Mathematical Programming*, 25(1):46–63.

Ventosa, M., Ba?llo, A., Ramos, A., and Rivier, M. (2005). Electricity Market Modeling Trends. *Energy Policy*, 33(7):897 – 913.

VENTYX (2012). VENTYX PROMOD IV Software. Retrieved May 22, 2012, from http://www.ventyx.com/en/enterprise/business-operations/business-products/promod-iv.

Wagstaff, K., Cardie, C., Rogers, S., and Schr, S. (2001). Constrained K-means Clustering with Background Knowledge.

Wallace, S. W. (2000). Decision Making Under Uncertainty: Is Sensitivity Analysis of Any Use? *Operations Research*, 48(1):20–25.

Wang, T. and Neufville, R. D. (2004). Building Real Options into Physical Systems with Stochastic Mixed-Integer Programming. In *8th Annual Real Options International Conference*, pages 23–32.

WECC (2011). 10-Year Regional Transmission Plan: 2020 Study Report. Technical report, Western Electricity Coordinating Council.

Wiser, R. and Bolinger, M. (2011). 2010 Wind Technologies Market Report. U.S. Department of Energy, Office of Energy Efficiency and Renewable Energy. Retrieved March 10, 2012, from http://www1.eere.energy.gov/wind/pdfs/51783.pdf.

Wiser, R., Namovicz, C., Gielecki, M., and Smith, R. (2007). The Experience with

Renewable Portfolio Standards in the United States . *The Electricity Journal*, 20(4):8 – 20.

Wong, W., Chao, H., Julian, D., Lindberg, P., and Kolluri, S. (1999). Transmission Planning in a Deregulated Environment. In *IEEE Transmission and Distribution Conference*, volume 1, pages 350–355.

Woolf, F. (2003). *Global Transmission Expansion: Recipes for Success*. Tulsa, OK: PennWell Corporation.

WREZ (2012). Western Renewable Energy Zones. Retrieved May 20, 2012, from http://www.westgov.org/rtep/219.

Wu, F., Varaiya, P., Spiller, P., and Oren, S. (1996). Folk Theorems on Transmission Access: Proofs and Counterexamples. *Journal of Regulatory Economics*, 10(1):5–23.

Vita

Francisco David Muñoz Espinoza was born on August 16, 1983 in the city of Talagante, Chile. After graduating with his high school diploma in 2001 from Colegio Melipilla, he attended Universidad de Chile for his Bachelors degree in Mechanical Engineering. In 2008 he was awarded a Fulbright fellowship, which allowed him to pursue a Ph.D. in Energy Economics and Operations Research in the Department of Geography and Environmental Engineering at the Johns Hopkins University in Baltimore, Maryland. His doctoral research, under the direction of Dr. Benjamin F. Hobbs, focused on engineering-economic methods for power transmission planning under market and regulatory uncertainties and renewable resource policies. Part of his research was done in collaboration with the Energy Research Centre of the Netherlands and Sandia National Laboratories. After graduation, he will join the Analytics group at Sandia as a postdoctoral researcher.